EXTRAGALACTIC ENERGETIC SOURCES

edited
by
V. K. KAPAHI

INDIAN ACADEMY OF SCIENCES
BANGALORE

Proceedings of the Winter School on

Extragalactic Energetic Sources

Organized by
Tata Institute of Fundamental Research
January 10–21, 1983, Bangalore

Edited by
V. K. Kapahi

a supplement to
Journal of Astrophysics and Astronomy

The Indian Academy of Sciences
Bangalore 560080

Acknowledgement for the cover picture

Cover picture of 3C 273 obtained with the MERLIN interferometer at 73 cm wavelength by R. G. Conway, R. J. Davis, A. Foley, T. Muxlow & T. Ray. MERLIN is owned and operated by Jodrell Bank, University of Manchester, England.

Edited by V. K. Kapahi for
The Indian Academy of Sciences, Bangalore 560080,
typeset by Macmillan India Ltd., Bangalore 560025,
and printed at Macmillan India Press, Madras 600041

Preface and acknowledgements

The winter school on *Extragalactic Energetic Sources* was held at the Indian Institute of Science, Bangalore during January 10–21, 1983. The participants, numbering nearly a hundred, consisted largely of interested scientists and research students from various institutions and university groups in India, together with several experts from different parts of the world. The main purpose of the school was to provide an overview of the different aspects of powerful extragalactic sources and to highlight the recent developments, both theoretical and observational, that have taken place in this area. The principal speakers and the areas covered by them were: R. A. Laing (extended radio structures), M. H. Cohen (VLBI and compact radio sources), P. A. Strittmatter (optical and infrared studies), S. S. Murray & L. van Speybroeck (X-ray studies), M. J. Rees (models of active galactic nuclei) and G. R. Burbidge (non-cosmological nature of redshifts). In addition there were about a dozen seminars given by the participants.

The present volume is a record of the proceedings of the winter school including some of the interesting discussions that took place following the various lectures. We note with regret that despite our best efforts we have been unable to include in the proceedings the contributions by Drs R. A. Laing, S. S. Murray and L. van Speybroeck.

The school was organized by the Tata Institute of Fundamental Research with excellent support from the Raman Research Institute, Bangalore and the Indian Institute of Astrophysics, Bangalore. The facilities for holding lectures and housing the participants were kindly provided by the Indian Institute of Science, Bangalore. It is a pleasure to thank Professor J. V. Narlikar who shouldred most of the responsibility for the academic and administrative organization of the winter school. I am also grateful to a large number of colleagues who helped to make the school a success.

I wish to thank The Indian Academy of Sciences for agreeing to publish the proceedings and Dr T. P. Prabhu and Ms Sandra Rajiva for providing invaluable editorial help. The radio photo of 3C 273 was very kindly made available by Dr R. G. Conway of Jodrell Bank.

V. K. Kapahi
TIFR Centre
Bangalore

Contents

Kapahi, V. K. (Ed.)
Extragalactic Energetic Sources
Indian Academy of Sciences, Bangalore, 1985, pp. 1–11

Inverse Compton X-rays and VLBI Radio Structures*

M. H. Cohen *Owens Valley Radio Observatory, California Institute of Technology, Pasadena, CA 91125, USA*

Contents

1. Introduction

The comparison of X-ray and VLBI radio data is particularly interesting and allows one, in some cases, to deduce that the emitting material is moving relativistically towards us. The analysis assumes that the radio radiation is incoherent synchrotron emission, so that the radio spectrum and angular size give the magnetic field strength and the energy spectrum of the relativistic electrons. The synchrotron photons collide with these same high-energy electrons, and X-rays are produced by the 'self-Compton' process. X-rays can also be produced by other mechanisms, of course, so the self-Compton calculation yields a lower limit to the X-rays. The calculation can first be made by assuming that the emitting material is at rest. In a few cases it is then found that the measured X-rays are many orders of magnitude weaker than the calculated lower limit, and the immediate conclusion is that the emitting material is moving towards us. Values of δ (Doppler-shift factor) calculated this way are of order 10. In our discussion below, however, we will not be concerned with ratios of measured to expected X-rays, but will include δ in the calculations from the beginning.

* In his lecture, Professor Cohen also discussed the observational status of superluminal radio sources. For a more recent review on this subject the reader is referred to an article by M. H. Cohen & S. C. Unwin, in *IAU Symp.* 110: *VLBI and Compact Radio Sources*, Eds R. Fanti, K. I. Kellermann & G. Setti, D. Reidel, Dordrecht, p. 95.—*Ed.*

The utility of combining radio and X-ray data in this way was first emphasized by Burbidge, Jones & O'Dell (1974; hereafter BJO), and more recently by Marscher *et al.* (1979) and by Marscher & Broderick (1981a, b; 1982a, b). An important point made by BJO and by Marscher & Broderick (1981a) is that the calculation is distance-independent. Actually, the distance d comes into the calculation twice, *via* the depth of the source $R = \phi d$. The optical depth is proportional to RN_0, where N_0 is electron density. But when N_0 is estimated from the synchrotron turnover it is proportional to R^{-1}, and d cancels. The redshift enters only in the ratio $(1+z)/\delta$ which controls the transformation of observables from one coordinate system to another.

2. Theory

We assume that the source is a homogeneous sphere of angular diameter ϕ containing an isotropic power-law distribution of relativistic electrons $N(E)\mathrm{d}E = N_0 E^{-p}\mathrm{d}E$ and a tangled magnetic field B. The sphere moves with Lorentz factor $\gamma = (1-\beta^2)^{-1/2}$ at an angle θ to the line of sight, giving a Doppler factor $\delta = \gamma^{-1}(1-\beta\cos\theta)^{-1}$.

Gould (1979) has calculated the radio and X-ray radiation from such a sphere. The spectrum is only a little different from the standard slab spectrum. A terrestrial observer measures the peak flux density $F_m = F_m^*[(1+z)/\delta]^{-3}$ at frequency $\nu_m = \nu_m^*[(1+z)/\delta]^{-1}$, where the starred quantities are the peak values that would be measured by a co-moving observer. A schematic spectrum is shown in Fig. 1. The point (ν_n, F_n) is the intersection of the low- and high-frequency asymptotes, and was used by BJO and Unwin *et al.* (1983); (ν_m, F'_m) was used by Marscher *et al.* (1979), Simon *et al.* (1983) and others. We shall use (ν_m, F_m). For a homogeneous sphere these frequencies and flux densities are related by factors of order unity which are given in Table 1 in the appendix. At frequency ν_n^* the optical depth along the diameter of the sphere is 1.5.

The cyclotron frequency and magnetic field can be calculated from γ_m, the

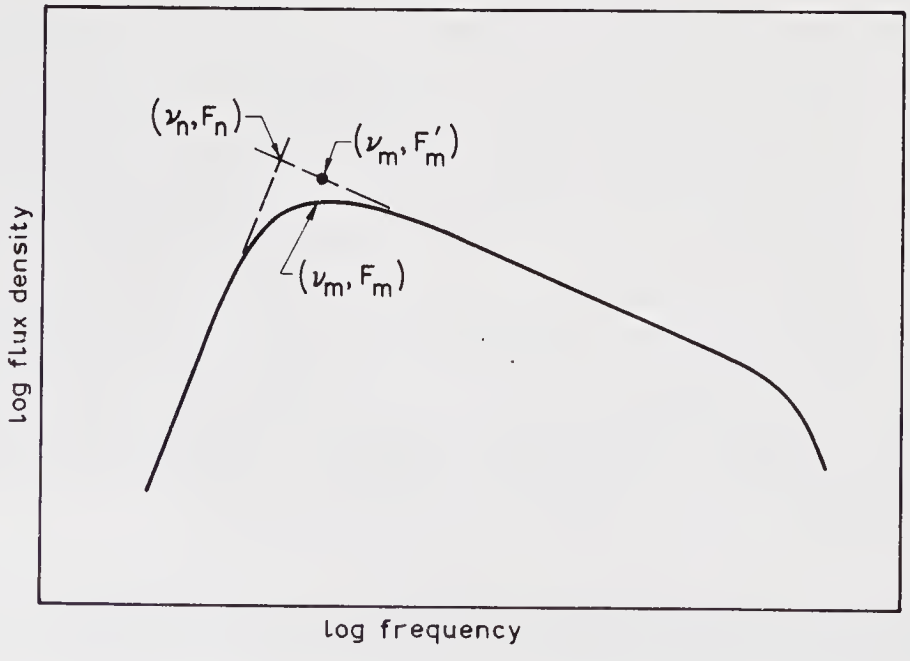

Figure 1. Schematic spectrum of a compact source illustrating the definitions used in the text.

characteristic energy (in units of mc^2) of the electrons radiating at ν_m^*:

$$\nu_B = \frac{eB}{2\pi mc} = \nu_m \gamma_m^{-2} \left(\frac{1+z}{\delta}\right) \tag{1}$$

and γ_m can be expressed in terms of the measured quantities F_m, ν_m, and ϕ. In practical units (Jy, GHz, milli-arcsec),

$$\gamma_m = 10^3 a(\alpha) F_m \nu_m^{-2} \phi^{-2} \left(\frac{1+z}{\delta}\right), \tag{2}$$

and

$$B = 10^{-5} b(\alpha) F_m^{-2} \nu_m^5 \phi^4 \left(\frac{1+z}{\delta}\right)^{-1} \text{ Gauss}, \tag{3}$$

where $a(\alpha)$ and $b(\alpha)$ are tabulated in the appendix. The $b(\alpha)$ used by Marscher (1983) is a little different because he used F'_m rather than F_m. In Equations (2) and (3) B and γ_m are the magnetic flux density and electron energy in the source, and unstarred frequencies and flux densities are measured by the terrestrial observer. The angular diameter ϕ is invariant in uniformly moving coordinate systems. The factor $(1+z)/\delta$ is readily understood in terms of the transformations between ν and ν^*, and F and F^*.

Equations (2) and (3) are often used to calculate γ_m and B, and it has been customary to set $\delta = 1$. When ϕ is unknown it is sometimes estimated from equipartition arguments, or from the variability timescale. In the latter case, there is a problem when the brightness temperature (proportional to γ_m) is above 10^{12} K, the 'inverse Compton limit'. The problem is cured by allowing $\delta > 1$. When ϕ is estimated from $c\tau^*/d$, the co-moving timescale τ^* should be expressed as $\tau[(1+z)/\delta]^{-1}$ where τ is the measured timescale, and so $\gamma_m \sim \delta^{-3}$. This strong dependence allows large temperature discrepancies to be reconciled with small values of δ; typically, $\delta < 10$. This calculation, of course, needs a specific value of the Hubble constant, and so is distance-dependent.

The source is assumed to be optically thin to X-rays and only single-scattering is important. Convenient formulae for the X-ray intensity from a sphere have been given by Marscher (1983) in terms of (ν_m, F'_m) and by Unwin *et al.* (1983) in terms of (ν_n, F_n). We give here the equivalent expression in terms of (ν_m, F_m). These frequencies and flux densities (Fig. 1) should be simply related, as shown in Table 1, and the three formulae are equivalent for a homogeneous sphere. If a good spectrum is in hand, the coefficients in Table 1 could be used as a test of homogeneity. If the source is not homogeneous the formulae are not strictly applicable, and any answers should be treated with caution. The formula for X-ray intensity is

$$(F_{x\nu}/\phi^2) = 10^{8\alpha-4} c(\alpha) \ln \Lambda (F_m/\phi^2)^{4+2\alpha} \nu_m^{-5-3\alpha} \nu^{-\alpha} \left(\frac{1+z}{\delta}\right)^{4+2\alpha} \tag{4}$$

where $F_{x\nu}$ is in Jy and $c(\alpha)$ is given in the appendix.

The parameter Λ is discussed by Gould (1979; he calls it Σ_c) and by Jones, O'Dell & Stein (1974); see also Marscher (1983). For a wide range of circumstances, it is approximately the ratio of upper to lower cut-off frequencies of the synchrotron spectrum. The important features of Equation (4) are that the X-ray brightness has a power-law spectrum with the same index as the high-frequency radio spectrum, and that it depends on high powers of the radio brightness, the synchrotron turnover frequency, and $(1+z)/\delta$.

In the literature, the main body of data on X-rays from compact objects comes from the Einstein Observatory. The X-rays are often reported as an integral over the energy range corresponding to 0.5 to 4.5 keV in the emitted reference frame, and for comparisons with these data Equation (4) must be integrated over the same range. When this is done, we have the self-Compton intensity in the energy range $(0.5\text{–}4.5)/(1+z)$ keV

$$S_x/\phi^2 = 10^{-9} d(\alpha)(1+z)^{\alpha-1} \ln\Lambda (F_m/\phi^2)^{4+2\alpha} \nu_m^{-5-3\alpha} \left(\frac{1+z}{\delta}\right)^{4+2\alpha}. \tag{5}$$

The coefficient $d(\alpha)$ is listed in the appendix. S_x is now in cgs units for convenience (erg cm^{-2} s^{-1}), F_m is in Jy, ν_m is in GHz, and ϕ is in milli-arcsec.

The X-ray intensity may be greater than that given by Equation (5), because the source may also emit thermal or other X-rays. Therefore, Equation (5) actually gives a lower limit to the X-rays, and from it we calculate δ_{min}, a lower limit to δ.

$$\delta_{min} = 10^{-2} e(\alpha) F_m \nu_m^{-p} \phi^{-q} S_x^{-r} (1+z)^s \tag{6}$$

where the units are as in Equation (5) and $e(\alpha)$, p, q, r, and s are tabulated in the appendix; we have taken $\ln\Lambda = 8$. Equation (6) is valid only for S_x covering the band $(0.5\text{–}4.5)/(1+z)$ keV. Most of the uncertainty in δ_{min} comes from ϕ, because it is uncertain and because q is bigger than the other exponents. In the homogeneous spherical model the angular diameter is well-defined, but a real source (even if spherical) might be inhomogeneous, and the effective diameter would change with frequency. The question then arises as to which diameter should be used in Equations (4) and (5). Gould (1979) has calculated the self-Compton radiation from certain classes of inhomogeneous spheres, but the effective angular sizes have not been calculated in detail. We conjecture that the measured diameter near ν_m is the appropriate one to use, because the photon density is highest there. However, it is very difficult to determine this angle directly, because the VLBI experiments typically have insufficient angular resolution. An upper limit is usually quoted for ϕ_m, which decreases δ_{min} and makes it less interesting. A stronger limit can be obtained by measuring ϕ at a higher frequency and making the risky assumption that ϕ is constant between ν and ν_m. Alternatively, a specific model can be chosen for $\phi(\nu)$, and ϕ_m calculated from ϕ_ν; *e.g.* in the Blandford-Königl (1979) model $\phi \sim \nu^{-1}$. Another poorly justified procedure uses the variation timescale with an assumed Hubble constant. In spite of the uncertainties, however, the VLBI and the variation timescale procedures yield self-consistent results for 3C 147 (Simon *et al.* 1983) and 3C 345 (Unwin *et al.* 1983). It appears that ϕ_m can be estimated to within a factor 2, and that errors in δ_{min} from this cause are no more than a factor 2.

As a practical point, VLBI observations usually yield only the half-power diameter (FWHM) of a gaussian which fits the visibility function. Marscher (1983) has shown that the value 1.8 × FWHM is a good estimate of ϕ when the sphere is optically thin and only partially resolved.

In equation (6) δ_{min} varies very slowly with S_x and large errors in its measurement can be tolerated. VLBI maps over a range of frequencies spanning the synchrotron maximum allow F_m and ν_m to be determined reasonably well, so that errors in ϕ dominate the errors in δ_{min}. The parameter Λ is very poorly known but fortunately δ_{min} varies only as $(\ln\Lambda)^r$ which is close to 1.5 for a wide range of parameters. Finally, all coefficients and exponents depend weakly on α, as shown in Table 1. The components

of a source often can be spatially separated with VLBI, and the individual spectral indices can be determined. However, the possibility may remain that the component under study is actually inhomogeneous, and that the spherical homogeneous model is a poor representation of the source. Even here, it may be possible to find limits to ϕ and ν_m such that a useful value of δ_{min} can be calculated, as Marscher & Broderick (1981a) did for NRAO 150.

A final interesting point in Equation (6) is that δ_{min} varies inversely with S_x; other things being equal, very weak X-rays imply relativistic motion. This follows directly from the transformations which produce the $(1+z)/\delta$ factors in Equation (4). A heuristic view of this is as follows. The fundamental parameters of the source are electron density N_0, index p, magnetic field B, and radius R. The ratio of (singly-scattered self-Compton) X-ray to (optically-thin) radio radiation is proportional to the product $N_0 R$ and depends on p but not on B (see Gould 1979, Equations 13, 15 and 20). If a source is deficient in high-energy electrons or is exceptionally small, then both the X-ray and radio radiation will be weak, and their ratio will also be weak. In general, such a source will not be prominent, but may become strong at centimetre wavelengths through Doppler boosting since $F \sim \delta^3$. The calculation described above for δ_{min} is independent of distance, and can be extended to provide a distance-independent upper limit to $N_0 R$. However, the calculation of N_0 by itself requires R which requires a distance.

3. Some observations

We now discuss some of the cases which have been reported in the literature. These include two cases where the X-ray data and the superluminal motion both suggest bulk relativistic motion (NRAO 140 and 3C 345), two cases where the radio and X-ray data are consistent with $\delta = 1$ (3C 84 and Mrk 501), one case where the radio and X-ray data strongly suggest $\delta > 1$ and a prediction of superluminal motion has been made (3C 147), three cases where an X-ray variability size is used, probably incorrectly, and the special case of 4C 39.25.

3.1 *NRAO 140*

In a series of papers, Marscher *et al.* (1979) and Marscher & Broderick (1981a, b; 1982a, b) report X-ray and radio observations of NRAO 140. They first showed that $\delta_{min} \sim 4$ and predicted superluminal motion of the components in NRAO 140, and then made second-epoch observations showing $v/c \simeq 10h^{-1}$, where $h = H_0/100$, H_0 being the Hubble constant.

Marscher & Broderick had limited radio data to work with and they picked a conservative decomposition of the overall radio spectrum, one which minimized the X-radiation. Their components A and B have similar values of F_m and ϕ but differ by a factor of 10 in ν_m, so the low-frequency component B, has the 'Compton problem' and is the source of most of the X-rays. For component B, $\phi \sim 0.24$ milli-arcsec, but it was measured at 10.7 GHz whereas ν_m is 2.7 GHz. Thus ϕ_m may be bigger than 0.24 milli-arcsec and δ_{min} smaller than 4. The measured proper motion gives $v/c = 10h^{-1}$ which implies $\gamma \geqslant 10(5)$ for $H_0 = 100(50)$. The uncertainties in the measurements of NRAO 140 are

rather large but the independent determinations of $\delta_{\min}$ and v/c are consistent with bulk relativistic motion with γ of order 5 or 10.

3.2 *3C 345*

Unwin *et al.* (1983) discuss two VLBI components in 3C 345, called D and C3, which represent the core and inner jet component, respectively. They derived ϕ from maps made at frequencies several times higher than ν_m, and used $\phi_D = 0.3$ milli-arcsec, $\phi_{C3} = 1.0$ milli-arcsec, giving $\delta_{\min,D} = 18$, $\delta_{\min,C3} = 8$. If the sphere model is wrong and diameters decrease with wavelength, as for example in the Blandford-Königl (1979) model, where $\phi \sim \nu^{-1}$, then corrected values are $\phi_D \sim 0.6$ milli-arcsec, $\phi_{C3} \sim 4$ milli-arcsec and $\delta_{\min,D} = 6$, $\delta_{\min,C3} = 1$. However, these corrections are too strong, as other observations near ν_m show that $\phi_D \leqslant 0.6$ milli-arcsec (Unwin *et al.* 1983, Fig. 2, epoch 1980.17) and $\phi_{C3} \leqslant 1.1$ milli-arcsec (Cohen *et al.* 1983, Fig. 5, epoch 1981.89). It appears that firm lower limits are $\delta_{\min,D} \geqslant 6$, $\delta_{\min,C3} \geqslant 7$.

These limits on δ are consistent with the superluminal motion seen in 3C 345, $(v/c)_{C3} = 7h^{-1}$, which by itself gives $\gamma \geqslant 7(14)$ and $\theta \leqslant 16°(8°)$ with $H_0 = 100(50)$ (Unwin *et al.* 1983, Fig. 10). If $\delta_{\min}$ is combined with the (v/c) values, we get $\gamma \geqslant 7(14)$ and $\theta < 8°(6.5°)$. The limit on component D, $\delta_{\min,D} \geqslant 6$, gives $\gamma \geqslant 3$ and $\theta \leqslant 9.5°$ for the core. A particularly interesting feature is that the radiating material in the core is moving relativistically, although the location of the core is generally assumed to be fixed. Relativistic beam models generally predict that all the components are Doppler-boosted, else there would be fortuitous agreement between the large boosting factor for the jet components, and the large intrinsic flux ratio between the core and jet components (Readhead *et al.* 1978). In some models the core is at the (stationary) location where the optical depth is unity (Blandford & Königl 1979; Scheuer & Readhead 1979).

3.3 *3C 84 (NGC 1275)*

Readhead *et al.* (1983) decomposed the nuclear radio source in NGC 1275 into a number of components with VLBI at 22 GHz, and by using measured angular sizes showed that the measured X-ray flux is consistent with self-Compton radiation with $\delta = 1$. The radio source 3C 84 is variable on a timescale of several years, which also is consistent with the measured diameter if $\delta = 1$. Romney *et al.* (1982) have presented evidence that the source is expanding with an apparent transverse velocity $(v/c) \sim 0.3\,h^{-1}$; but preliminary results of observations at 1.3 and 6 cm (Readhead & Unwin, unpublished) do not confirm this result. Readhead *et al.* (1983) have suggested that the one-sided curved morphology in the nucleus might be due to relativistic beaming, but otherwise there is no evidence for bulk relativistic motion in NGC 1275.

3.4 *Mrk 501 (1652+398)*

Kondo *et al.* (1981) made closely-spaced observations of Mrk 501 from 5×10^8 to 5×10^{18} Hz and presented a spectrum which is essentially free of errors due to variability. A single synchrotron cloud, with the optical, UV, and X-rays all produced by inverse-Compton radiation, fits the combined spectrum with $\delta = 1$ (no bulk

relativistic motion). To get this result, Kondo *et al.* used a diameter $\phi = 1.1$ milli-arcsec as given by Weiler & Johnston (1980) at 6 cm. This is nearly the same as the diameter reported by Pearson & Readhead (1981) at 6 cm, $\phi = 1.19$ milli-arcsec, but the agreement is fortuitous. The Weiler-Johnston result is derived from one (u, v) point in a one-baseline VLBI experiment, and assumes that the source is a circular Gaussian. The Pearson-Readhead result comes from 12 (u, v) points and is a better measure of the diameter; however, a reliable value can only come from a VLBI map made with hundreds of points. A serious objection to the Kondo *et al.* (1981) model is that the flux density in the Pearson-Readhead component is only half that in the total source (0.65 Jy *vs* 1.3 Jy) and therefore there are at least two components at centimetre wavelengths. At present there is no evidence for relativistic motions in Mrk 501, although VLBI maps at several wavelengths and a better model are clearly of interest.

3.5 *3C 147*

Simon *et al.* (1983) have VLBI maps of 3C 147 at 329 MHz showing a variable core with an overall diameter of 5-milli-arcsec. When this is combined with the X-ray observations, they calculate $\delta_{\min} = 3.6$. However, the spectrum of the core shows a peak at $\nu_m \sim 800$ MHz, so an angular diameter ϕ_m appropriate to ν_m should be used. Since ϕ_m must be smaller than 5 milli-arcsec, $\delta_{\min} = 3.6$ is a strong lower limit. They also estimate a variability timescale $\tau = 7.5$ yr, from which $\delta \geqslant 1.3 h^{-1}\theta$. The combination of this variability limit with the X-ray limit gives a stronger limit, $\delta \geqslant 4.3(6.7)$ for $H_0 = 100(50)$. Corresponding angles to the line of sight are $\theta \leqslant 12°$ (8.5°). Unless θ is much smaller than its upper limit, the source should show superluminal motion. Second-epoch observations (Simon *et al.* 1983; Wilkinson *et al.* 1984; Preuss *et al.* 1984), however, have failed to confirm this prediction.

3.6 *1218 + 304, 2155 − 304 and 0548 − 322*

Rapid variations in the optical or X-ray emission from quasars and BL Lac objects are indicative of a component of very small size. In a few cases, including the BL Lac objects 1218 + 304 (Weistrop *et al.* 1981), 2155 − 304 (Urry & Mushotzky 1982), and 0548 − 322 (Urry *et al.* 1982), this variability size has been used in the self-Compton formula to calculate δ. This is very risky, because the radio spectrum which is used in the same formula probably is not representative of the tiny region associated with the variability. Indeed, the discrepancy between the radio and optical variability timescales is one of the reasons why the optical continuum emission is presumed to arise in a region much smaller than the radio source. The X-ray variations are yet more rapid, and may come from an even smaller volume.

The basic problem in the analyses of these objects is the assumption of one uniform source out of which comes all the radio, optical, and X-ray emission. It is much more likely that there is a hierarchy of components, and it is necessary to use the radio size in the self-Compton calculation. For sources 1218 + 304, 2155 − 304 and 0548 − 322 the peak frequency ν_m appears to be a few GHz. Since $\lambda/d \geqslant 3$ milli-arcsec for terrestrial VLBI at 3 GHz, diameters smaller than about 1 milli-arcsec cannot be determined. However, measurements at higher frequencies show that components which peak at $\nu_m \leqslant 3$ GHz have $\phi > 0.2$ milli-arcsec; see *e.g.* the discussions for 3C 345 and NRAO 140

above. Also, the general lack of interstellar scintillations for extragalactic sources (Dennison & Condon 1981), including BL Lac objects, suggests $\phi > 0.1$ milli-arcsec, at least at metre wavelengths. If we assume $\phi \geqslant 0.2$ milli-arcsec rather than using the optical or X-ray variability as a guide to diameter, then the observed X-rays are consistent with $\delta = 1$ in all three sources. We maintain that at present there is no evidence for bulk relativistic motion in these objects.

3.7 *4C 39.25 (0923+392)*

4C 39.25 is a particularly interesting source because Shaffer (1984) has recently produced evidence that it is contracting superluminally. It is strong (5–10 Jy) with a high redshift ($z = 0.698$) and for a decade was a close stable double, with slow changes in flux density. In 1980, the double apparently began to contract, with a tentative velocity $v/c = 3$. This suggests that it has a relativistic beam which has a peculiar twist, so that in projection the luminous blobs are approaching each other. It is likely that 4C 39.25 is very similar to 3C 345.

The literature (Zamorani *et al.* 1981) contains one X-ray measurement of 4C 39.25, and a rough idea of the radio spectrum and diameter can be obtained from VLBI measurements (Shaffer *et al.* 1977; Bååth *et al.* 1981; Pearson & Readhead 1981). These suggest that $\delta_{\min} \sim 5$ and that there is bulk relativistic motion in 4C 39.25. This strengthens the conclusion that it is basically like the other superluminal sources. However, the radio data are incomplete, and more studies are necessary to confirm this.

Appendix

Self-Compton X-rays

The synchrotron spectrum from a homogeneous sphere is given by Gould (1979) in his Equation (36) and is depicted schematically in Fig. 1 here. In Table 1, we give the ratios ν_n/ν_m and F_n/F_m; which are also discussed by Gould. F'_m lies on the high-frequency asymptote and can be readily calculated if needed.

We have used Gould's calculation but have also expressed some of the results with the formalism of Burbidge, Jones, & O'Dell (1974). To help avoid confusion, we give here the correspondence between coefficients in these two papers.

Table 1. Dimensionless functions of spectral index.

α	ν_n/ν_m	F_n/F_m	$a(\alpha)$	$b(\alpha)$	$c(\alpha)$	$d(\alpha)$	$e(\alpha)$	p	q	r	s
0.25	0.52	1.29	4.71	1.61	2.30	1.48	1.73	1.28	1.56	0.22	0.83
0.50	0.68	1.44	3.95	2.29	1.51	0.66	2.21	1.30	1.60	0.20	0.90
0.75	0.79	1.53	3.87	2.39	1.28	0.39	2.84	1.32	1.64	0.18	0.95
1.00	0.86	1.59	4.12	2.10	1.35	0.30	3.65	1.33	1.67	0.17	1.00
1.25	0.91	1.62	4.48	1.78	1.54	0.25	4.59	1.35	1.69	0.15	1.04

$$k_{\alpha 0} = 2c(p)$$

$$j_{\alpha 0} = 2\pi(3/2)^{(p-1)/2}\, a(p)$$

$$i_{\alpha 0} = j_{\alpha 0}/k_{\alpha 0} = \pi(3/2)^{(p-1)/2}\, \frac{a(p)}{c(p)}$$

$$i_{\alpha 0}\, j_{\alpha 0}\, e^{\mathrm{sc}}_{\alpha 0} = \frac{3}{16\pi}\, \frac{b(p)}{c(p)}.$$

References

Bååth, L. B., Rönnäng, B. O., Pauliny-Toth, I. I. K., Kellermann, K. I., Preuss, E., Witzel, A., Matveenko, L. I., Kogan, L. R., Kostenko, V. I., Moiseev, I. G., Shaffer, D. B. 1981, *Astrophys. J.*, **243,** L123.

Blandford, R. D., Königl, A. 1979, *Astrophys. J.*, **232,** 34.

Burbidge, G. R., Jones, T. W., O'Dell, S. L. 1974, *Astrophys. J.*, **193,** 43 (BJO).

Cohen, M. H., Unwin, S. C., Lind, K. R., Moffet, A. T., Simon, R. S., Wilkinson, P. N., Spencer, R. E., Booth, R. S., Nicolson, G. D., Niell, A. E., Young, L. E. 1983, *Astrophys. J.*, **272,** 383.

Dennison, B., Condon, J. J. 1981, *Astrophys. J.*, **246,** 91.

Gould, R. J. 1979, *Astr. Astrophys.*, **76,** 306.

Jones, T. W., O'Dell, S. L., Stein, W. A. 1974, *Astrophys. J.*, **188,** 353.

Kondo, Y., Worrall, D. M., Mushotzky, R. F., Hackney, R. L., Hackney, K. R. H., Oke, J. B., Yee, H. K. C., Neugebauer, G., Mathews, K., Feldman, P. A., Brown, R. L. 1981, *Astrophys. J.*, **243,** 690.

Marscher, A. P. 1983, *Astrophys. J.*, **264,** 296.

Marscher, A. P., Broderick, J. J. 1981a, *Astrophys. J.*, **247,** L49.

Marscher, A. P., Broderick, J. J. 1981b, *Astrophys. J.*, **249,** 406.

Marscher, A. P., Broderick, J. J. 1982a, *Astrophys. J.*, **255,** L11.

Marscher, A. P., Broderick, J. J. 1982b, in *IAU Symp.* 97*: Extragalactic Radio Sources*, Eds D. S. Heeschen & C. M. Wade, D. Reidel, Dordrecht, p. 359.

Marscher, A. P., Marshall, F. E., Mushotzky, R. F., Dent, W. A., Balonek, T. J., Hartman, M. F. 1979, *Astrophys. J.*, **233,** 498.

Pearson, T. J., Readhead, A. C. S. 1981, *Astrophys. J.*, **248,** 61.

Preuss, E., Alef, W., Whyborn, N., Wilkinson, P. N., Kellermann, K. I. 1984, in *IAU Symp.* 110*: VLBI and Compact Radio Sources*, Eds R. Fanti, K. I. Kellermann & G. Setti, D. Reidel, Dordrecht, p. 29.

Readhead, A. C. S., Cohen, M. H., Pearson, T. J., Wilkinson, P. N. 1978, *Nature*, **276,** 768.

Readhead, A. C. S., Hough, D. H., Ewing, M. S., Walker, R. C., Romney, J. D. 1983, *Astrophys. J.*, **265,** 107.

Romney, J. D., Alef, W., Pauliny-Toth, I. I. K., Preuss, E., Kellermann, K. I. 1982, in *IAU Symp.* 97*: Extragalactic Radio Sources*, Eds D. S. Heeschen & C. M. Wade, D. Reidel, Dordrecht, p. 291.

Scheuer, P. A. G., Readhead, A. C. S. 1979, *Nature*, **277,** 182.

Shaffer, D. B. 1984, in *IAU Symp.* 110*: VLBI and Compact Radio Sources*, Eds R. Fanti, K.I. Kellermann & G. Setti, D. Reidel, Dordrecht, p. 135.

Shaffer, D. B., Kellermann, K. I., Purcell, G. H., Pauliny-Toth, I. I. K., Preuss, E., Witzel, A., Graham, D., Schilizzi, R. T., Cohen, M. H., Moffet, A. T., Romney, J. D., Niell, A. E. 1977, *Astrophys. J.*, **218,** 353.

Simon, R. S., Readhead, A. C. S., Moffet, A. T., Wilkinson, P. N., Allen, B., Burke, B. F. 1983, *Nature*, **302,** 487.

Unwin, S. C., Cohen, M. H., Pearson, T. J., Seielstad, G. A., Simon, R. S., Linfield, R. P., Walker, R. C. 1983, *Astrophys. J.*, **271,** 536.

Urry, C. M., Mushotzky, R. F. 1982, *Astrophys. J.*, **253,** 38.

Urry, C. M., Mushotzky, R. F., Kondo, Y., Hackney, K. R. H., Hackney, R. L. 1982, *Astrophys. J.*, **261,** 12.

Weiler, K. W., Johnston, K. J. 1980, *Mon. Not. R. astr. Soc.*, **190,** 269.
Weistrop, D., Shaffer, D. B., Mushotzky, R. F., Reitsema, H. J., Smith, B. A. 1981, *Astrophys. J.*, **249,** 3.
Wilkinson, P. N., Spencer, R. E., Readhead, A. C. S., Pearson, T. J., Simon, R. S. 1984, in *IAU Symp.* 110: *VLBI and Compact Radio Sources*, Eds R. Fanti, K. I. Kellermann & G. Setti, D. Reidel, Dordrecht, p. 25.
Zamorani, G., Henry, J. P., Maccacaro, T., Tananbaum, H., Soltan, A., Avni, Y., Liebert, J., Stocke, J., Strittmatter, P. A., Weymann, R. J., Smith, M. G., Condon, J. J. 1981, *Astrophys. J.*, **245,** 357.

Discussion

Ananthakrishnan: Does one always look for weak X-ray emission before deciding to observe a source for superluminal motion? Is this the only way to predict superluminal motion?
Cohen: The present superluminal sources were mostly found by looking at strong variables. The success rate in predicting superluminal motion from weak X-rays is now 50 per cent—positive with NRAO 140 and negative with 3C 147.
Gopal-Krishna: X-ray weakness like NRAO 140 has implied bulk relativistic motion along the line of sight. Bulk relativistic motion has also been invoked to explain the metre-wavelength flux variations observed in some sources. Accordingly, should these sources be expected to show superluminal expansion?
Cohen: Yes, I think many of them should. The difficulty is that superluminal effects are presently seen at 5 or 10 GHz with internal proper motions of 0.3 milli-arcsec yr^{-1} or so. At 0.5 GHz the angular resolution is poor and it would take ten years to see this proper motion. Unfortunately though, low-frequency outbursts might be less than ten years long.
Porcas: It may be that most of the low-frequency variable sources do show evidence of bulk relativistic motion. This does not necessarily mean that they should all show superluminal motion, however. They may just exhibit a single, 'core' component on milli-arcsec scale which could be 'stationary' (fixed region) but show radiation from matter with bulk relativistic motion (*i.e.* the trick employed by Scheuer & Readhead 1979).
Rees: If the low-frequency sources were indeed ultra compact there is one way in which the absence of interstellar scintillations could be explained. The line of sight may pass through one or more intergalactic clouds which might (analogously with the interstellar medium) produce enough scattering to make the apparent angular size too large to display interstellar scintillation, even if the source was intrinsically point-like. These clouds are known to exist from the data on QSO absorption lines (in the case of A0 0235 + 164 there is a galaxy along the line of sight, so the existence of clouds is even more likely.)
Narlikar: Do you have similar X-ray flux data for other superluminal cases like 3C 273, 3C 120 etc?
Cohen: These are now being investigated.
K. P. Singh: How do we interpret the rapid X-ray variability observed in some sources, *e.g.*, 2155 – 304? This rapid variability implies source size of 10^{-3} milli-arcsec which is much smaller than what is inferred from high-resolution radio maps.
Cohen: I don't know the origin of the rapid X-ray variability, but it surely comes from a volume much smaller than the radio synchrotron source.

Ramesh Narayan: Could you comment on the prospects of doing polarization observations with VLBI in future?
Cohen: Such experiments are difficult because great sensitivity is needed; also, the calibrations are difficult. Nonetheless several polarization experiments are in progress and there should be results in a year or two.

Kapahi, V. K. (Ed.)
Extragalactic Energetic Sources
Indian Academy of Sciences, Bangalore, 1985, pp. 13–51

Optical and Infrared Studies of Active Galactic Nuclei

P. A. Strittmatter *Steward Observatory, Tucson, Arizona 85721, USA*

Contents

1. Introduction

I will discuss in my lectures how data on the optical and infrared (IR) emission from active galaxies are obtained, and how these influence what we know about the sources. In doing so I will concentrate on the nuclei of active galaxies, rather than on the galaxies in which the nuclei are embedded. So I shall principally be talking about quasars, BL

This article has been put together by N. C. Rana, P. P. Deo, A. K. Kembhavi & V. K. Kapahi based on the four lectures delivered by Professor Strittmatter. Although care has been taken by the compilers to avoid mistakes, it must be noted that no editing has been done by the lecturer—*Ed.*

Lacs, the nuclei of Seyfert galaxies and so on, with reference to the accompanying stellar systems when necessary.

I will first talk about the many existing surveys of these objects and the basic properties of the sources at various wavelengths before going into their optical properties in some detail. In the next lecture I will take up polarization, which is a particularly important property in distinguishing non-thermal radiation but there has been very little discussion about this topic. The lecture after that will be mainly on the emission-line properties of various kinds of active galactic nuclei. The last lecture will contain some wild speculation and also some discussion on absorption-line properties and on how the combination of absorption- and emission-line properties of QSOs allows one to infer something about what is going on in their nuclei.

2. Existing surveys of extragalactic energetic sources

Active galactic nuclei are identified in surveys at various wavelengths, not necessarily in the optical band. The high-energy astrophysics game really began with the discovery of quasars and BL Lacs from radio surveys. As accurate radio positions became available, it was possible to optically identify some of the radio sources and as techniques improved, it became possible to study the IR properties of these sources. In recent times another good source of active galaxies has been the X-ray surveys. The two kinds of surveys are in principle capable of revealing the same kind of information, but this is always regulated by whatever influence the radio frequency emission or the X-rays have on the optical and IR properties of the objects. There have been surveys in the optical region of the spectrum as well, leading to the discovery of optically selected objects, but thus far there have been no surveys in the IR. The available samples of active galactic nuclei will therefore be biased against objects with certain infrared characteristics.

What one would ideally like to do is to have complete spectral information from the radio through the γ-ray region, on every one of the sources that it is conceivable to observe, down to limiting flux values in every region of the spectrum. This is obviously very hard to do. The character of the study is different in different regions of the spectrum. The radio observer tends to cover a very wide frequency range with a spectral resolution that is absolutely tremendous, but with absolutely no sampling at all over the frequency spaces in between. So it is very easy to fit smooth continua through the data. There is not much spectral information available in the X-ray band either. The data has so far been sampled only at very low resolution, and there is considerable difficulty in deciding whether the differences between the spectral channels are real or not.

The optical region is different in that the wavelength range covered is exceedingly narrow, in comparison with the radio and X-ray regions, with at most a factor of 3 covered in the energy of the photons; usually this factor is as small as 2. In the IR region the data is obtained somewhat separated in wavelength, basically due to the windows in the atmosphere. The field is still in its infancy but better resolution and spectral coverage are becoming available.

I shall not review radio surveys here, except to make the point that there have so far been many surveys, like 3C, 4C, Bologna, 5 GHz NRAO-Bonn, *etc.* These are all significant because they have been made at widely different wavelengths. In the X-ray region there was not much surveyed prior to the Einstein observatory. But in the optical

region there have been many surveys. One generally uses known optical properties of objects from those found in radio surveys, to pull out the required objects from survey plates. One of the criteria used to select quasars is that of colour. This is based on the distinction in the spectra of quasars as compared to those of stars: the former are relatively smooth compared to the spectra of stars which show very strong structure like the Balmer jump. If the spectrum of a star with an ultraviolet (UV) cutoff is compared to that of an object with a smooth spectrum stretching into the UV, it will be found that the latter contains more in the UV than in the blue or the visible, relative to the star. It is therefore possible, using two-colour pictures, with UV as one colour, to pick up candidates for smooth spectra. By widening the range and measuring at more than two colours, it is possible to refine the colour criterion. But if there is structure in the spectra, it is not possible to use the colour criterion.

One of the earliest surveys for quasars using the colour selection technique was done by Sandage & Véron (1965). The technique has been developed particularly by Braccesi and his group in Italy, using 4-band 3-colour work (*e.g.* Braccesi, Formiggini & Gandolfi 1970). All surveys based on colour selection have been listed by Véron & Véron (1982). A very important survey of quasars is the Palomar-Green two-colour survey (PG survey) aimed at finding all the bright quasars in the sky, that have UV excess (Schmidt & Green 1983). The Braccesi survey covers a rather small area, but goes down to about 19.5 mag. The PG survey, on the other hand, covers the whole sky but finds quasars only brighter than $\sim$ 16 mag.

A more recent optical selection technique makes use of the fact that quasars and related active galaxies have very strong emission lines. Using objective-prism and grism techniques much work has been done by Smith, Osmer, MacAlpine, Hoag, Hazard, Weedman and others (see Smith 1981 for a review). These slitless surveys contain biases too, selecting objects with strong emission-line spectra of a kind one is already familiar with. The surveys, for example, are very efficient in discovering quasars with redshifts 2 to 3, because this is where Lyman-α, the strongest line in the spectrum, is most readily detectable. Obviously these surveys will never detect any BL Lac type of objects. Such objects cannot easily be found in surveys using colour selection either, because the continuum spectra of BL Lac objects tend to be flat in the optical region and it is difficult to distinguish them using an UV excess criterion.

Here I want to make a few comments on the X-ray surveys. Apart from the deep Einstein surveys of various regions of the sky, there are the intermediate flux serendipitous surveys (*e.g.* Maccacaro *et al.* 1982), which consist of complete samples of sources discovered accidentally in the fields of stars and other objects that were the targets of pointed Einstein observations. The optical identifications of the surveys are not yet complete, and I think it is fair to say that proposed identifications are not always very secure. The proportion of galactic stars seems to be rather high in the deep surveys and that is not very interesting from the point of view of extragalactic astronomy. The basic result from the intermediate surveys is that almost all the sources are identified and there are hardly any empty fields. Roughly speaking, about 25 per cent of the serendipitous sources are stars, 50 to 70 per cent are active galactic nuclei, and approximately 15 per cent are clusters of galaxies. Surprisingly, out of a total of about 60 sources from two serendipitous surveys, one from Berkeley and the other a collaborative effort between CFA and Steward Observatory, there has been only one BL Lac object (Stocke *et al.* 1982). It perhaps tells us something about the evolution of their luminosity functions or could be something else.

3. Importance of studying same objects in different spectral windows

It is possible to make many deductions about sources found in radio surveys by seeing them in the optical and in the infrared region. Likewise a lot can be learnt about sources found in optical surveys by studying them in the radio and X-ray region.

Let me begin with radio sources. Radio surveys have been important in the discovery of quasars, in the realization that galaxies and galactic nuclei can be very strong radio sources, and somewhat later in the recognition that as far as their optical properties are concerned, there is a distinction between BL Lac objects and the other active galaxies.

3.1 *Empty Fields in Radio*

I think it is fair to say that one would have had great difficulty in recognizing from radio surveys alone, that there were separate categories of objects involved. Broadly speaking, one would have had resolved sources and unresolved sources. Unless they are optically identified, little can be understood of their chemical composition *etc.* When the radio sources do not seem to have any optical (or IR or X-ray) counterpart down to the limit of the stellar surveys, they constitute what are called empty fields. Over the last few years, our concept of empty fields has changed drastically. For example, 3C quasars when discovered were basically radio sources. Later on many of them were optically identified with stellar-looking objects. When their number distribution is plotted against their optical magnitudes, a peak is found to occur at around the 18th magnitude and then the distribution falls off. It implies two things. The radio power and the optical power are somehow correlated. Secondly, a strongly emitting radio source may not contain sufficient amount of visible matter in it. It may or may not even emit in the IR or X-rays. Over the last two years or so Rieke and his collaborators have been observing empty fields in the IR (mainly at 2.2 μm), just as Gunn, Longair and others have done in the optical. In the optical it has been possible in many cases to find objects as faint as the 24th magnitude associated with the empty field radio sources (*e.g.* Gunn *et al.* 1981; Peacock *et al.* 1981). IR observations at 2.2 μm indicate (*e.g.* Rieke *et al.* 1979, 1982) a success rate of nearly 100 per cent in the case of flat spectrum sources selected from 5 GHz surveys. Some of these empty fields were actually detected at relatively bright flux levels.

The results are the same in the case of steep-spectrum sources from the Jodrell Bank survey at 966 MHz that are classified as empty fields from the Palomar Sky Survey. About 95 per cent of these sources were detected in the IR (Lebofsky, Rieke & Walsh 1983). When the IR results are coupled with the optical searches, one succeeds in identifying very faint objects having optical magnitudes in the range 21–24 and occasionally a little fainter. In a few cases objects have been detected down to the 19th magnitude in the K band. This large magnitude difference between the optical and the IR counterparts of the same sources compels us to categorize them with very steep IR-to-optical spectra. Such objects are very red, and even if they are bright they would not be detected in any of the standard optical surveys.

3.2 *Average Spectral Slope over a Wide Range of Wavelengths*

In Fig. 1, the flux-density measurements of some classical Seyferts and a quasar are shown over the whole frequency range from the radio through optical to the X-ray

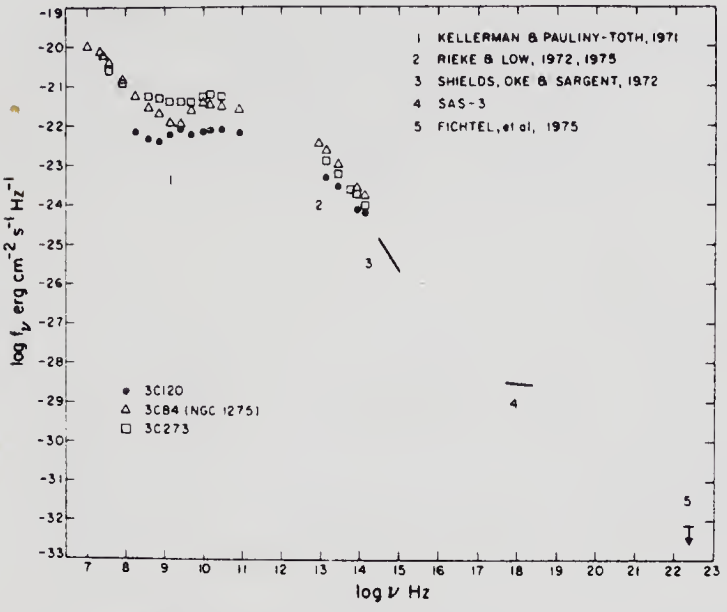

Figure 1. Composite spectra of some sources (from Giacconi 1978).

region. The exploration on the frequency scale has remained highly incomplete. It is seen that by and large all the classical sources lie on a line $f(\nu) \propto \nu^{-1}$ provided we join the distant islands on the frequency scale by straight lines. Scaled with the radio fluxes, the optical fluxes of the empty field sources lie far below this line, and what the IR studies of these objects show is that the IR fluxes lie right where they should on the ν^{-1} line. The same is true for the BL Lacs, a rough sketch of the flux behaviour of 0716 + 71 is shown in Fig. 2. It seems to me that everywhere that we care to look along the ν^{-1} line, the local slope is different from -1. In the radio we have flat, inverted and steep spectra; we have just recognized that there is a class of sources with very steep spectra between the IR and optical regions, and in the X-ray region it is routine to reduce data with slopes of -0.4 or -0.5. So nowhere that we can look in detail does the slope follow the overall slope of -1 between two, three or at most four islands.

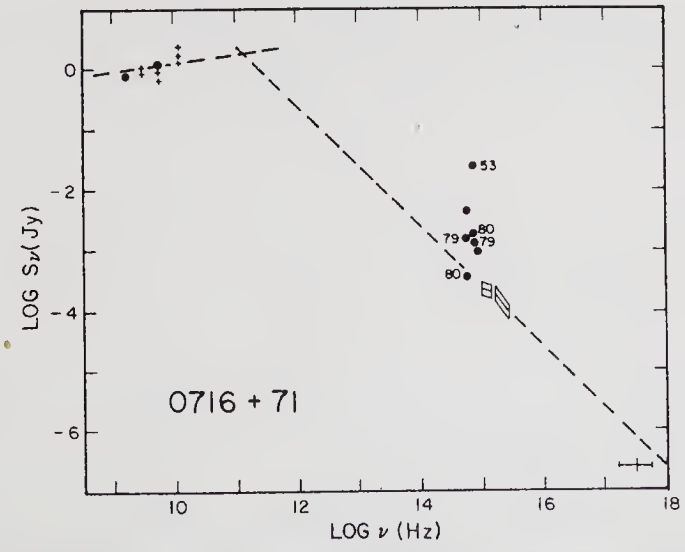

Figure 2. Spectrum of BL Lac object 0716 + 71 (from Biermann *et al.* 1981).

Why does the slope change locally just at the places we happen to look? Or, on the other hand, is the spectrum extremely complex? If we look into regions of the spectrum which have hitherto remained inaccessible, it might turn out that the spectra there too are very complex—for example, in the far infrared (FIR). One therefore has to be careful about fitting beautiful curves between known regions of the spectrum.

3.3 *Radio Observations of Optically Selected QSOs*

I mentioned empty fields in radio surveys and the distribution of optical and radio magnitudes of radio-selected quasars. It is also interesting to begin with optically selected quasars and find what the radio properties of these are. When this is done for the two brightest samples, one a spectral-line survey, namely the MCS survey, and the other, the PG survey based on the colour criterion, it is found in both cases that the number of quasars that are radio sources is rather low—only about 10–20 per cent are what I would call reasonably strong radio sources. The only meaningful way of defining 'reasonably strong radio sources' is through the distribution of their observed radio fluxes.

Fig. 3 is a schematic plot of radio fluxes (on a logarithmic scale) on the X-axis and the number of sources found in fixed logarithmic intervals of flux on the Y-axis. A strong peak is seen at about 1 Jy. There are few sources at low flux levels and there is a cutoff flux which depends on the sensitivity of the instrument used, and the observing time spent. The cutoff in the observed flux occurs at $\sim$ 1 mJy. The curve in Fig. 3 implies that the range of radio flux observed in optically selected quasars is comparable to the range of optical flux. When a radio survey is conducted only of the optically selected PG sample of bright quasars, one or two really bright objects like 3C 273 are found. On the other hand, the MCS sample of optical quasars is fainter by a factor of 2 or 3 and is over a relatively restricted area of the sky. It therefore does not have enough sources for the superbright objects like 3C 273 to be picked up. Nevertheless it is found that the ratio of radio fluxes to optical fluxes is the same.

3.4 *Relevance to Beaming Hypothesis*

This approach of examining the distribution of observed radio and optical fluxes tells us that for some reason the radio and optical output of the compact part of the sources

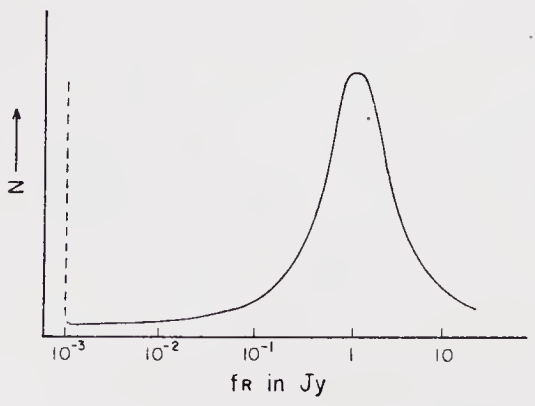

Figure 3. A schematic plot of the distribution of radio flux density for optically selected QSOs.

are very closely related. The approach also tells us something about the beaming hypothesis. If it is assumed that the radio fluxes in the compact components of strong radio sources are beamed because of ejection at relativistic velocities in the direction of the observer (*e.g.* Scheuer & Readhead 1979) then the fluxes of those sources that are not beamed in the direction of the observer are known as well. The nature of that distribution is expected to be linear as shown by dot-dashed lines in Fig. 4 for two different assumptions regarding the nature of the jets (Strittmatter *et al.* 1980). Now if the relativistic factor is only as large as 1.3 or 1.4, then nothing could be gained at those places where strong beaming effects are desired, as the curve T1 drops sharply above 1 Jy. If factors of 2 to 5 are chosen, on the other hand then the character of the distribution (see curve T2) does not agree with the observed distributions shown by the solid and dashed lines in Fig. 4. So one has to either assume that the optical flux is beamed too by the same amount or give up beaming as a general characteristic of radio sources that distinguishes between radio-quiet and radio-loud quasars. It is not necessary to give up the possibility of beaming occurring at all, but as a general characteristic it has to be rejected. Therefore, the radio fluxes cannot in general be dominated by beaming effects.

One way out is to assume that the optical flux is dominated by beaming effects too, but I do not see how that can be true because I do not believe that the thermal line emission can be beamed in the same way. Beaming of the optical continuum would require that where it occurred, the equivalent width of optical emission lines be smaller than where it did not occur and such a correlation is not seen. There is no distinction in

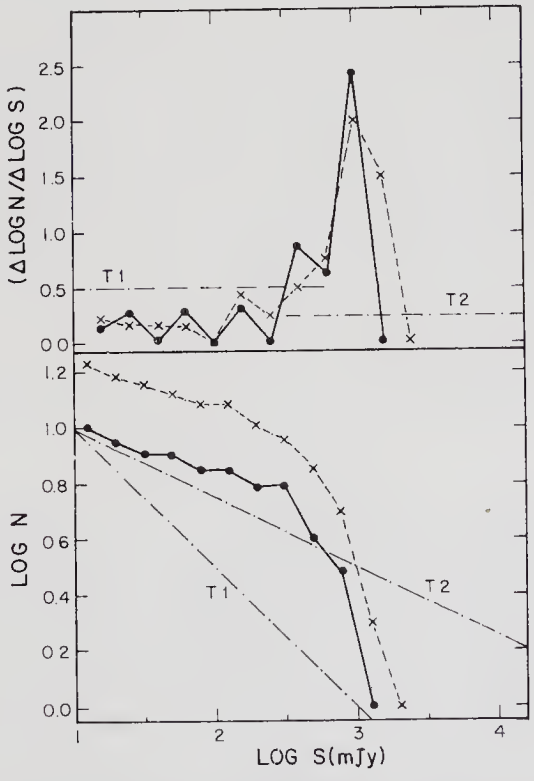

Figure 4. Differential (top) and integral (bottom) distributions of flux density of MCS quasars (from Strittmatter *et al.* 1980). T1 and T2 correspond to the expected distributions on the beaming hypothesis for different model parameters.

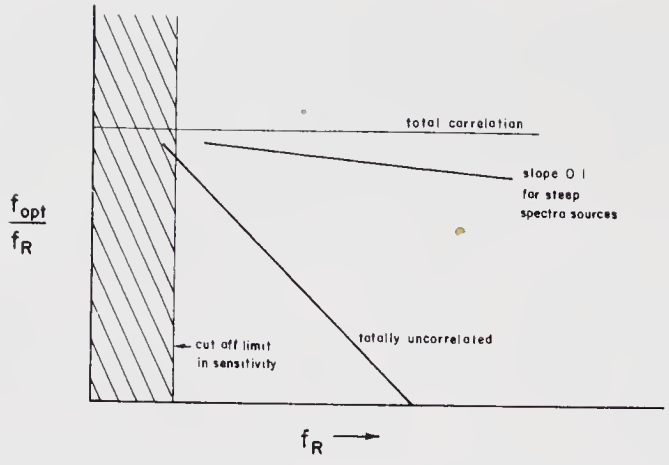

Figure 5. A schematic plot of radio flux density (f_R) against the ratio of optical to radio flux density, f_{opt}/f_R, for QSOs.

broad terms between the emission-line equivalent widths for those quasars that are detected as radio sources and those that are not.

One can in fact try to look for correlations directly between radio and optical brightnesses. Recently, in collaboration with Hans Steppe at Bonn, I took all the 5 GHz sources stronger than 0.25 Jy, that were also identified with quasars, and compared their 6 cm radio and optical flux densities and their ratios. Fig. 5 is a schematic plot of radio flux density (f_R) as the independent variable and the ratio of optical flux density to radio flux density (f_{opt}/f_R) as the dependent variable. Now if there is a correlation, a flat distribution will be obtained and if the radio and optical fluxes are totally uncorrelated a slope of -1 will be seen. There is of course a cutoff in the optical data at the 20th magnitude. This introduces a bias in defining the slope. But it is possible to bin the data and ask what is the distribution of upper bounds in each of the bins. If that is done, a slope for the upper bounds is obtained that is closer to 0 than -1. If a similar plot is made for steep spectrum sources, the ones that are by inference optically thin, curiously enough a slope of -0.1 is obtained, which is essentially flat. So again, from a direct analysis we arrive at the same inference as has been made from the radio study of optical quasars.

4. Continuum emission and polarization properties

4.1 *Seyfert Galaxies*

Seyfert galaxies are a rather heterogeneous group, with a variety of galaxies grouped under the same name. A crude definition of Seyferts is that these are galaxies with bright nuclei and strong emission lines. This group is further divided into two classes. Type 1 have broad permitted emission lines, tens of thousands of kilometres per second in width, but narrower forbidden lines with widths of thousands of kilometres per second. Type 2 Seyferts have sharper lines than type 1—the permitted lines are not very much broader than the forbidden lines. But like in all definitions we then define new categories like type 1.5, type 2.5 *etc.* (see Weedman 1977 for a review). It is possible to define these categories with a specific feature like the line spectrum, but so many other characteristics like the origin of radiation at various wavelengths just across optical and

IR are so different from object to object that one wonders what meaning these definitions have.

Seyfert galaxies are a class of objects that emit primarily in the infrared. Fig. 6 shows the optical and infrared continua of a number of Seyferts and Seyfert-like galaxies from Rieke (1978). Some of the spectra are smooth, while some of them, as in Mkn 231 show clear sharp spectral features. For many years it was fashionable to interpret the IR

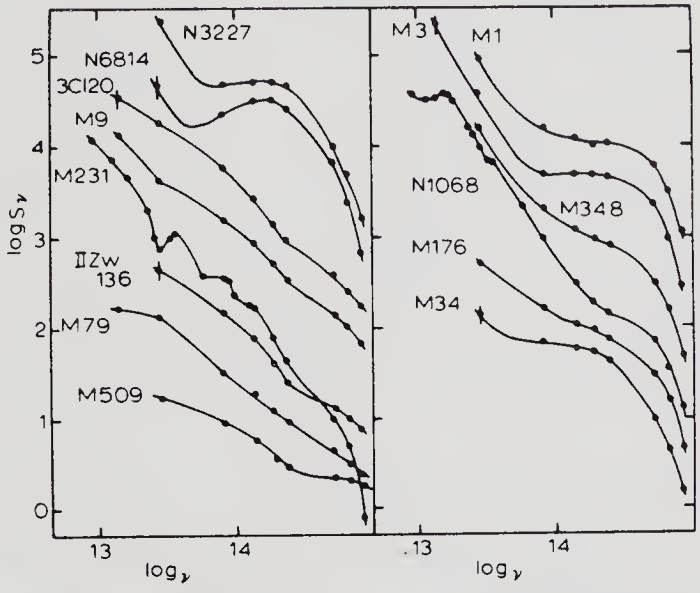

Figure 6. Continuum optical–IR spectra of some Seyferts and Seyfert-like galaxies (from Rieke 1978).

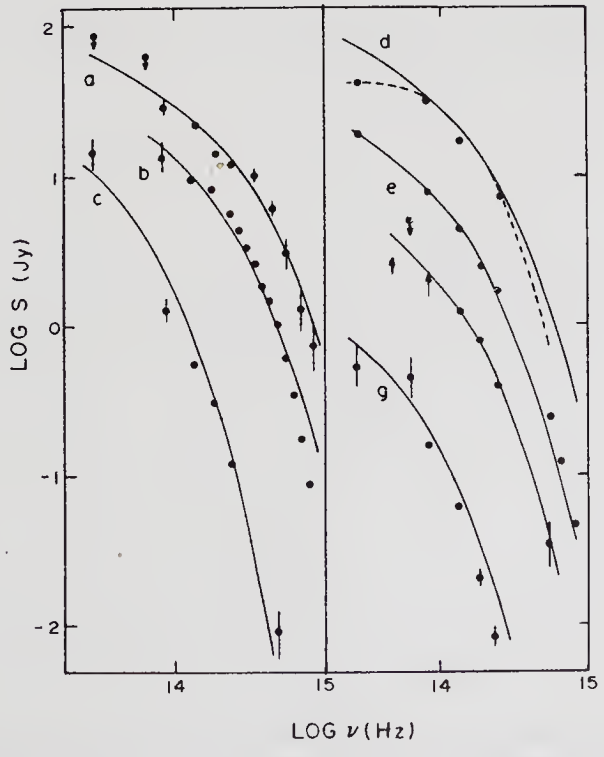

Figure 7. Optical–IR spectra of several nonthermal sources with sharp spectral cutoffs. Solid lines are theoretical synchrotron spectra (from Rieke, Lebofsky & Wisniewski 1982).

continuum as due to some incoherent synchrotron (nonthermal) process. The reason is explained in Fig. 7, which shows the optical and IR continua of a number of nonthermal radio sources that truly emit incoherent synchrotron radiation. Such continua tend to be very steep towards the optical and are sufficiently flat in the IR. Data seem to fit well with emission due to synchrotron mechanism with a single magnetic field and single electron-energy spectrum with an abrupt cutoff above a certain energy (Rieke, Lebofsky & Wisniewski 1982). One can however adjust the curvature and the steepness of the spectrum by changing the above parameters.

In recent years a lot has been studied of the optical and IR continua of Seyfert galaxies, their polarization, variability, line spectra *etc.* There seems to be a wide range of properties. One of the characteristics is made evident in Fig. 6. A good fit to the observations cannot be obtained for non-thermal synchrotron emission. Apparently there are two components—one optical and the other infrared. They are present in various proportions. It is now believed that in the IR as well as the FIR, the emission is likely to be thermal in nature, basically a reradiation by the dust component. The optical component in some cases is believed to be due to nonthermal processes. But it might as well come from a stellar population. Also, some absorption features are present which could be ascribed to dust particles (see Figs 8 and 9).

How can one tell the various contributions apart? Obviously the nonthermal spectrum is expected to be smooth and polarized. In the reradiation from dust one might hope to see certain spectral characteristics. One would also hope to see the temperature of the dust correlated in some way with the spatial extent over which the dust extends. Stars one would expect to identify directly from transition features in the spectrum, and scattering brings in polarization but of a different kind from that expected from synchrotron radiation. All these features are in fact found in one Seyfert galaxy or another.

The question of dust and the observation of polarization in one or two Seyfert galaxies (Angel *et al.* 1976) has prompted Martin *et al.* (1983) to carry out a survey of

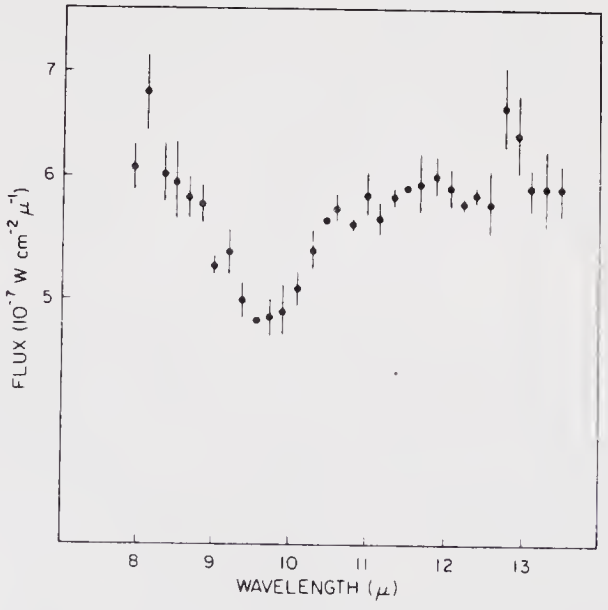

Figure 8. The 10 μm silicate absorption band in NGC 1068 (from Kleinmann, Gillet & Wright 1976).

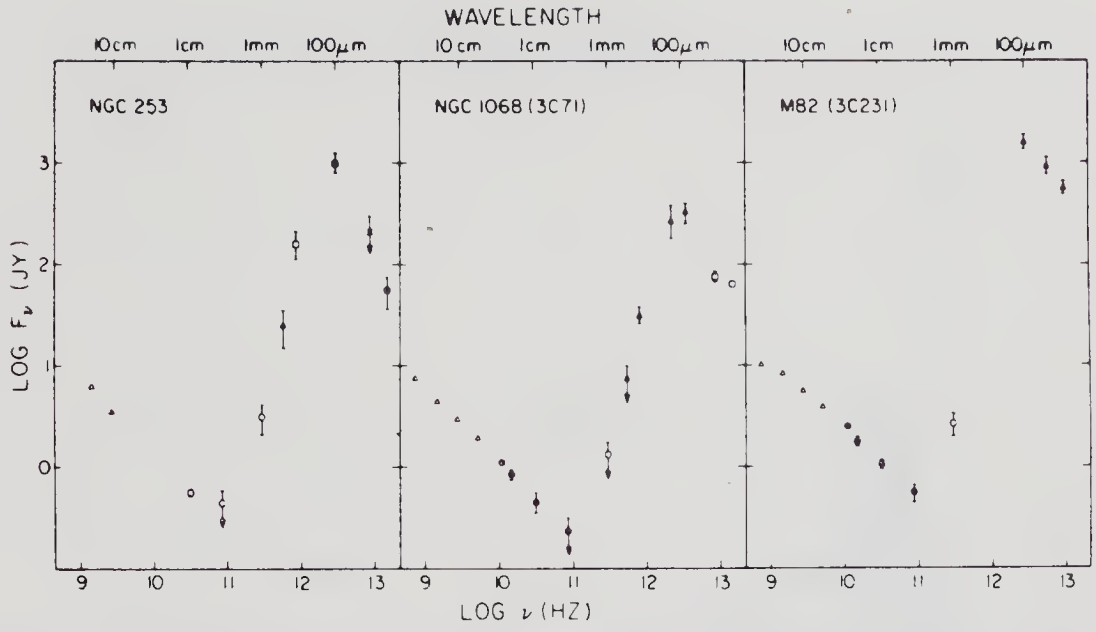

Figure 9. The millimetre-wave spectrum showing thermal reradiation (from Elias *et al.* 1978).

polarization in Seyferts. Their sample has 99 Seyferts, and amongst these only 14 show high polarization ($\gtrsim 2.5$ per cent), of which 10 are of Type 1 and 4 of Type 2. Multicolour polarimetry indicates that in most highly polarized Seyferts the polarization is much stronger in the blue than in the red, and the angle of polarization stays fairly constant with wavelength. If an observation is made with sufficient resolution, it is found that the lines and the continuum are polarized to the same degree. All this speaks very much for the polarization being due to scattering by dust, and this is of course consistent with the feeling that a large fraction of the IR emission is reprocessed radiation being emitted by the dust which also produces polarization.

Let us go through a few specific cases now. NGC 1068 is a particularly well-studied case. The degree of polarization is proportional to λ^{-3}, as one would expect from dust. The permitted lines are polarized but the forbidden lines are not. So there is already some kind of variation here. As one gets into the IR there is some evidence that the polarization does not continue to go down. There may be a residual component of polarization in the IR which is not due to scattering. There are several components in the nucleus of NGC 1068—a broad component that looks like reradiation by dust and a 2 μm bump which appears to come from a substantially smaller knot that has a residual polarization and also a continuum spectrum. A recent study by McCarthy *et al.* (1982) seems to show that it is unresolved to the limit that they can reach ($\sim$ 0.2 arcsec). This does not rule out thermal reradiation by hotter dust, with the temperature well-defined because of the bump at 2 μm, but this is not a very comfortable situation.

In NGC 1068 there is a nucleus that is quite clearly defined and there is a shoulder of lower brightness radiation. As one moves out one comes to what looks like a jet, the arms of a spiral galaxy. The nucleus is strongly dominated in the spectrum by the relatively broad emission lines. But as one goes out into the shoulder, the strengths of the emission lines drop. I do not know how the continuum behaves as one moves out of the nucleus.

At the top of Fig. 10 is shown the continuum spectrum with the emission lines, in the

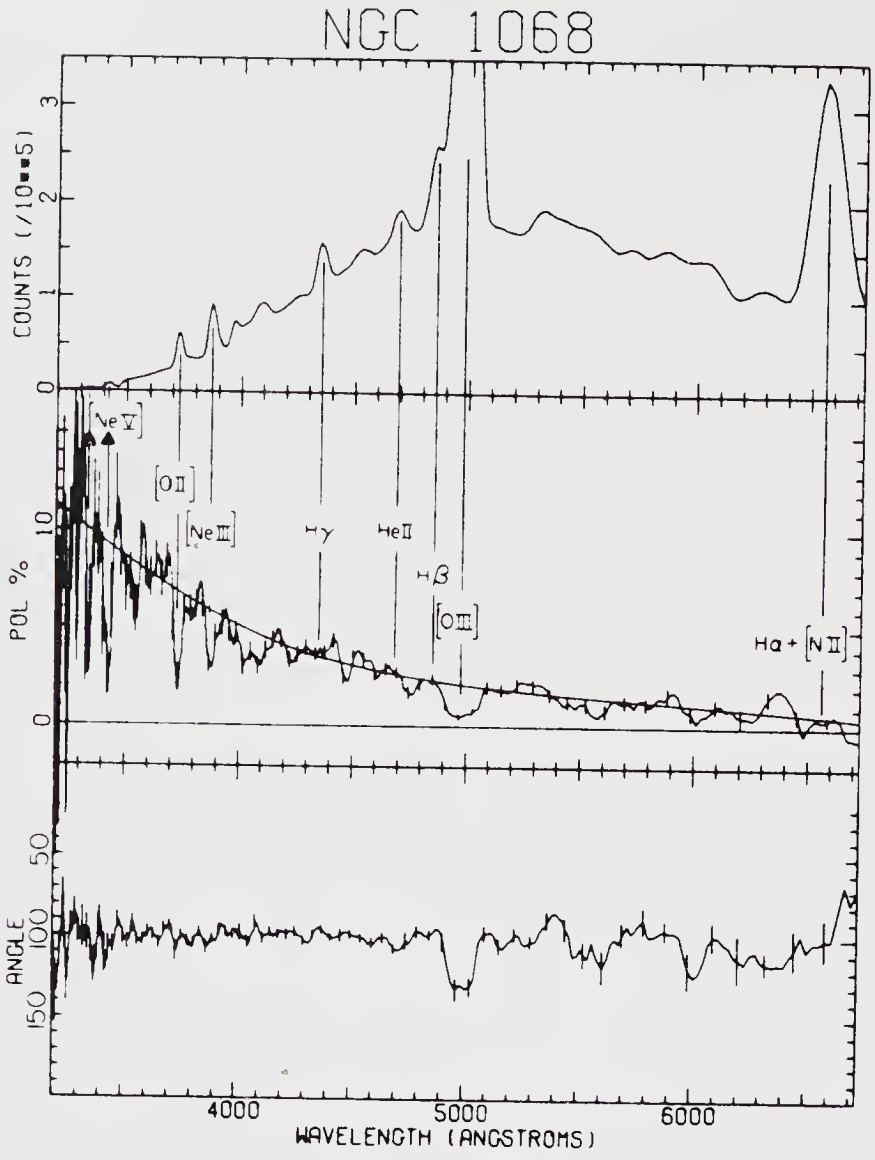

Figure 10. Spectropolarimetric data for NGC 1068 (from Angel *et al.* 1976).

middle is the polarization as a function of wavelength and at the bottom the polarization angle. The smooth line drawn in the diagram in the middle is a $1/\lambda^3$ curve showing the goodness of fit to scattering from dust. The strong Hγ line does not seem to produce any significant bump in the polarization whereas at the position of the [O III] forbidden line, the polarization drops significantly. This is the origin of the statement that the degree of polarization is the same in the continuum and permitted lines. One can also get some estimate of reddening in the permitted and forbidden lines and it appears that whatever is causing the reddening is the same for both types. How all this matches together is still rather uncertain. In the part of the diagram showing the angle of polarization as a function of λ, the only significant variations are where the forbidden lines occur.

In Fig. 11 is shown the spectrum of the nucleus of NGC 1068 in the region of H and K lines. Seen sharply are the two neon lines λ 3869 and 3968 Å. There is apparently a very strong absorption feature between them. This feature is associated with the K line of calcium. But the H line of calcium is seen here in emission. In the spectrum of the

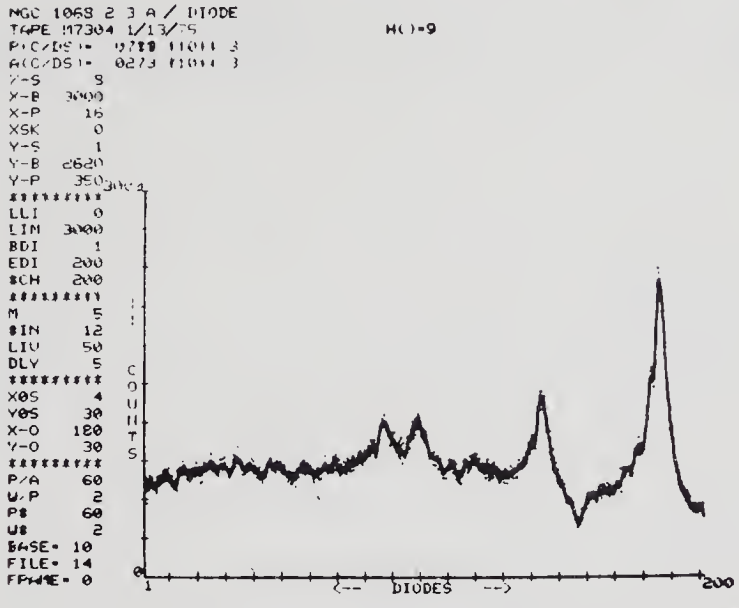

Figure 11. Optical spectrum of the nucleus of NGC 1068 in the region of the H and K lines.

nucleus the two emission lines due to sulphur disappear almost completely. One is left with a spectrum that looks like that of A or F stars, with strong broad H lines, *etc.* Now in the nucleus all the hydrogen lines and the H line of calcium are swamped by the emission lines but the K line is not. So one can compare the line profile here with that in the shoulder and ask how different they are. They are not very different at all, and one can estimate that any additional continuum that one wants to add in here has got to be less than 10 per cent. In the optical, I would say that in the nucleus of this particular Seyfert galaxy, one is clearly looking at a star-like spectrum and it is indistinguishable from what one presumes to be due to late and early types. That is not true for all Seyferts, but it is true in general that Seyfert galaxies seem to have fairly early type underlying spectra and generally this is associated with spirals.

In Fig. 12 are shown the spectrum and polarization plots for NGC 4151. What can be seen here is that wherever there is an emission line in the spectrum, the polarization goes down. This is a case where there is a continuum that is not totally independent of wavelength in its polarization. It looks somewhat interstellar, but is not peaked enough for that. The conclusion is that in addition to an interstellar component of polarization there is probably a nonthermal component of about 1 per cent and whenever the emission lines appear, polarization goes soaring down.

NGC 4151 is an exception to the dust scattering rule—its polarization is weak, variable; the continuum flux is variable, the angle of polarization is not varying and it is a case where—in the optical—one may be seeing a nonthermal component.

The other case that is special is NGC 1275. It is strongly polarized. The stellar background seems to be an elliptical galaxy with late-type stars, which is again strange. The angle of polarization varies strongly, and in the lines the polarization is weaker. This is a very good case for seeing directly a nonthermal component. The VLBI structure has a position angle of 170° compared to the 100–150° for optical polarization.

Obviously the Seyfert galaxies are a very heterogeneous group, the unifying feature being the definition which is purely optical and spectroscopic. Some show evidence for

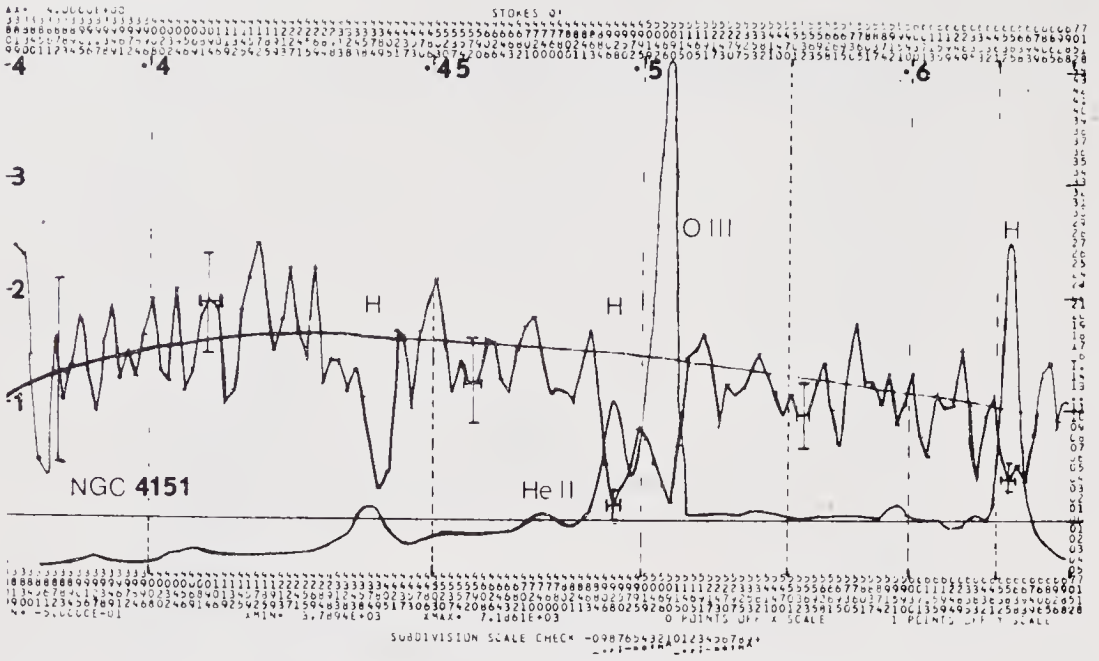

Figure 12. Spectropolarimetric data for NGC 4151.

a nonthermal continuum in the optical and IR, others seem almost totally to have thermal or stellar radiation. Generally the Seyfert galaxies are strong X-ray sources. The feeling therefore is that there is probably some kind of a similar engine in the middle of these things, but that the engine is well masked by thermal processes with the radiation being absorbed and re-emitted.

4.2 *BL Lac Objects*

The definition of BL Lac objects has changed over the years, but basically these are objects with either no lines in their spectrum or very weak ones, and polarized continuum. Nearly all BL Lac objects have been found because they are strong radio sources. This situation has changed only a little bit with the advent of the X-ray surveys. It is very difficult to do optical surveys for these objects based on any colour criterion because their colour is basically similar to that of most stars. The X-ray surveys have produced one BL Lac object and two have been found from the PG survey (apparently anomalous cases). These are X-ray sources but their radio fluxes are of the order of 10 mJy and they would not have appeared in any strong radio source catalogue.

The optical spectra of the objects are steeper (mean spectral index of about 2 in the optical region) than an average quasar spectrum and that is why they look redder. The spectral indices can range from about 1 to 3 or 4. Generally the IR spectrum shows a flattening closer to ν^{-1}, although the range over which the measurements are made is not sufficient to establish that one really has a power law spectrum. There is a wealth of IR data because of the steep rise from the optical to the IR, with the IR fluxes being high compared to the sensitivity limit attainable. Sometimes there are outbursts in the objects, and most of them are variable, with timescales as short as about 10 hours. The variability is such that changes of ~ 1 mag are not uncommon, with changes of 3–3½ mag being occasionally observed. Polarization is strong—it is a part of the

definition—and values from 0 to 40 per cent have been measured, with the typical value being of the order of 10 per cent.

The angles of polarization are variable, but this depends on the source. There are some without any favoured direction, any direction of polarization being equally probable at any time. BL Lac is an example where the direction of polarization is highly variable, while OJ 287 is one in which the angle does not vary at all. Most BL Lac type of objects are flat-spectrum sources in the radio band, showing variations in the radio flux. At least two show double radio structure and little variation. The double sources also seem to be relatively constant in their optical output.

In general it is found that the polarization is independent of wavelength, though there are exceptions which show a slight dependence on wavelength, particularly in the angle. When the object varies in brightness, there is no obvious connection between how bright the object is and how polarized it is. As the brightness goes up and down, the spectrum as a general rule does not change, though there are some cases in which a change has been observed. In 0235 + 164 the UV part of the spectrum has been seen to change during an outburst and revert to its original form afterwards. As the spectrum goes up there is a tendency for the longer λ to lag behind so that what one sees is almost an inversion. The projection of the steep spectrum down towards the X-ray region would lead one to undershoot the observed X-ray fluxes by a factor of order 100, which is much more than the normal amplitude of variations in these objects.

There are weak emission lines seen in a few BL Lac sources. To me they look like the narrow emission lines that are seen in galaxies in which the BL Lac objects reside. Several of the low-powered ones and the nearer ones clearly reside in elliptical galaxies, in contrast to Seyferts which tend to be spirals. It should be noted here that NGC 1275 has polarization properties nearly identical to those of BL Lac objects, and it also is an elliptical galaxy. There is certainly no evidence for any broad emission lines of any strength at all in BL Lac objects. Even when the objects are in a very faint stage in the continuum, there is no evidence for any emission lines in the spectrum. If any lines, particularly broad ones, are present at all, they must be very weak.

In my opinion, BL Lac objects do not have lines, or strong lines, because there is not much matter around them. Is this connected with the fact that when an underlying galaxy is visible, it is elliptical, and ellipticals are poor in gas content because the gas has gone into the stars, or black holes, or has been driven out of the galaxy? Certainly the elliptical galaxies had to have gas at sometime, and certainly quasars do have gas, and so I could say that BL Lac objects are engines that are still firing when the gas supply is removed, but I am sure there are many arguments against this point of view.

4.3 *Quasars*

QSOs have broad strong permitted lines sometimes, and very frequently forbidden lines. There are far fewer IR studies of quasars than of BL Lacs. This is because in quasars the optical spectrum is far flatter and for a given optical brightness the IR brightness is much weaker than in BL Lacs. Where they can be studied there are structures, but one is projecting up not too badly on a ν^{-1} spectrum. The optical region however shows very frequently other components. There is a range of optical indices with a mean of order unity (*e.g.* Richstone & Schmidt 1980). Basically the average quasar and average BL Lac optical spectral indices differ by unity. The range of spectral

indices actually goes right up to 6. These high values are very rare and it is not clear what they are due to. One cannot even rule out the possibility that some kind of reddening nearby has occurred in such cases.

There is a large class of quasars which have a deviation in the curve towards UV that is variously called a UV excess, a 3000 Å feature or a blue bump. It is not known conclusively what the bump is due to (see *e.g.* Grandi 1982). There has been some recent work by Puetter from San Diego to use the IUE to observe in the UV a small sample of quasars with very prominent blue excess. The word bump would be a misnomer for these objects. The excess appears to be more like a change in the continuum index, a hardening in the spectrum that seems to project essentially over the entire IUE range which is up to about 1200 Å. In many cases it does not seem to be a confined feature, which is what the original discussion was centred around. We could again be seeing a very heterogeneous group. By and large, objects which show this excess appear to be of low polarization type and those which do not, appear to be of higher polarization type. This is a very preliminary result but it does seem to hold up.

Samples of quasars have been surveyed for optical polarization (*e.g.* Stockman 1978; Moore & Stockman 1981). The histogram of observed polarization *vs* number is shown in Fig. 13. A clearly bimodal distribution is observed—quasars are either highly polarized (HPQs), or have significantly low polarization, of order of 1 or 2 per cent or less (LPQs). The origin of this bimodality is not known but it obviously has some connection with BL Lac objects.

Attempts have generally been made to observe polarization properties of quasars that have inverted spectra. Among these HPQs are the well-known sources 3C 279, 3C 345, 3C 446 and 3C 454.3. No radio-quiet quasar seems to be an HPQ, which clearly shows a connection between the optical and the radio. Whether a quasar is an HPQ or not does not seem to depend on its redshift. In the normal state there does not appear to be any obvious difference in the line spectrum of an HPQ and other quasars. But there is a clear distinguishing feature about the spectrum as a whole in that the HPQs tend to have steeper spectra in the continuum like BL Lac objects and vary dramatically in the optical. 3C 446 is a case of this type. The line-spectrum equivalent-width variation of

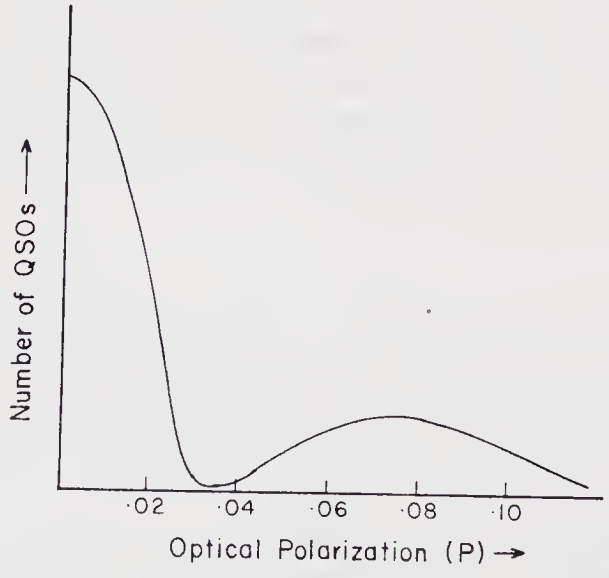

Figure 13. Schematic distribution of the observed optical polarization of QSOs.

3C 446 can be explained by a variation of the continuum alone, with no change in the line intensity. When the flare died away again, as far as I know, there has been no documentation of any subsequent change in the line features. This is a little surprising since the lines seem to stay constant regardless of what the central machine is doing.

Most quasars generally have small polarizations that are not strongly variable. Stockman, Angel & Miley (1979) were able to demonstrate, in my opinion quite conclusively, that if low polarization quasars are radio sources with a double structure, the direction of the axis of the double structure and that of the optical polarization **E** vector are closely correlated. This obviously points to some kind of a connection even though the optical polarization is disappointingly low. The fact that the polarization seems to be closely correlated with something that is a radio or nonthermal event clearly suggests that the radiation in the optical is being reprocessed here.

It is difficult to carry out a clear-cut optical survey for HPQs and BL Lacs, and this has not been done effectively. There may be some connection between these sources and relativistic beaming of the optical continuum radiation. The HPQs and BL Lacs seem to be related in their polarization properties. There is clearly a distinction between these and the LPQs. The two are easily separable. The continuum polarization distribution is clearly peaked in two places. The same is true of the line-intensity distribution in HPQs and BL Lacs. There does not seem to be a continuum of equivalent widths of lines between the HPQs and BL Lacs. Such a continuum is expected if the objects had basically the same property, with the BL Lacs simply having a higher level of continuum relative to the lines. I do not know what the explanation of all this is. It seems to me that in quasars there is gaseous material present, and there is some kind of an instability so that when the density of the material drops below a certain level, either the material gets blasted away or no longer gets put into the region where it can be illuminated. But there is another instability switch in there which at some point gives a bimodal distribution in the polarization property as well.

5. Emission-line properties

The line spectra of both Seyfert galaxies and quasars are remarkably similar in character, though obviously not identical. We come across a wide range of luminosity while going from quasars to the Seyferts. One intuitively feels that some correspondence between the luminosity and the size of the emission-line regions should exist. Most of the theoretical models that account for the origin of line emissions and the total luminosity do not spell out the exact cause of such a relationship but merely deduce it implicitly. These models are primarily invented to fit the existing data well and less attention has been paid to discover the overall guiding principle that reveals the underlying physics.

Another similarity between the Seyferts and the QSOs is that both show clear evidence for the so-called blue bump in their optical spectra. Normally the bump occurs somewhere around 3000 Å, but the details vary from object to object.

When it comes to the physical modelling of these objects, one finds that it is almost impossible to accommodate sufficient amount of dust particles in the emission-line regions of quasars. Here lies the main difference with the Seyferts which unlike the quasars must contain significant amount of dust in them. The emission-line regions of QSOs are required to be so hot that nothing can solidify in order to form dust particles,

whereas the Seyferts, being generally much less luminous, can host a lot of them. In fact, certain spectral features in the Seyferts are ascribed to the dust component only. Quasars, on the other hand, hardly show any evidence for exclusively dust-born features, for example, the noted 2200 Å feature in absorption. The basic goal of modelling these objects remains to interpret the emission lines and the spectrum with regard to their intensities and line profiles, and to describe the physical conditions, the chemical compositions and the dynamics of the entire region.

5.1 *A Few Specific Cases*

Before I proceed to modelling, I will describe the line features of some selected objects belonging to the two classes. Fig. 14 shows the optical spectrum of Mk 509, a typical type 1 Seyfert galaxy. The spectrum shows a number of narrow permitted lines and broad forbidden lines. The strange bump that appears at the left end of the spectrum is the aforementioned blue bump, though not quite at 3000 Å. It seems to have merged with the Balmer jump here. Table 1 gives an idea of the intensities of various lines, all relative to the intensity of Hβ, in another typical Seyfert galaxy, NGC 4151. The strongest are of course the [O III] forbidden lines.

Fig. 15 shows the optical spectra of a number of low-redshift quasars from Baldwin (1975). It shows the wide range of the forbidden to the permitted line ratios. As we follow the spectra from top to bottom in the figure, the forbidden [O III] 4959, 5007 Å emission lines keep getting stronger relative to the strength of Hα. They are nearly absent in 3C 273 but highly peaked in say, PKS 2135 – 14. If we closely examine the tip of the Hα line for all these quasars, we can further identify a sharp component of that line manifested differently in different quasars. Also noticeable is the blue bump common to all these quasars.

The spectrum of an intermediate-redshift quasar, H 1331 + 170 is shown in Fig. 16. Various recombination lines and forbidden lines of higher ionizations of carbon and oxygen, alongwith the Lα emission, are seen. They are more or less typical of the Seyferts also. The asymmetry of the Lα line is perhaps due to differential absorptions. Fig. 17 shows the spectrum of a high-redshift quasar, OH 471. The Lα and Lβ + O VI

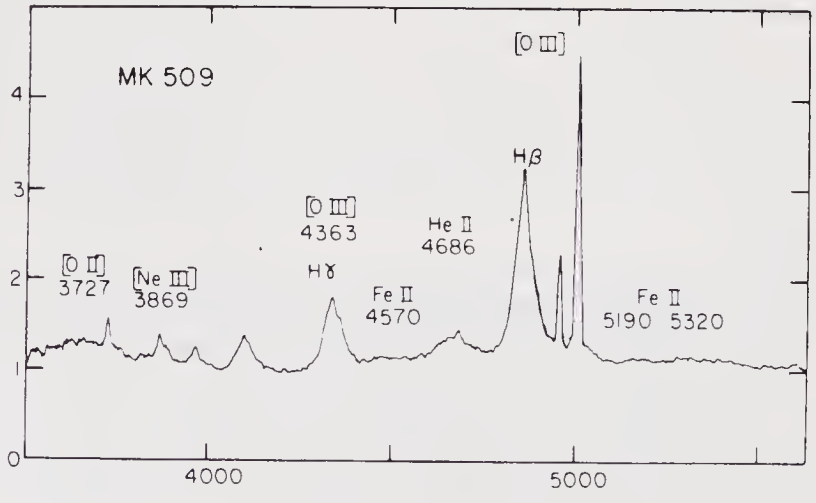

Figure 14. Optical spectrum of Mk 509 (from Osterbrock 1978).

Table 1. Relative line intensities.

Ion	(Å)	NGC 4151 (Omitting wings)
[Ne v]	3346	...
[Ne v]	3426	1.8
[O II]	3727	2.8
[Ne III]	3868	1.6
[Ne III]	3969	...
[S II]	4071	0.45
Hδ	4101	0.28
Hγ	4340	0.39
[O III]	4363	0.39
He I	4471	0.05
He II	4686	0.39
Hβ	4861	1.00
[O III]	4959	3.9
[O III]	5007	11.9
[N I]	5199	...
[Fe XIV]	5303	0.05
[Fe VII]	5720	0.22
[N II]	5755	0.17
He I]	5876	0.22
[Fe VII]	6087	0.39
[O I]	6300	1.00
[O I]	6364	0.22
[Fe X]	6374	0.11
[N II]	6548	0.28
Hα	6563	1.61
[N II]	6583	1.39
[S II]	6716	1.33
[S II]	6731	1.56

lines in this particular quasar are fairly representative of about one-third or half of all high-redshift quasars. Due to self-absorption the spectral flux is practically reduced to zero at still shorter wavelengths.

Table 2 lists a few emission lines that are seen in a typical quasar. The line strengths are indicated along with their wavelengths in a comparative sense. These lines mostly belong to the ultraviolet part of the spectrum, a part that had not been well studied in the context of Seyfert galaxies; but UV data on the Seyferts are now fast becoming available and proving to be quite interesting.

5.2 *Line-Emitting Regions*

The broad-line emitting regions (BLRs) do not emit any forbidden lines in the visible. This implies that the number density of particles in this region is $n_e \gtrsim 10^7$ cm^{-3}. We can also say something about the upper bound to this density. At very high densities, the intercombination lines like C III] are suppressed. Because these intercombination lines are present rather strongly in all quasars, the upper bound on the number density is roughly 10^{10} cm^{-3}. Since the spectral lines are broad, it gives an idea of the velocity

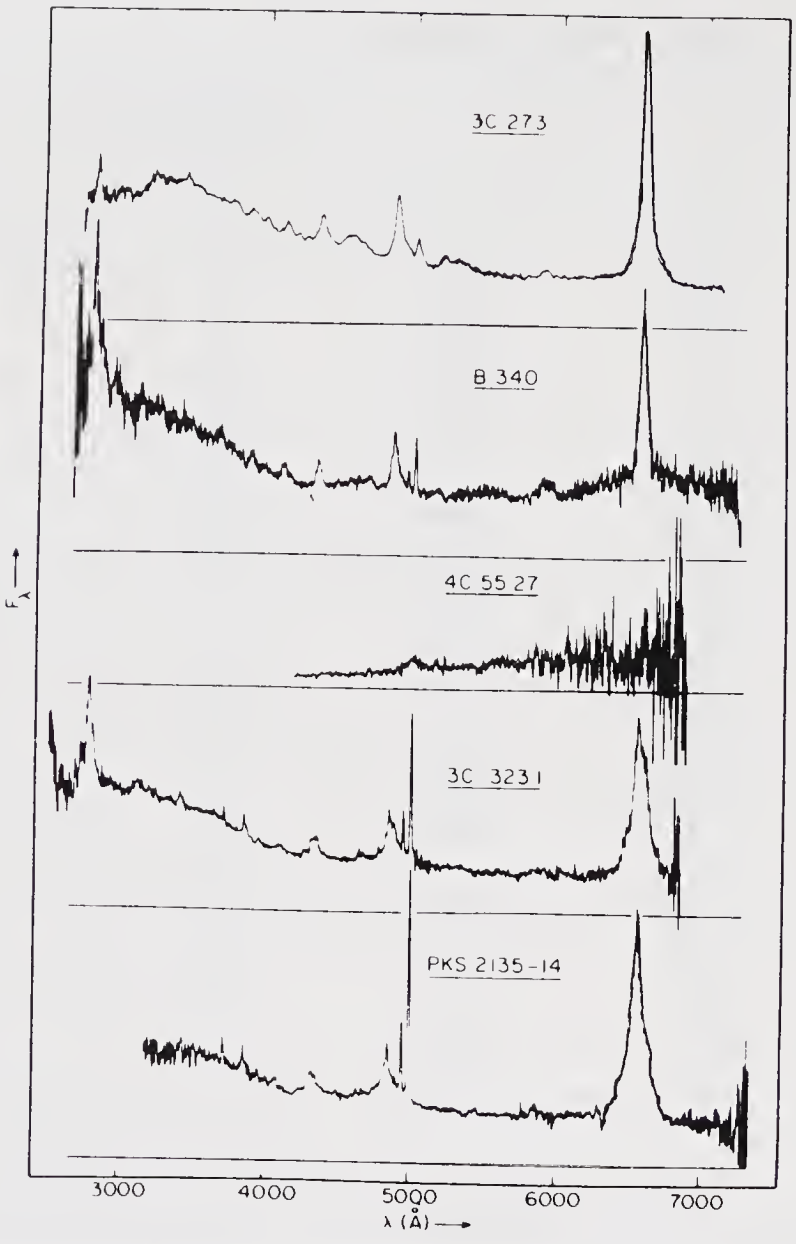

Figure 15. Spectra of some low-redshift QSOs (from Baldwin 1975).

dispersion of the emitting particles in that region. The typical velocities involved are generally higher than 10^4 km s^{-1}.

The narrow-line regions (NLRs) on the other hand are characterized by the presence of forbidden lines, implying $n_e \lesssim 10^7$ cm^{-3}. The velocities are also much lower. Because of the sharp differences in velocities and particle densities, presumably these two regions are physically distinct and separate, rather than being continuous or intermixed. Generally speaking, the size of the BLR in QSO's is roughly ~ 1 pc and that of NLR could be as large as several kpc. For Seyferts, however, both the dimensions are much smaller.

5.3 *An Independent Luminosity Indicator for QSOs*

The intrinsic luminosity of QSOs remains practically indeterminate if we do not accept the cosmological interpretation of QSO redshifts. Many desperate attempts have been

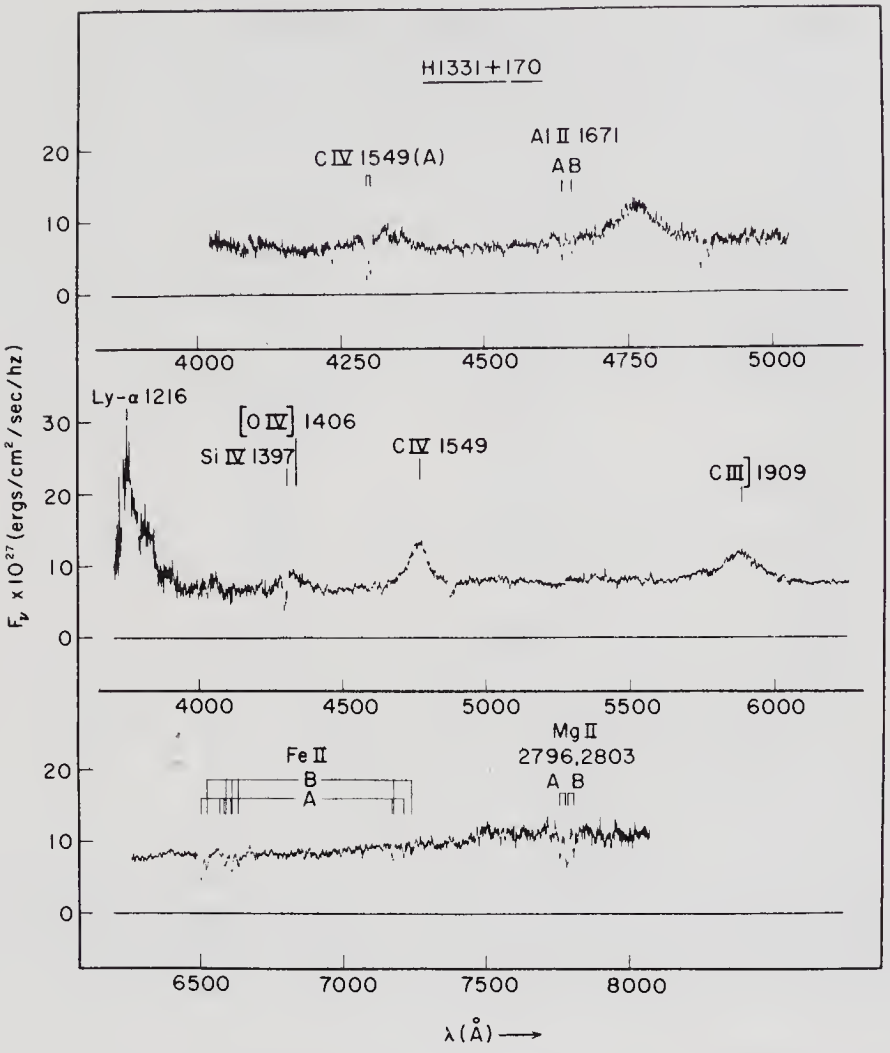

Figure 16. Spectrum of an intermediate-redshift quasar H 1331 + 170 (from Strittmatter *et al.* 1973).

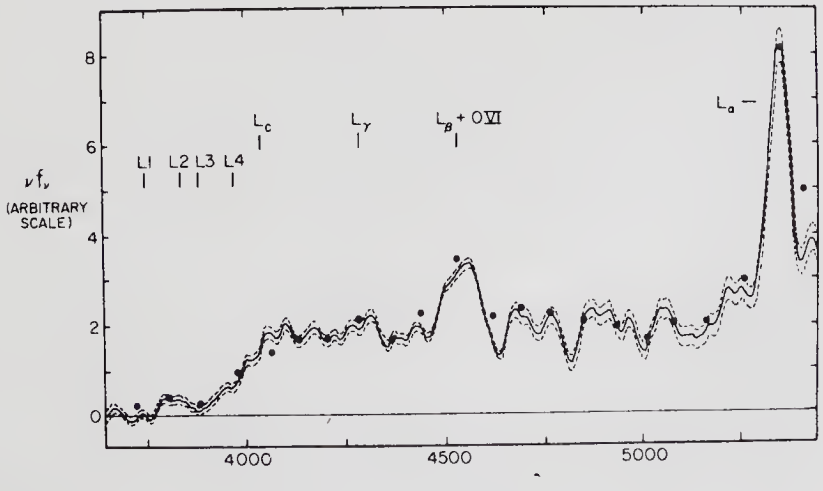

Figure 17. Smoothed spectrum of the high-redshift quasar OH 471 (from Carswell *et al.* 1975).

Table 2. Emission lines seen in a typical QSO.

Wavelength (Å)	Line	Strength*
1026	Lβ	0–M
1034	O VI	...
1216	Lα	S
1240	N V	0–M
1397	Si IV	0–W
1402	[O IV]	...
1549	C IV	S
1640	He II	0–M
1909	C III]	M–S
2798	Mg II	S
3426	[Ne V]	0–W
3727	[O II]	0–W
3869	[Ne III]	0–M
4686	He II	0–M
4861	Hβ	M
5007	[O III]	0–S
5876	He I	0–M
6562	Hα	S

* 0 = absent; W = weak; M = medium; S = strong

made to establish at least one independent luminosity indicator for QSOs, other than the redshift. It seems that Baldwin has got something. He has found (Baldwin 1977a) that the width of the C IV line shows an inverse correlation with the intrinsic luminosity in the continuum around that line (1549 Å). Fig. 18 shows the original plot of Baldwin

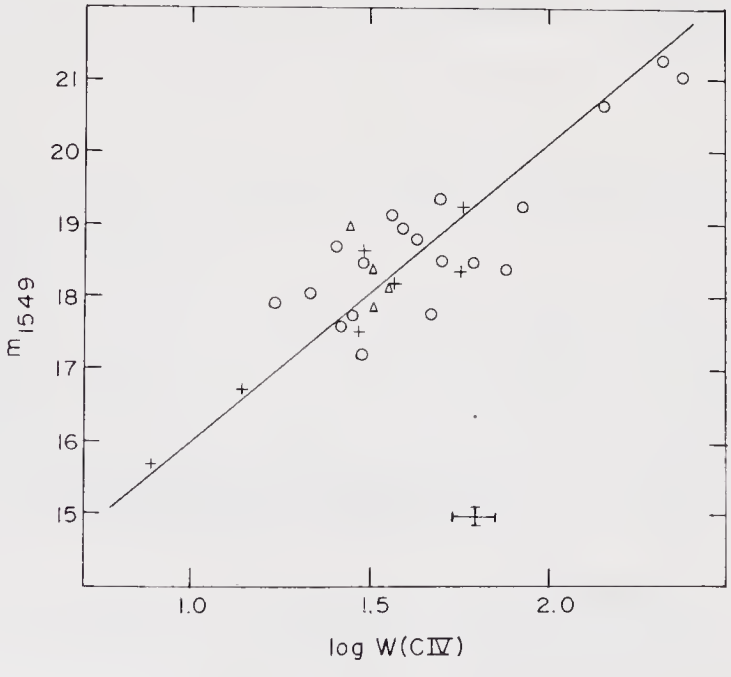

Figure 18. Baldwin's correlation between the width of the C IV line and the luminosity around 1549 Å.

for about 20 QSOs with some additional data. In the last two years, he has made further refinements, but the trend remains more or less the same. The empirical relation between the equivalent width of the C IV line, $W(\text{C IV})$, and the underlying luminosity of the continuum (L_c), is of the form $W(\text{C IV}) \propto L_c^{-2/3}$. There is no ready explanation for this correlation although it clearly provides some clue yet unspelt. Does this relationship hold all the way down to the luminosities of Seyfert galaxies? After a careful study of Seyferts over the last two years, Wampler has found that at the level of the luminosity of Seyfert galaxies, this dependence vanishes and the equivalent widths stay constant, that is, become independent of the intrinsic luminosity. I must mention however that measurement of the emission line widths is often difficult due to competing effects such as absorption.

5.4 *Simplest Modelling of the Line-Emitting Regions of QSOs*

The early calculations of the emission-line intensities (see Davidson & Netzer 1979; Baldwin 1979 for reviews) were rather simplified but they were amazingly successful. Such simple models usually assume that there is a central source that emits radiation with a power-law spectrum. The central source is surrounded by an envelope of gas at a distance of about 1 parsec from the centre. Whether this gas is in ionization equilibrium is determined by the power output of the central source and the *in-situ* (local) rate of ionic recombination in the gas. Except for the ionization continua of the gas elements, it is generally assumed that the gas is optically thin. Assuming certain density and chemical composition of the gas one calculates the ionization equilibrium for each species as a function of distance from the central source. The rate of ionization per unit volume is equated to the recombination rate per unit volume.

The line-strength equation has two parts, the first one being the collisional contribution from the ith species itself and the second being the recombination contribution from $(i+1)$th species. A filling factor ($f \simeq 10^{-4}$) representing the fraction of the entire volume that has actually got high-density gas for line emission is also required. It is usually arranged in such a way that the emitting region is ensured to have small optical depth for electron scattering under all conditions of variability as well as to satisfy the forbidden-line requirements. It is known that many quasars vary in their total light outputs on a timescale of a day or two and therefore one would like to argue that one always sees the central source right through the envelope. That means, the optical depth in electron scattering is under any circumstances small compared to unity. I think, this may not be generally true. For the vast majority of QSOs, we are probably not seeing all the way through to the centre. Most of them may not vary in timescales of a day or two. It is only the HPQs among the quasars for which the statement of low opacity can be justified.

Assuming the relatively normal abundances of the elements, the calculations of the line-strengths were found to be in excellent agreement with the available observations. It was indeed taken to be a great success, as the assumptions that went into the modelling were simple, and yet one could explain the relative strengths of all the lines that could be observed spectroscopically in the optical band. But that was a period when practically no UV or IR data were available.

5.5 *Limitations of the Simplest Models*

Based on the above model which basically advocates optical transparency as far as the origin of lines are concerned, one expects (*e.g.* Miller 1974; Davidson 1972) that the line-intensities of Lα should be about 20–40 times brighter than those of Hβ provided one further assumes that the continuum is fairly smooth throughout. But Lα and Hβ are separated by two octaves on the frequency scale, which is beyond the scope of optical spectroscopy. So the chance was very little of studying a single quasar in both the lines. Only the low-redshift quasars were seen in Hβ and the high-redshift ones in Lα. By combining data from these two different populations of quasars, Baldwin (1977b) estimated the ratio of Lα to Hβ line-intensities. The observed ratio turned out to lie in the range 3–6, rather than 20–40. This result was further supported by the IUE observation as well as by IR observations (see *e.g.* Davidsen 1980). For high-redshift quasars one can now compare the intensities of Lα to that of Hβ and for low-redshift quasars, Hβ to Pα. The latter ratio also disagrees by a similar factor (*e.g.* Puetter *et al.* 1978).

5.6 *A Plausible Explanation*

One of the popular explanations to the discrepant ratio of intensities of Lα to Hβ was that Lα is suppressed by dust reddening either outside or more likely inside the object. The clear indications of absence of dust in the spectra of quasars make this suggestion rather implausible, though in some cases some amount of reddening is present (see Baldwin 1977b).

Another explanation which I believe to be a plausible one is to bring in the optical-depth effects. The emission-line region may contain a number of emission-line clouds each of which is optically quite thick especially in the Lyman and Balmer continua. Hydrogen, being the most abundant element in these clouds, plays a dominant role with reference to the Lyman and Balmer continua only. But for developing a truly rigorous picture, one should also consider other elements and their characteristic continua, though it does not change the quality of the scenario. So let us now investigate the effect of introducing optical depth in the resonance lines of hydrogen only.

If the optical depth is high for Lα photons, they are simply trapped inside the cloud. As a result, a part of the neutral hydrogen (H I) pool will find itself populated in two levels rather than all being in the ground level. Depending on the density of the would-be-trapped Lα photons, the population distribution between two levels of the H I pool changes with time. As the second level becomes populated sufficiently, the temperature of the gas might be high enough to knock off the excited electron from the atom. Else, this can be done by another Lα or Balmer continuum photon. Then this ionized atom as a result of recombination can produce back a new Lα photon plus some other low energy photons. So we get back one Lα photon which will not be able to escape from the system but will now help populate the second level of some other hydrogen atom if it is at the ground state, or else knock off an electron from the second level. The net result is obviously the maintenance of the pool of Lα photons and production of some lower-energy photons.

Now let us see what happens to the Hβ or Balmer continuum photons. The Balmer continuum photons that are coming from the central source can ionize a hydrogen atom at the second level or higher. Subsequent recombination would produce a new Lα

photon plus some other photons. The Lα photon goes back into the pool keeping the level high, while some other lines are enhanced. Thus the net result is the enhancement of other line strengths with respect to Lα. This is basically the opposite of reddening, because instead of suppressing Lα we now enhance Hβ. Having populated this level, the same kind of process can be furthered to populate the next higher levels, depending of course on the number of photons of Hβ, Lα *etc.* The actual problem is fairly complicated.

There have been a number of analyses of this situation (*e.g.* Canfield & Puetter 1981). The resulting spectrum that is calculated seems to fit the data qualitatively better than the simple calculations in the optically thin case. At present they do not, of course, fit the data astoundingly well. These calculations are highly model-dependent (especially if we have a large number of clouds embedded in the region), geometry-dependent, interpretation-dependent, *etc.* It seems to me that this kind of explanation, in which the emission-line region is made up of a large number of fairly small but optically very thick clouds in which fairly complicated radiative-transfer processes are going on, is going in the right direction.

5.7 *The Blue Bump*

Th enhancement of the Balmer continuum in the above scenario could very well be used for explaining the blue bumps that I have mentioned earlier. The intensity of the blue bump may be a direct reflection of the optical depth in the Balmer continuum.

There are also other explanations for the origin of the blue bump, contributed by say, several Fe II lines or 2-photon continuum, or some blackbody emissions *etc.* (see *e.g.* Grandi 1982, for references). I will not go into the details of all these alternative explanations. To some extent all these effects might contribute collectively, or any of them selectively in particular cases. For example, the kind of population mechanism that I have described here can affect the Balmer continuum hypothesis, a variation in the density of iron can affect the Fe II line mechanism, and so on. This is perhaps the reason why the details of the blue bump vary from object to object. If the 2-photon mechanism is prevalent for some source, the bump would likely occur around 2400 Å rather than around 3600 Å which is when the Balmer jump mechanism is favoured. These mechanisms can however account for blue bumps of only a fraction of all the UV-excess objects.

Another popular mechanism due to Malkan & Sargent (1982) suggests that the blue bump can be fitted well to emission from a blackbody ($T_B \sim 2\text{–}3 \times 10^4$ K) that is possibly associated with the accretion disc in the central source. This radiation is then transmitted through the low-opacity gas and we see the bump. But this may not be the case in general due to the following reason.

Note a particular observation that UV excess is absent in blazars (BL Lac objects and HPQs). Wherever there is this excess, there seems to be only low polarization. But how are they related? Perhaps when there is enough gas, the opacity is high and trapping of photons is more efficient. This will result in reprocessing of radiation that comes from the central engine to such a degree that most of the memory of the variability, polarization *etc.* is lost. It is only when the opacity is low, that one can see all this right through the gas envelope, but then one does not find the UV excess. So the UV excess may not directly originate in the central engine. Before we jump to such a conclusion, we should of course carry out a careful comparison of the HPQ lines and the

continuum excess and see whether one finds any difference between their spectra and of those QSOs which are remarkably nonthermal.

For high optical depths not only in Lyman lines but also in Balmer lines, one starts reprocessing Lα photons also by O I fluorescence mechanism. This process results in O I lines in the spectrum, the line strengths of which will depend on the amount of O I and the optical depth in Balmer lines. This argument leads us to say that one should never detect any O I in HPQs. But there are definitely some signatures of O I. Though it is a minor point, one has yet to find a satisfactory explanation.

5.8 *Cloud Dynamics and Line Asymmetries*

We have seen that the simplest model for the emission-line regions in quasars—assuming a central source surrounded by clouds—does not fit well with the details of observations. A number of considerations lead to some revision, namely that the clouds have to be optically thick in the Lyman continua and much more so in the lines. This at least qualitatively explains the otherwise anomalous Lα to Hβ intensity ratio. It is then found that the best fitting parametres for the line-emitting clouds would be the following. The individual clouds have a typical size of $\sim 10^{13}$ cm and particle density $n \sim 10^{9}$–10^{10} cm^{-3}, giving mass $M \sim 10^{25}$ g. The temperature is quite high, $T \sim 20{,}000$ K and the clouds are moving with velocities $v \sim 10^{4}$ km s^{-1}.

The size of the central engine is often inferred from the observed timescale of variability of the object in the optical, and that of the whole emission-line region from the line-intensity fitting procedure which is of course model dependent. The total size of the emission-line region turns out to be $r \sim 10^{18}$ cm. The dynamics of the clouds, though a matter of controversy, can roughly be understood from the nature of broadening of the broad spectral lines. The general consensus is that the clouds are moving out radially, rather than rotating as a whole or moving randomly inside the region. Turbulence could be another likely candidate, because it can also give rise to the observed asymmetry and shifts of the lines.

Fig. 19 represents the model schematically. The high-velocity, optically thick clouds surround the central source that is responsible for heating up the clouds. The sides of

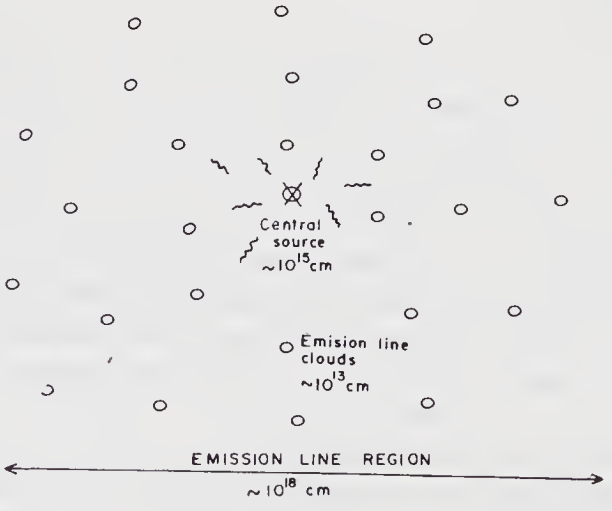

Figure 19. A schematic model of the emission-line region.

the clouds facing the central source are heated up and become highly ionized. Due to the optical thickness, the far sides are less heated and are therefore less ionized. If the lines are optically very thick, we have to look through the body of the cloud that lies between us and the central source, in order to see those lines produced in the other half of the same cloud. So it is the clouds that lie behind the central source that contribute principally to the observed line-intensities, provided the intercloud gas is optically thin. Since the clouds have high velocities in general, depending on the direction of their motion with respect to us, the spectral lines will be shifted either towards the red or towards the blue. Now if the clouds are moving randomly with respect to each other, it will hardly give rise to any line asymmetry. But if the clouds are systematically expanding radially, some kind of line asymmetry will arise. The exact amount will depend on the significance of electron scattering in the intercloud medium, that tends to shield the direct view of the rear half of the cloud. So these are two competing processes, the radial expansion and the intercloud attenuation. Some of the lines, especially the resonant ones, are likely to be optically thick in the clouds, whereas the intercombination lines (*e.g.* C III]) are not. Therefore one expects different effects in the line profiles depending on the type of line, the optical thicknesses in that line and electron scattering effects in the intervening region. Not only do these details differ significantly from source to source, one even faces severe difficulty in explaining all the line asymmetries of a single source. The emission-line profiles of Lα, C IV λ 1549 Å and C III] λ 1909 Å in PHL 957 are shown superposed on one another in Fig. 20. From the relative positions of the profiles, minute redshift differences of each line can clearly be recognised. The profile of the C III] line here is perhaps representative of many quasars.

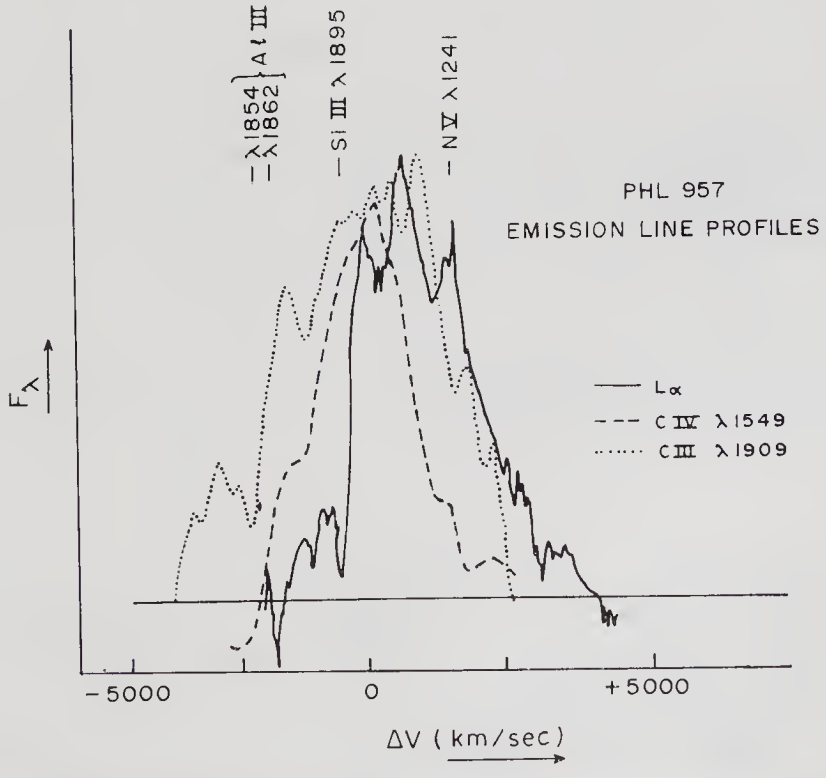

Figure 20. Profiles of three different emission lines in PHL 957 reduced to a common redshift (from Coleman *et al.* 1976).

It has a strong blue wing, a feature that can be explained by assuming optical transparency of the line through individual clouds but not quite through the expanding intervening region. The other two profiles are somewhat difficult to explain due to the much more discrete nature of absorption that completely distorts the profile. Sometimes the asymmetries that are seen in C IV line profile are of the opposite kind to that of C III] line. In any case, the best explanation for the line asymmetries seems to be in terms of optical depth competition of one kind or another and the radial expansion of the cloud system.

It has been a long-standing problem to understand what exactly holds a cloud together. I think, we have understood it partially, if at all. Left to itself a cloud will double its size in a time perhaps a thousand times shorter than its average ELR crossing time, assuming that the entire velocity spread in the lines is due to motion. Therefore, to confine the clouds, one assumes that there is some kind of low-density high-temperature gas between the clouds. If the clouds are in pressure balance with the intercloud medium and are in relative motion with respect to the confining gas, the clouds and the gas tend to act as a gluey material in the sense that the latter offers efficient dragging on the former to the point of stopping it, if the temperature of the confining gas is below 10^8 K. Furthermore, at such low temperatures, the intercloud medium may as a whole begin to collapse. All this suggests on the one hand that the temperature of the intercloud gas is very high, probably well above 10^8 K, and on the other hand, that this confining gas is not static, perhaps it is expanding like a wind and dragging the clouds with it. A number of groups (*e.g.* Weymann *et al.* 1982, Krolik, McKee & Tarter 1981) are investigating these aspects in great detail. Before discussing this I would like to consider other evidences for the windlike outflows in quasars.

5.9 *Broad Absorption Lines in QSOs*

Fig. 21 shows the spectrum of PHL 5200, a high-redshift quasar ($z = 1.980$), taken by M. Burbidge and her collaborators. The C III] intercombination line at λ 1909 Å does not show any absorption features. But at shorter wavelengths the resonance lines C IV λ 1549 Å, Si IV λ 1397 Å, N V λ 1243 Å and Lα, all show very broad absorption features ($v \sim 10^4$ km s^{-1}), sharp towards red and rather gradual towards the blue. The characteristic Lα emission is seen to be very weak compared to other lines. This is perhaps because of the very broad N V absorption which has strongly suppressed Lα. It is also seen that the strength of emission of the C IV line is very much lower than that of absorption, a feature that cannot be explained by adjusting the radial outflow and

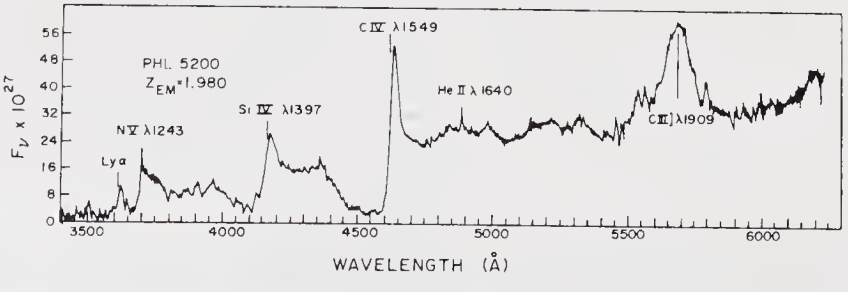

Figure 21. Spectrum of PHL 5200 showing the broad absorption features.

electron-scattering parameters, simply because what is taken out from the beam at one velocity should come back with another.

After the discovery of broad absorption lines in PHL 5200 (Lynds 1967), another quasar, RS 33, was found (Burbidge 1970) to have similar absorption characteristics. For a long time these were the only two quasars that showed broad absorption-line (BAL) features. In recent years of course many more have been found. It immediately became clear that the BAL characteristics are much more heterogeneous than one had thought from RS 33 and PHL 5200. The reason so few were found in early years is just another selection effect. It turns out that there are essentially no good cases of BAL quasars that are radio loud, and quasar detection was done largely through the radio surveys. There are in fact only two radio-loud quasars (PKS 1157 + 014 and GC 1556 + 335) which show very marginal BAL characteristics. I will give a few more examples, all from the optical surveys.

Fig. 22 shows a high-resolution spectrum of MCS 141. I have chosen this to exemplify a difference in character of the C IV line in absorption. It seems that it has somehow shifted from the position of the emission line; it has a rugged blue and a red wing, and there is quite a bit of structure everywhere. Fig. 23 is the spectrum of the same object at higher resolution and over a narrow range. It is extremely rich in structure, compared to PHL 5200. It is believed that there is an absorbing medium having a wide range of velocities in it but seemingly clumpy in that range of velocity. Fig. 24 shows a high-resolution spectrum of another quasar, MCS 232, that resembles P Cygni absorption features with respect to the emission lines. The shift in the positions of some of the absorption lines is several times the width of the emission lines.

Absorption seems to take place always blueward of the emission lines, possibly implying an outflow of the absorbing medium. It is generally accepted that such features are associated only with quasars and that the velocity of outward motion of $\sim 10^4$ km s^{-1} happens to be the same as that of the broad emission-line region. One might naturally ask whether there is any connection between these two regions.

A histogram of the observed distribution of sharp absorption-line features associated with the C IV line in the intermediate-redshift sample is shown in Fig. 25 as a function of the velocity of the absorption system relative to the quasar. It has been taken from the work of Williams, Weymann and others. Most of the C IV absorption

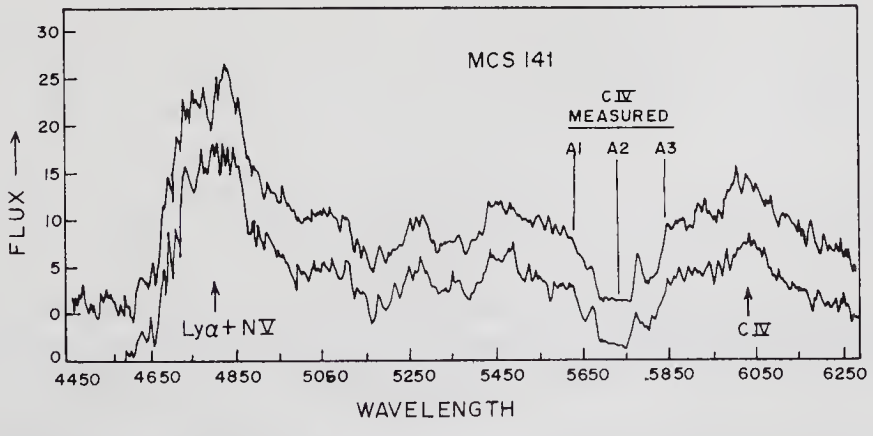

Figure 22. Spectrum of MCS 141 showing the broad-absorption features associated with the C IV line (from Turnshek *et al.* 1980).

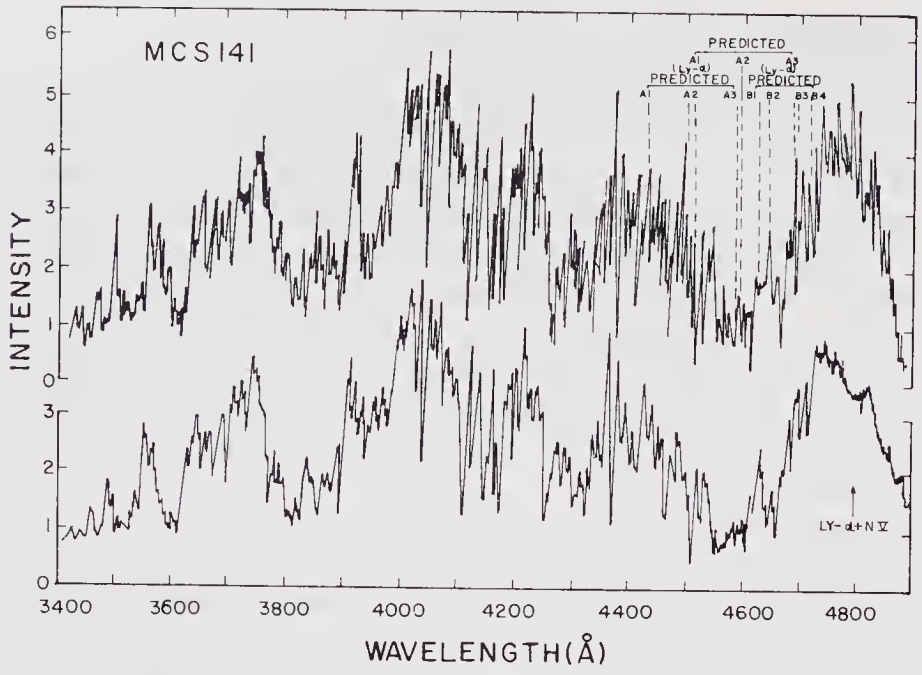

Figure 23. High-resolution spectrum of MCS 141 showing the rich structure in the absorption lines (from Turnshek *et al.* 1980).

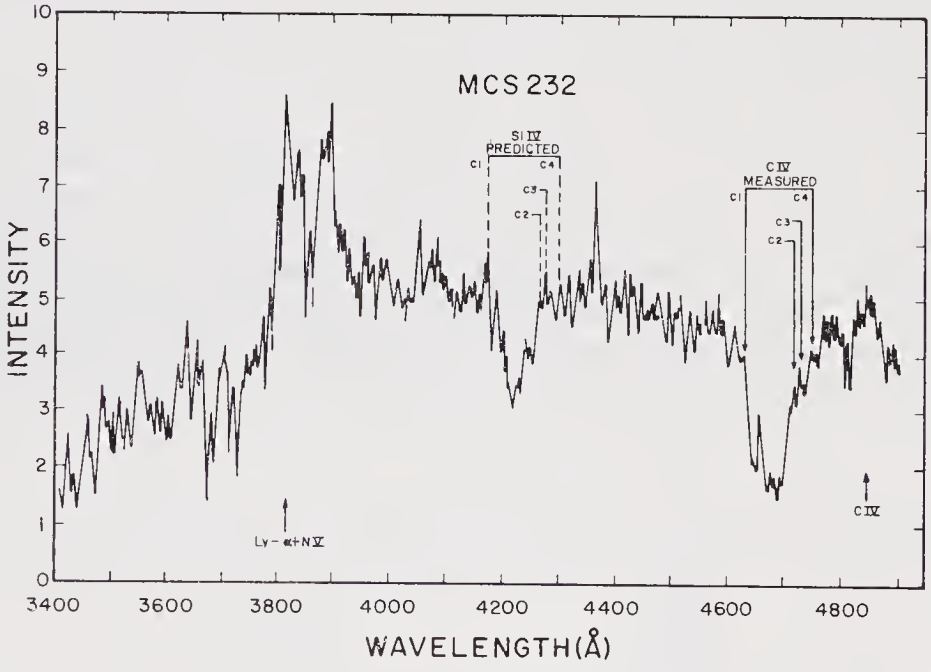

Figure 24. High-resolution spectrum of MCS 232 (from Turnshek *et al.* 1980).

systems occur near the emission redshift and the distribution has a tail extending from the peak out to velocities $\sim 2 \times 10^4$ km s^{-1}. Although these investigators could not come to unique conclusions, they have suggested some alternative explanations. Such a peaked histogram with an extended tail might indicate that there exists a local and randomly moving absorbing cloud system around the quasar as a part of the galaxy or the cluster with which it is associated, or located somewhere between us and the quasar.

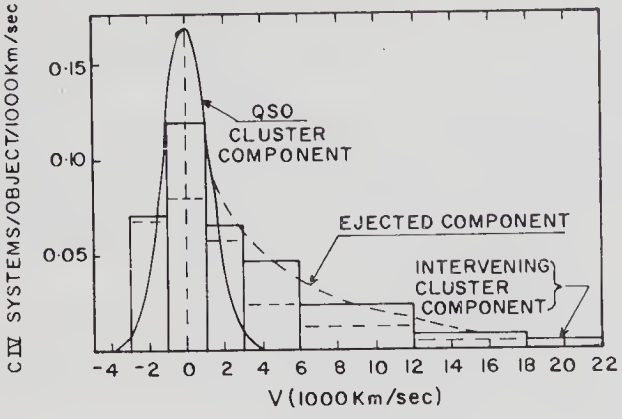

Figure 25. Velocity distribution of sharp-absorption features associated with Civ line in a sample of intermediate-redshift quasars.

However, what one finds between PHL 5200 and MCS 141 is a smooth absorption system changing into a broader one with much fine structure. Again in the radio-selected samples, which occasionally show incipient absorption features, these consist of sharp lines that occur in strong bunches. This shows that a kind of natural evolution has taken place from PHL 5200 to MCS 141. This kind of line sharpening in absorption *i.e.*, breaking up of broad absorption-features into many sharper ones, occurs in novae during their rapid evolution.

Let us now summarize the properties of BAL QSOs.

(1) Roughly 3 per cent of the optically selected quasars show BAL features in them. The number is of course quite uncertain.
(2) High ionization seems to be a characteristic of BAL features in quasars.
(3) By studying the nature of broad absorption lines, one can understand what kind of gas might produce them. By studying the Lyman continuum absorption one finds that unlike the emission clouds, these jets of gas are optically thin in Lyman continuum.
(4) The Lα emission is often suppressed by the broad absorption in the Nv line. It tells us something about the relative location of the emission-line region and the broad absorption-line-forming gas.
(5) Some of the BAL quasars have exceedingly sharp red wings, but none has a really sharp blue wing. The blue wings are generally rugged.
(6) The asymmetry implies that one can rule out the spherically symmetric scattering case for producing these BAL features. One can also estimate the covering factor for not seeing the BAL features that exist intrinsically. The hints lie with the observed fraction of the population of quasars showing BAL features, and say, the distribution of the absorption depths in lines. Sometimes they go right to zero indicating that the absorption clouds are probably covering the emission-line region. We know that the size of the emission-line region is a few parsecs. Thus the covering factor for a quasar in general is believed to be about 10 per cent. Since we have seen only 3 per cent of the optically selected quasars to have BAL features, this 10 per cent covering factor would imply that about 30 per cent of the quasars in fact have BAL features, which would have been seen if viewed from the correct angle.
(7) The red absorption edges are often displaced a few times their widths away from the emission-line systems.

(8) Several QSOs show multiple BAL features. This does not normally happen in a star showing a P Cygni type profile due to the accelerating wind from the surface of the star as in novae or B stars.
(9) The broad absorption clouds are well outside the emission regions. They have a size that is at least comparable to the latter, because observed lines often go to zero intensity or sometimes 50 per cent intensity. They often have very significant radial velocities ($\sim 10^4$ km s^{-1}) with respect to the centre of emission in the emission-line region. Sometimes one finds two of them in the line of sight.
(10) No true BAL QSO is a strong radio source. There are only two radio-loud quasars that show marginal BAL characteristics. PHL 5200 is the only BAL quasar that is polarized in the optical. However this property seems to be unique to PHL 5200.
(11) Lines break up into sharper components.

Many of the above properties are also present in purely sharp-line QSOs. The general conclusion is that the absorbing clouds are well outside the emission-line regions and have sizes comparable to ELR. The clouds have significant radial velocity with respect to ELR.

6. Radiative acceleration mechanism for expanding gas clouds

Over the past ten years or so, various radiative acceleration mechanisms for radially expanding gas clouds have been proposed, originally to explain the sharp-line features over a very wide range of velocities. Basically there are two approaches. The first one is the pure radiation-pressure mechanism (*e.g.* Blumenthal & Mathews 1979). The radiation from the central source is absorbed and reemitted or scattered by the gas around the source. In this process a net momentum is transferred to the gas by radiation causing the whole region to expand. One can of course do the ballistics of these gaseous projectiles, but before doing so one has to circumvent the problem of confinement of these gas clouds.

The other approach assumes that the acceleration is provided by a steady wind emanating from the central source. The problem then reduces to one analogous to the solar wind. The classical wind equations are

(a) $$V\frac{\mathrm{d}V}{\mathrm{d}r} = -\frac{GM}{r^2} - \frac{1}{\rho}\frac{\mathrm{d}P}{\mathrm{d}r} + \frac{1}{\rho}\frac{\Phi}{c}$$ (steady-state momentum equation),

(b) $$\frac{1}{r^2}\frac{\mathrm{d}}{\mathrm{d}r}(\rho V r^2) = 0$$ (mass-conservation equation),

(c) $$V\frac{\mathrm{d}}{\mathrm{d}r}\left(\frac{3}{2}\frac{P}{\rho}\right) = \frac{PV}{\rho^2}\frac{\mathrm{d}\rho}{\mathrm{d}r} + \frac{\Phi}{\rho}k - \frac{\Phi}{\rho}$$ (energy-conservation equation),

(d) $$P = \frac{2\rho kT}{m_{\mathrm{H}}}$$ (equation of state).

Here P, ρ, V and T are the pressure, density, velocity and temperature of the wind

respectively. r is the radial distance from the central source that has mass M. Φ represents the basic energy flow from the central source that maintains the push; depending on the mechanism, it could be the radiation pressure per unit time and/or something else. One can see that the steady-state momentum equation contains the gravity term, the pressure-gradient term and finally this radiation-pressure term. Since this radiation pressure can also heat up the system, it also appears in the energy conservation equation. The last term of the third equation provides the internal energy per unit mass. The second and fourth equations complete the formality for giving the steady-state solutions for the four wind parameters as functions of r.

However the equation for velocity as a function of r turns out to be fairly complex with all redshift terms in the numerator and a factor $(V^2 - c_s^2)$ in the denominator, where c_s is the sound speed. Thus there exists a critical condition, what is called the sonic point, where the denominator becomes zero. If we want to get a regular solution around the sonic point, we have to make the numerator also vanish at the sonic point. This has been a standard practice with the classical wind theory and one obtains some kind of eigen-condition on what is happening.

Let us consider pure radiation pressure. First of all the temperature of the gas is determined by the radiation field from the central source, and seems to be relatively low for the gas. Then at the point where the sonic condition is satisfied, one also obtains certain conditions on the radiation forces and the gravity at that point. In the pure radiation pressure scenario, it is hard to get the required driving force once the sonic point is crossed. The terminal velocity is comparable to the speed of sound and that is usually not very interesting unless the sound speed is $\sim 10^4$ km s^{-1}. If we try to heat up the gas by radiation field alone such a high sound speed is difficult to achieve. One has to artificially devise some other means of building up high speeds. It seems to me that the radiation pressure mechanism does not provide a natural solution.

How can one get a high temperature? Though there are many ways, I would like to concentrate on the one that has been analysed by my colleagues (Weymann *et al.* 1982). The novelty of their approach is that they use the presence of relativistic electrons to dump energy into the gas. In that case the standard calculations for the emission-line regions get modified. All the previously published results on the ELR calculations were done without taking into account the effect of the presence of relativistic electrons in the confining medium, though in many cases, at least in radio-loud quasars, there is relativistic plasma around on a scale exactly the same as that of ELR. It is inconceivable that there is no interaction between the relativistic plasma and the thermal plasma we see. So the earlier calculations were based on many simplified assumptions.

Now let us see in the present context how one should modify the wind equations. The radiation pressure terms in the energy and the momentum equations are to be replaced by the corresponding ones for the relativistic plasma. To start with one assumes a high luminosity in the relativistic plasma, or more precisely in the electrons, that is comparable to that in the electromagnetic radiation, *i.e.*, $L_{rel} \sim L_{em} \sim 10^{46}$ erg s^{-1}. The exchange of energy between the electrons and the gas is not by Coulomb interactions but by a much more efficient process, the so-called oscillating two-stream instability process. It principally heats up the gas with the energy deposition rate per unit area

$$\Phi = 1.6 \times 10^{-4} \frac{n_{rel}^3}{n_{th}^{3/2}} \frac{1}{\gamma} \text{ erg cm}^{-3} \text{ s}^{-1},$$

where n_{rel} and n_{th} are the number densities of the relativistic electrons and the thermal

gas particles respectively and γ is the relativistic gamma factor for the electrons. With this Φ, the sonic point condition to be satisfied at a radius, r_{sonic}, is given by

$$r_{\text{sonic}} \simeq \left(\frac{L_{46}^{3/5} T_{10}^{1/5}}{\gamma_3^{4/5} P_{-2}^{1/2}} \right) \text{pc}.$$

So it mainly depends on the luminosity and the γ factor, again each of which may have some implicit temperature dependence. It has been assumed that $T \sim 10^{10}$ K. But as one can see from the expression, the explicit dependence on temperature is rather weak, so also with the pressure of the thermal gas. For pressure balance between the emission-line clouds and the confining medium, a reasonable value of the radius of the sonic point turns out to be $r_{\text{sonic}} \sim 1$ pc. As we have already argued that beyond the sonic point radius the whole system begins to diffuse away, this radius should faithfully represent the scale size of the emission-line region. One feels happy to note that the size of the ELR in quasars estimated otherwise is around the same value.

Noting that the radius of the sonic point depends on the luminosity to its 3/5th power, one may wonder why Seyfert galaxies and quasars have very similar spectra, very similar ionization conditions *etc.*, in spite of their widely different luminosities. To answer this, we must first find a parameter that really reflects the conditions of having similar spectra and similar ionizations. Among the common properties, for example, Seyfert galaxies and quasars both have broad lines. The densities are such that one finds C III] in the broad-line region but not much of [O III]. This requires densities $\sim 10^9$–10^{10} cm^{-3} in the emission clouds. However, from spectral lines alone, one can not distinguish a Seyfert galaxy from a quasar; the intrinsic luminosities have to be known. What then matters is the ratio of the number densities of photons (n_{ph}) and thermal electrons (n_{el}). This ratio can be regarded as an ionization parameter which basically depends on the temperatures of the clouds and the wind and also on the luminosity in the following way

$$\frac{n_{\text{ph}}}{n_{\text{el}}} \sim \frac{T_{\text{cloud}}}{L^{1/5} T_{\text{wind}}^{2/5}}.$$

Since the dependence on the luminosity is so weak, the state of ionization in Seyfert galaxies as well as in quasars should not be very different.

The emission-line regions in general extend up to a maximum of twice the sonic point radius of a steady-state wind powered by a relativistic plasma. The temperature around the sonic point is about 10^{10} K, and therefore the sound speed in wind is $\sim 10^4$ km s^{-1}. A large number of emission-line clouds are embedded in the confining gas. We know the particle densities in the clouds, but not their sizes, excepting some rough estimates. Once we leave such a cloud inside the steadily flowing wind, the question is whether the clouds will stay stationary to the wind and go out through the sonic point. Obviously, the emission-line clouds inside the wind are under the action of gravity produced by the whole region and of the ram pressure of the wind. The two act in opposite directions (Fig. 26). Using the normal ELR parameters of the clouds one can calculate the acceleration of these clouds. It is found that the ram pressure of the wind wins and that the clouds are accelerated to the speed of the wind on a length-scale much shorter than the sonic point radius. The clouds on the border of ELR are being continuously pushed out by the wind. This constitutes a constant rate of mass-loss from the system, which is estimated to be roughly 20 $M_\odot$ yr^{-1}.

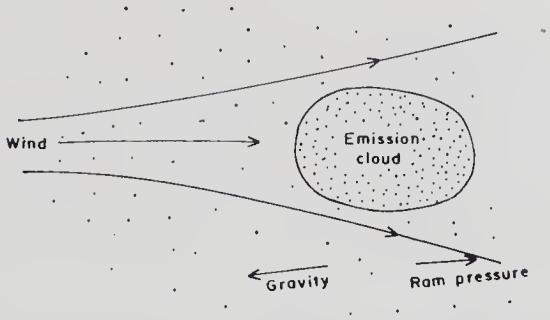

Figure 26. Gravity and ram pressure of the wind act in opposite directions on a line-emitting cloud.

The model does not answer all the questions, namely the origin of the wind, the origin of the cloud system, the supply of the relativistic electrons in radio-quiet quasars *etc.* Can we really make some inference from optical studies of the radio-quiet quasars about the existence of relativistic electrons in them? So far not. Obviously the model is oversimplified; nevertheless it can explain many of the observed features.

6.1 *Are BAL Quasars Embedded in Spiral Galaxies?*

Let us assume that the BAL quasars are embedded in spiral galaxies. As the wind comes out of the central region of the quasar it interacts with the interstellar medium. With the kind of density of the interstellar medium, the wind ram pressure of the quasar wins all the way through 5 kpc or more. We know that the interstellar medium is clumpy in nature and the low temperature clouds of size about 1 pc, having number density of particles of $\sim 10^3\,\mathrm{cm}^{-3}$ and mass $\sim 10\,M_\odot$, are abundant. Those which fall on the streamline of the wind (Fig. 27a) at a distance of about 1 kpc from the centre of the galaxy will be accelerated to velocities of order $10^4\ \mathrm{km\ s}^{-1}$ on a timescale of 10^6 yr while pushing themselves by the action of the wind through the distance of about

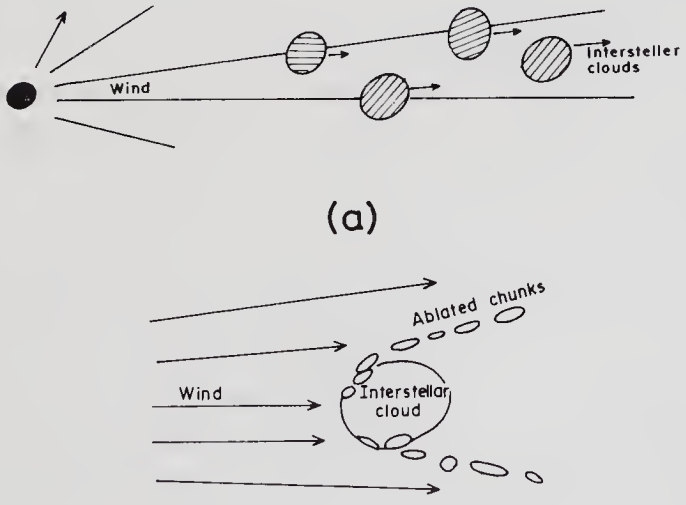

Figure 27. Schematic model of the interaction of the interstellar clouds with the wind.

10 kpc. Such clouds receive the radiation from the central engine and also the blow of the wind from the same direction.

I have investigated a model case for such a cloud. Calculations show that as the acceleration of a cloud begins under the above circumstances, instabilities of the Rayleigh-Taylor kind are developed on the front. Chunks of the cloud are pulled off from the surface and they also begin to accelerate independently of the cloud (Fig. 27b). Depending on the position of the observer with respect to the geometry of the cloud–cloudlet system, the observer may directly see the light coming from the emission-line region or fairly well-defined absorption due to the main cloud. Whatever velocity this cloud has with respect to the observer constitutes the centre of the absorption-line spectra. Each cloudlet having some definite velocity, appreciably different from the main cloud velocity, may produce a distinctly sharp absorption line. And the total effect, if blurred, would give rise in general to a very broad absorption line. One can have several clouds in favourable locations with respect to the observer to essentially explain all BAL features in QSOs.

One should of course remember that this is merely one way of looking at it. What we need for explaining BAL features is the presence of wind from the centre, having a required property to accelerate the central clouds, if the latter be present in the surrounding galaxy within a few kpc distance from the centre. Why spiral galaxies? Because BAL QSOs and spiral galaxies are both generally radio weak.

7. The nature and evolution of the central engine

Finally the study of the central engines in various types of active galactic nuclei may provide clues to their origin. In the framework of the cosmological hypothesis, one considers accumulation of matter basically on the galactic scale and certain aspects of the early active phases of the galaxies. We are required to find processes that lead to the release of large power in the central engines. Accretion of matter by massive black holes may be one such. One generally neglects the role of the angular momentum in such scenarios. It is rather unlikely that matter is everywhere accreted in a state of zero angular momentum. There will be some kind of gradations, some with low angular momentum and some with very high.

If one imagines anything condensing down to the scale of a black hole or singularity and it has any angular momentum, it is going to form a disc in the inner regions. If it has a large enough angular momentum and the black hole has galactic mass, the accretion disc may extend well up to 20 kpc from the centre. I will call that a spiral galaxy. It is now rotating, though most of the matter is at low rotational velocity and spread over a large distance. Any evolution in that disc due to friction or anything else takes a very long time. The less angular momentum the gas has, the more easily it goes towards the centre and more rapid becomes the evolution. The disc structure on a reasonable timescale (depending on the mass and angular momentum) can go anywhere from 20 kpc down to the smallest, say 1 pc. It seems to me that the primary variable is the angular momentum. The rate at which matter falls on to the black hole is related to the specific angular momentum (h) and the mass of the black hole at the centre. I think, an elliptical protogalaxy will generally have a smaller h and therefore higher $\dot{M}$, and a typical spiral protogalaxy will have large h and therefore smaller $\dot{M}$ in its disc.

We know that a black hole itself cannot accrete matter at a rate exceeding the

Eddington rate. So even if the mass-supply rate from outside exceeds the Eddington rate, the black hole can grow only at the Eddington rate and the rest of the infalling matter has to be blasted off some way or other. When a black hole continues to grow at the Eddington rate, its mass exponentiates on a timescale of order 10^8 yr (assuming that the Eddington limit is obtained on the basis of the free electron-scattering opacity alone) and its luminosity is given by the Eddington luminosity of the black hole. Fig. 28 shows some idealized curves for the evolution of the luminosity, mass and external mass-outflow rate for two given inflow rates on to the black hole system. Mass and luminosity, both continue to increase exponentially with time up to a point limited by the external mass-supply rate. Once the luminosity becomes equal to the equivalent of the external mass-supply rate, the luminosity begins to stay practically constant (solid line), provided the mass-supply rate also remains a constant, but the mass keeps on increasing linearly with time (dashed line). During the earlier phase when the rate at which the black hole was swallowing matter was below the supply rate from outside, the leftover portion had to be blasted off in the form of a strong wind or something else. This mass-loss rate from the black hole system as shown by the dashed-dotted line in Fig. 28, gradually decreases with time till it reaches the critical point where everything begins to be swallowed and nothing escapes beyond that. The two sets of curves are shown for two different mass-supply rates; higher this rate, later is the turning point reached and higher is the value of the constant luminosity beyond.

Let us now describe the scenario in terms of the objects we know—like the QSOs, BL Lacs, galaxies *etc.* To start with, the black-hole system has a very low luminosity and a constant, high rate of mass inflow which just reverses the direction before reaching the black hole. Such an object defies any detection from a distance. Then the luminosity builds up gradually, but still there is a lot of gas around the black hole. This is the region where one should not only see a high intrinsic power output but also the gas should be excited and one should see many emission lines. The entire region would be optically very thick in electron scattering, hiding the central engine. Such a scenario may plausibly apply to radio-quiet quasars or more generally to the optically selected quasars.

As the luminosity of the above system continues to build up further, it approaches the critical state and more and more matter is being swallowed by the central black hole.

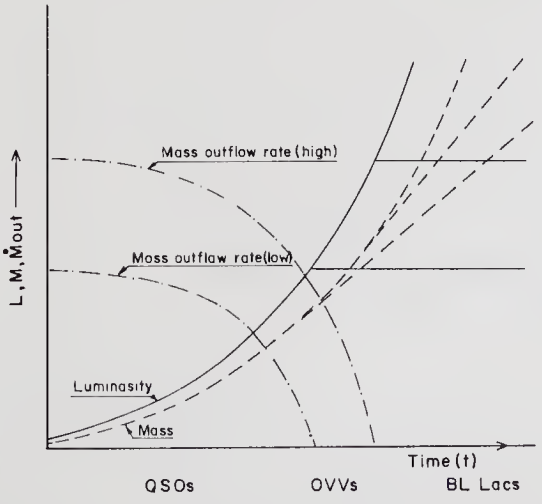

Figure 28. The evolution of luminosity and mass.

The gaseous envelope becomes more and more dilute. One would now begin to see the central engine but some line emissions from the hot gaseous envelopes would still be visible. The object behaves like an OVV (optically violently variable). Once one reaches the critical point the luminosity attains its peak and the gaseous envelope practically disappears. One would be able to see the central engine straightaway. However, as long as the mass is coming in through the disc, the whole region would still shine but there would be very little thermal emission. Such an object may be called a BL Lac object. Finally the object ceases to emit any radiation when the external supply of mass is switched off. It becomes an ordinary galaxy, the nucleus of which is generally seen not to be very active.

So we get an evolutionary sequence for active galactic nuclei; a radio-quiet quasar going over to a radio-loud quasar which turns into an OVV, a BL Lac and finally into an ordinary galaxy. This sequence would follow for any given specific angular momentum. If we start with low angular momentum, and hence with a high mass-supply rate towards the centre, we would expect to go through the whole sequence rapidly under high luminosity and the end result is an elliptical galaxy. On the other hand, a high angular momentum system like a spiral galaxy has its mass-inflow rate so low that the activity of the central engine remains poor all the time and most of the gas will still be seen out there in its spiral arms.

References

Angel, J. R. P., Stockman, H. S., Woolf, N. J., Beaver, E. A., Martin, P. G. 1976, *Astrophys. J.*, **206,** L5.

Baldwin, J. A. 1975, *Astrophys. J.*, **201,** 26.

Baldwin, J. A. 1977a, *Astrophys. J.*, **214,** 679.

Baldwin, J. A. 1977b, *Mon. Not. R. astr. Soc.*, **178,** 67P.

Baldwin, J. A. 1979, in *Active Galactic Nuclei*, Eds C. Hazard & S. Mitton, Cambridge Univ. Press, p. 51.

Biermann, P. *et al.* 1981, *Astrophys. J.*, **247,** L53.

Blumenthal, G. R., Mathews, W. G. 1979, *Astrophys. J.*, **233,** 479.

Braccesi, A., Formiggini, L., Gandolfi, E. 1970, *Astr. Astrophys.*, **5,** 264.

Burbidge, E. M. 1970, *Astrophys. J.*, **160,** L33.

Canfield, R. C., Puetter, R. C. 1981, *Astrophys. J.*, **243,** 381, 390.

Carswell, R. F., Strittmatter, P. A., Williams, R. E., Beaver, E. A., Harms, R. 1975, *Astrophys. J.*, **195,** 269.

Coleman, G., Carswell, R. F., Strittmatter, P. A., Williams R. E., Baldwin, J., Robinson, L. B., Wampler, E. J. 1976, *Astrophys. J.*, **207,** 1.

Davidsen, A. F. 1980, in *IAU Symp. 92: Objects of High Redshift*, Eds G. O. Abell & P. J. E. Peebles, D. Reidel, Dordrecht, p. 235.

Davidson, K. 1972, *Astrophys. J.*, **171,** 213.

Davidson, K., Netzer, H. 1979, *Rev. mod. Phys.*, **51,** 715.

Elias, J. H. *et al.* 1978, *Astrophys. J.*, **220,** 25.

Giacconi, R. 1978, *Phys. Scripta*, **17,** 159.

Grandi, S. A. 1982, *Astrophys. J.*, **255,** 25.

Gunn, J. E., Hoessel, J. G., Westphal, J. A., Perryman, M. A. C., Longair, M. S. 1981, *Mon. Not. R. astr. Soc.*, **194,** 111.

Kleinmann, D. E., Gillett, F. C., Wright, E. L. 1976, *Astrophys. J.*, **208,** 42.

Krolik, J. H., Mckee, C. F., Tarter, C. B. 1981, *Astrophys. J.*, **249,** 422.

Lebofsky, M. J., Rieke, G. H., Walsh, D. 1983, *Mon. Not. R. astr. Soc.*, **203,** 727.

Lynds, C. R. 1967, *Astrophys. J.*, **147,** 396.

Maccacaro, T., *et al.* 1982, *Astrophys. J.*, **253,** 504.

Malkan, M. A., Sargent, W. L. W. 1982, *Astrophys. J.*, **254,** 22.
Martin, P. G., Thompson, I. B., Maza, J., Angel, J. R. P. 1983, *Astrophys. J.*, **266,** 470.
McCarthy, D. W., Low, F. J., Kleinmann, S. G., Gillett, F. C. 1982, *Astrophys. J.*, **257,** L7.
Miller, J. S. 1974, *A. Rev. Astr. Astrophys.*, **12,** 331.
Moore, R. L., Stockman, H. S. 1981, *Astrophys. J.*, **243,** 60.
Osterbrock, D. E. 1978, *Phys. Scripta*, **17,** 137.
Peacock, J. A., Perryman, M. A. C., Longair, M. S., Gunn, J. E., Westphal, J. A. 1981, *Mon. Not. R. astr. Soc.*, **194,** 601.
Puetter, R. C., Smith, H. E., Soifer, B. T., Willner, S. P., Pipher, J. L. 1978, *Astrophys. J.*, **226,** L53.
Richstone, D. O., Schmidt, M. 1980, *Astrophys. J.*, **235,** 361.
Rieke, G. H. 1978, *Astrophys. J.*, **226,** 550.
Rieke, G. H., Lebofsky, M. J., Kinman, T. D. 1979, *Astrophys. J.*, **232,** L151.
Rieke, G. H., Lebofsky, M. J., Wisniewski, W. Z. 1982, *Astrophys. J.*, **263,** 73.
Sandage, A., Véron, P. 1965, *Astrophys. J.*, **142,** 412.
Scheuer, P. A. G., Readhead, A. C. S. 1979, *Nature*, **277,** 182.
Schmidt, M., Green, R. F. 1983, *Astrophys. J.*, **269,** 352.
Smith, M. G. 1981, in *Investigating the Universe*, Ed. F. D. Kahn, D. Reidel, Dordrecht, p. 151.
Stocke, J., Liebert, J., Stockman, H., Danziger, J., Lub, J., Maccacaro, T., Griffiths, R., Giommi, P. 1982, *Mon. Not. R. astr. Soc.*, **200,** 279p.
Stockman, H. S. 1978, in *Pittsburgh Conference on BL Lac Objects*, Ed. A. M. Wolfe, Univ. Pittsburgh, p. 149.
Stockman, H. S., Angel, J. R. P., Miley, G. K. 1979, *Astrophys. J.*, **227,** L55.
Strittmatter, P. A., Carswell, R. F., Burbidge, E. M., Hazard, C., Baldwin, J. A., Robinson, L., Wampler, E. J. 1973, *Astrophys. J.*, **183,** 767.
Strittmatter, P. A., Hill, P., Pauliny-Toth, I. I. K., Steppe, H., Witzel, A. 1980, *Astr. Astrophys.*, **88,** L12.
Turnshek, D. A., Weymann, R. J., Liebert, J. W., Williams, R. E., Strittmatter, P. A. 1980, *Astrophys. J.*, **238,** 488.
Véron, P., Véron, M. P. 1982, *Astr. Astrophys.*, **105,** 405.
Weedman, D. W. 1977, *A. Rev. Astr. Astrophys.*, **15,** 69.
Weymann, R. J., Scott, J. S., Schiano, A. V. R., Christiansen, W. A. 1982, *Astrophys. J.*, **262,** 497.

Kapahi, V. K. (Ed.)
Extragalactic Energetic Sources
Indian Academy of Sciences, Bangalore, 1985, pp. 53–86

Radio Sources and Galactic Nuclei: Models and Problems

Martin J. Rees *Institute of Astronomy, Madingley Road, Cambridge CB3 0HE, U.K.*

Contents

1. Introduction

In these lectures I intend to discuss some theoretical ideas about the central energy source in active galactic nuclei. Let me begin by briefly explaining the organization of the topics. I shall start with some introductory remarks about the various length-scales involved in the problem. Then I will try to argue that a natural evolutionary sequence is likely to lead to a supermassive collapsed object in the centre of a galaxy. I shall next discuss the basic physics of accretion discs around a black hole (ion-supported or radiation-supported). Of special importance is the possibility of extracting the rotational energy of a black hole by coupling it magnetically to the accretion disc and thereby augmenting the power output per unit mass accreted. I will then discuss the stability, propagation and confinement of the jets which are produced by the central engine, and what they are made of (ordinary plasma, e^+-e^- pairs, or Poynting flux), and the role of e^+-e^- 'photospheres' around compact objects in 'processing' the X-ray and optical continuum emission; and then consider superluminal motion, concentrating on some of the difficulties faced by simple models. I shall also briefly discuss the subject of source statistics and whether any of the nearby active galaxies contain black holes.

2. Scales of structure in active galaxies

In discussing active galactic nuclei we are talking about an incredible range of length-scales and variety of phenomena. Fig. 1 illustrates the length-scales from about one

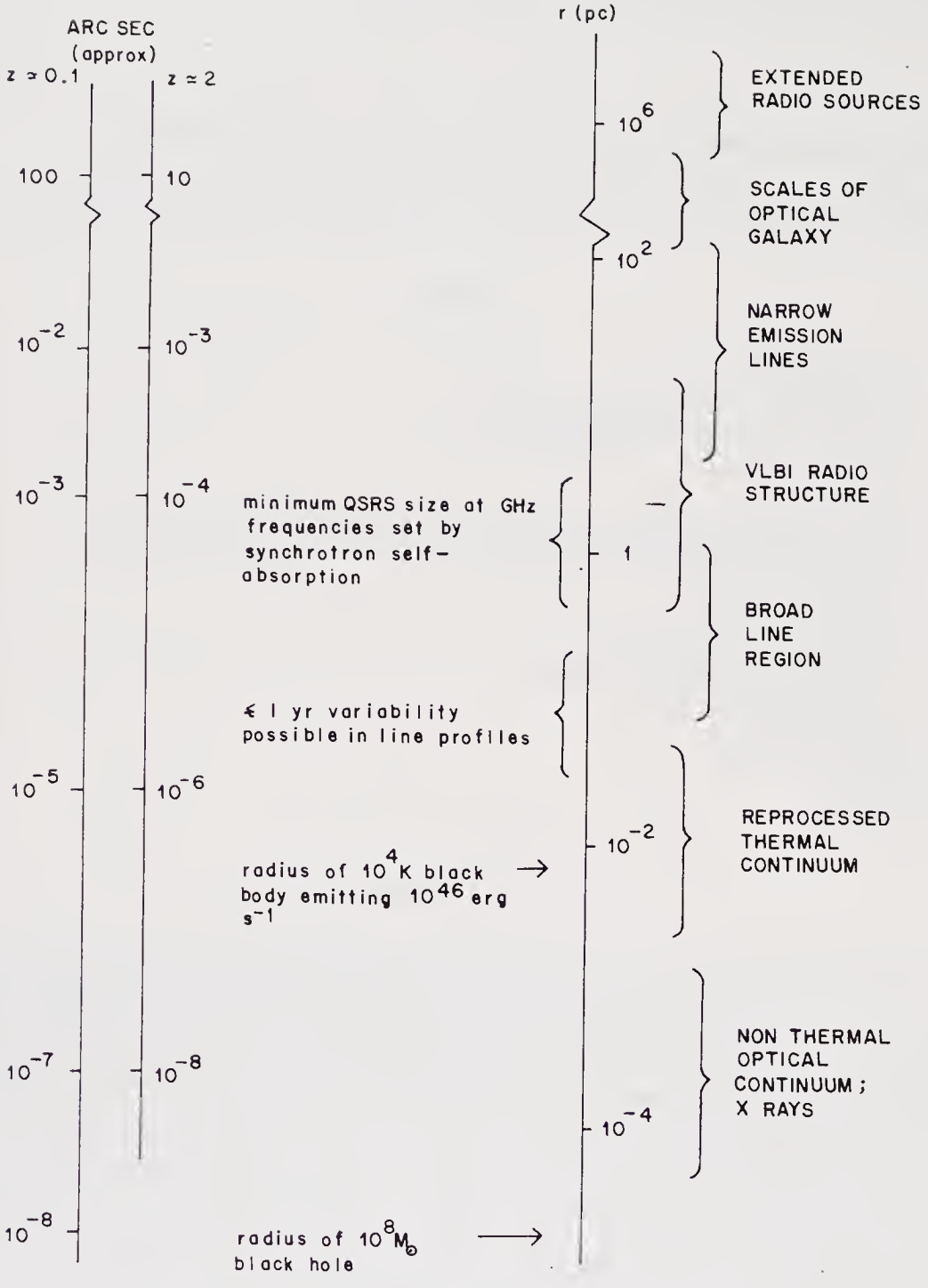

Figure 1. Scales of structure in a typical active galaxy.

light day to around 10^6 pc. The VLBI radio structure appears on the scale of parsecs, but large-scale radio sources may be $\gtrsim 1$ Mpc in size. However we know that these objects emit in various other frequencies as well; the length-scales associated with these emissions are also shown in Fig. 1. The optical emission lines are normally classified into narrow lines (with velocity dispersion of the order of the galactic dispersion) and broad emission lines. We do not know for sure the length-scales associated with the narrow lines; it could be about a hundred parsecs (larger in the more luminous quasars).

Broad-line regions contain higher-density gas and probably occupy scales less than one parsec.

The figure also shows some other relevant length-scales one can infer from simple theoretical considerations. For example, synchrotron self-absorption gives a minimum size for quasars of about one parsec at radio wavelengths. Again the observed variability of the broad emission lines gives an upper bound (about 1 light year) for the broad-line emission regions. Though these are quite small compared to the extended radio source scales (10^6 pc), the length-scale associated with the central engine is still smaller. The region from which the X-ray and optical continuum radiations emerge must be less than a light day across to account for the variability observed in some cases. The figure also shows the necessary size for a blackbody at 10^4 K to emit the observed 10^{46} erg s^{-1}. The size is of the order of 10^{-2} pc; optical emission lines must originate at larger length-scales. Also it is clear that any optical continuum which is rapidly varying must be essentially nonthermal.

The central engine is as far removed (in logarithmic scale) from the VLBI structure as the VLBI structure is from the extended radio structure. If one represents the central region by 1 cm, the radio lobes will be separated by the size of the Earth.

We have enough data on the emission lines to infer some major features of the emission-line region. One finds that no forbidden transition of [OII] is observed implying densities higher than 10^7 cm^{-3}. At the same time, one does see [CIII] (1909 Å) lines which puts an upper bound on the density of the order of 10^{10} cm^{-3}. This high-density cloud must be photo-ionized by the ultraviolet (UV) radiation from the central object; so the clouds are at about 10^{18} cm from the central source. The densities and physical conditions are closer to those in solar prominences than in ordinary HII regions. The current picture models this region as a large number of fast-moving 'clouds' in a rarefied background medium, held by static or ram-pressure balance, but it is unclear how they are moving (outflow? rotational motion? infall?).

3. The role of massive black holes

I shall now describe the 'conventional' model for the central engine which is powered by a black hole. Fig. 2, which is essentially a propaganda poster taken from an earlier paper (Rees 1978), illustrates various runaway processes that can take place in the central core of the galaxy. If you follow the evolutionary track it is hard to escape the conclusion of a black hole. The end point of a dense stellar cluster (such as might exist at the centre of galaxies) can be a supermassive star; a supermassive star could alternatively form directly from infall of gas into the central potential well. However, it is well known that such supermassive objects are quite 'fragile'. For a given central temperature, the radiation pressure dominates the matter pressure for masses above $\sim 10\,M_\odot$. When $P_{\rm rad} > P_{\rm gas}$, the virial theorem implies that, for a given M/R, $aT^4_{\rm central} \propto \rho \propto M^{-2}$, so $T_{\rm central} \propto M^{-1/2}$. This implies $P_{\rm gas} \propto M^{-5/2}$, leading to $(P_{\rm gas}/P_{\rm rad}) \propto M^{-1/2}$. Because of this,

$$(\gamma - \tfrac{4}{3}) \propto M^{-1/2},$$

and thus heavier the star, the closer it is to the verge of instability. But there is a general relativistic correction which makes the critical γ *larger* than 4/3 by an amount of order

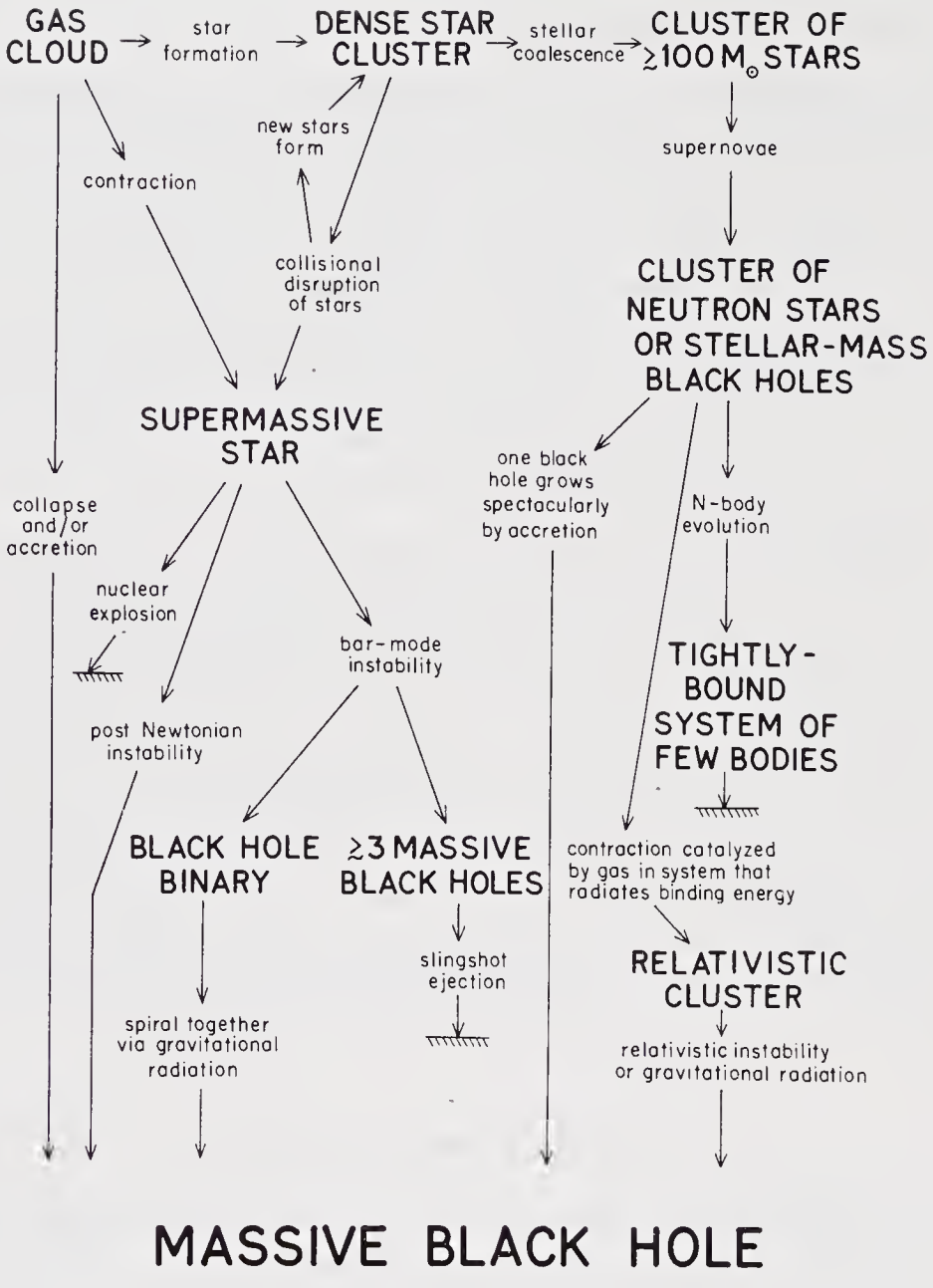

Figure 2. Processes leading to the formation of massive black holes in galactic nuclei.

$(P/\rho c^2)$. It turns out that this instability sets in for $r < r_{\rm inst}$, where

$$\frac{r_{\rm inst}}{r_{\rm Sch}} \simeq \frac{1}{(\gamma - \frac{4}{3})},$$

where $r_{\rm Sch}$ is the Schwarzschild radius. Thus for supermassive objects this instability sets in at much larger radius than the Schwarzschild size. From Fig. 3 we see that a contracting supermassive star with $M > 10^6\, M_\odot$ will become unstable and collapse before it can efficiently produce thermo-nuclear radiation. This leads, again, to a massive black hole.

To summarize, the formation of a black hole is inevitable once a threshold is crossed; if we want the most efficient energy source for our central engine then it is preferable to

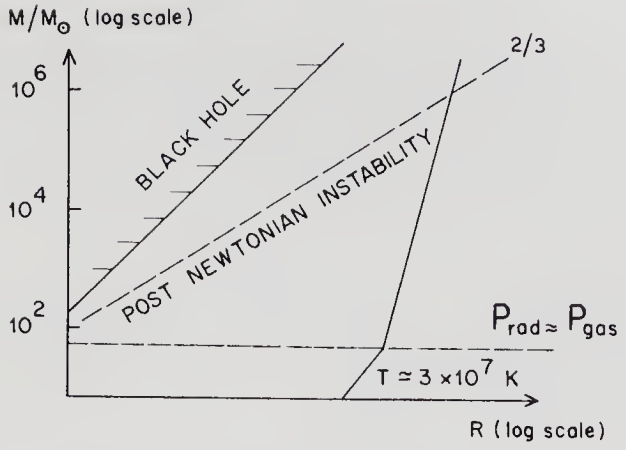

Figure 3. Stability of a supermassive star.

use a black hole. Needless to say, the various evolutionary tracks in Fig. 3 have to be investigated in greater detail, but it is unlikely that the precursors to the black hole will produce a serious alternative model for the most powerful sources (though they may be relevant to lower-level activity in some galactic nuclei).

With this motivation in mind, let us now look at the various processes which occur around the black hole. The Schwarzschild radius of a black hole is given by,

$$r_{\rm Sch} = \frac{2GM}{c^2} = 3 \times 10^8 \left(\frac{M}{10^8\, M_\odot} \right) \text{km}.$$

In other words, black holes with masses $\sim 10^8\, M_\odot$ will have $r_{\rm Sch}$ of about a thousand light seconds. This mass-scale ($10^8\, M_\odot$) is the relevant one for two reasons: (i) It is at this mass-scale that gravity can compete with radiation pressure for quasar luminosities. (ii) This is the sort of value which is required, to produce the energy stored in the extended radio lobes.

It is easy to achieve energies of the order of 100 MeV/nucleon for the material orbiting around the hole at distances less than, say, $10\, r_{\rm Sch}$. This energy release can lead to what may be called a trans-relativistic plasma saturated with e^+-e^- pairs. The effective blackbody temperature for our system—which is the temperature of the blackbody with same radius and luminosity—is given by,

$$T_{\rm bb} = a^{-1/4} \left(\frac{L}{4\pi R^2 c} \right)^{1/4} \simeq 10^6 \left(\frac{L}{L_{\rm E}} \right)^{1/4} \left(\frac{R}{R_{\rm Sch}} \right)^{-1/2} M_8^{-1/4}\ \text{K}.$$

Here we have scaled the luminosity with respect to the Eddington luminosity $L_{\rm E} = 4\pi GMm_{\rm p}c\sigma_{\rm T}^{-1} = 1.3 \times 10^{46}\, \text{M}_8\, \text{erg s}^{-1}$. This value for $T_{\rm bb}$ implies some very general conclusions about the nature of the radiation that escapes from $\lesssim 10\, R_{\rm Sch}$. First of all, X-rays (thermal or nonthermal) can escape and propagate: X-rays require a gas of $\sim 10^8$ K, which is not going to be optically thick at this equivalent blackbody temperature. In the optical band, however, it is not possible to produce thermal radiation (from distances $\sim 10\, R_{\rm Sch}$) and any emission must be nonthermal—with a brightness temperature $\gg$ its colour temperature. In other words the observed thermal component in the optical band must be the result of reprocessing at much larger radii. Again, it is not possible to have any significant radio emission even *via* relativistic synchrotron processes which permit brightness temperatures $\sim 10^{12}$ K. (The syn-

chrotron self-absorption turn-over occurs at a few microns, in the IR region.) Lastly, it turns out that no γ-rays can escape either. This is because in the central regions the pair production cross-section is extremely high, which converts γ rays into e^+-e^- plasma.

In the simplest model one takes the accretion flow into the black hole to be the main source of power. If the accretion flow is denoted by $\dot{M}$, we have

$$\dot{M} = 1.5 \times \left(\frac{\varepsilon}{0.1}\right)^{-1} \left(\frac{L}{10^{46}\,\mathrm{erg\,s^{-1}}}\right) M_\odot\,\mathrm{yr}^{-1},$$

ε being the efficiency factor for converting rest mass into energy. We can also write down expressions for particle density, electron opacity and equipartition magnetic field in this model, with the usual scalings

$$n \gtrsim 10^{10} \left(\frac{L}{L_E}\right)\left(\frac{V_{ff}}{V_{in}}\right) M_8^{-1}\,\mathrm{cm}^{-3},$$

$$\tau_{\text{elec. scattering}} \simeq \left(\frac{L}{L_E}\right)\left(\frac{V_{ff}}{V_{in}}\right),$$

$$B \lesssim B_{eq} = 10^4 \left(\frac{L}{L_E}\right)^{1/2} \left(\frac{V_{ff}}{V_{in}}\right)^{1/2} M_8^{-1/2}\ \text{Gauss}.$$

These expressions depend critically on the ratio of free-fall velocity (V_{ff}) to inflow velocity (V_{in}). The inflow is related directly to the viscosity parameter which, of course, is quite uncertain from a theoretical point of view. For a thin disc one can also write down the ratio of disc thickness, h, to disc radius, R, as

$$\left(\frac{h}{R}\right)^2 \simeq kT_{gas}\left(1 + \frac{P_{rad}}{P_{gas}}\right)\left(\frac{R}{R_{Sch}}\right)\left(\frac{1}{m_p c^2}\right),$$

which is essentially the ratio of thermal energy to gravitational energy. From this it is clear that, to maintain a thick disc ($h \gtrsim R$) at distances of the order of R_{Sch} requires either $P_{rad} \gg P_{gas}$ (*i.e.* $L \simeq L_E$) or $kT_{gas} \gtrsim 100$ MeV. We come to these two possibilities later.

In addition to providing the energy, we also expect the central engine to be responsible for the collimation observed in radio jets. This collimation obviously requires a physically unique direction. One way of modelling this is to consider the central engine to be in a rotating oblate gas cloud in the centre of a galaxy. This was the mechanism in the original Blandford & Rees (1974) model. However there are at least two different reasons for suspecting the collimation to occur very close to the compact object in a relativistically deep potential well: (i) This is the most propitious place for generating a high energy per particle; (ii) long-term stability of the jet axis can be ensured by the 'gyroscopic' effect of the central spinning body—in other words, one can use the rotation axis of the black hole to provide the collimation of the jet.

If the collimation of the jet takes place so close to the black hole, then one has to consider the general-relativistic effects seriously. It turns out that three such effects play an important role. We will discuss them one by one.

The first is what is called the 'dragging of inertial frames'. A rotating black hole tends to drag orbiting objects along with it. More precisely, the orbits around a rotating black hole precess with a period,

$$t_{prec} \simeq t_{Kepler}\left(\frac{r}{r_{Sch}}\right)^{3/2}\left(\frac{J}{J_{max}}\right)^{-1}.$$

If we have an accreting disc around such a black hole, this precession tends to align the disc material around the hole to be axisymmetric with respect to the hole axis. This generally occurs, as shown by Bardeen & Patterson (1975), for distances smaller than a critical radius (r_{BP}) which is the radius at which the precession timescale equals the inflow timescale. Thus the spin axis of the black hole provides the necessary collimation direction. This axis is quite stable and can change only very slowly, on a timescale $\sim M/\dot{M}$.

The second relativistic feature is that circular orbits cannot exist too close to a black hole—there is a minimum angular momentum for a stable or bound circular orbit. If one considers particle orbits around a black hole there arises a region where no stationary flow pattern can exist. In other words particle 'orbits' in the funnel region have either (i) sufficient energy to escape to infinity or (ii) sufficiently low angular momentum to be swallowed by the black hole. Thus an axisymmetric flow pattern around such a black hole can never extend into the funnel region around the rotation axis (Fig. 4).

Detailed models have been developed for thick accretion discs (or tori) where radiation pressure balances the gravitational and centrifugal pull throughout the disc (Fig. 4). In the funnel region, the radiation flux must balance very strong centrifugal effects, giving a large 'effective gravity' for this part of the torus (and thus there will be more radiation along the funnel). The rest of the torus radiates thermally at about the Eddington luminosity. The detailed structure, equilibrium and stability of these thick tori are still subjects of active research and controversy.

This general picture may be correct for a radio-quiet quasar, which emits a good

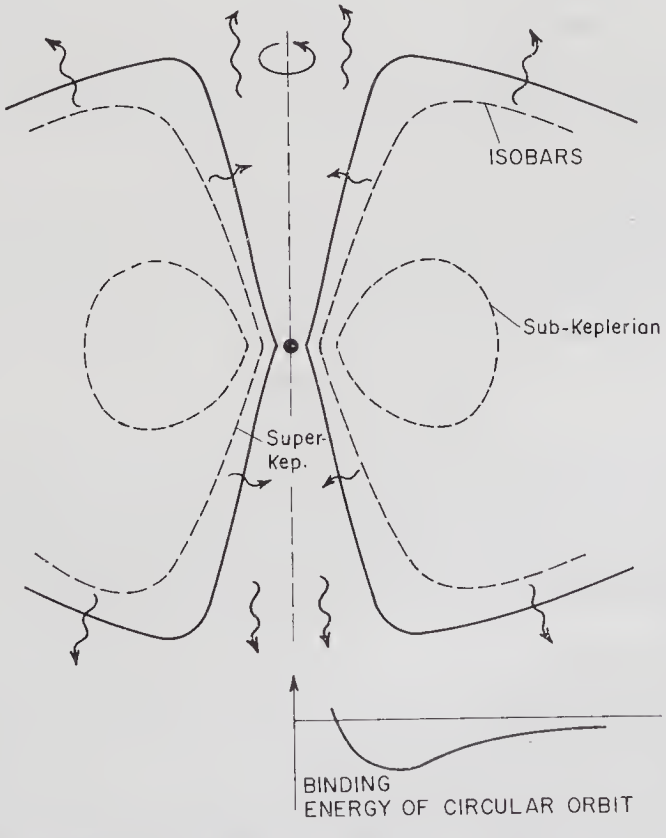

Figure 4. Thick accretion disc supported by radiation pressure.

amount of optical and UV thermal radiation. However, there does exist another class of objects, the so-called strong radio galaxies (*e.g.* Cygnus A). In such objects rather little thermal radiation is seen from the nucleus, but a large power is nevertheless being beamed out to the radio lobes. The total energy content of these lobes implies that the central mass involved must be $\gtrsim 10^7 M_\odot$. A radiation-supported disc certainly cannot do the job here. I shall discuss later a model in which thick tori are supported by the (high temperature) gas pressure.

The third distinctively relativistic effect is that a spinning black hole is a latent source of enormous power; magnetic fields threading a black hole can drive a current system to extract its rotational energy. I shall return to discuss this later.

An important class of accretion flows are those where a thick accretion disc or torus, supported by radiation pressure, acquires a narrow funnel along the rotation axis along which radiation is preferentially leaking out. I mentionud earlier that even though this sort of model might be relevant for radio-quiet quasars, it might not be the correct model for radio-loud galaxies like Cygnus A. This is because in such objects, no thermal radiation at the Eddington luminosity ($\gtrsim 10^{45}\,\mathrm{erg\,s^{-1}}$ for $M_{\mathrm{BH}} > 10^7 M_\odot$ which is relevant for Cygnus A) is seen from the nucleus, in contrast to what is predicted by the radiation-supported disc models. This motivates one to consider a different class of accretion flows for such strong radio galaxies, the so called *ion-supported tori.*

In ion-supported tori (Fig. 5), the accretion rate is very low and the material is held up by gas pressure rather than radiation pressure. We now consider the consequences of an accretion rate which is very low, far lower than required for emission at the Eddington luminosity. Radiation pressure is then unimportant. Further, if the density is very low, then cooling time may be long compared to the dynamical timescales and eventually if we make the density sufficiently low, it may happen that gas swirls all the way into the black hole, before it has time to cool. It will then acquire a temperature such that $kT \simeq GM/r$ from viscous dissipation; gas pressure may thus support a thick disc structure when the inward drift timescale is shorter than the cooling timescale (it may also then be shorter than the electron–ion coupling timescale). If these conditions hold, then much of the energy liberated in the accretion process (remember we have kinetic energies of ~ 100 MeV per particle available) would remain as thermal energy of the *ions* and not be radiated away, even though relativistic *electrons* can almost always radiate efficiently by synchrotron or Compton processes. We then have the possibility of a thick structure supported by ion pressure. The condition for this 'inefficient cooling' is

$$\frac{\dot{M}}{M_{\mathrm{crit}}} < 50 \left(\frac{V_{\mathrm{in}}}{V_{\mathrm{ff}}}\right)^2.$$

If the material were falling almost radially inwards the above condition is very easy to satisfy; but even for a low viscosity (so that V_{in} is very small compared to V_{ff}, more time is available for cooling, and there is a higher density for a given $\dot{M}$) this condition can be fulfilled for sufficiently low $\dot{M}$. From now on we consider the case where this condition can be satisfied.

What we will then have (Rees 1982) is the same sort of geometry as before, a thick torus, but held up by the pressure of the hot gas (primarily by the ions since $T_{\mathrm{i}} > T_{\mathrm{e}}$). This situation prevails, however, only for very low accretion rates and inefficient cooling; one may therefore feel that this is a doubly unpromising model for energizing something as powerful as a radio galaxy. That would be the case if it were not for the third of the inherently relativistic effects, which I mentioned last time.

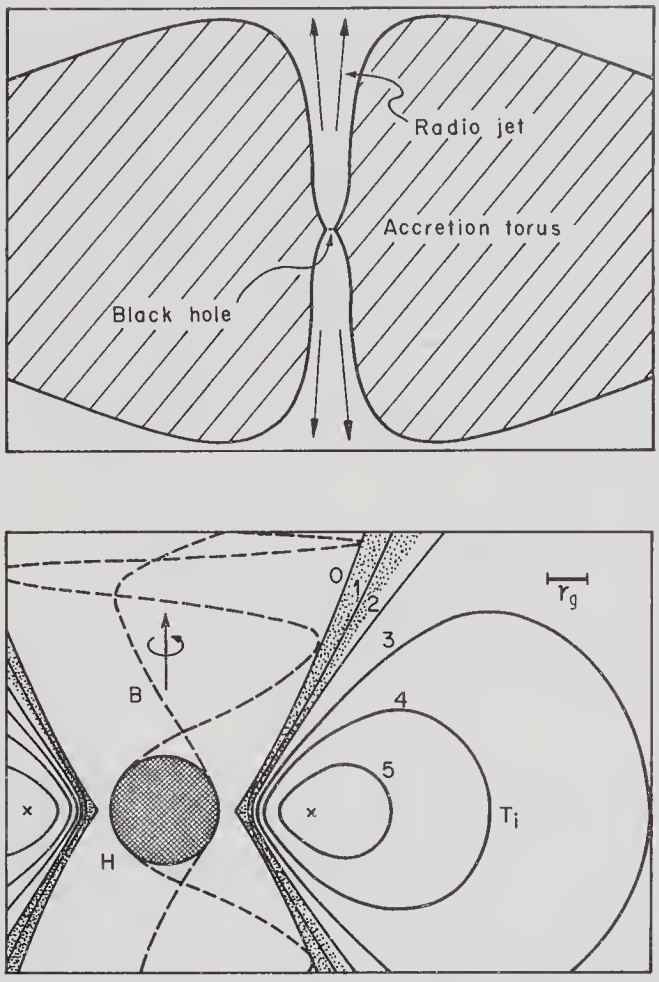

Figure 5. Accretion torus surrounding a spinning black hole supported by ion pressure. Contours of ion temperature (in units of 10^{11} K) are shown in the inner regions of the torus. (Adapted from Rees 1982).

This is an effect whereby you can actually extract energy from a spinning black hole, provided magnetic fields coupled to some external current system thread the horizon. Loosely, the horizon around such a black hole resembles an inside-out light cylinder around a pulsar, where strong $\mathbf{E} \cdot \mathbf{B}$ forces generate energy which will go preferentially into fast particles. The discussion of this is rather technical and I will not go into the details. Work on black holes and black-hole horizons in the last few years has shown that there are very close analogies between the horizon of a black hole and a rotating conductor. The essential reason for this is that if you consider electromagnetic fields near black holes, there is in effect only a certain angle at which the electric and magnetic lines of force can cross the horizon. This is analogous to the case for an ordinary conductor: the electric field must be normal to the conductor surface for a perfect conductor; for a spinning imperfect conductor in an imposed electromagnetic field, the angles made by the **B**-field, and the $\mathbf{E} \cdot \mathbf{B}$ forces can be calculated. Consider a highly artificial situation where we have a rotating black hole in the centre and at large radius we have a shell of some small resistance, say copper, around it (see Fig. 6). (You must be familiar with the laboratory situation of the unipolar inductor, where one has a rotating conductor inside a conducting sphere and generates electric potential and currents around the circuit.) It turns out that for a rotating black hole which has magnetic fields

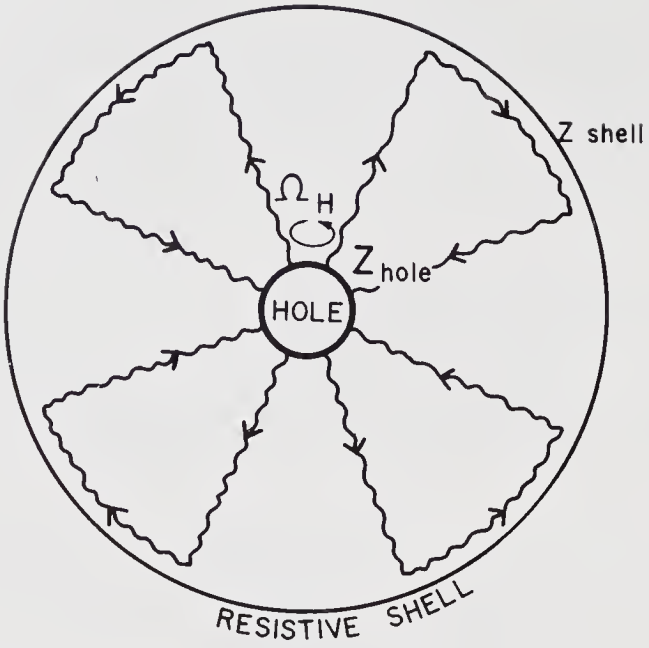

Figure 6. Rotating conductor analogy for black hole and its horizon.

threading the hole, you can get a similar effect. Pioneering work on this was done by Blandford & Znajek (1977) and later by Macdonald & Thorne (1982) and Phinney (1983). Three requirements must be fulfilled: (i) a magnetic field system, threading the hole; (ii) a current system flowing 'through' the hole (which is schematically shown in Fig. 6) and (iii) for maximal power dissipation in the 'shell' one needs to have a matching of the effective resistances of the shell and the hole: *i.e.* $Z_{\rm shell} \simeq Z_{\rm hole}$ (where $Z_{\rm hole}$ is $\sim$ 30 ohm, the effective resistance in free space). This is an idealised situation, but it illustrates how a substantial fraction of a hole's rotational energy (up to 29 per cent of its total mass-energy) can in principle be extracted.

If a magnetic field B threads the hole, then one can estimate the power which can be extracted from the spin energy of the hole to be $\sim B^2 r_{\rm grav}^2 (J/J_{\rm max})^2 c$. This is, roughly speaking, (the magnetic stress) $\times$ (the area of the hole) $\times$ (velocity of light) $\times$ (the angular momentum parameter of the hole)^2; $J/J_{\rm max}$ is the Kerr parameter a/m. The magnetic field must be produced by currents *outside* the hole—any external field due to material that falls into the hole would decay away on a timescale $\sim r_g/c$. The main role of the torus in these accretion flows is thus to 'anchor' the magnetic field lines that thread the hole. The torus therefore has to be a good enough conductor so that currents which produce magnetic fields can be set up in it. Even though the torus itself may not release much energy it acts as a catalyst for the efficient extraction of the black hole's spin energy. To give some idea of the large amount of energy available, let us consider some large but not absurd parameters for the black hole. Suppose you have a $10^9\ M_\odot$ black hole with $J \simeq J_{\rm max}$, then enough rest-mass energy can be extracted as spin energy and this can power a source of luminosity 10^{45} erg s^{-1} for several times 10^9 yr. This may be a way therefore to power nonthermal nuclear sources in galaxies.

Let us go back to the physics of how this might happen. We argued that the torus heats up to about 100 MeV per nucleon. This will be the temperature of the ions (the electrons may be cooler since they will radiate but we assume that they are not strongly coupled to the ions). Fig. 5 shows the ion temperature in units of 10^{11} K (10 MeV) near

the black hole. Now this torus is not radiating very much, but anything it does radiate will primarily be γ-rays (from bremsstrahlung of the relativistic electrons). All we need is that a few pairs of these γ-rays interact with each other in the funnel region and produce electron–positron pairs. These can then drive a current system made up of electrons and positrons. One can calculate that enough pairs are produced to set up the current system. In this way one can have a current system, with currents (as well as magnetic fields) going 'into' the rotating hole. This of course results in enormous electric fields near the hole along the rotation axis in analogy with the case of a unipolar inductor (an enormous $\mathbf{E} \cdot \mathbf{B}$ term), and can generate very-high-energy particles going out along the funnel.

One would like to know exactly what form this wind will take and whether one can in principle get the necessary efficiency. Shown in Fig. 7 is the engineers' version of the same circuit (from Phinney 1983). The potential that is available is very large:

$$V = 10^{19}\left(\frac{B}{10^4\,G}\right)\left(\frac{M}{10^8\,M_\odot}\right)\frac{\Omega^H}{\Omega^H_{\max}}\ \text{Volts.}$$

People who know about pulsar theory would not be surprised by this—there again the maximum available $\mathbf{E} \cdot \mathbf{B}$ is very large. This is the upper limit to which you can accelerate particles, but if too many particles are injected the field is 'shorted out' and this limit is never reached.

Let us come back again to the physics of the accretion torus and the consistency requirements that we had outlined earlier. One of these was that the ion–electron coupling timescale should be greater than the inflow time. This is to ensure that the ions do not cool down even if the electrons do, but remain at a high enough temperature ($kT_i \simeq GM/r$) to support the torus. (This is the reason for the nomenclature *ion*-supported torus rather than *plasma*-supported torus). In calculating this (Rees 1982) we have assumed that the coupling between electrons and ions is provided by Coulomb scattering alone. One question which arises is whether in this context there will be other more efficient collective plasma processes which will couple the ions and the electrons? If there are, then the model may not work in this form and the torus will deflate. I have tried to consult a lot of plasma physicists on this question, but do not yet have an agreed answer. There are bound to be shearing motions, due to the differential rotation in the torus, which generates local pressure anisotropies in the ion plasma and the electron plasma. There are certain instabilities which isotropize the ion plasma and also those which isotropize the electron plasma. The key question—which still seems open—is whether these isotropization processes which act on ions and on electrons transfer energy *from* ions *to* electrons. If they did, then the electrons would drain away the thermal energy of the ions and a thick torus supported by ion pressure would be

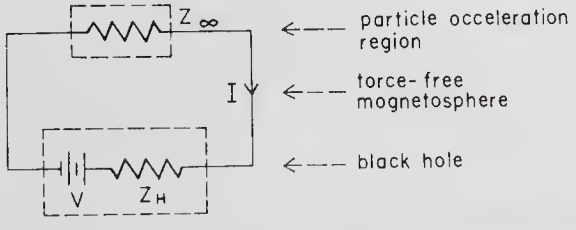

Figure 7. Engineer's version of high-energy-particle generation in the funnel region (from Phinney 1983).

impossible. We might still be able to have a thin magnetized disc [as Blandford & Znajek (1977) envisaged] but then may be unable to get the good initial collimation that a thick disc provides. To summarise, the ion-supported torus offers a way of producing energy in the form of ultra-relativistic electron-positron jets, without producing a lot more energy from thermal radiation at the same time.

I conclude this section with a brief digression for the benefit of relativists who may be concerned about the electric charge on the black hole. When a gravitating system is electrically charged, the gravitational effect of the charge (and, more generally, of the electromagnetic field) modifies the Kerr metric to the more general Kerr–Norman form. The charge Q becomes significant if $Q^2 \simeq M$, which requires a fractional deviation f from charge neutrality of order $\mathcal{N}^{-1/2}$, where $\mathcal{N} = e^2/Gm_p^2 \simeq 10^{36}$. Any gravitating plasma body (even the Sun) acquires a charge such that the electrical and gravitational binding energy of an electron are comparable. However, the value of f needed to provide a surface potential of even 10^9 V is $\mathcal{N}^{-1}$, and for this value, Q^2/M itself is only of order $\mathcal{N}^{-1} \simeq 10^{-36}$. Even if the hole is charged to the potentials $\sim 10^{20}$ eV discussed above, the value of Q^2/M is still only of order 10^{-15}. [A related statement is that the magnetic energy density in realistic accretion flows is $\lesssim 10^{-15}$ of $(M/r_g^3)\,c^2$.] We are thus justified by a large margin, in treating the space-time as given by the ordinary Kerr metric.

4. Scaling laws

Although I introduced these accretion flows (the radiation and the ion-supported tori) in the context of $10^8\,M_\odot$ objects, which are relevant perhaps for the nuclei of radio galaxies, there is really no preferred scale in the relevant physics. We can genuinely imagine scaled-down versions. To make this explicit, let us consider an object with a given mass M and luminosity L. Let us now consider a 'miniature' version with mass $M' = xM$ and luminosity $L' = xL$ with $x \ll 1$. Clearly we have done the scaling in such a way that the ratio L/L_E is the same, *i.e.* the relative dynamical effects of radiation pressure and gravity are the same. But the nontrivial point is that under this scaling one automatically gets another ratio to scale, namely the ratio of the cooling time to the dynamical time. This is because we have, for a given efficiency $\dot{M}' = x\dot{M}$, and the density $\rho' = x^{-1}\rho$ (since $\rho \propto \dot{M}/r^2$ and $r' \propto xr$). The cooling time t_{cool} (which is $\propto \rho^{-1}$) therefore scales as $t'_{cool} = xt_{cool}$. This scaling holds not just for two-particle cooling processes such as bremsstrahlung, but also for synchrotron cooling rates ($\propto B^2$) if B scales $\propto \rho^{1/2}$ so that the magnetic stresses are a fixed fraction of total pressure. Now the dynamical timescale at a given multiple of the gravitational radius scales as $t'_{dyn} = xt_{dyn}$, since all linear dimensions like r_g have scaled down by x ($r'_g = xr_g$). This implies that the ratio of the cooling timescale to the dynamical timescale is the same in both the original and the scaled-down version. And it is basically this ratio which determines what the temperature is going to be at a given part of the disc (though opacity effects may complicate the picture somewhat). So there is more than a crude analogy between the scaled-down object and the original one. There might therefore be a genuine physical similarity between quasars and smaller-scale phenomena. This at least, motivates one to search for a classification scheme for different types of galactic nuclei. We outline below such a classification scheme.

The flow pattern, and the question of whether we have a radiation-supported torus

Table 1. Physical classification of active galactic nuclei.

M	$(L_A/L_E) \gtrsim 1$ Smothered	$(L_A/L_E) \ll 1$ Semi-starved
$10^9 M_\odot$	Optically-selected QSOs	M 87; Radio galaxies
$10^6 M_\odot$	Seyfert galaxies	Galactic centre
$(1–10) M_\odot$	SS 433	Radio stars; γ-ray sources

or an ion-supported one, depends on the accretion rate $\dot{M}/\dot{M}_{crit}$ (or L_A/L_E, where L_A denotes the accretion-powered luminosity). We can then distinguish two cases which I call the 'smothered' case and the 'semi-starved' case: in the first, the accretion luminosity is greater than the Eddington luminosity and we have radiation-supported tori; in the second it is much less than the Eddington luminosity, but the cooling is low enough so that we can set up an ion-supported torus. The tentative suggestion I wish to make is that when the masses are 10^8–$10^9 M_\odot$, the smothered case may be relevant to the bulk of quasars which are basically radio-quiet and where the main radiation mechanism in the optical could resemble the photosphere of a hot star (Table 1). (There could be some polarization but only what arises from electron scattering in non-spherical geometry.) On the other hand, the radio galaxies like Cygnus A and M 87—where there is reason to believe that there may be very massive black holes, but where one does not see much thermal radiation from the nucleus—must be cases where $\dot{M}$ is low, but an ion-supported torus extracts energy from a spinning black hole. These 'semi-starved' holes generate primarily nonthermal phenomena and jets. Of course, we have to consider where radio-loud quasars fit in: these could have a thermal luminosity at the Eddington limit, but also have strong radio jets. There are two uncertainties here, if we hope to formulate a 'unified' model for all active nuclei. One is the uncertainty about orientation effects, which could be very important especially if there is relativistic beaming. The other uncertainty concerns whether a 'smothered' black hole, radiating $L \simeq L_E$ thermally, could also be releasing some extra energy from its spin if magnetic fields anchored deep in the radiation-supported torus are threading it. (Although we discussed this process for ion-supported tori, there is no reason in principle why a similar process cannot operate also in a radiation-supported one. In this case one could get *much more* than the Eddington limit by extracting the spin energy of the black hole and at the same time have thermal radiation coming out at the Eddington limit.) This could be relevant to some class of quasars.

5. Physics of radio jets

Let us now turn to the physics of largescale radio jets. Any theory of radio sources has in effect three basic ingredients. In the beam-type model the basic picture involves: (i) a source of relativistic plasma in the centre, (ii) some bifurcation and collimation mechanism, *i.e.* a way in which relativistic plasma can be squirted out preferentially in two opposite directions, and (iii) a place far away where the beam of relativistic plasma is stopped by interaction with the intergalactic medium, in a shock front. In this region one has a hot spot, and also a surrounding cocoon (composed of material which came out in the beam and was shocked) extending sometimes all the way back to the central source. The speed of advance of the beam, V, is governed by ram pressure balance—the

balance between the momentum density in the beam and the $\rho_{ext} V^2$ pressure force exerted by the surrounding medium. The beam energy is randomized by a shock when it impinges on the external medium; the particles here are accelerated and these regions are identified with the 'hot spots' in the radio source components. The relativistic plasma then accumulates in a cocoon of lower energy density and lower radio emissivity (see Fig. 8).

I would like to re-emphasize (*cf.* Fig. 1) that many powers of ten difference in scale are involved: even if collimation is initiated on the scales of 10^{15} cm or less, the jets may face many vicissitudes before they can actually get out to the much larger distances where we observe the radio phenomena. They may be destroyed and recollimated; they could even change direction. The smallscale jet may be lined up with the direction of the rotation axis of the central massive object while the largescale one may lie along the rotation axis of the galaxy.

A few comments now about the 1–100 kpc jets which are mapped with the VLA. The first point to emphasize is that we are probably justified in thinking of jets as basically fluid phenomena and using fluid dynamical analogies, the reason being that the gyro-radius, $m_e v_e \gamma_e / eB$, for the particles in the jet, and the debye length, $(kT_e / n_e e^2)^{1/2}$, are both always *much* less than the jet dimensions. This means that charge neutrality is closely satisfied, (unless the particles have energies of 10^{19} eV) since you can only separate the charges to a length-scale of the order of a Debye length; also the relative velocities of the electrons and ions are small. In effect, the flow is fluid-like and the MHD approximation is valid. (As in the solar wind, even though the mean free path for two-particle collisions is very large, the presence of even small amounts of magnetic fields makes the plasma fluid-like.)

What confines the jets? The first thing to consider is whether they are just confined by the external pressure. Do they just widen as the external pressure drops, going first from the galactic nucleus out to the body of the galaxy, and then from the galaxy to the intergalactic medium? If so, and assuming that the material flows along the beam just like an adiabatic fluid, one can use Bernoulli's equation to work out how the beam widens as the external pressure drops off. When the flow is supersonic the beam widens only gradually, the diameter d changing as $p_{ext}^{-(0.2-0.3)}$, depending on the equation of state of the beam material. [Note that the gross features of the model for VLA-scale jets do not require the plasma in the beam to be all relativistic, in the sense of having p/ρ

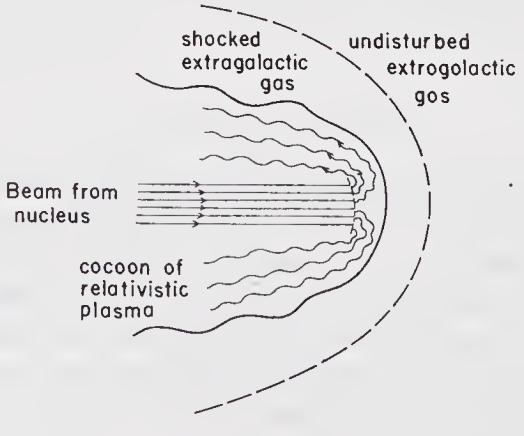

Figure 8. A very schematic picture of the structure of a radio source component. (More realistic flow patterns have been computed by e.g. Norman *et al.* 1983).

$\simeq 1/3\,c^2$ and containing no 'cold' material. All that is important, is that $(p/\rho)^{1/2}$ (the internal sound speed) should exceed the escape velocity from the galaxy so that the beam is unaffected by gravity. Actually the jet cannot be strictly adiabatic since some internal dissipation has to take place to accelerate the relativistic electrons which make the jet detectable. The pressure inside the jet must really, therefore, fall off more slowly than in the adiabatic case, and hence the jet should widen slightly faster.]

The other possibility is that the jets are not confined at all and are what are called 'free jets'. This is possible if the jet is flowing at a speed which is very large compared to its internal sound speed. If one took away the external pressure, the jet would widen transversely at its internal sound speed, but if this were very much less than the outflow speed then the jet could remain a fairly narrow one. A 'free jet' requires the Mach number to satisfy $M > \theta^{-1}$, where θ is the opening angle. It could be that some of the observed jets alternate between being confined and free as they move out. This would happen, if at some stage in the jet's journey through the galaxy, the external pressure dropped so fast that the jet material could not expand sufficiently rapidly to come to pressure equilibrium. At this stage the jet would be 'free'. Later, farther away from the centre of the galaxy when it has once again reached pressure equilibrium, it may again be confined. When the jet is free, dissipation is less and such regions might be identified with gaps along the jet.

What about magnetic fields in the jet? If $v_{\rm jet}$ is uniform over the jet cross-section (*i.e.* there is no shearing motion), and if there is no entrainment of magnetic fields, then flux conservation implies that the magnetic field's perpendicular component $B_\perp \propto d^{-1}$ and the parallel component along the jet $B_\parallel \propto d^{-2}$. This means that as the jet moves out, the field switches from predominantly parallel to perpendicular. This picture is however complicated by shear, since even quite a small velocity gradient could regenerate $B_\parallel$ from $B_\perp$: all one would need is $\Delta v/v \gtrsim d/l$, where l is the length of the jet.

Now there are some observed jets, whose minimum internal pressure is inferred from equipartition arguments, where pressure balance seems incompatible with what we know about the external medium. This has led some people, particularly Henriksen and collaborators, to propose 'magnetic self-confinement' of jets. I am not quite sure how plausible this is on stability grounds, but it is certainly physically possible for a jet to be confined not by external pressure but by a magnetic field. This requires a magnetic field wound around the jet; a nonzero B_ϕ decreasing away from the axis roughly as d^{-1}. The external pressure could then be balanced by $B_\phi^2(d_{\rm max})/8\pi$, the core of the jet (of diameter, $d_{\rm c} \ll d_{\rm max}$), being overpressured by a factor $(d_{\rm max}/d_{\rm c})^2$. Of course one of the problems is that the polarization data tell us that the magnetic field does not seem to have this configuration.

Another way out of the problem that is posed by some jets, whose internal pressure seems too large to be balanced by an external medium, is to say that perhaps they are not really confined at all. The possibility here is that a rather cold jet is in some places being shocked, and the radiation that one sees is coming from the shocked material. This might happen in the following way. Supposing the nozzle which is squirting out the jet ejects material with a velocity that is not constant. Then the fast bits will tend to catch up and try to overtake the slower bits ejected earlier. (If you moved at the mean velocity of the jet, you would see some parts of the jet lagging behind, and some parts gaining on you.) Internal shocks would then develop in the jet, where the relative kinetic energy of the fast and slow bits would be randomized. These could be sites where particles are accelerated which then escape sideways without being confined. If these

shocks continue one always has freshly accelerated particles. If you saw regions like this you might be misled into inferring that the jet had to be confined by a pressure equal to the pressure in the shocked regions. It is possible that most of the jet material is cold and one is not seeing it; the regions one sees are places where there are internal shocks and randomization of some of the bulk kinetic energy in the jet.

Realistically, the contents of the jets are going to be just as complex and inhomogeneous as the interstellar medium is. In principle the beam material could consist of cool cloudlets embedded in hotter material. This colder material could be produced by entrainment of cool gas, by thermal instabilities or by cooling behind internal shocks. This is relevant to some cases where there is evidence for emission lines with generally low velocities associated with the jet. In SS 433 we certainly know that material is moving out at $\sim c/4$ but is in the form of tiny cloudlets that are emitting optical emission lines. We should remember therefore that the beam contents can be rather complicated.

As jets propagate out, we expect there to be entrainment. This could be due to Kelvin–Helmholtz instability at the boundary or sweeping-up of material expelled from stars along the jet's path; it could be important in decelerating low-powered fast jets.

Apart from the confinement problem, there are other environmental effects which are going to have an influence on jet shapes, and which one infers must be present from the complicated and asymmetric structures that are revealed by the VLA. One such environmental effect is 'side winds'. If a jet is exposed to an external medium moving transversely to it, then a sideways pressure gradient will cause the jet to bend. This situation could obtain if (say) the parent galaxy were moving through the intergalactic medium. This is almost certainly what is happening in the radio trails of NGC 1265. One can work out the details of jet bending due to 'side winds'. If R is the radius of curvature of the jet's path and M is the Mach number, then one requires that $M \lesssim (R/d)^{1/2}$. If this inequality is fulfilled then one has $\Delta P/P \simeq (d/R)^{1/2} M$, where ΔP is the extra external pressure on one side of the jet. For a side wind blowing at its internal sound speed, $\Delta P \sim P$, applied to NGC 1265 and similar sources, this model can account for the drastic bending observed (Begelman, Rees & Blandford 1979). Some people (Smith & Norman 1981 and references cited therein) have considered whether buoyancy effects could cause bending in some sources. In general this can only be a 'gentle' effect since $\Delta P/P \approx (d/\text{scale height})$, and this is in general small for narrow jets.

The other type of distortion (which I shall return to later) is 'precession'. Some sources have so-called 'inversion symmetry' (or S-type symmetry). It is uncertain whether these really involve precession (since the phenomenon can be interpreted otherwise); and even if it is precession it is not clear whether it stems from precession of the central source, or is an effect on the scale of the whole galaxy.

The amazing thing about the jets that we see is their stability. Jets in tailed radio sources can bend through 90° without breaking up. How can we learn more about jets and their stability? I am pessimistic about doing analytical work on jet instability because one can only tackle very idealized cases. One way of studying jets is by detailed numerical computations. Norman *et al.* (1982) have done 2-dimensional hydrodynamical computations which show that it is indeed possible to propagate a jet without instabilities destroying it completely, at least as far as their 2-D code is able to address the question. Eventually 3-D computations will be needed to understand jet

flows. Another possible way of learning about jets is by wind-tunnel experiments. One can in principle learn a lot by firing a jet sideways into a supersonic flow and seeing if one can simulate anything like a bent source. One could also perhaps do the experimental analogue of this problem by firing particle beams or laser beams into the atmosphere.

Let me just interject a comment about how one is going to learn more about this subject. In Section 3, I talked about rather exotic physical processes which occur in regions less than a light day across, involving plasmas under much more extreme conditions than those which people normally study (e^+–e^- plasmas, *etc.*) and involving some inherently relativistic effects. We are using here physics that we do not know too well. Moreover, we know Einstein's theory really well only in the weak field limit. It would be interesting in this context to try and get hold of a diagnostic, by using our study of active nuclei, to *test* strong-field general relativity; to learn whether the spacetime around a rotating black hole is indeed described by the Kerr-metric. This is an extra motivation for our study of active galactic nuclei.

In extended sources, the physics is not so exotic. However it is here that I am more pessimistic about making progress. This is because around the compact object discussed earlier on, even though the physics is exotic, it is a fairly clean problem: axisymmetric flow in a calculable gravitational field. On the other hand, in the largescale sources environmental effects are plainly crucial: it is rather like meteorology. Weather prediction is difficult even though it does not involve exotic physics, and it may be correspondingly hard to interpret the detailed morphology of these sources. If we want to learn something of novelty and importance for physics, it is more important to understand the compact sources (also it is in a sense easier). To use a possibly unsavoury analogy, a mushroom cloud reveals rather little about the initiating thermonuclear event; by scrutinizing the shape of these big double radio sources, you don't learn much about what generates the energy and produces the relativistic jets.

It seems, from the above discussion, that jets may originate as relativistic plasma. We also know that on the VLBI scale there does exist evidence for relativistic motion. This leads one to explore the question: What is the velocity of the material which we observe at much longer, VLA lengthscales? Are the jets relativistic, or are they of much slower velocity?

Let me first examine arguments *in favour* of relativistic velocities for the jet. Basically there are three reasons for this belief. First, if the jets are relativistic to begin with, then it is very difficult to slow them down (in going from VLBI to VLA scale) without dissipating much of their energy. This would vastly reduce the energy content of the jets and thus the deposit of energy on the hot spots. This shows that if the small-scale structure is relativistic, then it is unlikely that the largescale structure is not.

The second argument is based on the powerful sources like Cygnus A. In order to have an energy deposit of $> 10^{44}$ erg s^{-1}, one does require high velocities if the mass flux has to be kept to 'reasonable' values. In other words, a plausible upper bound to the mass that is available for transport sets a lower bound on the jet velocity.

The third argument concerns the existence of one-sided jets. When the jets are one-sided the VLA scale and VLBI jets point in the same direction. The conventional interpretation uses the concept of 'Doppler favouritism' to account for this, which again involves relativistic velocities. It is worth emphasizing that the restriction on orientation of the jet in this case is not at all severe (unlike, for example in the explanation of superluminal separation). In the case of jets shown in Fig. 9, the Doppler

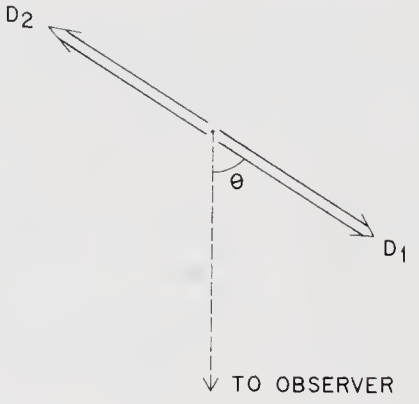

Figure 9. Geometry of the jets relative to the observer.

factors for jet 1 and jet 2 are

$$D_1 = \frac{1}{\gamma_{\text{beam}}[1-(v/c)\cos\theta]},$$

$$D_2 = \frac{1}{\gamma_{\text{beam}}[1+(v/c)\cos\theta]}.$$

Thus, in a steady jet, the surface brightness goes in the ratio of

$$R = \left(\frac{1+(v/c)\cos\theta}{1-(v/c)\cos\theta}\right)^{2+\alpha}.$$

For $v \simeq c$, R can be quite large even for a 'typical' orientation. In a random distribution, $\theta < 60°$ in 50 per cent of the cases; for $\theta < 60°$ the ratio is larger than 20. If we take θ less than 45° (which may occur in some 30 per cent of the cases) the ratio is larger than 150. This shows that as long as jet velocities are relativistic, one-sided jets are easily explained in the above manner without requiring any special orientation. (Compare this with the case of superluminal motion where one needs $\theta < 12°$ to get a value of $v_{\text{app}} > 5c$). The above numbers, of course, get somewhat modified when we take v/c to be less than one, but the basic point does not change.

Let us now look at the counter-arguments which suggest that the jet velocities are smaller (*i.e.* the jet is nonrelativistic). The first argument is based on the existence of bent jets in many sources (van Groningen, Miley & Norman 1981). This bending causes a large change in the Doppler factor if the jets are relativistic. The absence of any drastic change in the surface brightness across the bend puts a bound on the velocity. This argument of course assumes that the bend physically changes the direction of the jet.

There exists a 'model-dependent' argument which suggests $v \ll c$ for sources which have an inversion or reflection symmetry: an interesting model for such sources invokes the effect of galactic environment (Blandford & Icke 1978), which is not possible for $v \sim c$. One needs the jet to be very slow to make this model work.

Evidence for internal Faraday rotation (*e.g.* in NGC 6251) would require thermal plasma in the jet. The energy flux would then be embarrassingly high unless the jet velocity were less than about $10^4\,\text{km s}^{-1}$. However, it is extremely difficult to obtain reliable values for Faraday rotation, and hence it is not really possible to use this criterion in practice. But one can use the fact that any jet will be sweeping out the material ejected from stars (stellar winds, supernova remnants, *etc.*) in its path to put an

independent bound on the energy flux. This argument rules out $v \sim c$, at least in the low-powered jets.

If one takes the point of view that jet velocities are nonrelativistic, then one-sidedness cannot be attributed to Doppler favouritism and must be an intrinsic property. There could be a 'flip-flop', the jet being ejected in one direction for some time and in the opposite direction after the 'flip'. Evidently, the timescales for these reversals must be larger than the intrinsic jet timescale,

$$t_j = (\text{jet length})/(\text{jet velocity}),$$

but must be smaller than the overall age of the source. These constraints suggest a value around 10^6 yr for NGC 6251 or M 87. One notices that this is of the order of dynamical scale in the central few parsecs of a galaxy. Thus if the central engine were slightly displaced from the origin of the potential well, the periods of oscillation would be of this order, which suggests one possible mechanism for 'flip-flop'. An alternative possibility is that there are jets on both sides, but for some reason related to the nuclear environment, one jet is more dissipative (*e.g.* has more internal shear) and is a stronger radio emitter.

6. Some physical processes: Particle acceleration and pair production

One essential ingredient of radio source models is an *acceleration mechanism* both in the compact and the extended sources. The standard Fermi process gives a power law, but one whose slope depends on the ratio of two quantities—the escape and acceleration timescales—which are *prima facie* unrelated. A Fermi-type process involving *shock fronts*, however, avoids this problem and offers the promise of producing a standardized power law. The general idea is the following: consider a strong, nonrelativistic shock front in an essentially thermal medium. We know that the density contrast across the shock (we work in the frame in which the shock is at rest) may be of the order of 4 or so. The trajectory of a particle which is moving at speeds higher than that of the shock ('super-thermal particle') will be as shown in Fig. 10. Such

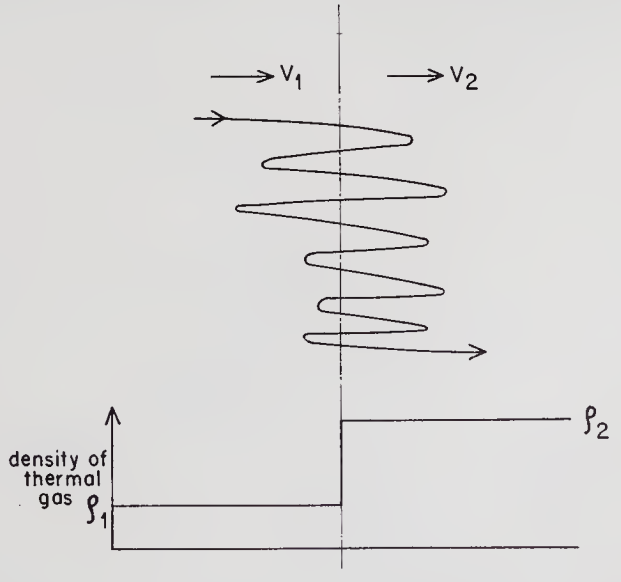

Figure 10. First-order Fermi acceleration in shock fronts.

a particle crosses the shock front roughly (c/v_1) times and each time its energy gets boosted by a factor of order $(v_1 - v_2)/c$. In other words this acts as a first order process with cumulative energy gain of the order of original energy. A more detailed calculation shows that the particles acquire a power-law spectrum whose slope depends on the compression factor $q = (v_1/v_2)$. The mean energy gain (for each double passage through the shock) is $\Delta E/E = 4/3\ v_1/c(1 - q^{-1})$. The escape probability (per double passage) due to the mean flux is $\eta = v_2/(c/4)$, assuming that the relativistic particles are almost isotropic in the shock frame. After x passages, a particle of initial energy E_0 has energy $E = E_0 \exp[4/3x(v_1/c)(1 - q^{-1})]$. The probability of completing x passages is $(1 - \eta)^x$, so $N(E) \propto E^{-(2+q)/(q-1)}$. If $q = 4$, this simple argument gives an E^{-2} slope. The main attraction of this type of mechanism for acceleration is that it produces a fairly standard type of power-law spectrum. For this reason, and because shock formation is ubiquitous, this mechanism has become quite popular in many astrophysical contexts.

Let us now come back to the compact sources and some of the processes therein—in particular the X-ray and nonthermal optical emission which, we believe, 'samples' the central source about a light day across. There are some problems confronting any theory trying to generate large amounts of hard photons from a small volume. Fig. 11 presents the plethora of physical processes that can be going on in the compact region: we will concentrate on just two particular aspects, *viz.* Comptonization and pair production.

Comptonization occurs where a set of photons are injected into a system of electrons whose mean thermal energy exceeds the photon energy. It is easy to see that for a photon of frequency ν, the mean energy gained per scattering will go as,

$$\frac{\delta\nu}{\nu} \simeq \left(\frac{V_e}{c}\right)^2 \simeq \frac{kT_e}{mc^2} \quad (m_e c^2 \gg kT_e \gg h\nu).$$

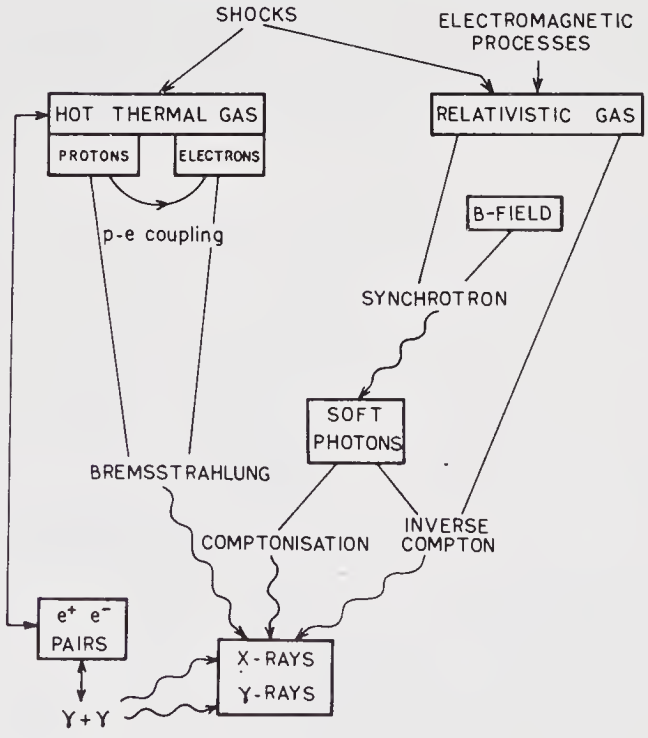

Figure 11. Physical processes in compact regions.

If the optical depth of the system is τ, then for optically thick source, τ^2 represents the typical number of scatterings before a photon escapes. Thus the relevant parameter that describes the evolution of the photon spectrum is

$$y = \tau^2 \left(\frac{kT_e}{mc^2} \right).$$

Fig. 12 shows schematically the evolution of an original monochromatic photon spectrum for different values of y. As y increases, the effect becomes more and more pronounced; for large values of y, the photons come into equilibrium with the electrons, acquiring a Wien-law spectrum (*i.e.* a relativistic Maxwellian) with mean energy of order (kT_e). For intermediate values of y, one obtains a power-law spectrum of photons, and this is an attractive mechanism for any source with nonthermal spectrum. However, one must notice that observed sources seldom display the bump in Fig. 12 and hence some additional physics must always be invoked to suppress it.

The second process that comes up in our scenario is electron–positron pair production. There are two conventional methods (that is, excluding 'exotic' processes like vacuum breakdown *etc.*) for producing e^+e^- pairs. In a region with γ-rays and X-rays such that

$$\varepsilon_\gamma > \frac{2(m_e c^2)^2}{\varepsilon_X}$$

(where ε_γ is the characteristic γ-ray energy and ε_X is characteristic X-ray energy), pair production is possible. Now since the cross-section for the process, a factor ~ 2 above threshold, is of the order of Thomson cross-section it cannot be neglected in our model. The optical depth for γ-rays in such a region is of order

$$\tau_\gamma = 10^2 \left(\frac{L_X}{L_E} \right) \left(\frac{\varepsilon_X}{m_e c^2} \right)^{-1}$$

(L_X is the X-ray luminosity). Thus unless the X-ray luminosity is very small, any process that produces γ-rays will also generate e^+e^- pairs. This effect is important even when L_X is some one percent of the Eddington luminosity.

The second process—'thermal' pair production—occurs whenever the electron temperature is greater than $(m_e c^2)/k$. This can take place even in ion-supported tori

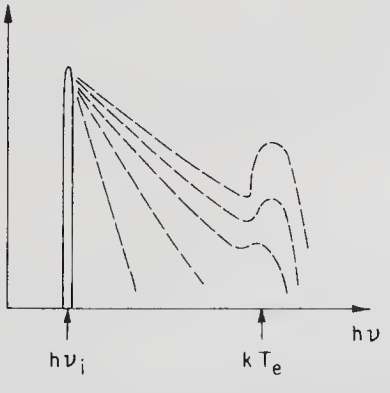

Figure 12. Comptonization of a monochromatic photon spectrum for different values of the parameter Y.

(discussed in Section 3) and has the important effect of increasing the cooling rate more steeply than one would have expected from bremsstrahlung alone.

Before leaving this topic let us discuss one simple model of compact sources wherein the pair-production process is important. Consider a spherical source of size R, relevant to the continuum-emitting region of quasars, perhaps one light day across. It is easy to see that for standard (equipartition) values of the magnetic field the synchrotron lifetime for relativistic electrons would be far less than (R/c). In other words, the electrons must undergo local acceleration at various regions dispersed throughout the source. Suppose that such local regions produce a power-law spectrum of photons between $(\nu_{\min}; \nu_{\max})$ with an index α (say) (as would be expected if the acceleration occurs *via* shock waves). What happens when $h\nu_{\max} > m_e c^2$, so that pair production is possible?

Let us define a parameter l through the equation,

$$L = l(m_e c^3/\sigma_T)R, \quad i.e. \quad l = \left(\frac{m_p}{m_e}\right)\left(\frac{R}{R_{Sch}}\right)^{-1}\left(\frac{L}{L_E}\right).$$

Clearly, when $l > 1$, pair production effects are dominant. However, as we noted previously, in many realistic situations l *is* greater than unity. Now if we denote by f_γ the fraction of the luminosity carried by primary photons in the range $h\nu > m_e c^2$, then pair production will prevent these photons from escaping for $f_\gamma l > 1$; e^+e^- will then be produced copiously, and, of course annihilate back, leading soon to an equilibrium situation. In such a source the Thomson optical depth due to e^+e^- pairs will be,

$$\tau_{e^+e^-} = (xf_\gamma l)^{1/2}[\sigma_T c/A]^{1/2}.$$

Here, x is the mean number of pairs per MeV of luminosity above the threshold and A is the annihilation rate. The expression in square brackets is of the order of unity for sub-relativistic pairs and goes as γ^2 for relativistic pairs. This implies immediately that when $(xf_\gamma l) > 1$, the depth $\tau_{e^+e^-} > 1$ is maintained in the source. In other words all the radiation is 'processed' through an e^+e^-, optically thick, cloud.

This Comptonization again depends on the parameter

$$y = (kT_{e^+e^-}/m_e c^2)\tau^2_{e^+e^-},$$

and since there cannot be catastrophic Comptonization, with $y \gg 1$, as there is not enough energy to turn all the low-energy photons into γ-rays, e^+e^- plasma *must* be sub-relativistic (that is $kT \ll m_e c^2$, since $\tau_{e^+e^-} > 1$). Under these conditions the 'reprocessed' spectrum has the form shown in Fig. 13. The photons with $h\nu > m_e c^2$ reappear at lower frequencies with a sharp cutoff at around $(m_e c^2/\tau^2_{e^+e^-})$. Such a source will exhibit reprocessed radiation concentrated typically in the hard X-rays. Moreover, there will be no survival of any original synchrotron polarization (see Guilbert, Fabian & Rees 1983, for fuller discussion).

7. Superluminal VLBI components

The idea of superluminal velocity goes back a long way. In fact there is a paper by Couderc written in 1939, discussing the phenomenon called 'light echoes' as applied to Nova Persei (which exploded in 1901). When this nova went off, enhanced reflection off the circumstellar clouds was seen after a certain time delay which was less than the

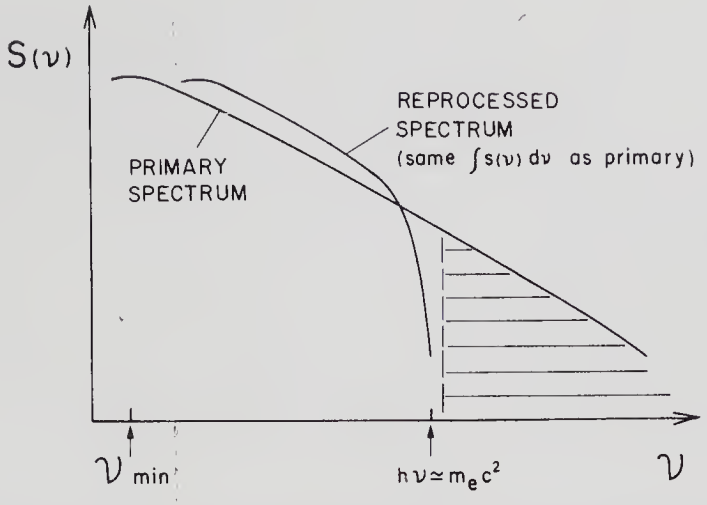

Figure 13. Reprocessed spectrum due to Comptonization.

apparent transverse travel time (at speed c) to those clouds. And it was realized in 1939 (if not before) that this could be explained if the cloud was somewhat nearer to us than the nova. Then the locus of points from which reflected radiation reaches a distant observer with a given time delay is a paraboloid and this gives superluminal light echoes from all points in the forward hemisphere. So, that was certainly a very 'classical' phenomenon in astronomy; fast moving material with high Lorentz factor (but with v not quite at c) gives essentially the same possibility, although the paraboloid then turns into an ellipsoid (Rees 1966).

The theorist's view, therefore, of what the observers (*cf.* the lectures by Marshall Cohen) are telling us is that the typical superluminal source is made up of a high-surface-brightness region (identified with the nucleus itself) and blobs which are moving outwards with superluminal apparent transverse velocity.

The model which is frequently discussed, and popularized particularly by Blandford & Königl (1979) and by Scheuer & Readhead (1979), involves the idea that the superluminal velocities are along narrow jets. If the Lorentz factor is γ_{beam} then the apparent transverse velocities can be up to $\gamma_{\text{beam}} \times$ (actual velocity), (*i.e.* essentially $\gamma_{\text{beam}} c$ in the ultra-relativistic case). This requires that the angle which the beam makes with the line of sight (θ) is of the order $1/\gamma_{\text{beam}}$. Therefore, Lorentz factors of 5 can give rise to apparent transverse motion with $\sim 5c$, when the angle θ is about 12°. You get, of course, enormous Doppler favouritism in this case. Recall that the Doppler favouritism was dramatic even for quite general orientations, which could explain the absence of counterjets in these cases. However, in this kinematic model we cannot avoid having the matter moving at a small angle to the line of sight, and therefore one does require to some extent, a special orientation.

So much for superluminal motion in the radio band; what about any other evidence for relativistic beaming? I am not quite sure how strong this evidence is—it is perhaps only marginal. However Angel & Stockman (1980) have studied in particular the optical variability of the sources B2 1308 + 164 and AO 0235 + 164 which are extreme optically violently variable (OVV) objects, sometimes called BL-Lac objects, or blazars. (It was in fact E. Spiegel's prime contribution to extragalactic astronomy—in an after-dinner speech at the Pittsburg BL-Lac conference in 1977—to coin the term *blazar* to denote BL-Lac objects and the most extreme variable quasars.) Angel & Stockman

(1980) have been monitoring high polarization and intensity variations in a number of blazars, which are atypical among quasars in that most quasars display only a very small amount of polarization (an amount which can readily be interpreted as just due to electron scattering). For some of the blazars, however, the polarization can be as much as ~ 30 per cent. These extreme objects involve powers up to $10^{49}\,\mathrm{erg\,s^{-1}}$ if isotropic and vary in intensity and polarization on timescales of $\lesssim 1$ week. It has been speculated by Angel & Stockman (1980) and others that these may be members of a beamed population with the beam pointing towards us. In fact Angel & Stockman did claim some supporting evidence for this idea (though again I would not make too much out of this). They discussed the polarization variations in the objects they studied and found that for most of them, despite a variation in the polarization angle, there was a preferred long-term axis for the polarization vector. But in the two objects mentioned earlier they claimed that the polarization vector varies over 'all points of the compass'; there was no preferred long-term axis. This they claimed was consistent with the idea that there was a directed outflow *towards* the observer in these two objects, whereas in other sources the beam makes a larger angle to the line of sight. If this is true, it would be evidence for beaming on a smaller scale, probably, than the tens of parsecs that one is talking about in the superluminal radio sources.

Now if the jets are initiated from a scale of (say) 10^{15} cm, then any relativistic *random* motions that were produced at that time would have decayed away by adiabatic losses. Therefore one has to assume that the blobs in superluminal sources are places where re-acceleration has occurred. There must be some *in situ* reconversion of the bulk kinetic energy into relativistic particles and this could be due to obstacles in the beam or the kind of internal shocks which arise from velocity variations. If one does adopt this sort of interpretation, then there is no natural reason to believe that you could trace back a particular blob all the way to its nucleus. For instance, supposing the nozzle was squirting out material whose Lorentz factor went up and down between (say) 3 and 5, then the fast bits would eventually catch up with the slow bits; but if the timescale for the variation was of the order of years, then the material traverses many light years before the shock forms (because $\Delta v/c$ is small even when $\Delta\gamma_{\mathrm{beam}}/\gamma_{\mathrm{beam}} \simeq 1$, if $\gamma_{\mathrm{beam}} \gg 1$). Therefore it would be a very interesting test for this kind of model to see if a particular blob can be traced back to the centre, or if on the other hand the blob seems actually to start off at some place removed from the centre.

The beam model that I have just sketched has of course been discussed in great deal, but I would like to emphasize what seems to me a big problem for this model: *i.e.* the superluminal motion in 3C 273. The problem here is that 3C 273 is already an exceptional object on the basis of its optical apparent magnitude alone. In the Schmidt–Green (1983) survey for instance, we know that there are not very many other objects like it in the sky—there are not very many other objects which are as apparently bright in the emission lines. We have therefore an object which is already exceptional; and if we have a theory which requires it to have an orientation which has only 1 per cent probability, it seems a big embarrassment for the theory. An already exceptional object has to be ~ 100 times more exceptional. This problem only arises for 3C 273, because in the case of (say) 3C 466 there could perfectly well be 100 times as many objects which have the same optical appearance but which are not strong radio sources. It could be argued by some that this problem is not serious since 3C 273 is a unique object (just like Cygnus A is exceptionally bright); and we must in any case accept as a 'coincidence' that it has a much higher $L_{\mathrm{rad}}/L_{\mathrm{opt}}$ than most quasars. But it does seem to

me that if someone came up with a theory that did not require this extra factor of 100, one would be a good deal happier.

One way slightly to ease the problem would be through an idea which I pointed out a couple of years ago which somebody else called the 'spray' model. This is a modification of the simple jet model which does allow you to see superluminal effects over a range of angles larger than $1/\gamma_b$. The suggestion here is that a relativistic jet is pointing towards the largescale jet. But one assumes that the material is not unidirectional but is being squirted out with a large Lorentz factor $[\gamma_b]$ of ~ 5 in a range of directions about the main jet axis, the intensity falling off with increasing angle to the jet axis. Now let us suppose that our line of sight does not make a particularly small angle to the jet axis, so we are not within an angle $1/\gamma_b$ of the main beam. However we will see superluminal effects from material whose angle to our line of sight is less than γ_b^{-1}, *i.e.* from material ejected at angles between $(\phi - \gamma_b^{-1})$ and $(\phi + \gamma_b^{-1})$ where ϕ is the angle the jet axis makes with our line of sight. Of course the superluminal effects from $(\phi - \gamma_b^{-1})$ will be seen projected in the direction of the main jet, but those from the $(\phi + \gamma_b^{-1})$ direction will be projected on the other side. Therefore if this is to be a consistent model where we see superluminal motions preferentially along the largescale jet then the fall-off in the intensity with angle must be such that we have a lot more intensity along the $\phi - \gamma_b^{-1}$ direction than the $\phi + \gamma_b^{-1}$ one. Provided this constraint were satisfied, observers, for whom $\phi \gg \gamma_b^{-1}$ would see superluminal blobs moving in the general projected direction of the largescale jet. Of course (in this model) if we were looking at 3C 273 almost along the jet (at angle $\phi < \gamma_b^{-1}$) then we would detect a huge flux of hundreds of Janskys. Probably that is not an embarrassment because in comparison with the other superluminal sources, the ratio of 3C 273's radio flux to its optical output is lower than for (say) 3C 446. If you brought 3C 446 as close as 3C 273 and kept it lined up along our line of sight then its radio luminosity would much exceed that of 3C 273. So you could tolerate being, as it were, in the 'radio side lobes' for 3C 273, in a way you cannot for others. And it is only in 3C 273 that one needs to invoke an explanation of this kind. The basic assumption which is being dropped therefore is that the ultra-relativistic matter is directly beamed in one direction; it is instead assumed that there is some range of angles. Incidentally in this type of spray model blobs produced by shocks would not necessarily all appear exactly projected in the same direction. There could therefore be blobs moving in a direction which does not appear to be pointing quite along the largescale jet. The data (on 3C 345) which Marshall Cohen attributed to possible 'precession', could alternatively indicate merely that successive blobs are being shot out in slightly different directions. We shall have to wait for the next blob in 3C 345 to see whether there is actual precession, or whether the effect is just due to a spray about the overall mean jet direction.

If relativistic particles are freshly accelerated in the superluminal blobs, then there is no reason why the electron energies should not extend up to the values needed to give optical emission. And the spectrum might be such that they emit more energy in the optical than in the radio. Of course, even the MMT will not have the resolution adequate to resolve those features but in principle there is no reason why the superluminal sources should not be like the M 87 jet where there is more power radiated in the optical than in the radio. And it could be that some fraction of the optical nonthermal continuum from superluminal sources is not coming directly from the nucleus but is coming from the superluminal jet. (I do not know how one could check that, unless possibly there were absorption due to an intervening galaxy detectable in

Lyman lines and the 21 cm line. Contributions from different places might be distinguishable if they pass through HI with different velocity or column density. That is the only hope, I think, until we have optical interferometry with milli-arcsec resolution).

The one conclusion which is hard to avoid in superluminal sources is that bulk motions with high Lorentz factors are involved. For an electron–ion plasma, this would imply 5–10 GeV per ion in the flow. This in turn implies that some fraction of the matter may have to get more than its 'fair share' of energy, because in most accretion-type processes the average amount of energy given to the matter is $\lesssim 100$ MeV per ion.

Another possibility is that we are observing an electron–positron flow. Then, of course, instead of needing (say) 5 GeV per electron to get a γ_{beam} of 5, we only need 5 MeV, since the electron in this case is charge-neutralized by a positron, and not by an ion. It is therefore interesting to speculate about relativistic electron–positron beams. I have discussed already how electrons and positrons can be produced in a galactic nucleus, either by conventional processes (turning γ-rays into pairs) or by more exotic electrodynamic processes. One can set some constraints on electron–positron beams if they are initiated on scales as small as 10^{15} cm. There is a limit on the energy flux because a beam in which the initial e^+–e^- density were too high would just annihilate. The net result is that, if a powerful electron–positron jet emerges from dimensions of order of a Schwarzschild radius, it must start off with a large bulk Lorentz factor: for a given amount of power a smaller density of electron–positron pairs is then needed, and in their co-moving frame the time available for annihilation is reduced by the time-dilation factor.

Another constraint is that a beam with high γ_b, even if the electrons and positrons escape annihilation, may be braked by 'Compton drag' as it moves through the ambient radiation field in a quasar. This sets an upper limit to γ_b. The combined effect of these constraints could be evaded in a 'radical' model where an electron–positron jet is produced, then *does* annihilate (to give a beam of γ-rays), and the γ-rays convert back into electron–positron pairs by colliding with X-rays after travelling a few parsecs. You can make a model of that kind, but it seems ingenious rather than plausible.

Another class of acceleration mechanism utilizes radiation pressure. This of course is more efficient for electron–positron plasma than for electron–ion plasma. But it turns out that it is still very hard to get Lorentz factors γ_b much more than 5, the reason being that once the particles are moving out relativistically the radiation coming from the back appears redshifted, and so the acceleration is less. A further effect is that if the radiation source is not a 'point', then in the frame of a relativistically moving particle, aberration tends to make the radiation appear to come from the forward direction. This means that however intense the radiation is, you can never (at a radius r) get up to a Lorentz factor which is larger than r/r_{source}. In other words to get a Lorentz factor of 10 one has to go to a radius ten times that of the photon source (otherwise the radiation will decelerate the particles); but, of course, the farther away one goes the weaker becomes the radiation pressure. People have tried to calculate this in detail, both for spherical symmetry and for tori: it does prove rather hard using radiation pressure to get Lorentz factors more than about 5 even for electron–positron plasma.

These problems with collimating and accelerating plasma to high bulk Lorentz factors suggest that the directed outflow is perhaps primarily in the form of Poynting flux rather than particles. This electromagnetic energy can then be converted into relativistic plasma at larger distances.

8. Precession effects?

Another issue related to compact sources, and to whether collimation occurs on really small scales, is the question of whether 'reflection-symmetric' sources (or some of them, anyway) arise from the precession of the central nozzles. If they are indeed manifestations of precession, this could be precession on the scale of the entire galaxy, or it could alternatively be precession of a central nozzle. In an earlier paper (Begelman, Blandford & Rees 1980), we discussed whether it is in principle possible for a nozzle to precess if it is produced by a flow pattern around a black hole. The nozzle can then precess only if the black hole itself does. This is hard, because a black hole is very compact, and things like the tidal force of the galaxy are entirely negligible. The only way in which a black hole could be made to precess would be if there was a very dense mass very near. In fact the only realistic context for applying a large enough torque to a spinning black hole is if it is orbiting around another black hole. Now one might at first sight deride this as a very contrived notion. But, on the contrary, if black holes lurk in galactic nuclei, then binary black hole formation is *almost inevitable*. The reason is that *galaxy mergers* occur. (Some people even believe that *most* ellipticals form *via* mergers.)

If two galaxies collide, and each harbours a black hole in its core, then the massive holes will spiral to the centre of the merged stellar system by dynamical friction. We can then ask if the holes themselves coalesce completely, or if there might be a chance of forming a durable binary with the kind of separation that is needed in order to give precession on the correct timescale. (This precession is, incidentally, not only relevant to the S-symmetric sources; it has also been advanced as a possible explanation of the misalignment between the most compact VLBI jets and the more extended structure). I shall not go through the details here, but Fig. 14 shows calculations of the timescale for two black holes of mass $\sim 10^8\, M_\odot$ to spiral together, as a function of their separation in units of their Schwarzschild radius. When the separation is more than ~ 10 pc, the

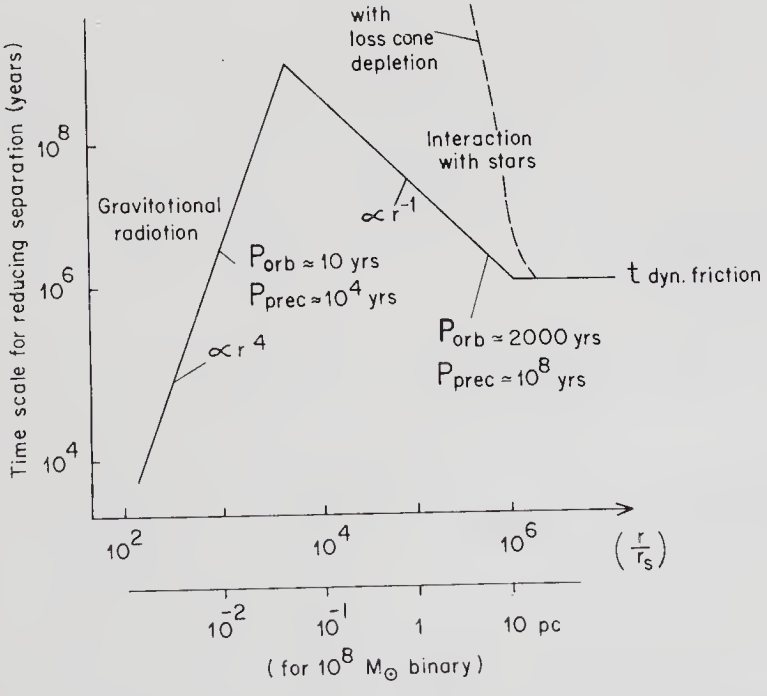

Figure 14. Timescales involved in the coalescence of two $10^8\, M_\odot$ by black holes.

black holes do not feel each other's gravitational potential: they just spiral down due to dynamical friction, striving for equipartition with the (much lighter) stars. However when they get closer than about 10 pc (in these units) they start feeling each other's gravitational potential. As they get closer together, their relative velocity, which down to this point has essentially been the galactic dispersion velocity, starts to increase as $r^{-1/2}$ (where r is the separation between the black holes), and they become a binary. As this binary becomes more and more compact, dynamical friction effect on the stars becomes less and less efficient—a tight binary has a smaller cross-section for interaction with stars. That means that the timescale for reduction in r, starts to increase as r^{-1}. (It may increase even more steeply if the binary kicks out of the system all the stars whose orbits come anywhere near it. It cannot then evolve until those stellar orbits are repopulated, and that happens only on the much longer timescale of star–star interactions in a galaxy). When the black holes get close enough, the gravitational radiation governs the timescale for driving them together, giving a timescale which goes as r^4 and is of course very short when they approach final coalescence. But the key point is that a black hole binary would persist for a timescale of order of 10^8 yr (or still longer if the stars near it were depleted), with a separation of $\sim 10^4$ Schwarzschild radii, but would not last long with smaller r because of gravitational radiation. Now one can work out the precession and the orbital periods, which are also indicated in the figure. Timescales $> 10^8$ yr are expected only for a definite range of r. At the minimum of this range (*i.e.* in the timescale $\propto r^4$ region) the orbital period $P_{\rm orb} \simeq 10$ yr and the precession period $P_{\rm prec} \simeq 10^4$ yr. The precession might then give rise to a misalignment between compact and extended structures, and also—as Gaskell (1983) found in one or two quasars—it could give the broad emission lines (which may be tied to one of the orbiting objects) a large velocity relative to the galaxy they are in. At the upper end of the range (where the timescale for coalescence goes as r^{-1}) the orbital period is around 2000 yr while the precession period is $\sim 10^8$ yr. This latter timescale is appropriate for explaining the overall asymmetry of the very extended structures in S-type sources. If black holes do exist in a large number of galaxies, then, given that mergers occur, there is a good chance of 'catching' galaxies in an active phase where they contain a binary black hole with precession periods $10^4 \simeq 10^8$ yr. Indeed if the loss cone effects prevent dynamical friction from driving the components together, the binary could sit around, in the r^{-1} part of the curve, for perhaps a Hubble time. The only thing that could then cause coalescence would be infall of gas into the system, with friction of the gas driving them together. That same gaseous dissipation could activate the galactic nucleus, so one would always automatically 'catch' a galaxy in the active stage while it contained a precessing binary.

What happens in the final coalescence? Specialists in gravitational-wave astronomy are interested in whether they could detect gravitational-wave bursts from extragalactic objects. In principle, if supermassive objects of $10^8.M_\odot$ collapse, or if two large masses collide, a burst of gravitational waves may emerge whose characteristic period (duration) would be of the order of hours. This would be in the wavelength range that can be probed by doppler tracking of interplanetary spacecraft *etc.*, rather than by ground-based detectors (which work best at higher frequencies). But even if we do believe that massive black holes exist, most evolutionary tracks (see Fig. 2) cause them to form in such a gradual way that they do not yield a single intense pulse: if the hole grows by gradually swallowing stars or gas, or if it grows by gradual collapse of the gas cloud, not much gravitational radiation need emerge at all. Coalescence of two pre-

existing black holes is the only route which guarantees a highly efficient burst in the final coalescence. But the bad news is that even though this burst would have an amplitude detectable by foreseeable high-precision techniques for tracking spacecraft, the estimated rate of galaxy mergers out to the Hubble radius is such that (even if there were a black hole in all those galaxies) the pulse rate predicted would be only about one per century—depressing even to those who are prepared to devote their entire lives to the quest of gravitational waves.

9. Evolution and statistics

My next topic is the evolution with redshift of radio sources and quasars and the issue of how many *dead* quasars there might now be. I will not talk about the detailed work on actually fitting models to the evolution of the luminosity function. As everyone here probably knows, you can fit a wide variety of models to the evolution; the general trend of most of them is that the evolution is more drastic for the most powerful radio sources; Schmidt & Green (1983) claim this also for the most optically-powerful quasars. The co-moving density of the most powerful sources is about 1000 times higher at a redshift of 2 than at present. It is important to be clear about what is meant by the evolution of source population with redshift. The individual lifetime of a powerful source is probably very short compared to cosmic evolution timescales. Therefore when we talk about evolution of the source population (or luminosity function), we are not talking about the same objects at all times—we are envisaging a z-dependence in the birthrates, the life duration, or the peak luminosity at different epochs. One can speculate on the various redshift-dependent effects that might control the evolution of sources. The *epoch* of *galaxy formation* is obviously a relevant factor: one does not expect to see any powerful quasars or radio sources until the stage in the universe when galaxies have formed and settled down, at least to the stage having well-defined nuclei in which some kind of runaway activity can occur. We would also like to know how the nucleus and the fuelling rate onto a central object depend on the age of a galaxy. Another question, especially for radio sources, is how the radio emission, particularly the extended lobes, depends on the gaseous environment on the galactic and intergalactic scale. This depends on the epoch in a complicated way. In earlier studies, people tried to fit models where the intergalactic gas density went something like $(1+z)^3$. That is obviously an over-simplification if the gas is falling into clusters. The density of gas in a *cluster now* is probably *higher* than the density of intergalactic gas *anywhere* at a redshift of 2, before the clusters had formed. So it is not at all obvious how the mean external gas density with which an extended radio source interacts depends on redshift.

How many dead quasars would there be? Rough estimates can be made as follows. If one knew the lifetime, one could say how many generations there would be in the Hubble time; one then inserts an extra evolutionary factor, allowing for the number of quasars at $z = 2$ having been a thousand times more per co-moving volume that it is now. Such estimates yield the ratio of 'dead' to living quasars in the range 10^2–10^6 (extremely uncertain).

A new and rather ingenious attack on this problem was made by Soltan (1982). His argument gives some handle on the number of quasar remnants which evades the big uncertainty about the active lifetime. Even though we have some evidence on how long an extended radio source lasts (we know roughly how long it takes to inflate the

extended lobes), we have no idea at all how long the active phase of a compact quasar lasts. Therefore it is an improvement if the question of quasar lifetimes is bypassed. Soltan worked out the integrated background light due to all observed quasars: it amounts to about 10^{67} erg Gpc^{-3}. The uncertainty here is due to the source counts at faint magnitudes. (He in fact went down to the 22nd magnitude assuming 200 degree^{-2} at that magnitude.) If we know the energy density generated by quasars we can infer how much energy is being put out per galaxy. This sets some lower limits on the mean mass of the remnants left in typical galaxies. To produce 10^{67} erg $(\mathrm{Gpc})^{-3}$, the number of solar rest masses that should be converted is 8×10^{13} $(\mathrm{efficiency}/0.1)^{-1}$ $M_\odot$ Gpc^{-3}. If the remnant masses are 10^8–10^9 $M_\odot$, then this tells us that there must be between 10^5–10^6 remnants per Gpc^3. Alternatively, on the hypothesis that all quasars are associated with 'bright' galaxies of magnitude < -21.3 (whose number per Gpc^3 is known), we can say that the mean mass of the remnants left in these galaxies has to be $> 2 \times 10^7$ $(\mathrm{efficiency}/0.1)^{-1}$ $M_\odot$. This argument is of course uncertain, since we do not know the efficiency (nor how much to allow for radiation in other wavebands), but it does avoid any presumption about lifetimes.

10. Black holes in nearby galaxies?

Even if one does not believe that active quasars involve black holes, it seems hard to escape the conclusion that *dead* ones *must* be black holes and must exist in profusion (unless you invoke a theory where gravity becomes repulsive on a short scale.) And if these holes are spinning they could even be reactivated by feeding new material onto them. What about nearby galaxies? There was a claim 4–5 years ago of having found evidence from stellar distributions that there was a dark central mass in the centre of M 87. Young *et al.* (1978) plotted the surface brightness as a function of distance and found a high brightness 'cusp', and also anomalously high stellar velocities, near the centre. They claimed on this basis that there was a central dark mass of 3–5×10^9 $M_\odot$. This conclusion has been subject to various kinds of doubts, and at this stage the arguments still seem confused. If the stellar velocities are not isotropic, one can explain the observations without invoking a large central dark mass; and even if there is one, it does not have to be a black hole, but could be a star cluster with a large mass-to-light ratio. We have to await the space telescope to get data with better resolution.

In Centaurus A, one of course does not have the same sort of data that Young *et al.* (1978) have for M 87, since the nucleus is not seen so well optically. But this is the nearest galaxy to us which we have reason to believe spewed out a great deal of energy in the past. We also know that it has a very compact radio and X-ray nucleus, with a jet coming out; there is therefore some residual activity. But the only reason for believing that there is some large ($\gtrsim 10^8$ $M_\odot$) mass at the centre is that Centaurus A's extended radio lobes (if one applies the classic Burbidge argument) pose extremely high energy requirements.

There is a unique compact radio source in our Galactic centre (which again Marshall Cohen mentioned) which is still almost unresolved. Its dimensions are $\lesssim 10^{14}$ cm. Another peculiar phenomenon towards the Galactic centre is a strong electron–positron annihilation line, which there is strong reason to believe is variable. The variability is claimed on the basis of obtaining different results on balloon flights six months apart. The radio source is certainly very compact and probably variable on

timescales of days or less (Brown & Lo 1982). We nevertheless have evidence against there being a monster ($\gtrsim 10^9\ M_\odot$) black hole in our Galactic centre. We know from the IR data on the neon line, that if there is a black hole there at all its mass cannot be more than $3 \times 10^6\ M_\odot$: that is the mass inferred if one interprets the Ne velocities as virial velocities; but it is not mandatory to interpret them that way—they could be ejection velocities—and therefore this is just an upper limit. There is really no firm evidence for a black hole in the Galactic centre. However, I would argue that there are two phenomena which are unique to the Galactic centre—the radio source and the fact that a large fraction of the γ-ray energy is coming out in the electron–positron line. If we do have a unique phenomenon in a unique location in the Galaxy, it is not necessarily *ad hoc* to invoke a special kind of object; and black hole models can account for both these. But this is the only reason to believe that there is possibly a collapsed object of more than a stellar mass in the Galactic centre.

Now for some details of the compact radio source. The luminosity is quite low, about 10^{34} erg s^{-1}. We do not know the radius directly because any apparent angular extent could be due to small-angle interstellar scattering. (But the self-absorption limit to the radius, if it is synchrotron radiation, is $\gtrsim 3 \times 10^{13}\, B^{-1/4}$ cm at 8 GHz, B being measured in Gauss). The dimensions are consistent therefore with a very compact source which is self-absorbed. If there were a black hole at the centre, then this radio source could be due to synchrotron emission from electrons at radius $4–5 \times 10^{13}$ cm around it. If low-level accretion occurs onto a black hole of $10^6\ M_\odot$, then the magnetic field at this radius ($\sim$ 100 Schwarzschild radii) is quite large (of order 10–100 Gauss). Since the field is high the radio emission can come from electrons with very modest γ's. It could be that the radio emission is coming from essentially thermal electrons in an accretion torus, with energies of a few MeV. In fact a model of that kind can even yield a spectrum consistent with the radio data, and where of course the intrinsic angular size does increase towards low frequencies (Rees 1982).

In connection with whether there is positive evidence for a black hole in the Galactic centre, an important counter-argument has been advanced by Ozernoy (1979) and his collaborators. They have argued against the idea of a black hole of more than $100\ M_\odot$ or $200\ M_\odot$ in the Galactic centre, on the grounds that there is a high star density at the centre and if there were a black hole of $10^6\ M_\odot$, then tidally captured stars would generate a higher mean luminosity from the Galactic centre than is consistent with the data. If the density of stars within the central parsec is about 10^6 pc^{-3}, and the velocity dispersion ~ 200 km s^{-1}, the capture rate of stars turns out to be almost 10^{-3} per year for a hole of $10^6\ M_\odot$. This number is, I think, hard to argue with unless you appeal to loss-cone depletion. Ozernoy has claimed that this would give excessive growth of the black hole and excessive X-ray luminosity. However in making this argument, he has assumed that when a star is disrupted, it takes a long time ($\gg 10^3$ yr) for the debris to drain away, so that the luminosity is sustained until the next star falls in. So he is assuming that at a typical time one would see something not far from the average luminosity. Moreover in estimating the mean luminosity he assumes that the material is all swallowed and radiates with high efficiency. But these assumptions may not hold good. There is an uncertainty in how long it takes for a star to be torn apart and digested. If we get only a brief flare when the star falls in, then for most of the time there is no sort of activity. Another question is how much of the debris from a tidally disrupted star actually goes down the hole rather than being expelled, and with what efficiency it gets converted into energy.

Tidal disruption has often been discussed in the general context of galactic nuclei as a way of feeding material into the hole, but I shall consider it just in the context of the Galactic centre where we at least have a handle on the star density. If a star's orbit brings it close enough to the hole, then it will be sheared apart by tidal disruption. The tidal radius for an ordinary star passing near a $10^6 M_\odot$ black hole is at about 100 Schwarzschild radii. The debris from such a star would fly out in a very eccentric orbit. This is because the only orbital kinetic energy that has actually been lost in this fly-by is enough energy to unbind a star, which is about 10^{-5} of its rest mass. Therefore this material still has a chance to spray out to about $10^5 r_{\rm Sch}$. It will subsequently settle down to some sort of axisymmetric configuration whose angular momentum is that of a closely bound orbit. The orbital period at the tidal radius is only about one day. Therefore when the material settles down to become axisymmetric, it is in a configuration whose dynamical timescale is only one day. Unless the viscosity is very low, it could be that after a very short time (compared to the intervals between successive swallowings), it is all over, the material having all either gone down the hole or been blown away. Since quite a lot may be blown away we might just get a brief flare. It is thus not clear that Ozernoy's argument rules out a black hole of $10^6 M_\odot$ at the Galactic centre.

Let me conclude these comments on the Galactic centre by suggesting a possible way to test whether there is a black hole of $10^6 M_\odot$ there. If a star passed close enough to the black hole to be captured but was not finally destroyed, it might be gradually 'ground down' into an orbit at essentially the Roche limit for the massive black hole. If that happened, then we would have a star whose orbital period was about one day (this would depend on the type of the star but be independent of $M_{\rm h}$). The orbital *velocity* however would be very large (about $0.1\, M_{h6}{}^{1/3} c$). Gravitational radiation would of course be pulling it in closer, but the timescale for this turns out to be very long. There may be other drag forces, but in principle such a star could survive until another star fell into a similar orbit and collided with it. If one did find $\lesssim 1$ day periodicities, associated with evidence for very high velocity, that would strongly favour there being a large massive hole. Only if the hole mass is very large can an ordinary star be in orbit around it undisrupted by tidal effects, but still close enough to have an enormous orbital velocity.

11. Concluding remarks

I intended to say a bit more about scaled-down prototypes of extragalactic phenomena—things like SS 433 and Sco X1 where jets are also seen—and also about the rather exciting recent evidence that in protostars there is a highly collimated ejection, which gives rise to clouds of about the mass of the Earth moving out at $\sim 200\,{\rm km\,s^{-1}}$. But in view of the time I will not say any more. However, let me reiterate my main theme: it does seem mainly from radio data, but also from other (*e.g.* X-ray) evidence and from objects like SS 433) that jets are an ubiquitous feature of high energy astrophysics. Flow patterns around compact objects must generically give rise not only to a lot of energy but also to this kind of directed outflow. This is now becoming the 'conventional' interpretation; but I believe it is leading to progress, at least to the extent that it suggests which well-posed problems are worth concentrating on. These processes may turn out not to work, but only if future theory or data convinces us of this will we be justified in invoking more radical explanations.

Figure 15.

Just to finish, let me show my one and only slide (Figure 15)—you can interpret it as you like. Some would interpret it by saying that we must not close our eyes to *present* evidence that points towards 'new physics'. But on the other hand some of us may regard it as a caricature of those people who are unwilling to accept that 'conventional' ideas have at *least* permitted some progress over the last decade towards understanding extragalactic phenomena.

Acknowledgements

I am grateful to the organizers of the Winter School, and to many of the participants, for interesting discussions, and for kind hospitality. I am extremely indebted to T. Padmanabhan and K. Subramanian for their skill and effort in preparing a full draft of this manuscript, based only on my oral presentation and semi-legible viewgraphs.

References

Angel, J. R. P., Stockman, H. S. 1980, *A. Rev. Astr. Astrophys.*, **18,** 321.
Bardeen, J. M., Petterson, J. A. 1975, *Astrophys. J.*, **195,** L65.
Begelman, M. C., Blandford, R. D., Rees, M. J. 1980, *Nature*, **287,** 307.
Begelman, M. C., Rees, M. J., Blandford, R. D. 1979, *Nature*, **279,** 770.
Blandford, R. D., Icke, V. 1978, *Mon. Not. R. astr. Soc.*, **185,** 527.
Blandford, R. D., Königl, A. 1979, *Astrophys. J.*, **232,** 34.
Blandford, R. D., Rees, M. J. 1974, *Mon. Not. R. astr. Soc.*, **169,** 395.
Blandford, R. D., Znajek, R. L. 1977, *Mon. Not. R. astr. Soc.*, **179,** 433.
Brown, R. L., Lo, K. Y. 1982, *Astrophys. J.*, **253,** 108.
Couderc, P. 1939, *Ann. Astrophys.*, **2,** 271.
Gaskell, C. M. 1983, in *Proc Liège Coll. 24: Quasars and Gravitational Lenses*, Inst. d'Astrophys., Univ. Liège, p. 473.
Guilbert, P. W., Fabian, A. C., Rees, M. J. 1983, *Mon. Not. R. astr. Soc.*, **205,** 593.
Macdonald, D., Thorne, K. S. 1982, *Mon. Not. R. astr. Soc.*, **198,** 345.
Norman, M. L., Smarr, L., Winkler, K-H. A., Smith, M. D. 1982, *Astr. Astrophys.*, **113,** 285.
Ozernoy, L. M. 1979, in *IAU Symp. 84: Large-Scale Characteristics of the Galaxy*, Ed. W. B. Burton, D. Reidel, Dordrecht, p. 395.
Phinney, E. S. 1983, in *Astrophysical Jets*, Eds A. Ferrari & A. Pacholczyk, D. Reidel, Dordrecht, p. 201; and work in progress.
Rees, M. J. 1966, *Nature*, **211,** 468.

Rees, M. J. 1978, *Observatory*, **98**, 210.
Rees, M. J. 1982, in *The Galactic Center*, Eds. G. R. Riegler & R. D. Blandford, AIP publications, p. 166.
Rees, M. J., Begelman, M. C., Blandford, R. D., Phinney, E. S. 1982, *Nature*, **295**, 17.
Scheuer, P. A. G., Readhead, A. C. S. 1979, *Nature*, **277**, 182.
Schmidt, M., Green, R. F. 1983, *Astrophys. J.*, **269**, 352.
Smith, M. D., Norman, C. A. 1981, *Mon. Not. R. astr. Soc.*, **194**, 771.
Soltan, A. 1982, *Mon. Not. R. astr. Soc.*, **200**, 115.
van Groningen, E., Miley, G., Norman, C. A. 1981, *Astr. Astrophys.*, **90**, L7.
Young, P. J., Westphal, J. A., Kristian, J., Wilson, C. P., Landauer, F. P. 1978, *Astrophys. J.*, **221**, 721.

Discussion

Cowsik: (1) What is the fraction of the energy made available in the formation of the black hole that is radiated; do we have any observational evidence for this energy release? (2) What is the maximum energy that can be stored in the rotation of the black hole and what fraction of it can later be released?
Rees: (1) If the hole grows gradually *via* accretion, a large amount of energy may be radiated. But if it forms *via* (for instance) dynamical instability of a supermassive star, then not much energy would escape during the collapse. (2) The maximum 'reducible mass' of a hole with $J = J_{\max}$ is about 30 per cent. In principle this can be extracted with 50 per cent efficiency by electromagnetic processes.
Padmanabhan: If one takes the 'inevitability of black hole formation' seriously, what percentage of galaxies will have a dead/alive black hole in the centre? What percentage of these will be active galactic nuclei?
Rees: Most large galaxies would harbour massive black holes. The level of activity must be low in general, presumably because the holes are 'starved' of gas.
Ghosh: The Lense–Thirring effect producing the jet-alignment works only when the black hole has enough angular momentum. What kind of upper bounds on the black hole's initial angular momentum can be put from the expected conditions at birth?
Rees: It depends on how the hole forms. If it forms from a rotating supermassive star, or grows by accretion of material with a constant angular momentum vector, then $J \simeq J_{\max}$ is possible.
Ghosh: In order to specify a 'Polish doughnut' completely, does not one have to specify both the angular momentum distribution and the surface gravity/flux distribution on the disc surface.
Rees: I think the surface angular momentum distribution is sufficient to specify the shape of the surface, and therefore (since the 'surface gravity' is then determined) the radiation flux per unit area.

Kapahi, V. K. (Ed.)
Extragalactic Energetic Sources
Indian Academy of Sciences, Bangalore, 1985, pp. 87–103

Noncosmological Redshifts in Galaxies and Quasars

G. R. Burbidge *Kitt Peak National Observatory, Tucson, Arizona 85726, USA*

Contents

1. Introduction

During the 1950s evidence for violent events in galaxies came through radio astronomy with the discovery of nonthermal radio sources. Radio luminosities of the order of 10^{43-44} ergs s^{-1} were observed from some galaxies. It was clear by the late 1950s that synchrotron mechanism is responsible for the radio emission. The synchrotron theory tells us that the energy content of these sources is at least $\sim 10^{60}$ erg for the most powerful sources. A proper understanding of this output of energy involves a lot of questions and uncertainties like the estimates of distances to these sources, equipartition arguments *etc.*

Radio astronomy led us to explosive events in galaxies. But radio emission is not the only manifestation of violence. In the early sixties, it was shown that the optical emission of several sources is due to explosive events (Burbidge, Burbidge & Sandage 1963). Seyfert nuclei have broad optical emission lines which show that the kinetic energy associated with them is very large. The nuclear components of these galaxies have continuum emission which is nonthermal in character so that normal stellar evolutionary processes cannot explain this energy release.

Many disturbed galaxies (like NGC 520 and the exploding galaxy M 82) have been found. Tidal effects were initially suggested as an explanation for these disturbances, but they were shown to be totally inadequate to explain the violent phenomena observed. The jet in M 87 (Fig. 1) which is due to synchrotron radiation poses many problems of confinement, reacceleration *etc.*

A fundamental discovery of enormous consequence came in the mid-1960s with discoveries of radio variables like CTA 102 and 3C 273. The period of variability in some cases was of the order of only a few days. These short periods make the problem very difficult due to the severe limitations they impose on the sizes of the emitting regions. One is thus led perhaps to question the distance estimates based on redshifts, or to highly relativistic motions (so-called superluminal effects). VLBI measurements

Figure 1. The optical jet in M 87.

showed the existence of small-scale structures. The same technique has revealed superluminal motions, again casting doubts on the distance estimates. Recently, X-ray observations have been made of these extragalactic energetic sources. Thus we are led to a variety of problems connected with these powerful sources, their energetics, sizes and dynamics. While gravitational energy sources are most favoured, the details of the models are being worked out involving black holes, accretion discs, multiple supernovae, star clusters etc. The problems posed by the enormous redshifts of QSOs are very basic whether the redshifts are cosmological or noncosmological. Considerable ingenuity is employed in trying to fit a variety of observations with conventional models. It may be worthwhile to concentrate on a few objects that can be probed in considerable detail rather than on a large number of diverse objects.

Currently, the world is divided into two camps—one group holding on tenaciously to the traditional views, and the other believing that the new astronomical discoveries are ushering in new physics. In short, we can say that astronomy at present is in the same situation as physics was during the latter part of the nineteenth century.

2. Bright galaxies

I will now discuss the various relations that have been found between the redshifts and apparent magnitudes or distances of bright galaxies. It is well known that the nature of QSO redshifts has been a subject of great controversy ever since the discovery of these objects about twenty years ago. But questions have been raised even for galaxies over the last sixty years.

From about 1929, when Hubble first gave the initial redshift–distance relation, the conventional view has been that the redshifts of all the extragalactic objects, excluding small effects, are both due to, and evidence for, the expansion of the universe. For small redshifts a linear relation between velocity and distance is obtained, but for larger redshifts different cosmological models predict specific departures from linearity. The linear velocity–distance relation (for small redshifts) together with the discovery of the microwave background radiation and its generally accepted explanation as being the

relic blackbody radiation from a hot big bang are the two bases for the general belief in an expanding universe of Friedmann type.

This simple view has been borne out by the original work of Hubble (1929), followed up and extended in a large number of investigations, notably by Sandage & Tammann (1974, 1975). The relation has been extended from velocity shifts of about 3000 km s^{-1} or less to clusters of galaxies with redshifts of about 0.5. But the situation for the bright galaxies is more complex as the following discussion will show.

Investigations by Hawkins (1962), de Vaucouleurs (1972) and Segal (1980) indicate that for the comparatively bright nearby galaxies, the simple linear relation does not hold. Hawkins and Segal have argued in favour of a quadratic dependence of velocity on apparent magnitude. However, Sandage and his associates as well as Soneira (1979) have counter-argued that the nonlinearity is due to selection effects, particularly due to the Malmquist effect, which in turn is denied by Nicoll & Segal (1980). The plots obtained by Segal and Soneira are shown in Figs 2 and 3 respectively.

An interesting approach to the problem is to review the original data of Hubble. This is done in Fig. 4. We have chosen only those nebulae for which Hubble gave distances. The velocity–distance plot based on modern data for these is compared with the original plot of Hubble. Now we can ask ourselves the question whether looking at the modified 1980 plot, Hubble would have obtained a linear velocity–distance relation.

The second line of evidence, uncomfortable for the conventional view, is that of periodicities in z or $\log(1+z)$. If redshifts are indeed measures of distances we cannot expect to find sharply preferred values of z. But Tifft (1976) has shown that there is a correlation between the nuclear magnitudes of galaxies in clusters and their differential redshifts, with a 'quantized value' of $\Delta v = 72.5\,\mathrm{km\,s^{-1}}$. He has found similar effects in the redshift differences in double galaxies. In Fig. 5, which is based on redshift measurements on double galaxies by Peterson (1979), we can see clear evidence of a periodicity in Δv, contrary to the expectation of a smooth distribution of redshift differences. Tifft's result is certainly startling. If it is genuine, it suggests that on a small scale at least a component of the redshifts of galaxies may have a non-Doppler origin.

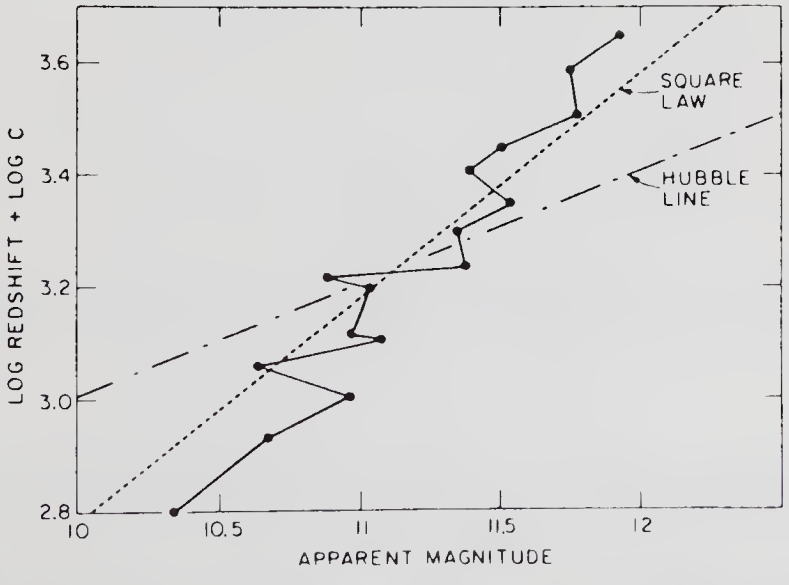

Figure 2. The m–z relation for galaxies brighter than 12.5 mag (Segal 1980).

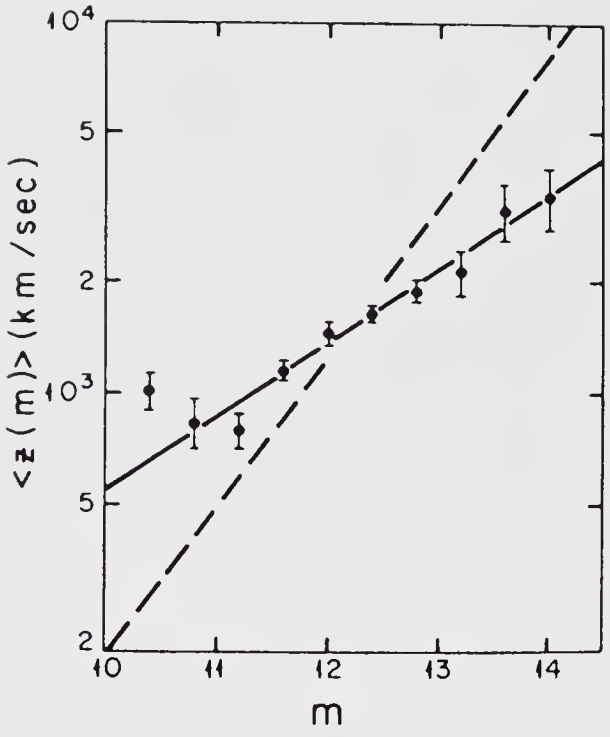

Figure 3. The *m–z* relation for bright galaxies (Soneira 1979). The dashed line represents the square law and the solid line the Hubble law.

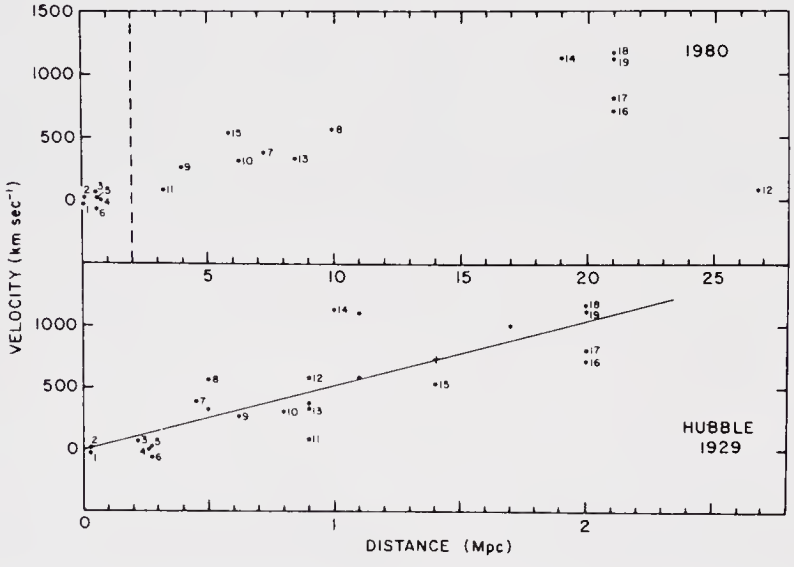

Figure 4. The velocity-distance relation for galaxies used by Hubble. Modern velocities have been used in both parts of the figure. But the distances in the lower part are from Hubble and in the upper part from modern estimates.

The third line of evidence comes mainly from the work of Arp (1971a, 1978, 1980a) who found several pairs of galaxies which are apparently physically associated, but have very different redshifts. Two examples are shown in Figs 6 and 7. Fig. 7 is of particular interest in that a compact galaxy having a large redshift apparently lies in front of a larger galaxy NGC 1199 with a smaller redshift. The redshift differences in all the cases

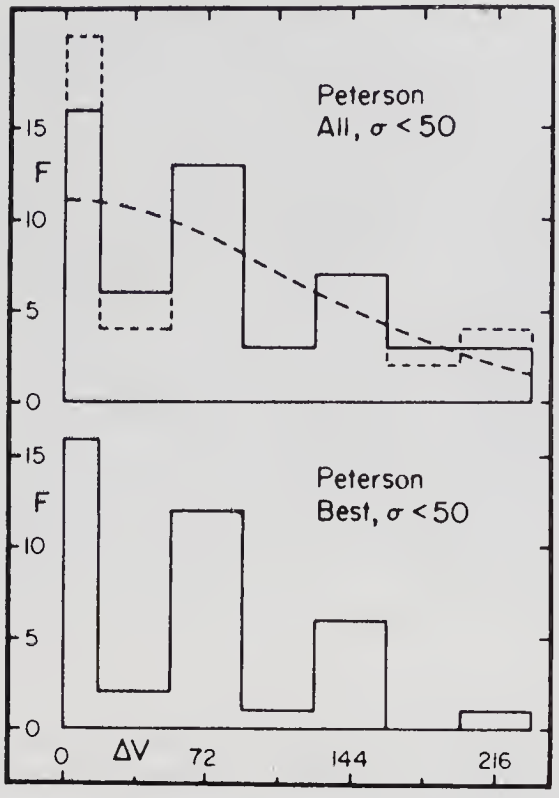

Figure 5. Distribution of redshift differences for double galaxies (Tifft 1980).

Figure 6. A companion galaxy to NGC 53, with a discrepant redshift (Burbidge 1981).

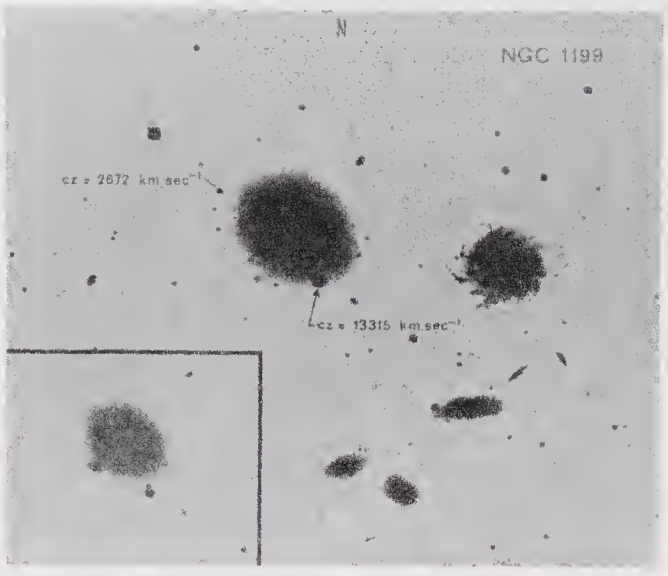

Figure 7. A compact galaxy with a much larger redshift lying in front of NGC 1199 (Burbidge 1981).

noted by Arp are far too great to be due to peculiar motions. In fact, if galaxies in general had such large peculiar motions, no Hubble relation would have been discernible in the first place. It has been pointed out, however, that in all the cases discovered so far the smaller galaxy has the larger redshift. This, in a way, supports the conventional interpretation of redshifts as being distance indicators. This has prompted the most common rebuttal of Arp's findings *viz.* that all the configurations are accidental. My opinion is that, considering the comparative variety of bright galaxies and the extremely limited observing time one has, it is unlikely that all the configurations are chance occurrences. Moreover, luminous connections between the two members are highly visible in some of the cases.

If we accept the view that many bright galaxies may have a noncosmological component of redshifts comparable to the cosmological component, the apparent nonlinear relation between redshifts and apparent magnitudes which we discussed above may perhaps be explained. The simplest explanation for noncosmological redshifts is that the compact galaxies are ejected from the parent galaxies and the redshift excess is due to the local Doppler effect. This interpretation cannot of course account for the absence of blueshifts.

3. The nature of QSO redshifts

I shall now consider evidence against the cosmological nature of QSO redshifts and in particular discuss the large body of evidence that now exists, which shows that many QSOs are physically associated with galaxies with very different redshifts.

In the most recent optical catalogue of QSOs (Hewitt & Burbidge 1980) are listed about 1500 QSOs with measured redshifts. The very first QSOs to be discovered had much larger redshifts than those of the majority of galaxies for which information was available. Hence it was natural on the basis of the Hubble relation to suppose that the QSOs were the farthest and most luminous objects, though there was no independent

evidence for this assumption. Terrell (1964) was the first to interpret the QSOs as local phenomena. He put forward the hypothesis that QSOs were ejected from our Galaxy. The ejection hypothesis was given in a slightly different version by Hoyle & Burbidge (1966) who suggested the nearby galaxies like NGC 5128 as the likely seats of ejection.

Let us start by looking at the Hubble diagram for QSOs (Fig. 8). It is a complete scatter diagram, and there is no obvious indication of any relation between redshift and magnitude. It is no doubt possible to attribute the large scatter to wide variations in the intrinsic luminosities of the objects. Also a somewhat tighter fit can be obtained by choosing a particular class of QSOs, *e.g.*, only those with steep radio spectra. But what should be noted is the clear absence of correlation between redshift and apparent magnitude, when the whole sample is considered. This does not mean that it is not possible to assume that the redshifts are of cosmological origin, but at the same time it does not give any support for the idea. The situation here is very different from that encountered by Hubble and Humason in the case of galaxies where a strong correlation was used as a direct proof of the existence of an expanding universe. In my opinion it is fair to say that if Hubble and Humason had investigated the QSOs first and not the galaxies, they would not have considered that they had found evidence for an expanding universe.

The second line of evidence comes from the rapid optical and radio variability of these objects which puts severe limits on the sizes of the region producing the variable flux. On the assumption of cosmological redshift the high redshifts of QSOs make them very distant and consequently highly luminous objects. The high luminosity confined within a small region means a very high photon energy density and it was shown by Hoyle, Burbidge & Sargent (1966) that a paradoxical situation occurs. Several proposals have been made to avoid this paradox. The severe physical problems can be allayed only either by assuming that the QSOs are local, or by appealing to extreme relativistic effects. At present there does not exist a single well-worked-out model which can account for the continuum source properties and avoid the paradox, if the QSOs are at cosmological distances. It should be noted that the paradox largely disappears if the QSOs are at noncosmological distances (less than or about 100 Mpc). The same can be said about the 'superluminal' objects for which speeds of expansion exceeding that of light are obtained if the objects are assumed to lie at cosmological distances.

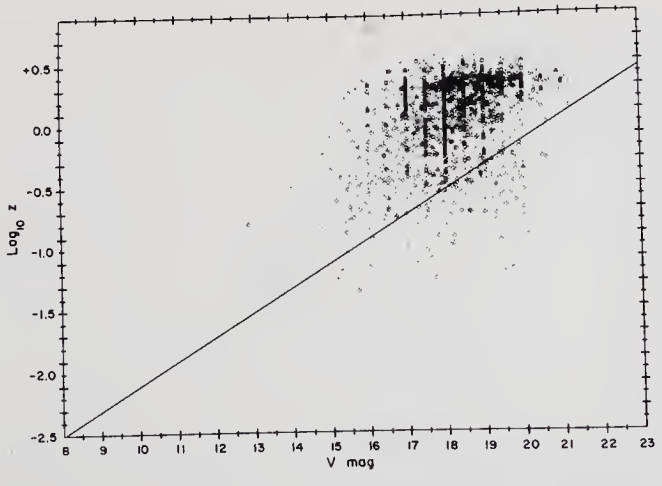

Figure 8. The redshift–magnitude diagram for QSOs (Hewitt & Burbidge 1980).

The distribution of redshifts of the QSOs constitutes the third line of evidence against the cosmological interpretation. From Fig. 9 we can see that there are distinct peaks on a scale of $\Delta z = 0.1$ at $z = 0.3, 0.6, 1.4$ and in particular 1.95. It is unlikely that selection effects can be the cause for such a distribution (Burbidge 1978). At the same time it is very difficult to demonstrate statistically the existence of very sharp peaks with $\Delta z = 0.01$ (Burbidge & O'Dell 1972). If z_c, z_r, and z_i are the cosmological, random-motion and intrinsic components of the total observed redshift z_o, we have

$$(1 + z_o) = (1 + z_c)(1 + z_r)(1 + z_i).$$

It follows that the peaks produced by discrete values of z_i can easily be destroyed by the smearing caused by a small range in the values of z_c and z_r. Thus it is indeed remarkable that peaks are found at all. It has been estimated that the peaks are periodic with $\Delta \log (1 + z_i) = 0.089$.

All the evidences that I have discussed until now can be termed indirect. The direct way to attack the redshift problem is to look for associations between QSOs and galaxies, and also between QSOs themselves. A well-established association of a QSO with a galaxy of the same redshift will be an evidence in favour of the cosmological nature of the QSO, assuming that the galaxy redshifts are always cosmological, whereas evidence of association with galaxies of different redshifts will mean that the QSOs have noncosmological redshifts. Similarly, confirmed associations between QSOs with different redshifts will imply that at least the differences in redshifts are non-cosmological.

Before discussing in detail the evidence supporting the noncosmological interpretation, let me first point out that there is evidence that some QSOs and galaxies have the same redshifts. This comes mainly from the work of Stockton (1978). From a sample of 27 QSOs with $z \leqslant 0.45$, Stockton found 13 galaxies in 8 fields with the same redshifts as those of the QSOs within a distance of 45 arcsec. The probability of chance coincidence was estimated to be $\sim 1.5 \times 10^{-6}$. Hence Stockton's observations provide

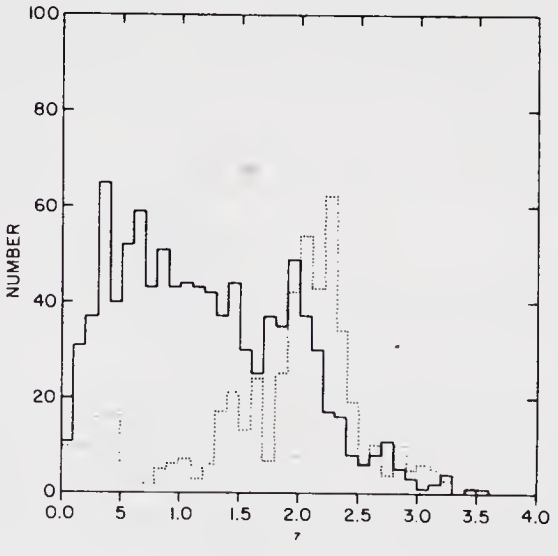

Figure 9. Redshift distributions of QSOs: discovered by colour creteria or by positional coincidences (solid line), discovered by objective prism or grism techniques (dotted line) (Hewitt & Burbidge 1980).

a strong evidence that some QSO redshifts are cosmological. However it does not prove that all QSO redshifts are cosmological. Secondly it has been tacitly assumed that the other cases where the redshift values do not agree are accidental and there is no evidence that this is really true.

Markarian 205 was the first QSO found near a bright galaxy, NGC 4319 (separation 43 arcsec), with a discrepant redshift. Arp (1971b) has shown that there appears to be a luminous connection between the two objects. The reality of this apparent luminous connection has often been questioned in the literature. However, Sulentic (1983) on the basis of image processing of unpublished plates has recently confirmed the existence of the luminous connection between the two objects.

Burbidge *et al.* (1971) were the first to analyse a chosen sample of 3 CR QSOs as compared with the galaxies in the Shapley–Ames Catalogue. When a logarithmic plot of the angular separation between the QSOs and the galaxies (which are within 10 arcmin of each other) and the galaxy redshift was made it was found that the points were remarkably close to a straight line of slope -1 implying that the QSOs all lie at approximately a constant distance of 10 to 15 kpc from the galaxies. This effect was statistically significant. However analysis of a sample of Parkes QSOs and galaxies in the Zwicky catalogue did not yield statistically significant results (Burbidge 1979). But more recently a similar plot for all the galaxy–QSO systems listed in Hewitt–Burbidge catalogue was done (Burbidge 1979). A least-square solution gives the best fit line to $\log z$–$\log \theta$ of the form

$$\log \theta = -1.17 \log z + \text{const.}$$

At 99 per cent confidence level, the range of the slope for this line is between -0.93 and -1.56. The correlation coefficient $r = 0.68$ is significant.

A large number of QSOs is now known to lie near bright galaxies (Burbidge 1981). In some cases they have been discovered by accident and many through systematic searches by Arp. Some of the configurations are illustrated in Burbidge (1981).

I shall now discuss some statistical tests for which we restrict ourselves to those QSOs which lie within 10 arcmin of the galaxies (Table 1). If N is the number of galaxies that have been looked at (assumed to be 300), and Γ the sky density of QSOs (in deg^{-2}) brighter than m, then the number of QSOs expected to lie within θ arcsec of arbitrary points is

$$\langle n \rangle = 2.4 \times 10^{-7} N \Gamma \theta^2.$$

The values of the sky densities chosen are 0.3, 1, 3 and 10 QSOs deg^{-2} down to 17, 18, 19 and 20 mag respectively (Burbidge 1979). Table 2 lists the values of $\langle n \rangle$ for different angular diameters, where they are compared to the total number actually observed (N_o) and that has been found by Arp, N_{oA}. We can clearly see that for distances about 1 to 2 arcmin the numbers found are much greater than those expected by chance. This is powerful statistical evidence for physical associations. For QSOs further out the results become progressively less significant till at distances > 5 arcmin fewer are found than those expected by chance. This means either they have not been looked for as carefully as have those at smaller angular distances, or that the overall sky density is lower than the values which were used to calculate $\langle n \rangle$. If the latter is true the significance of the objects found very close is enhanced.

Even more striking than this are the cases of the clustering of several QSOs around one galaxy, the alignment of QSOs with different redshifts, and the existence of at least

Table 1. All QSOs known to lie within 10 arcmin of bright galaxies or their companions.

QSO coordinate designation	QSO	Galaxy	Separation (arcsec)	m_v (QSO)	z (QSO)
0007 + 106	III Zw2	B	50	15.4	0.089
0018 + 006	UM 228	NGC 78B	516	17.0	0.102
0024 − 018	UM 245	NGC 120	240	18.0	(1.46)
0027 + 018	UM 247	NGC 132	300	18.9	2.35
0032 − 082	BSO 1	NGC 157 companion	119	19.0	0.756
0038 − 019	PKS	NGC 227 companion	67	18.5	1.690
0038 − 020	PKS	NGC 227 companion	~ 400	18.0	1.178
0040 − 017	UM 268	NGC 227	456	18.0	(1.66)
0106 + 013	PKS	ZW 0106.1 + 0123	192	18.39	2.107
0112 − 017	PKS	NGC 448	600	17.41	1.365
0121 + 108	MC 2	ANON	40	18.0	0.510
0132 − 075(g)	UB 1	NGC 615	235	18.5	1.64
0133 + 004	UB 1	NGC 622	71	18.5	0.91
0133 + 004	BSO 1	NGC 622	73	20.2	1.46
0151 + 045	PHL 1226	IC 1746	54	17.5	0.404
0156 + 187(g)	UB 2	NGC 772	352	19.4	2.61
0219 + 428	3CR 66A	3CR 66B	390	15.2	(0.444)
0225 − 014	PKS	NGC 936 companion	302	18.0	2.037
0226 − 014	UB 1	NGC 936 companion	101	19.6	1.13
0240 − 002	BSO 1	NGC 1073	104	19.8	1.945
0240 − 002	BSO 2	NGC 1073	117	18.8	0.599
0240 − 002	RSO	NGC 1073	84	20.0	1.411
0243 − 007(g)	UB 1	NGC 1087	170	19.1	2.147
0317 − 023	4C − 02.15	NGC 1298	228	19.50	2.092
0809 + 558	UB 1	NGC 2534 (MKN 85)	121	18.7	2.40
0814 + 579	BSO 1	NGC 2549 companion	134	18.9	2.40
0841 + 499	U 1	NGC 2639 companion	188	18.8	1.177
0844 + 319	—	NGC 2402	30	18.87	1.834
0846 + 513	W 1	NGC 2681 companion	12	19.5	1.860
0853 + 515(g)	UB 1	NGC 2693	188	19.5	2.31
0855 + 539	UB 1	NGC 2701 companion	110	19.4	0.243
0916 + 513	UB 2	NGC 2841 companion	200	18.7	0.120
0917 + 514	UB 1	NGC 2841 companion	407	18.5	2.028
0917 + 513	UB 3	NGC 2841 companion	220	16.5	0.553
0921 + 349	U 1	NGC 2859 companion	60	(19.2)	0.23
0923 + 349	U 2	NGC 2859 companion	66	(19.7)	2.25
0923 + 345	U 3	NGC 2859 companion	73	(20.3)	1.46
0924 + 301	—	B2	480	21.0	2.02
0932 + 219	UB 1	NGC 2916	216	19.2	0.238
0932 + 220	UB 2	NGC 2916	370	17.6	0.793
0933 + 218	UB 4	NGC 2916	586	19.3	1.868
0952 + 698	HOAG 1	M82 (NGC 3034)	382	20.0	2.048
0952 + 698	HOAG 2	M82 (NGC 3034)	512	21.0	2.054
0952 + 698	HOAG 3	M82 (NGC 3034)	585	21.0	2.040
0955 + 326	3C 232	NGC 3067	114	15.8	0.533
0958 + 558	UB 1	NGC 3073 (MKN 131)	144	18.8	1.53
0958 + 557	UB 2	NGC 3073 (MKN 131)	530	17.3	2.091
1015 + 415	UB 3	NGC 3184 companion	339	19.1	(0.92)
1015 + 414	UB 4	NGC 3184 companion	278	18.1	2.029
1021 − 006	PKS	ZW 1022.0 − 0036	126	18.22	2.547
1039 + 140(g)	UB 2	NGC 3338 companion	251	19.7	2.14

Table 1. Continued.

QSO coordinate designation	QSO	Galaxy	Separation (arcsec)	m_v (QSO)	z (QSO)
1039 + 140(g)	UB 1	NGC 3338 companion	218	20.4	(2.04)
1046 + 128	UB 1	NGC 3389	265	19.4	1.111
1046 + 129	UB 13	NGC 3384	149	20.6	(0.497)
1049 + 616	4C 61.20	NGC 3407	173	16.3	0.422
1107 + 036	4C 03.21	ANON	20	18.9	0.96
1108 + 289	QS	NGC 3561	66	20.0	2.192
1130 + 473(g)	BSO 1	NGC 3726 companion	100	18.4	1.13
1153 + 534	W1	NGC 3992 companion	280	20.3	1.75
1205 − 008	PKS	ANON	9.4	18.6	1.002
1206 + 439	3CR 268.4	NGC 4138	174	18.4	1.400
1219 + 755	MKN 205	NGC 4319	42	14.5	0.070
1222 + 102	WDM 6	NGC 4380	88	17.6	cont.
1223 + 338(g)	UB 1	NGC 4395 companion	145	18.7	1.265
1223 + 338(g)	B 6	NGC 4395 companion	329	18.4	1.038
1218 + 339	3CR 270.1	NGC 4395 companion	303	18.6	1.519
1223 + 338(g)	UB 1	NGC 4395	370	19.2	0.77
1233 + 125	WDM 8	NGC 4550	44	17.2	0.728
1241 + 166	3CR 275.1	NGC 4651	210	19.0	0.557
1253 + 104	MC 2	ANON	90	18.0	0.824
1316 + 423	UB 1	NGC 5055 companion	315	18.3	0.910
1319 + 388	UB 1	NGC 5107	40	19.5	0.949
1342 + 440	BSO 1	NGC 5296	55	19.3	0.963
1428 + 498(g)	UB 2	NGC 5660	483	17.3	0.205
1430 + 101	UB 1	NGC 5669 companion	70	17.7	0.766
1432 + 489	BSO 1	NGC 5682	95	19.2	1.940
1441 + 522	3C 303C	3C 303	20	19.97	1.570
1458 + 718	3CR 309.1	NGC 5832	372	16.78	0.905
1505 + 559(g)	BSO 1	NGC 5866	436	18.1	0.706
1537 + 595	UB 1	NGC 5981	107	19.0	2.132
1545 + 210	3C 323.1	ANON	370	16.69	0.264
1548 + 114	MC 2	ANON	9	19.0	1.901
1749 + 701	W1	NGC 6503	324	16.5	(0.76)
2020 − 370	PKS	ANON	21	17.5	1.048
2158 − 134	BSO 1	IC 1417	76	17.8	0.73
2252 + 129	3CR 455	NGC 7413	24	19.7	0.543
2259 + 157	UB 1	NGC 7465	128	19.2	1.66
2305 + 187	4C 18.68	ANON	7	16.5	0.313
2315 − 049(g)	UB 1	NGC 7592	415	18.7	1.410
2333 + 019	UB 1	NGC 7714–15 companion	120	18.0	1.871
2334 + 019	UB 2	NGC 7714–15 companion	480	19.0	2.193

one very tight group of QSOs with different redshifts (Hazard, Arp & Morton 1979).

A striking case is that of three QSOs with $z = 0.594$, 1.40 and 1.95 lying within 2 arcmin of the centre of the galaxy NGC 1073 (Burbidge 1981). The probability of clustering is estimated to be about 0.01. Similarly interesting cases are of the QSOs associated with NGC 2639 (Arp 1980b) and NGC 3379 (Arp, Sulentic & di Tullio 1979).

Arp & Hazard (1980) have found what is surely the most striking case of alignments of QSOs discovered so far. They discovered two triplets of QSOs (A, B, C) and (X, Y, Z)

Table 2. A comparison between the numbers of QSOs found near bright galaxies (N_o or N_{oA}) and the number expected by chance ($\langle n \rangle$).

Apparent magnitude	θ(arcsec) $\leqslant 60$			$61 \leqslant \theta$ (arcsec) $\leqslant 120$			$121 \leqslant \theta$ (arcsec) $\leqslant 180$			$181 \leqslant \theta$ (arcsec) $\leqslant 300$			$301 \leqslant \theta$ (arcsec) $\leqslant 600$		
	N_o	$\langle n \rangle$	N_{oA}	N_o	$\langle n \rangle$	N_{oA}	N_o	$\langle n \rangle$	N_{oA}	N_o	$\langle n \rangle$	N_{oA}	N_o	$\langle n \rangle$	N_{oA}
$\leqslant 17$	3	0.08	0	1	0.24	0	1	0.36	1	1	1.23	1	5	5.8	1
$\leqslant 18$	7	0.25	1	6	0.78	3	1	1.29	1	2	4.2	1	12	19.5	5
$\leqslant 19$	11	0.78	1	12	2.32	9	7	3.6	5	9	12.3	5	19	58.6	12
$\leqslant 20$	17	2.60	5	19	7.8	14	9	12.9	7	14	41.2	9	24	194	16

as shown in Fig. 10, where each triplet is precisely aligned and the redshifts of (A, Y), (B, X), and (C, Z) are nearly the same. Moreover the lines joining the QSOs with similar redshifts are approximately concurrent. It has been suggested that this region could be the seat of explosion from where the QSOs might have originated. Most recent calculations show that the probability of finding two such systems aligned at random is as low as $\sim 10^{-4}$ (Narlikar & Subramanian 1982). In fact another pair of triplets has been noticed by Saslaw in an adjacent region on the same plate. The probability of finding four triplets is even lower.

In the grouping of QSOs around galaxies two things are worth noting *viz.* alignments and similarities in redshifts. Let us consider similarities in redshifts. In several cases there are two or more redshifts closely the same, but often there are others which are quite different. It is often argued that pairs of QSOs with similar redshifts lie at the same cosmological distance and hence are indicators of the existence of superclusters. But it is conveniently ignored that the same proximity arguments indicate that both the bright galaxy and the other QSOs with different redshifts, if present, are also physically associated.

Alignments always imply physical associations. The alignment of double radio lobes with a galaxy placed symmetrically is taken as the characteristic property of radio sources associated with galaxies. But only when the aligned objects have very different redshifts is the physical association doubted.

I shall finally briefly discuss pairs of QSOs. Till now several close pairs have been discovered (Hewitt & Burbidge 1980, Table 5). Some well-known examples are 1548 + 114a & b, with a separation of 5.5 arcsec (Wampler *et al.* 1973); the famous 0957 + 561a & b (Walsh, Carswell & Weymann 1979) with a separation of 5.7 arcsec; and

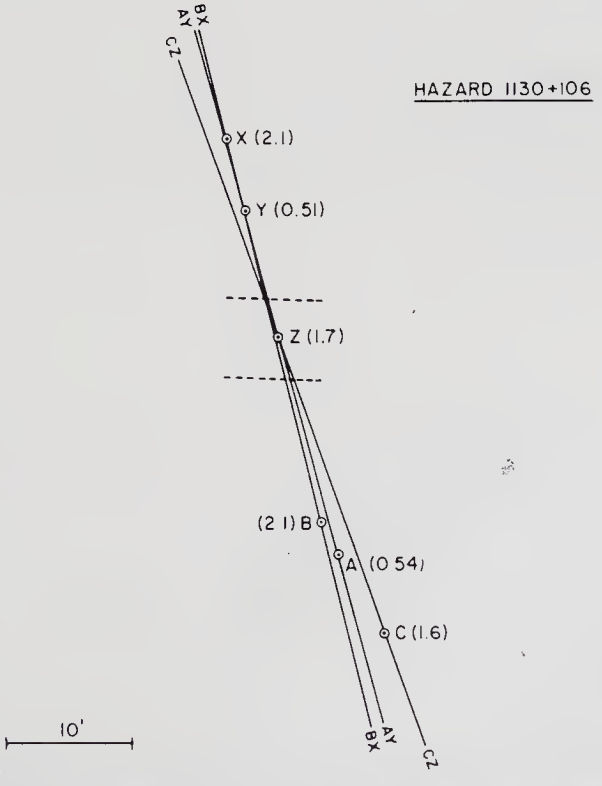

Figure 10. The two quasar triplets of Arp & Hazard (1980), shown with lines drawn to join QSOs with similar redshifts (Burbidge 1981).

3C 345 and 1641 + 398 where the separation is about 8 arcmin (Margon, Chanan & Downes 1981). What is interesting is that different interpretations are given for each of these systems. 0957 + 561a & b have been widely accepted as twin images of a single QSO due to a gravitational lens, since the redshifts are identical. But the first case is dismissed as a chance coincidence since the redshifts are different. In the third case, though the redshifts and other physical properties are very similar for the two QSOs, Margon, Chanan & Downes (1981) have argued at length against it being a gravitational lens phenomenon, since the QSOs are widely apart. I feel that it is far more sensible to attempt a common explanation for the double QSO problem.

4. Concluding remarks

I shall conclude this series of lectures with an assessment of the existing situation. For galaxies there is no doubt that most of the redshifts are cosmological. But we cannot ignore the possibility that some part of the redshift of some galaxies may not be due to the expansion of the universe. The evidence bearing on this is found in galaxies with small redshifts, $z \lesssim 0.01$. Hence the noncosmological component also must necessarily be small.

For QSOs the situation is different. The evidence for noncosmological redshifts is much stronger. We can relate all the evidences we discussed if we accept the unifying idea that galaxies of various types can eject radio sources, other galaxies and QSOs. Usually the existence of alignments is accepted as proof for physical associations. Only when alignments involve objects with very different redshifts or apparently normal galaxies are involved the instinctive belief that alignment implies physical association is doubted. This is more due to the deep-seated belief that all redshifts are indicators of distances, than any objective analysis of the evidence. The lack of any well-established theory for noncosmological redshifts and for explaining ejection of compact bodies from massive centres along a preferred axis only worsens the situation. It leads to a chain reaction—the evidence is doubted, statistical arguments are criticized and hence no serious attempts are made to explain the phenomena. The problem is not solved, because it is not worked upon.

References

Arp, H. C. 1971a, *Astrophys. Lett.*, **7,** 221.
Arp, H. C. 1971b, *Astrophys. Lett.*, **9,** 1.
Arp, H. C. 1978, *Astrophys. J.*, **220,** 401.
Arp, H. C. 1980a, *Astrophys. J.*, **239,** 469.
Arp, H. C. 1980b, *Astrophys. J.*, **236,** 63; **240,** 415.
Arp, H. C., Hazard, C. 1980, *Astrophys. J.*, **240,** 726.
Arp, H. C., Sulentic, J. W., di Tullio, 1979, *Astrophys. J.*, **229,** 489.
Burbidge, G. R. 1978, *Phys. Scr.*, **17,** 237.
Burbidge, G. R. 1979, *Nature*, **282,** 451.
Burbidge, G. R. 1981, in *10th Texas Symp. Relativistic Astrophys.*, Eds R. Ramaty & F. C. Jones, *Ann. N.Y. Acad. Sci.*, **375,** 123.
Burbidge, G. R., Burbidge, E. M., Sandage, A. R. 1963, *Rev. Mod. Phys.*, **35,** 947.
Burbidge, E. M., Burbidge, G. R., Solomon, P. M., Strittmatter, P. A. 1971, *Astrophys. J.*, **170,** 233.

Burbidge, G. R., O'Dell, S. L. 1972, *Astrophys. J.*, **178,** 583.
Hawkins, G. S. 1962, *Nature*, **194,** 563.
Hazard, C., Arp, H. C., Morton, D. C. 1979, *Nature*, **282,** 271.
Hewitt, A., Burbidge, G. R. 1980, *Astrophys. J. Suppl. Ser.*, **43,** 57.
Hoyle, F., Burbidge, G. R. 1966, *Astrophys. J.*, **144,** 534.
Hoyle, F., Burbidge, G. R., Sargent, W. L. W. 1966, *Nature*, **209,** 751.
Hubble, E. 1929, *Proc. Nat. Acad. Sci.*, **15,** 168.
Margon, B., Chanan, G. A., Downes, R. A. 1981, *Nature*, **290,** 480.
Narlikar, J. V., Subramanian, K. 1982, *Astrophys. J.*, **260,** 469.
Nicoll, J. F., Segal, I. E. 1980, *Astr. Astrophys.*, **82,** L3.
Peterson, S. D. 1979, *Astrophys. J. Suppl. Ser.*, **40,** 527.
Sandage, A. R., Tammann, G. A. 1974, *Astrophys. J.*, **190,** 525; **191,** 603; **194,** 223, 559.
Sandage, A. R., Tammann, G. A. 1975, *Astrophys. J.*, **196,** 313.
Segal, I. E. 1980, *Mon. Not. R. astr. Soc.*, **192,** 755.
Soneira, R. M. 1979, *Astrophys. J.*, **230,** L63.
Stockton, A. N. 1978, *Astrophys. J.*, **223,** 747.
Sulentic, J. W. 1983, *Astrophys. J.*, **265,** L49.
Terrell, J. 1964, *Science*, **145,** 918.
Tifft, W. G. 1976, *Astrophys. J.*, **206,** 38.
Tifft, W. G. 1980, *Astrophys. J.*, **236,** 70.
de Vaucouleurs, G. 1972, in *IAU Symp.* 44*: External Galaxies and Quasi Stellar Objects.*, Ed. D. S. Evans, D. Reidel, Dordrecht, p. 353.
Walsh, D., Carswell, R. F., Weymann, R. J. 1979, *Nature*, **279,** 381.
Wampler, E. J., Baldwin, J. A., Burke, W. L., Robinson, L. B., Hazard, C. 1973, *Nature*, **246,** 203.

Discussion

Narlikar: Can you say something about powerful X-ray and IR sources?
Burbidge: Historically the X-ray and IR sources have not been so important. This is because neither X-ray nor IR observations were made in the early days. We now know that many QSOs and Seyfert nuclei are powerful X-ray sources, probably generated by Compton scattering, though in some cases they may be thermal. Observations have been made in the near IR of many QSOs and galaxies, but very few in the far IR. There is still considerable uncertainty as to whether the IR flux is thermal in origin or is synchrotron radiation. Much of it may be thermal radiation from dust grains which are being irradiated by a central compact non-thermal source.
Cohen: Several radio astronomers attempted to verify Sholomitski's early announcement of variability in CTA 102. They were unsuccessful. That is what led to a general disbelief in variability.
Burbidge: I can only reiterate that the fact that we knew it had a large redshift led us to disbelieve the variability when it was first announced.
Porcas: Just an interesting historical note regarding CTA 102. This is now one of the best confirmed cases of low-frequency radio variability. I spoke to Sholomitski recently, however, and he is inclined to discount his own original result as having arisen from instrumental problems.
Thakur: Excuse me if I comment that you acted as an iconoclast this morning. The departure from the Hubble plot may arise due to luminosity evolution. Further, while expecting a linear relation, it was tacitly assumed that galaxies do not evolve in luminosity and that all galaxies have the same mass to luminosity ratio.
Burbidge: The Hubble relation for QSOs cannot be taken as positive evidence for cosmological redshifts though the relation can be explained in this way if you first

accept the premise that the redshifts are cosmological. We should be looking for positive evidence not just compatibility with strongly held belief.

Ramadurai: Is it not true that helium abundance is also another evidence in favour of hot big-bang models?

Burbidge: Helium is not the primary evidence. I consider that it is secondary evidence for a hot big bang, (a) because there are other ways to produce it and (b) because I am not convinced that the abundance is the same in all galaxies.

Narlikar: Of the quasar–galaxy associations found by Stockton, he considered only those in which the redshift difference was small. Why did he ignore (without discussion) all those cases (more than 50 per cent of his total) in which the redshift difference was uncomfortably large?

Burbidge: Obviously because he assumed that they were all accidental. However I suspect that this is not the case.

Nityananda: Has there been any study of possible spectral differences between those quasars for which the redshift is believed to be cosmological and the others?

Burbidge: No detailed work has been done. But as far as we can tell using low-dispersion spectra, there appear to be no differences.

Cowsik: Whereas one may account for an efficiency of ~ 0.1 for the conversion of accretion energy into energy of the plasma as due to gravitational radiation or absorption by the black hole, once the plasma is formed all its energy would ultimately be radiated away in some band or the other. Further, in view of the expectation that the various efficiencies are sensibly independent of the mass of the central black hole, bringing the quasi-stellars nearer would reduce the total energy requirements by $\sim d^2$ but the spatial density goes up by $\sim d^3$ so that the nett energy demand per unit volume of the universe goes up as d^{-1}. In view of the large redshifts one cannot push them too far away either or the energy demands would go up again. Indeed the cosmological hypothesis seems to fit to the situation of minimum energy generation in the universe. In any case bringing them very near will only aggravate the energetics problem.

Burbidge: The number of objects will increase and the total energy budget of the universe may change. But as far as I know there is no objection to this. As far as the efficiency of energy release is concerned I agree that most of the energy will go into gravitational waves, neutrinos and heat. If we could detect some of this or even find sources where this was dominant, they would be good candidates for the black hole theories.

Porcas: In your lecture you made the point that one good way to do science is to have a theory and then make a prediction. When Walsh, Carswell & Weymann found identical spectra and redshifts in the double quasar 0957 + 561A,B, they made predictions based on the theory that a single quasar, at a distance given by its redshift, gave rise to two images because of the gravitational lens effect. They predicted that the flux ratio should be the same over all parts of the electromagnetic spectrum and that one should find an intervening galaxy. Roeder & Dyer predicted the galaxy redshifts as ~ 0.4. All these predictions were subsequently confirmed. The VLBI radio structures are also similar. Does not this, by your own criteria, give confidence in the 'scenario'?

Burbidge: If 0957 + 561 were the only close pair I would agree that the argument is good. However we already know of a number of close pairs, one at least with a separation less than 0957 + 561. We now have to argue since all close pairs are likely (statistically) to be physically connected that (a) close pairs which have the same redshifts are gravitational lenses, (b) slightly wider pairs with similar redshifts are in

superclusters and (c) those pairs with different redshifts, are accidental configurations; *i.e.* three different explanations for close pairs. Surely one should look for one explanation for all close pairs. And in any case it is premature to invoke gravitational lenses until one has hard evidence that redshifts are cosmological.

Laing: You mentioned A. Webster's work (1982, *Mon. Not. R. astr. Soc.*, **200**, 47P; **201**, 179) on quasars near companion galaxies and on quasar alignments and then dismissed it: are you saying that his technique is incorrect? If not, do you accept the implications?

Burbidge: While we all know how we should use statistics, when we discover something we usually take up a position and then use statistical arguments to bolster our position. Conversely opponents of new ideas and observations use statistical arguments to decry them. It is well-known that the school from which Webster comes is not unbiased. But above all, I consider that direct evidence such as 3 QSOs in NGC 1073 or the bridge between NGC 7603 and its companion will ultimately survive all attempts at statistical demolition.

Kapahi, V. K. (Ed.)
Extragalactic Energetic Sources
Indian Academy of Sciences, Bangalore, 1985, pp. 105–112

Relativistic Motion in Quasars

D. J. Saikia *Radio Astronomy Centre, Tata Institute of Fundamental Research, Post Box 1234, Bangalore 560012.*

Abstract. Using a large sample of well-observed, double-lobed quasars, we examine simple predictions of the relativistic beaming hypothesis and find the data to be broadly consistent with this scenario. We also review briefly other evidences in the literature which suggest that relativistic beaming does appear to play an important role in the observed radio properties of quasars.

Key words: quasars—relativistic beaming

"We dance round in a ring and suppose,
But the Secret sits in the middle and knows."
Robert Frost, *The Secret Sits*

1. Introduction

It is now generally believed that energy is supplied to the extended regions of extragalactic radio sources by oppositely-directed beams of fluid squirting from active galactic nuclei. These collimated beams possibly have highly relativistic velocities close to the nuclei of their parent optical objects, but they perhaps slow down as they burn their way through the surrounding interstellar or intergalactic medium. Dissipation of energy by these beams as they traverse outwards can often give rise to narrow, elongated features in the brightness distribution of a source. Such features, called jets, have been detected in recent years in a large number of sources, and have perhaps provided the strongest evidence in support of the above scenario. The jets range in scale from the VLBI ones with sizes of $\sim$ a few milliarcsec to those which extend upto many tens of arcsec and have been mapped by aperture synthesis techniques.

If the flow velocity is large, the flux-density of the approaching jets will be significantly enhanced by relativistic beaming when the ejection axis is close to the line of sight. Over the last few years, there have been attempts to build 'unified models' which seek to identify the core-dominated quasars with those whose core flux-density has been significantly Doppler boosted due to a small viewing angle and a relativistic bulk velocity. In these unified schemes, quasars with their jet axes close to the plane of the sky have been identified with either the radio-quiet quasars (Scheuer & Readhead 1979) or the ones whose radio emission is dominated by the extended lobes (Orr & Browne 1982).

Although a wide variety of observations of active galactic nuclei have since been interpreted in the relativistic beaming framework with a reasonable degree of success,

there are problems with the simple unified schemes which have been suggested so far. In this short review we shall concentrate only on quasars and summarize some of the evidence which suggests that relativistic beaming for both nuclear and extended jets does appear to play an important role in some of the observed properties of these sources.

2. Relativistic beaming in nuclear jets

Several recent statistical studies indicate that the fraction of emission from the core, f_c, might be a reasonably good statistical measure of the orientation of the ejection axis to the line of sight (*cf.* Moore *et al.* 1981; Orr & Browne 1982; Kapahi & Saikia 1982, hereinafter referred to as KS82). For a sample of well-observed quasars, KS82 examined the correlations of f_c with other parameters which also depend on the viewing angle, such as the projected linear size, l, the supplement of the angle formed at the core by the outer hot spots, Δ, and the ratio of separations, R_θ, of the hot-spots from the nucleus. The results appeared to be broadly consistent with the predictions of the relativistic beaming model.

In this section, we first re-examine the f_c–l, f_c–Δ and the l–Δ correlations using a larger sample of well-observed quasars. While investigating the f_c–R_θ correlation, it was earlier assumed that the component further from the nucleus is indeed the approaching one. Since it has recently been shown by Saikia (1984a) that this often may not be the case, we have not examined this relationship in the present paper. Here, we also do not consider the correlation of f_c with the flux-density ratio, R_s, of the outer hot-spots, since this parameter is plagued by a number of uncertainties such as the identification of the approaching component, a reliable estimate of the flux-density of the hot-spots and an understanding of the evolution of their luminosity with age.

2.1 *The f_c–l relation*

If the core-dominated sources are indeed inclined at small angles to the line of sight, one might expect an inverse correlation between f_c and the projected linear size, l. To look for such a relation, Hine & Scheuer (1980) considered a sample of 3CR double-lobed sources while KS82 compiled a reasonably homogeneous sample of 78 well-observed quasars selected from low-frequency catalogues. While the 3CR sources appeared to be consistent with the model predictions, the sample of quasars showed a significant correlation, consistent with the predictions of the relativistic beaming hypothesis.

Here we re-examine the f_c–l relation using all quasars which have a measured redshift, have been mapped with at least 3 resolution elements along their main axes and have a total flux-density at 178 MHz $\geqslant$ 2 Jy. It is relevant to note here that to compile a sample largely independent of orientation, the flux-density limit for completeness should be defined for the extended lobes only. However, if the core generally contributes only a small fraction of the total flux-density at 178 MHz, the sources in the sample should be more or less randomly distributed in the sky.

The final sample consists of 140 quasars, 131 of which have lobes on opposite sides of the nucleus while 9 appear one-sided with only a single extended lobe. These 9 have been observed to be one-sided from observations with high dynamic range and sensitivity either at the VLA or MERLIN. The f_c–l diagram for the entire sample is

shown in Fig. 1. The parameter f_c has been estimated for an emitted frequency of 8 GHz while l has been calculated in an Einstein–de Sitter universe with $H_0 = 50\,\mathrm{km\,s^{-1}\,Mpc^{-1}}$. There is clearly a deficit of sources with $f_c \gtrsim 0.3$ and $l \gtrsim 400$ kpc which is unlikely to be due to any selection effect. The two very discrepant quasars are marked in the figure. The predicted upper-envelopes to the f_c–l diagram corresponding to $f_c(90°) = 0.033$ (see KS82) and bulk Lorentz factor $\gamma = 2$ and 5 are also shown in the figure. It is of interest to note that the one-sided sources usually have strong cores and small linear sizes, consistent with the possibility that their jet axes are close to the line of sight (*cf.* Kapahi 1981). A Kolmogorov–Smirnov test shows that the f_c-distributions for the two roughly equal groups with $l >$ and $l < 200$ kpc are different at a level of significance of ~ 95 per cent. The level of significance is not overwhelming, perhaps largely due to the intrinsic size distribution of quasars.

2.2 *The f_c–Δ Relation*

Readhead *et al.* (1978) had pointed out that the large misalignments between VLBI and large-scale structure in core-dominated sources might be due to amplification of small intrinsic misalignments by projection effects. This result was extended to a large sample of double-lobed quasars by Saikia & Kapahi (1982) who reported a positive correlation between f_c and Δ, the supplement of the angle formed at the core by the outer hot-spots, consistent with the predictions of the relativistic beaming model.

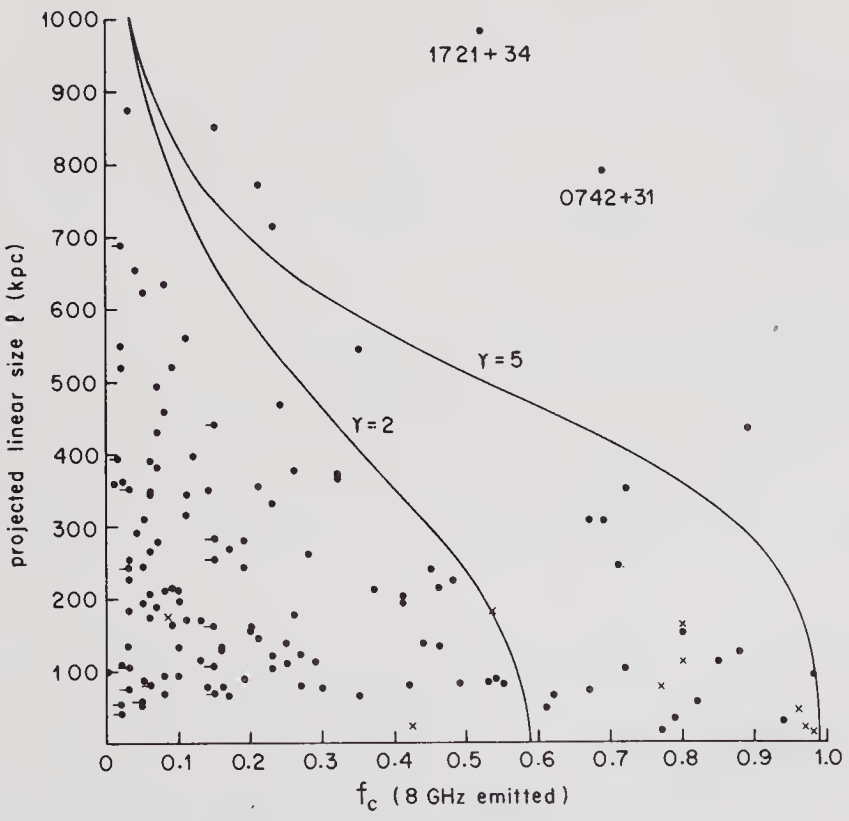

Figure 1. The f_c–l diagram, where f_c is the fraction of radio emission from the core, and l, the projected linear size. The double-lobed quasars are shown by filled circles, while the crosses represent those with only a single extended lobe. The predicted upper envelopes for bulk Lorentz factors $\gamma = 2$ and 5, as explained in the text, are also shown.

We re-examine the f_c–Δ relation using only those quasars, from the sample described earlier, which have been observed with at least 6 resolution elements along their major axes. This criterion reduces errors in the values of Δ. The f_c–Δ diagram and the Δ-distributions for those with $f_c \leqslant 0.15$ and > 0.15 for the resulting sample of 106 quasars are shown in Figs 2 and 3 respectively. Although there is a large scatter, there appears to be a trend for quasars with more prominent cores to appear more misaligned. A Kolmogorov–Smirnov test shows the two distributions in Fig. 3 to be different at a level of significance of ~ 99.99 per cent.

2.3 *The l–Δ Diagram*

Since sources with prominent cores appear more misaligned and also have small projected sizes, it is to be expected that l and Δ will be correlated in the sense that the more misaligned sources have smaller linear sizes. KS82 reported the existence of such a correlation, which has since been confirmed by Hintzen, Ulvestad & Owen (1983). The l–Δ correlation for the present sample of 106 quasars, shown in Fig. 4, confirms the earlier results.

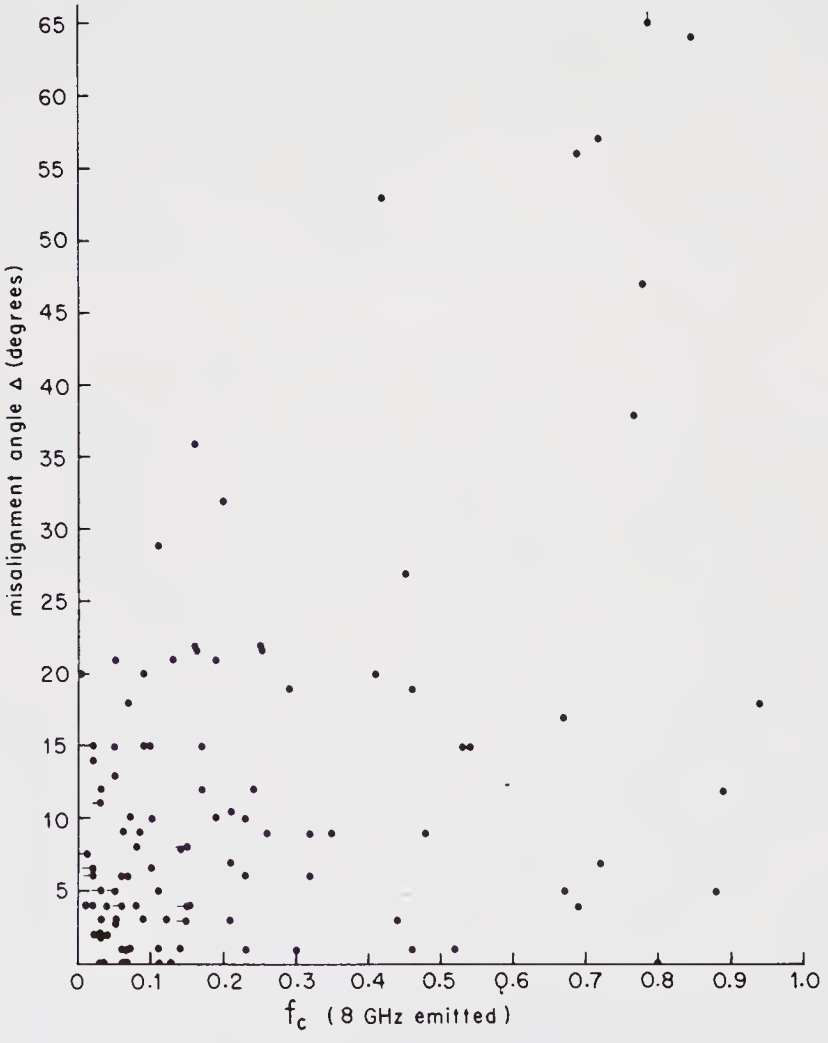

Figure 2. The f_c–Δ diagram, where Δ is the supplement of the angle formed at the core by the outer hot spots.

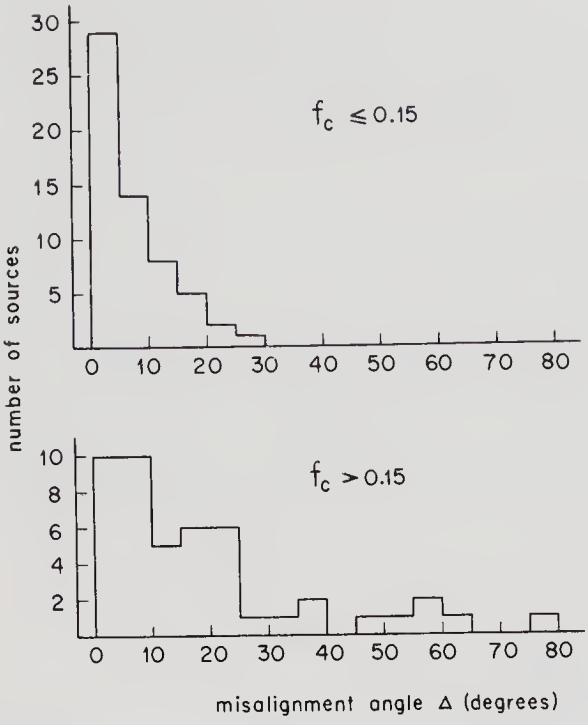

Figure 3. The distributions of Δ for sources with $f_c \leqslant 0.15$ and > 0.15.

2.4 *Summary of Additional Evidence*

Here we briefly summarize some of the additional evidence in support of the relativistic beaming scenario for nuclear, VLBI-scale jets.

(a) Superluminal motion: The superluminal motion of knots in VLBI-scale jets can be understood if they are ejected with a velocity $\sim c$ along an axis close to the line of sight (Behr *et al.* 1976; Blandford, McKee & Rees 1977; Scheuer & Readhead 1979; Blandford & Königl 1979).

(b) One-sidedness of jets: The nuclear jets tend to be one-sided, even when the outer extended lobes are approximately symmetric. Their apparent one-sidedness finds a natural explanation in the relativistic beaming model. (*e.g.* Scheuer & Readhead 1979; Blandford & Königl 1979).

(c) Low-frequency variability: The assumption of bulk relativistic motion in the nuclear regions of low-frequency variables can decrease the inferred brightness temperature below the inverse-Compton limit (Fanti, Padrielli & Salvati 1982; Jones 1982).

(d) Inverse-Compton X-ray flux: The problem of detecting much lower compton X-ray flux in some compact radio sources can also be alleviated by invoking bulk relativistic motion in the nuclear regions (Marscher & Broderick 1981; Cohen 1985).

(e) Source counts of quasars: The proportion of flat-spectrum sources in flux-density-limited samples selected at different frequencies and also the number/flux-density counts of flat-spectrum sources appear to be consistent with the predictions of the relativistic beaming scenario (Orr & Browne 1982).

(f) Misalignments: While the VLBI structure of weak-cored sources appear to be reasonably well-aligned with the large-scale emission, those in core-dominated sources

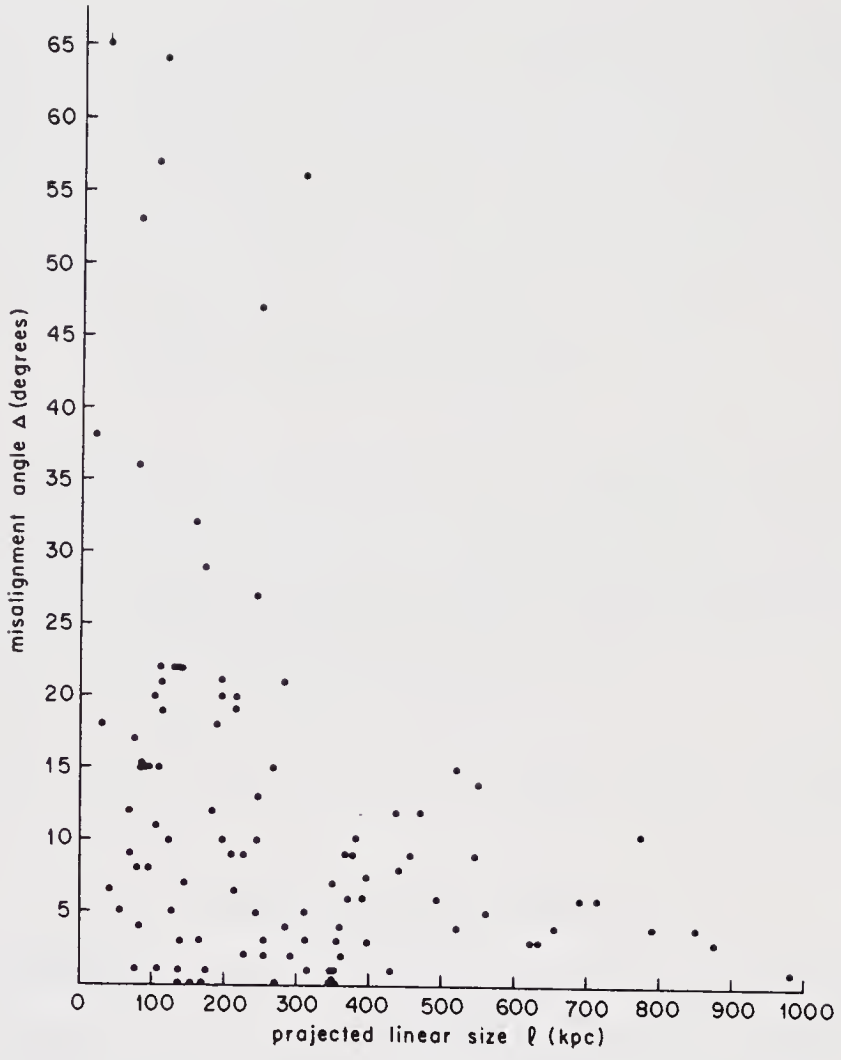

Figure 4. The l–Δ diagram.

exhibit strong curvature and are often misaligned with the extended emission. As discussed earlier, this can be understood if the core-dominated sources are viewed at small angles to the line of sight (Readhead *et al.* 1978, 1983).

This result has been extended to a large sample of quasars by Saikia & Shastri (1984) who have used the core-polarization E-vector at $\lambda 6$ cm to infer the direction of the nuclear elongation. Their result is consistent with the earlier VLBI studies and in broad agreement with the relativistic beaming model.

3. Relativistic beaming in extended radio jets

The extended radio jets in quasars also tend to be one-sided, even when the outer extended lobes are approximately symmetric. To explain their apparent one-sidedness in the relativistic beaming model, a mildly relativistic velocity of $\sim 0.5\,c$ is often sufficient. Since it is known that the extended and nuclear jets tend to occur on the same side of the nucleus (*cf.* Bridle & Perley 1984; Rees 1985), it is tempting to speculate that the observed asymmetry of the extended jets is also due to relativistic beaming. A more

detailed investigation shows that almost all sources with prominent cores tend to have extended jets, while those without jets almost always tend to have weak cores (Saikia 1984b). This suggests that sources with extended jets are indeed inclined at small angles to the line of sight. The tendency for quasars with jets to appear more misaligned is also consistent with such an interpretation.

However, there does appear to be a population of quasars which have one-sided radio jets and weak cores. These sources often do not have prominent hot-spots at the end of the jets (*cf.* Saikia 1984b). The jets in these sources are perhaps extremely dissipative and slow-moving, and can be observed even at angles close to the plane of the sky. If the asymmetric dissipation of energy in these sources is influenced by the external medium, it is extremely unlikely that the medium $\sim$ 100 kpc from the nucleus can persuade the VLBI-scale jet to occur on the same side of the nucleus as the large-scale jet. VLBI observations of high sensitivity would be extremely interesting to study the orientation of the nuclear and extended jets in such sources.

4. Discussion

The radio data appear to be broadly consistent with the Orr–Browne type unified scheme where core-dominated quasars have small viewing angles while the weak-cored ones are inclined at large angles to the line of sight. One of the difficulties with this scheme has been the reported tendency for extended lobe-dominated sources to have weaker Fe II emission and broader lines than the core-dominated ones (*cf.* Miley & Miller 1979; Steiner 1981). The difference in the Fe II emission for the two types of radio structures has, however, not been confirmed by Bergeron & Kunth (1984). In the Scheuer–Readhead model, the quasars with their ejection axes close to the plane of the sky were identified with the radio-quiet ones. Initial radio surveys of optically selected QSO samples were not consistent with the predictions of this model (Strittmatter *et al.* 1980; Condon *et al.* 1981; Shaffer, Green & Schmidt 1982). However, recent, deep observations with the VLA of the Palomar sample of bright quasars appear to be consistent with the model predictions provided the strong, extended and perhaps unbeamed quasars are excluded (Kellermann *et al.* 1984). But it is important to note that there are statistically significant spectroscopic differences between the radio-loud and radio-quiet quasars (*cf.* Bergeron & Kunth 1984), which are unlikely to be due to orientation effects.

While broader unified schemes are definitely required to understand the varying degrees of activity in galactic nuclei and their properties at all wavelengths, the purpose of this short review has been to merely show that relativistic beaming does appear to play an important role in the observed radio properties of one class of active objects, namely quasars. Attempts have also been made over the last couple of years to understand the BL lac type objects and highly polarized quasars in the relativistic beaming framework with a reasonable degree of success.

Acknowledgements

I thank Vijay Kapahi for numerous useful discussions and also a critical reading of the manuscript.

References

Behr, C., Schucking, E. L., Visveshwara, C. V., Wallace, W. 1976, *Astr. J.*, **81,** 147.
Bergeron, J., Kunth, D. 1984, *Mon. Not. R. astr. Soc.*, **207,** 263.
Blandford, R. D., Königl, A. 1979, *Astrophys. J.*, **232,** 34.
Blandford, R. D., McKee, C. F., Rees, M. J. 1977, *Nature*, **267,** 211.
Bridle, A. H., Perley, R. A. 1984, *A. Rev. Astr. Astrophys.*, **22,** 319.
Cohen, M. H. 1985, in *Proc. Extragalactic Energetic Sources*, Ed. V. K. Kapahi, Indian Academy of Sciences, Bangalore, p. 1.
Condon, J. J., Condon, M. A., Jauncey, D. L., Smith, M. G., Turtle, A. J., Wright, A. E. 1981, *Astrophys. J.*, **244,** 5.
Fanti, R., Padrielli, L., Salvati, M. 1982, in *IAU Symp. 97: Extragalactic radio sources*, Eds D. S. Heeschen & C. M. Wade, D. Reidel, Dordrecht, p. 317.
Hine, R. G., Scheuer, P. A. G. 1980, *Mon. Not. R. astr. Soc.*, **193,** 285.
Hintzen, P., Ulvestad, J., Owen, F. N. 1983, *Astr. J.*, **88,** 709.
Jones, T. W. 1982, *Low Frequency Variability of Extragalactic Radio Sources*, Eds W. D. Cotton & S. R. Spangler, NRAO, Green Bank.
Kapahi, V. K. 1981, *J. Astrophys. Astr.*, **2,** 43.
Kapahi, V. K., Saikia, D. J. 1982, *J. Astrophys. Astr.*, **3,** 465 (KS82).
Kellermann, K. I., Sramek, R., Shaffer, D., Schmidt, M., Green, R. 1984, in *Proc. Liège Coll. 24: Quasars and Gravitational Lenses*, Inst. d'Astrophys., Univ. Liège, p. 81.
Marscher, A. P., Broderick, J. J. 1981, *Astrophys. J.*, **247,** L49.
Miley, G. K., Miller, J. S. 1979, *Astrophys. J.*, **228,** L55.
Moore, P. K., Browne, I. W. A., Daintree, E. J., Noble, R. G., Walsh, D. 1981, *Mon. Not. R. astr. Soc.*, **197,** 325.
Orr, M. J. L., Browne, I. W. A. 1982, *Mon. Not. R. astr. Soc.*, **200,** 1067.
Readhead, A. C. S., Cohen, M. H., Pearson, T. J., Wilkinson, P. N. 1978, *Nature*, **276,** 768.
Readhead, A. C. S., Hough, D. H., Ewing, M. S., Walker, R. C., Romney, J. D. 1983 *Astrophys. J.*, **265,** 107.
Rees, M. J. 1985, in *Proc. Extragalactic Energetic Sources*, Ed. V. K. Kapahi, Indian Academy of Sciences, Bangalore, p. 53.
Saikia, D. J. 1984a, *Mon. Not. R. astr. Soc.*, **209,** 525.
Saikia, D. J. 1984b, *Mon. Not. R. astr. Soc.*, **208,** 231.
Saikia, D. J., Kapahi, V. K. 1982, *Bull. astr. Soc. India*, **10,** 42.
Saikia, D. J., Shastri, P. 1984, *Mon. Not. R. astr. Soc.*, **211,** 47.
Scheuer, P. A. G., Readhead, A. C. S. 1979, *Nature*, **277,** 182.
Shaffer, D. B., Green, R. F., Schmidt, M. 1982, in *IAU Symp. 97: Extragalactic radio sources*, Eds D. S. Heeschen & C. M. Wade, D. Reidel, Dordrecht, p. 367.
Steiner, J. E. 1981, *Astrophys. J.*, **250,** 469.
Strittmatter, P. A., Hill, P., Pauliny-Toth, I. I. K., Steppe, H., Witzel, A. 1980, *Astr. Astrophys.*, **88,** L12.

V. K. Kapahi (Ed.)
Extragalactic Energetic Sources
Indian Academy of Sciences, Bangalore, 1985, pp. 113–117

3C 179 and Superluminal Source Statistics

R. W. Porcas *Max-Planck-Institut für Radioastronomie, Auf dem Hügel 69, D5300 Bonn, FRG*

Abstract. Recent observations of the superluminal source 3C 179 are presented. The statistical incidence of superluminal motion is discussed and an observational programme to test the relativistic jet model is described.

Key words: quasars—superluminal motion—relativistic jet

During the course of his lectures, Marshall Cohen spoke quite extensively about the phenomenon of superluminal motion. This subject is one of the most intriguing in extragalactic research and so I needn't apologise for devoting my seminar to one aspect of the topic. Marshall concentrated his discussion with reference to the quasars 3C 345 and 3C 273. Here I shall talk about 3C 179 and what light it sheds on the statistics of superluminal motion if the relativistic jet explanation is correct, and then report on some further observational tests which are underway using the new, sensitive Mark III VLBI recording system.

Fig. 1 presents a radio map of the quasar 3C 179 showing the structure on the arcsec scale. This map was obtained using the Jodrell Bank radio-linked array, MERLIN, at 408 MHz. The source exhibits nearly all the features mentioned by Robert Laing during his lectures: double lobes of emission, straddling a central, compact core and a jet pointing towards the western lobe which contains a hot spot. The fraction of the total flux contained in the core is about 8 per cent; a remarkably similar VLA map at 5 GHz (courtesy of Owen & Puschell) of comparable resolution shows that the core has a flat spectrum, however, and accounts for ~ 40 per cent of the emission at that frequency.

I have been doing a series of transatlantic VLBI observations of the core of 3C 179 at 10.7 GHz, giving a resolution of 0.5 milli-arecsec *i.e.* 1000 times smaller than this map. The results of the first 2 experiments, in 1979 October and 1980 December, revealed that the core itself has an 'inner' double structure. Unfortunately, the core is too weak to easily employ the hybrid mapping schemes mentioned earlier in this Winter School, but fitting models to the visibility functions showed that the separation of the two inner components increased by 0.15 milli-arcsec. This corresponds to a separation velocity of 7.6 times the speed of light (assuming a Hubble constant of 55 km s^{-1} Mpc^{-1} and that the redshift of 3C 179 *does* indicate its distance) and demonstrated superluminal motion in the core (Porcas 1981).

Since then I have obtained observations at three more epochs at 10.7 GHz and one at 5 GHz. Fig. 2 shows the 'expansion graph' of 3C 179, a plot of the separation of the inner double components at each observing epoch. Interesting features to notice are:

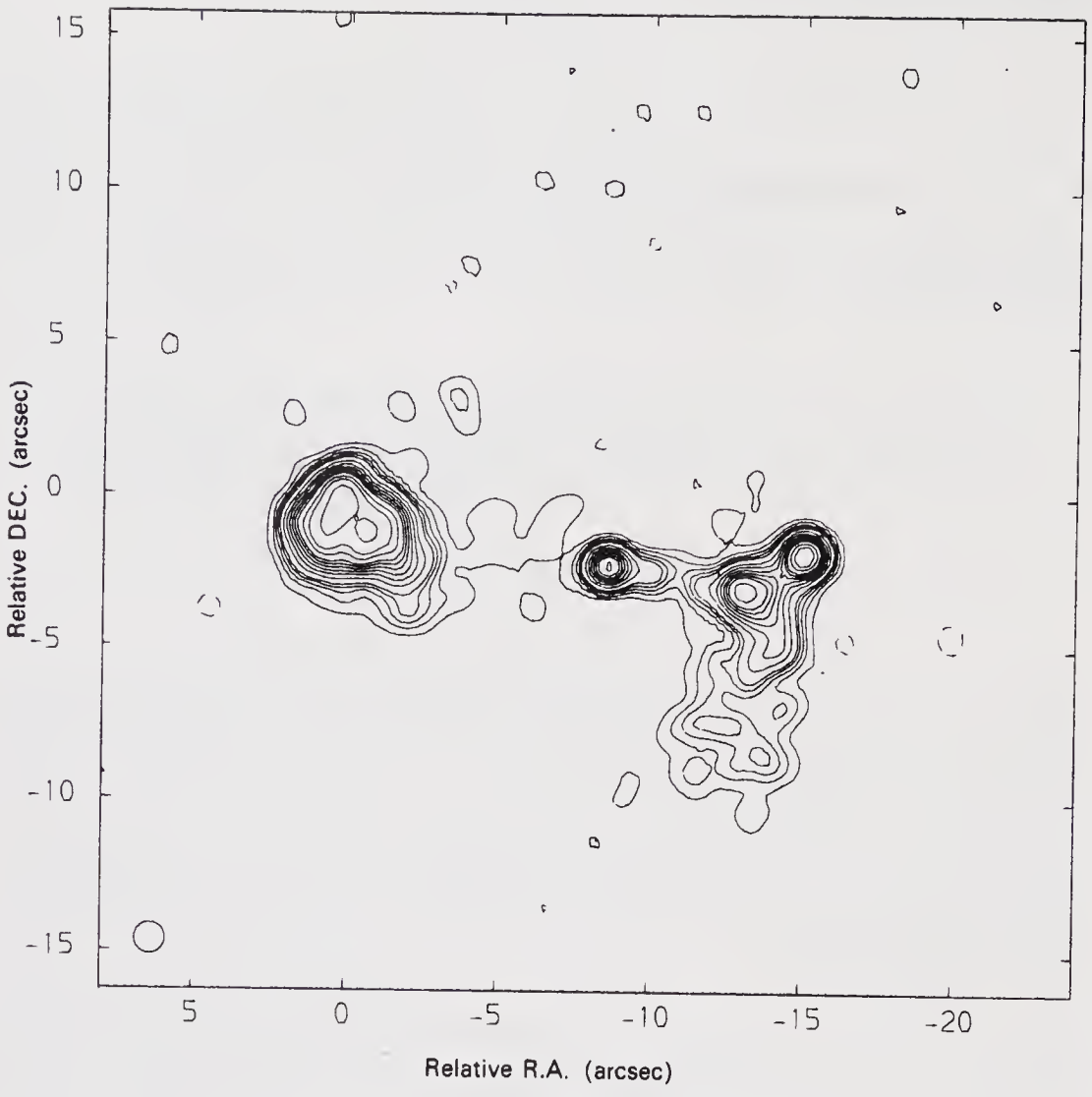

Figure 1. 408-MHz MERLIN map of 3C 179.

(i) the superluminal motion is confirmed as the separation continues to increase with time, (ii) the last 2 points at 10.7 GHz are above an extrapolation from the previous 3 and (iii) the 5 GHz point does not quite agree with those at 10.7 GHz. One explanation for (ii) would be that the motion has indeed accelerated (Marshall mentioned that a similar acceleration may have occurred for the outer component of 3C 345). An alternative explanation is that it results from the inadequacies of model fitting. Imagine that in addition to a constant, linear separation velocity, other changes occur just below the resolution limit. The eastern component may itself have sub-components on the 0.1 milli-arcsec scale (the model fitting indicates component extensions of this order); if the relative flux density of these sub-components changes, the measured separation of the centroids of the eastern and western components will be affected. If, in addition, the two sub-components have different spectral indices, the centroid separation will be frequency dependent.

Most of the properties of 3C 179 (except its prominent double lobe structure) have been exhibited by the other superluminal sources, such as 3C 345 and 3C 273. Although 3C 179 is at a more convenient declination (67°) than the others for studying with

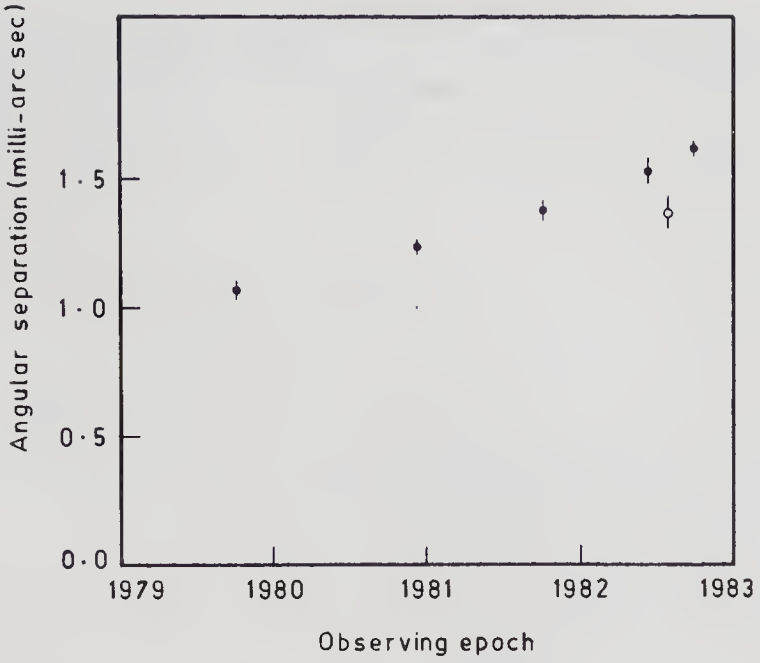

Figure 2. Separation of the nuclear components of 3C 179 versus observing epoch. Observations are at 10.7 GHz (filled circles) and 5 GHz (open circle).

current VLBI arrays, its core is only ~ 300 mJy (*i.e.* 100 times weaker than 3C 273) and one can ask why the more difficult observations of 3C 179 are important. The answer to this lies in the history of VLBI observations and the way radio astronomers select quasars for study.

As Geoff Burbidge has mentioned, most of the quasars in his master list are in fact radio quasars. These are found by first surveying the radio sky down to some limiting flux density, and then attempting to find optical objects associated with individual radio sources in the survey. Some of these, when studied spectroscopically, turn out to be quasars. VLBI observers have required their quasars to have 2 characteristics: (i) they must be strong (because the narrow recording bandwidth only yields adequate signal-to-noise on strong sources) and (ii) they must be compact (because the unfilled aperture of VLBI arrays can only 'see' compact sources). This second requirement is roughly equivalent to demanding that a quasar has a flat radio spectrum, since this is strongly correlated with compactness. Thus, early VLBI observers concentrated on studying the strongest flat-spectrum sources, mostly chosen from radio surveys at 5 GHz. Superluminal motion was discovered quite early (Whitney *et al.* 1971) and was found in quite a high proportion (~ 50 per cent) of the sources studied, suggesting that it is a very common phenomenon.

Satisfactory explanations of superluminal motion have been more difficult to invent. Geoff Burbidge has tried to persuade us that the redshifts do not indicate distance, whilst Professor Chitre has suggested that the phenomenon is an illusion brought about by an intervening gravitational screen. One of the more popular explanations is the 'relativistic jet', a beam of fast moving plasma moving with high Lorentz factor, γ, at a small angle, θ, to the observer's line of sight. Under special circumstances it is possible for a radio-emitting region moving in the jet to appear to move superluminally, because the observer's view of the early part of the motion is delayed with respect to later parts, and hence the apparent duration of the motion is shortened. This is an attractive

explanation because it fits in with theories about the origin of the outer, extended structure of radio sources and can explain the rapid flux density variations seen in some quasars. However, it does require very special viewing geometry. In order to see an apparent velocity Qc, a Lorentz factor of at least Q is required and the angle of the jet θ, with respect to the observer must be Q^{-1}. Since Q is observed to be ~ 7, θ must be $\sim 8°$, which can be expected only in $\sim Q^{-2}$ sources (*i.e.* 1 in 50). Thus the statistical prediction of the model is that the superluminal phenomenon should be rare.

This apparent contradiction between observation and model is resolved by realizing that a radio emitter moving relativistically at a small angle to the observer has an enhanced flux density, because of 'relativistic beaming'. Thus the sample of strong sources observed by VLBI is biased to contain sources with small angles simply because they are strong. How can one proceed to test the prediction of the model, that the superluminal effect should be rare amongst sources selected without bias with respect to their jet angles? Put another way, what and where are the sources which do *not* show superluminal motion because their jets do not point at us?

This is where the significance of 3C 179 comes in. At low frequencies, most of its flux density does not come from the relativistic jet which supposedly exists in the core but, rather, from the outer, extended emission regions—the double lobes. We know that these regions cannot move with velocities near the speed of light, because of the high degree of flux and separation symmetry with respect to the core which they exhibit (Longair & Riley 1979; Swarup & Banhatti 1981). Therefore, the flux density of the lobes does not depend on the source orientation, and we may take samples of sources selected on the basis of lobe flux density as being unbiased with respect to θ.

3C 179 was selected from just such a sample. The Jodrell Bank 966-MHz survey contains sources between declinations 40° and 70° with flux densities greater than 0.7 Jy. Of these, there are some 30 quasars brighter than 19 mag, and with overall size greater than 10 arcsec. Since these should be unbiased with respect to jet angle, the $\sim Q^2$ counterparts of 3C 179 (*i.e.* quasars with double lobes but unfavourable jet alignments) must be amongst the other 29 quasars. (Note that there is no room in the sample for quasars with low Lorentz factors. All the remaining quasars are 'used up' as the unaligned counterparts of 3C 179 with Lorentz factors ~ 7.) Orr & Browne (1982) have developed a scheme in which sources such as 3C 345 and other core-dominated sources are the extremes of a single population of radio quasars, with relativistic jets and double lobes, and whose observed properties simply reflect the observer's viewing angle.

We can proceed further with observational tests of the model by making VLBI observations of the cores of some of the other quasars in this sample. Toni Zensus and I have begun such a project at the MPIfR. We are observing 4 or 5 more quasars with a view to deciding whether they are indeed the unaligned counterparts of 3C 179 (as the relativistic jet model requires), or whether they look intrinsically different, or may even exhibit superluminal motions. Since the cores of these quasars are even weaker than that of 3C 179, we are using the new Mark III VLBI recording system. This consists essentially of 28 Mark II systems recorded in parallel, giving a factor of over 5 improvement in signal-to-noise ratio. The 28 'tracks' are separately correlated and then added coherently by means of an injected phase calibration signal. Some interesting features of the system are (i) the tape speed is 11 ft s^{-1}, (ii) a full tape only lasts 13 min, (iii) it takes 5 min to rewind the tape, and (iv) each tape costs around $ 300! It turns out in practice that our observing time is limited by the costs of tape purchasing and shipping!

We have already had 2 observing periods for this project and data for two of the sources have just been processed with the new MPIfR Mark III processor in Bonn. The increased sensitivity of this new VLBI system enables us now to observe 50 mJy cores, and we hope shortly to be able to shed some light on the question of the occurrence of superluminal motion in sources with unaligned jets!

References

Longair, M. S., Riley, J. M. 1979, *Mon. Not. R. astr. Soc.*, **188,** 625.
Orr, M. J. L., Browne, I. W. A. 1982, *Mon. Not. R. astr. Soc.*, **200,** 1067.
Porcas, R. W. 1981, *Nature*, **294,** 47.
Swarup, G., Banhatti, D. G. 1981, *Mon. Not. R. astr. Soc.*, **194,** 1025.
Whitney, A. R., Shapiro, I. I., Rogers, A. E. E., Robertson, D. S., Knight, C. A., Clark, T. A., Goldstein, R. M., Marandino, G. E., Vandenberg, N. R. 1971, *Science*, **173,** 225.

Kapahi, V. K. (Ed.)
Extragalactic Energetic Sources
Indian Academy of Sciences, Bangalore, 1985, pp. 119–126

Faraday Rotation and Magnetic Fields in QSO Absorption-Line Clouds

P. P. Kronberg *Scarborough College, Toronto, Ontario M1C 1A4, Canada & David Dunlap Observatory, University of Toronto, Richmond Hill, Ontario L4C 4Y6, Canada*

Abstract. An intercomparison of the Faraday rotation of quasars and their absorption-line spectra shows, for the first time, that we are detecting magnetic fields in absorption-line systems. By estimating the electron column density from the absorption-line spectrum we can make a statistical estimate of the magnetic field strength. For quasars with sufficient column density in their absorption-line systems, these estimates suggest fields of a few microgauss, or upper limits near that level.

For a few quasars, the implied field strengths are at milligauss level. This may reflect the existence of a much larger column density of intervening material than that deduced from the absorption-line spectra. This additional material may be very hot, and therefore not detectable in the optical window. Since Faraday rotation is insensitive to the temperature of the ionized gas, it could, for some quasars, be a useful signature of an additional, hot gas component in absorption-line systems. Alternatively, the high field levels could be genuine, particularly if they are in dense clouds associated with the quasar.

Key words: quasars, radio polarization—quasars, absorption lines—Faraday rotation—magnetic fields

1. Introduction

As the number and quality of radio polarization data for extragalactic radio sources has improved, we are able to determine the Faraday rotation measure (RM) of the integrated emission from a large sample of extragalactic radio sources.

$$\mathrm{RM} = \frac{\mathrm{d}\chi}{\mathrm{d}\lambda^2} = 8.1 \times 10^5 \int_0^{l_s} n_e B_\parallel \, \mathrm{d}l \quad \mathrm{rad\,m^{-3}}, \tag{1}$$

where n_e is the electron density ($\mathrm{cm^{-3}}$), $B_\parallel$ the line-of-sight magnetic field (G) and l_s the distance (pc) to the radio emitter. A source's RM is the sum of (1) a contribution from our Galaxy (GRM), (2) that intrinsic to the source itself (IRM), and finally, (3) an intervening line-of-sight contribution (LSRM). It is the latter which I shall discuss in this lecture. However, since LSRM and IRM, being both extragalactic, cannot easily be separated, I shall discuss the measurements of RRM (= LSRM + IRM), the 'residual' or extragalactic rotation measure after we have subtracted the GRM from the measured value (RM).

The current radio polarization data over 2–22 cm permit us to determine RM's for nearly 600 extragalactic sources. An updated version of the all-sky plot of Simard-Normandin & Kronberg (1980) is shown in Fig. 1. At most galactic positions at $|b| \gtrsim 25°$ the average RM is small, which means that RRM (and IRM and LSRM) are usually small. Furthermore the sign of RM is autocorrelated over $\sim 30°$ at high $|b|$ (Simard-Normandin & Kronberg 1980). This shows that we can, at least statistically, remove the GRM to obtain an estimate of RRM for each source.

In this lecture I shall discuss the evidence for Faraday rotation in intervening clouds between us and the quasars. From the optical and/or 21-cm absorption spectrum of a quasar, we can estimate the column density of electrons, $N_e = \int_c n dl$ for an intervening cloud at absorption redshift z_a. Then it is possible to compare this with the Faraday rotation which is influenced by the same N_e and associated line-of-sight magnetic field $\langle B_\parallel \rangle$. Following Kronberg & Perry (1982) we define the electrondensity-weighted mean line-of-sight magnetic field as

$$\langle B_\parallel \rangle = \frac{\int n_e B_\parallel \, dl}{\int n_e \, dl}. \tag{2}$$

Equation (2) shows that we can estimate $\langle B_\parallel \rangle$ of an intervening absorption-line cloud by dividing its contribution to RRM by its electron column density, N_e. We can estimate the latter from its absorption-line spectrum by measuring the line equivalent widths; then, using an ionization model and, if necessary, abundance ratios (if only heavy-element lines are observed), we can convert the column density of a particular atom to an electron column density, N_e. A single cloud at absorption-line redshift, z_a, having N_e (cm^{-2}) and $\langle B_\parallel \rangle$ (G) as defined above will produce a contribution to the observed RRM which is given by

$$\mathrm{RRM} = \frac{\beta N_e \langle B_\parallel \rangle}{(1+z_a)^2} \quad \mathrm{rad\,m^{-2}} \tag{3}$$

where $\beta = 2.63 \times 10^{-3}$. The $(1+z_a)^2$ factor arises from the fact that $d\lambda^2$ (observed) (see Equation 1) is larger than $d\lambda^2$ (cloud) by $(1+z_a)^2$.

2. Results of a rotation-measure–absorption-line analysis

In a recent analysis of the most recent RM and absorption-line spectra of QSO's, Judith Perry and I have found that there is indeed a tendency for quasars having strong absorption lines to have an excess RRM (Kronberg & Perry 1982). This has led to the first estimates of the magnetic field strengths in the absorption-line clouds in some QSO's. I shall illustrate the evidence for an RRM–absorption-line association as follows: Within a sample of 37 quasars with well-observed spectra and reasonably reliable RRM, we could divide these into 21 with weak or no detectable absorption, and 14 which had strong absorption (2 were classified as uncertain), on the basis of their optical spectra. We found that only one of the 21 weak absorbers has $|\mathrm{RRM}| > 30\,\mathrm{rad\,m^{-2}}$. Statistical tests using these two 'populations' show that the excess RRM for the strong absorption set is significant at a confidence level of $\gtrsim 98.8$ per cent (see Fig. 2).

Some further remarks concerning this result can be made: It is well known that

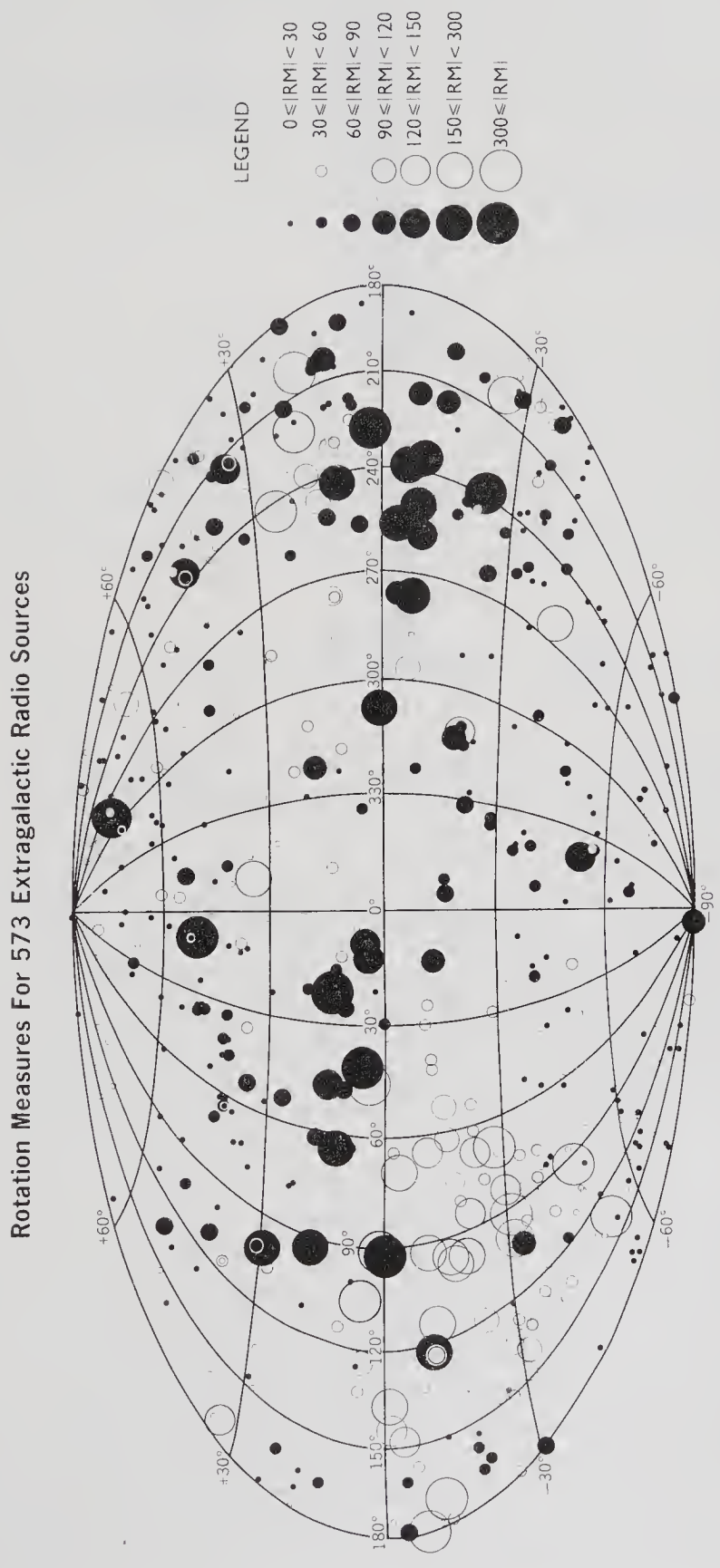

Figure 1. A Hammer-Aitoff equal-area projection showing the rotation measures (RM) of 573 extragalactic radio sources.

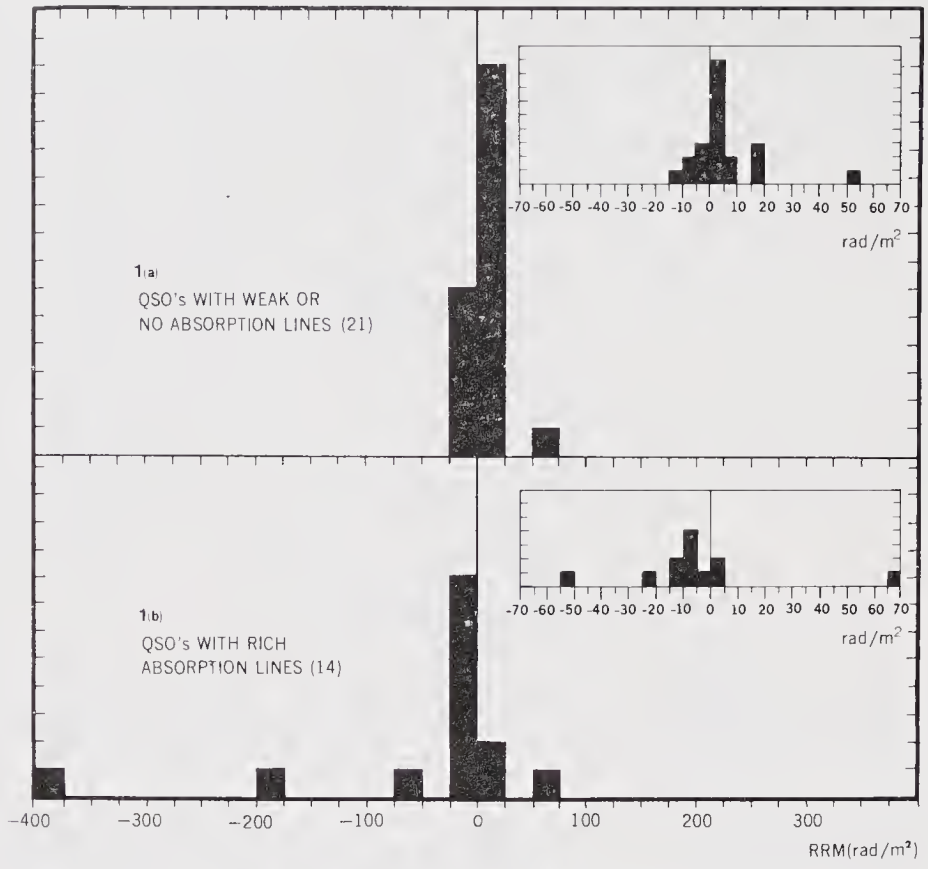

Figure 2. Histograms showing the distribution of RRM for quasars having strong and weak absorption. The insets show the low-RRM portion for smaller RRM intervals.

strong absorption-line systems occur preferentially in spectra of highly redshifted QSO's, a fact which is consistent with the higher probability of intersection with an intervening object for lines of sight originating at larger distances. Indeed, the average z_e of our 14 'strong absorbers' is roughly twice that of the 21 'weak absorbers' (2.01 and 1.02 respectively). If we assume the obvious alternative explanation for the excess RRM's, namely that they arise in the quasars themselves (or their host clusters, *etc.*), then because of the strong watering down of the observed RRM for highly redshifted objects [$\propto (1+z)^{-2}$—see Equation 3] we should see the *opposite* effect to that found, namely that higher RRM occurs for the low-z quasars. (This expectation includes the assumption that the typical excess RRM does not increase faster than $(1+z)^2$ due to evolutionary effects or a source luminosity effect.)

I shall also comment on 3C 309.1, the single exception which does not have strong optical absorption but has a significant RRM of $\sim 52\,\mathrm{rad\,m^{-2}}$. In an investigation of possible galaxy–QSO associations, Burbidge *et al.* (1971) called attention to the fact that its line of sight passes only 6.2 arcmin (14 kpc for $H_0 = 75$) from the nucleus of NGC 5832 at $z = 0.002$. A galaxy–QSO superposition of this kind is very unusual, having an *a priori* probability of ~ 0.001. In this case, even though its absorption spectrum does not show strong lines, we have independent evidence for an intervening object which can easily produce the observed excess RRM. If I were to remove 3C 309.1 from the 'weak absorber' set on these grounds, then the count above would be 0 out of 20 excess RRM's for the weak absorbers, and would reinforce the statistical result even further.

Now that I have, I hope, convinced you that we are detecting the presence of magnetic fields in some QSO absorption clouds I must mention a property of some of the radio sources which makes the application of Equation (3) problematic. This is that radio angular size of some quasars corresponds to several kiloparsecs at z_a, which means that the *Faraday* rotation line of sight can be up to a few kiloparsecs different from the *optical* ray path which is relevant to the absorption lines. Some of our estimates of $B_\parallel$ which I shall discuss below will therefore be subject to uncertainty resulting from this fact. Obviously the ideal quasar for probing absorption-line magnetic field strengths should have small radio size—and of course a high intrinsic radio polarization.

My final comment on our RRM–absorption results is that not *all* of the 14 strong absorbers have an excess RRM at our current level of detection (typically 15 rad m^{-2}). Three obvious reasons why this might be so are the following: (1) The radio ray path might not intersect the absorption-line cloud in some cases where the radio emission is significantly extended, (2) some clouds have intrinsically small Faraday rotation and/or magnetic fields which, combined with the $(1+z_a)^{-2}$ reduction of RRM puts their RRM below our detection limit, and (3) magnetic field reversals are such that significant cancellation of $n_e B_\parallel$ might occur in some cases.

3. What the intervening Faraday rotators could and could not be

The intervening objects which we know, or which have been postulated, are (1) haloes of galaxies, (2) clusters, (3) galaxy groups, (4) wind-driven shells of matter close to the QSO, and finally (5) the Lyman-α 'forest' clouds recently discovered and discussed by Sargent *et al.* (1980) and others.

The space densities and cross-sections of objects (1)–(3) are all such that at most only small numbers should be intersected—a fact which is at least roughly consistent with the statistics of QSO absorption-line systems. Massive, Coma-like clusters are too rare to be common absorption-line objects, however the haloes of large spiral galaxies are possible candidates (*cf.* Wagoner 1967) and the recent discovery of hot, extended gas clouds in galaxy groups suggest that galaxy groups, being much more numerous than large clusters (Bahcall 1980) may, perhaps in a pre-evolved form, also be absorption-line objects.

The only known class of object for which *many* intersections occur out to $z \simeq 3$ are the interesting Lα absorption clouds which are seen at a very large number of z_a's shortward of the Lα emission line in some QSO's. They are too numerous to be any of the objects (1)–(3), are of sub-galactic mass, and since they have too little mass to be gravitationally bound, they are presumably pressure-confined by a hot ambient gas, as suggested by Sargent *et al.* (1980). Using parameters similar to those deduced by Sargent *et al.*, which are summarized in Table 1, Kronberg & Perry (1982) investigated the possible effect of the Lα clouds on the rotation measure of QSO's, and concluded that they would *not* produce an observable RRM at the present epoch. Their discussion and conclusions can be briefly summarized as follows.

The effect on RRM of intervening clouds can be expressed as a z-dependent variance $\sigma^2_{\mathrm{RRM}}(z)$. For the Lα clouds, whose space density is assumed to scale as $(1+z)^3$ about the redshift range in which they have been observed ($\langle z \rangle = 2.4$), the σ^2_{RRM} can be shown

Table 1. Typical Lα cloud parameters deduced from the analysis of 6 QSO's by Sargent *et al.* (1980).

Number density, n_c, of clouds at $\langle z \rangle = 2.4$	$200\,\mathrm{Mpc}^{-3}$
Assumed cloud column density, N_e	$10^{19}\,\mathrm{cm}^{-2}$
Cloud radius, r_c	17 kpc
Cloud temperature	$3 \times 10^4\,\mathrm{K}$
Assumed equipartition magnetic field	$9 \times 10^{-8}\,\mathrm{G}$

under simple assumptions to be

$$\sigma^2_{\mathrm{RRM}}(z)_{\mathrm{L}\alpha\ \mathrm{clouds}} \simeq 4.1 \times 10^{-50} n_c(0) \beta^2 N_c N_e \langle B_\parallel(0) \rangle^2 \left[(1+z)^4 - 1\right] \mathrm{rad}^2\,\mathrm{m}^{-4}, \quad (4)$$

(Kronberg & Perry 1982), where N_c is the average total number of electrons per cloud, (assumed to be epoch-independent), N_e is the electron column density (cm^{-2}), β the constant in Equation (3), $n_c(0)$ the present-epoch number density of clouds (Mpc^{-3}). The '$\simeq$' results from the fact that Equation (4) is the solution to an integral which is only exact if $q_0 = 0$, *i.e.* approximately correct for $2q_0 z \ll 1$. The minimum detectable variance in the current RRM data is $\sim 20\,\mathrm{rad}^2\,\mathrm{m}^{-4}$. This, at $z = 3$ and for the parameters in Table 1, means that B would need to be ~ 25 times that for equipartition in the Lα clouds in order to have $\sigma^2 = 20\,\mathrm{rad}^2\,\mathrm{m}^{-4}$—a situation which is very unlikely. We can therefore conclude by calculation that the optically visible Lα 'forests' are not likely to be detected as Faraday rotators.

Having ruled out the Lα clouds, the only other known candidates are haloes of large galaxies, galaxy-group haloes (both in an earlier evolutionary state) or quasar-intrinsic excited clouds. We pointed out earlier that at best only *very few* galaxy haloes or groups will lie between us and a given high-z QSO. For the case of a few (m) such clouds, each with randomly oriented $\langle B_\parallel \rangle_i$, Kronberg & Perry (1982) have given the formal relation between the RRM, N_{ei} and $\langle B_\parallel \rangle_i$ (assuming that the latter are all of comparable magnitude). Given the RRM contribution from a single cloud (Equation 3), it can be shown that for m clouds, the typical 'deprojected' magnetic field strength estimate can be expressed as

$$\langle |\mathbf{B}| \rangle \sim \frac{2.2(1 + \langle z_a \rangle)^2 \mathrm{RRM}}{\beta \sqrt{m} N_e} \quad (5)$$

(Kronberg & Perry 1982). Estimates of the electron column density by various authors or by Kronberg & Perry have been combined with the latter's RRM data. An extract from these results is shown in Table 2. The $\langle |\mathbf{B}| \rangle$ estimates are obviously scaled to the electron column densities (column 4), and are normalized by the nearest 'likely' logarithmic electron column density (*e.g.* $N_{20} = N_e / 10^{20}\,\mathrm{cm}^{-2}$) as estimated either by Kronberg & Perry, or by other workers cited by them. Three categories of magnetic field estimates are quoted: (1) those which are not upper limits and a few microgauss (2) three which have only upper limits, corresponding to RRM upper limits, and (3) two further ones which give high (*i.e.* milligauss order) implied magnetic field strengths.

Table 2. Estimates of magnetic field strength in absorption clouds of different quasars.

	Source	No. of absorption systems used m	Redshift z_e	Redshift $\langle z_a \rangle$	Best current estimate of $\langle \lvert \mathbf{B} \rvert \rangle$ μG	Comment
Best estimates	3C 191	2	1.953	1.95	$\sim 30/N_{20}$	
	1331 + 170	1*	2.082	1.776	$\sim 13/N_{20}$	
Upper limits at $\langle \lvert \mathbf{B} \rvert \rangle \lesssim 250\,\mu$G	PKS 0119 − 046	4	1.948	1.97	$< 6/N_{20}$	
	OQ 172	2	3.53	2.78	$< 65/N_{18}$	RRM assumed to come from only two of the four z_a systems.
	4C 05.34	7	2.877	2.43	$< 230/N_{19}$	Effectively the higher of the two possible upper limits. (*cf.* Kronberg & Perry 1982).
Large implied fields	PKS 0458 − 02	1	2.285	2.28	$\sim 1600/N_{19}$	Single, broad-line system having $z_a \simeq z_e$.
	4C 24.61	1	2.328	2.363	$\sim 400/N_{20}$	$z_a > z_e$ for the strongest system. Galactic RM still uncertain.

*One (of 5) z_a system appears to dominate in hydrogen column density.

4. General comments and summary remarks

At this preliminary stage of estimating magnetic fields in absorption-line clouds, it is—at least in most cases—not clear how close we are coming to effectively dipping a probe into the cloud and measuring the true $|\mathbf{B}|$ value. The main question to be answered for a given QSO is: how well can we determine the electron column density? To answer this question we must ask if the optical absorption spectrum tells us enough information to reliably measure N_e. At present we cannot be certain whether there is a further component of hot gas which has not been detected. One could turn the statement around, and argue that when milligauss level fields result from Equation (5), we are really detecting a missing large component of very hot gas, not visible in the optical window. If there is 10^{21}–10^{22} cm^{-2} of very hot gas close to the QSO, the magnetic fields for PKS 0458−02 and 4C 24.61 come down to microgauss levels. This may be the best explanation for the large implied field values for PKS 0458−02 and 4C 24.61 in Table 2. However it is also interesting that, for these two sources $z_a \gtrsim z_e$, and they could be indicating genuinely, large magnetic fields in, for example, a QSO-intrinsic, ejected or wind-driven shell.

The combination of the best currently available rotation measure and absorption-line data on QSO's shows that we are now able to detect magnetic fields in extragalactic systems up to the largest observable redshifts. This is an exciting development, and will help to reveal the physical conditions in galactic and protogalactic haloes, and perhaps QSO intrinsic absorption clouds. The major uncertainty in many sources remains the hydrogen column density in the absorbing systems. Far ultraviolet spectroscopy is needed to determine the extent of very hot gas in intervening systems. Some of the absorbing clouds at $z_a \lesssim 1.5$ should be directly observable with the space-telescope resolution. In the meanwhile, RM measurements on more quasars are in progress.

References

Bahcall, N. A. 1980, in *Highlights of Astronomy*, **5**, Ed. P. A. Wayman, D. Reidel, Dordrecht, p. 699.
Burbidge, E. M., Burbidge, G. R., Solomon, P. M. Strittmatter, P. A. 1971, *Astrophys. J.*, **170**, 233.
Kronberg, P. P., Perry J. J. 1982, *Astrophys. J.*, **263**, 518.
Sargent, W. L. W., Young, P. J., Boksenberg, A., Tytler, D. 1980, *Astrophys. J. Suppl. Ser.*, **42**, 41.
Simard-Normandin, M., Kronberg, P. P. 1980, *Astrophys. J.*, **242**, 74.
Wagoner, R. V. 1967, *Astrophys. J.*, **149**, 465.

Kapahi, V. K. (Ed.)
Extragalactic Energetic Sources
Indian Academy of Sciences, Bangalore, 1985, pp. 127–131

Thick Accretion Discs—Luminosity Limits and Mass Outflow

Rajaram Nityananda & Ramesh Narayan *Raman Research Institute, Bangalore 560080*

Abstract. Thick accretion disc models for energetic extragalactic sources—predict a narrow funnel giving out a high, collimated luminosity. We discuss the interaction of the emerging radiation with the funnel walls and conclude that a significant mechanical luminosity in the form of a particle beam should result. An attempt to calculate the particle luminosity allowing for mixing of the surface layers with the bulk is described. Some constraints on the luminosity can also be placed by examining the internal equilibrium of the thick disc, particularly if the source of the released energy is concentrated near the central mass.

Key words: accretion disc—Eddington limit—particle beam

The idea of disc accretion around black holes as the process for releasing gravitational energy in quasars and other active galactic nuclei goes back to Lynden-Bell (1969). The same author (1978) noted the steep funnels (vortices) in models of differentially rotating fluid masses round a black hole, and suggested that these would provide a mechanism to collimate the energy outflow, possibly accounting for the double structure of extragalactic radio sources. This concept of a thick accretion disc has now been extensively studied, notably by Paczyński and his collaborators at the Copernicus Institute in Warsaw. A clear introduction to this subject can be found in the paper by Paczyński & Wiita (1980) which also pointed out a remarkable property *viz.* that the luminosity in the funnels is well in excess of the Eddington limit L_E at which radiation pressure would overcome gravity in a spherical geometry. Much of our work in this field has been aimed at understanding what kind of limits one can place on the luminosity in a funnel geometry.

Fig. 1(a) shows an element dA of a surface of revolution, emitting a luminosity dL normal to itself. The flux F multiplied by κ/c (κ = opacity) gives the outward force, and the arguments sketched in the figure show how to compare the maximum luminosity allowed by vertical equilibrium to the differential Eddington luminosity corresponding to the solid angle $d\Omega$ subtended by the element. In the notation of Fig. 1(a), vertical equilibrium gives

$$\frac{GM}{R^2}\sin\theta \geqslant \frac{dL\cos(\alpha-\theta)}{R^2\, d\Omega/\sin\alpha}$$

i.e.

$$dL \leqslant \frac{d\Omega}{4\pi} L_E f_1(\alpha), \quad L_E = \frac{4\pi GMc}{\kappa}.$$

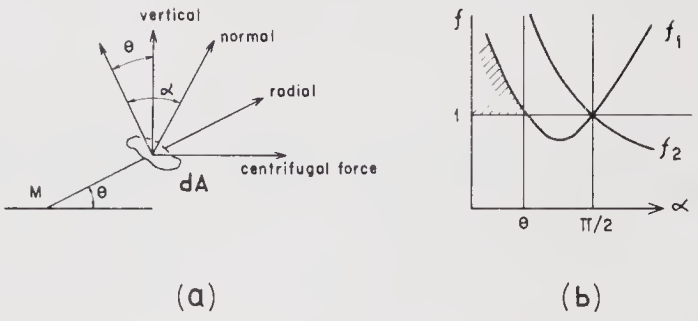

Figure 1. (a) Geometry of forces acting on an element of a surface of revolution. (b) The maximum luminosity allowed by vertical equilibrium (f_1) and horizontal equilibrium (f_2) *vs* the angle α. The shaded area corresponds to super-Eddington luminosities neglecting the reflection effect.

Centrifugal force being positive gives a second condition *viz.*,

$$dL \leqslant \frac{d\Omega}{4\pi} L_E f_2(\alpha) \quad \text{with } f_2(\alpha) = \frac{\cos\theta}{\sin\alpha \sin(\alpha - \theta)}.$$

The two functions f_1 and f_2 are plotted against α in Fig. 1(b) and we see that we need $\alpha < \theta$ if we want $L > L_E$. The essential point is that one can get super-Eddington luminosities only for a re-entrant surface. But this is also precisely the case when radiation from one part of the surface strikes another part, thus complicating the situation.

This so-called 'reflection effect' was neglected in the earlier work and was first seriously considered by Sikora (1981) who studied a general relativistic funnel model due to Jaroszyński, Abramowicz & Paczyński (1980) with a luminosity of $8.5\,L_E$. In the presence of the reflection effect, apart from the self-radiation flux F_s emanating normally from a surface element under consideration (Fig. 2), there is also another flux impinging externally which may be conveniently described in terms of a normal component F_n and a tangential component F_t. The net normal flux $(F_s - F_n)$ in Fig. 2

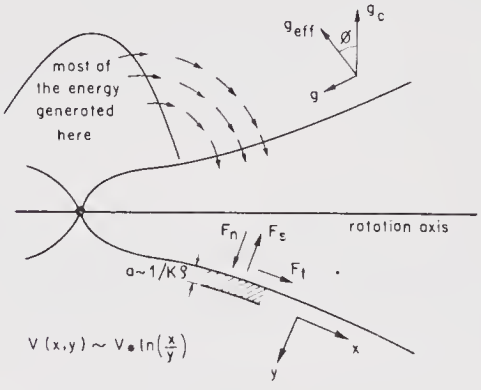

Figure 2. Centrifugal force g_c and gravity g combine to give an effective gravity g_{eff} normal to the funnel surface. The definition of the self flux F_s, as well as normal and tangential fluxes F_n and F_t are shown. The arrows show the direction of the normal to the unit area over which the corresponding flux is measured. The shaded layer of thickness a feels an accelerating force due to F_t. The interior layers move with a velocity $v(x, y)$. Top left: Application of the Eddington limit to an interior surface enclosing a large fraction of the energy generation.

has to balance the 'effective gravity' $g_{\rm eff}$ which is the resultant of gravity g and centrifugal force $g_{\rm c}$. Consequently, $F_{\rm s}$ becomes much greater than for a non-re-entrant surface. The possibility of accelerating particles by this enhanced collimated flux has been explored by Sikora & Wilson (1981). However, we note that the surface tangential flux $F_{\rm t}$ in the funnel region is also greatly enhanced, and one can no longer have strict equilibrium in the tangential direction. In our study (Nityananda & Narayan 1982), completed just before Sikora's work appeared, we in fact found that tangential forces in these models exceeded gravity by a factor ϕ^{-3} where ϕ is the funnel semi-angle ($\sim L_{\rm E}/L$). The numbers in Sikora's work bore this out, giving $F_{\rm t}\kappa/cg \sim 600$, which compares well with $(8.5)^3$. Turning the argument around, we thus see that if we require strict equilibrium at the funnel surface, then the luminosity will not be $L_{\rm E}/\phi$ as found in the standard models, but is limited to $\sim \phi^2 L_{\rm E}$.

Although the failure of equilibrium seems to be large in the funnel region in current models, one should really compare the tangential force to the larger forces in the problem like $g_{\rm eff}$ or $F_{\rm s}\kappa/c$. This was done in our paper where we used the famous α factor of Shakura & Sunyaev (1973) relating tangential and normal stresses. Since $g_{\rm eff} \simeq g/\phi$ from Fig. 2., the result is thus to weaken the earlier limit by a factor α/ϕ. That is, whereas we had a luminosity limit $L_{\rm E}\phi^2$ for strict equilibrium (which is just the Eddington luminosity cut down by the solid angle), allowing a friction coefficient α at the walls gave a limit $L_{\rm E}\alpha\phi$. Any luminosity higher than this would accelerate the walls since tangential momentum is being fed in faster than it can be removed to the interior.

Our paper gave some simple estimates of the acceleration obtained, but we have recently (in collaboration with Paul Wiita) tried to improve this, incorporating the mixing of the surface layers with the interior (Narayan, Nityananda & Wiita 1983, unpublished). The point is that the forces due to the reflection effect essentially act on a layer of optical depth unity which has a thickness $a = 1/\kappa\rho$ (ρ = density). The mixing is expected to be effective in a time a/v or $a/c_{\rm s}$, whichever is longer. (Here, v = velocity of the surface layer relative to the next layer, $c_{\rm s}$ = sound velocity.) It turns out that this timescale is less than that required by a surface element to traverse the length of the funnel, implying that mixing will be efficient. To quantify the effects, we used some results from turbulent shear flows. The velocity v_* of the turbulent eddies is related to the shear σ being transmitted at the surface by $\sigma = \rho v_*^2$ while the mean velocity at any point, compared to an element deep inside the disc, depends only logarithmically on the distance along, and depth below, the funnel walls (Fig. 2). However, when v_*^2 crosses $\alpha c_{\rm s}^2$ with $\alpha \sim 1$, the turbulence becomes supersonic and the tangential momentum transfer saturates (Shakura & Sunyaev 1973). In this case the surface layer can take off on its own.

Two interesting effects act to enhance the acceleration of the walls over what one might at first expect. Radiative acceleration is usually weakened by the Doppler effect when the matter recedes from the source. Further, even transverse radiation is swung forward by aberration and exerts a retardation. In fact, these two effects limited the Lorentz factors (γ) found by Sikora & Wilson (1981) to 1.15. However, when one accounts for the motion of the walls and notes that both the accelerating and the retarding radiation arise mostly from the moving walls, it is clear that these effects are reduced considerably.

The final values of the outflow velocity and the mechanical luminosity $L_{\rm p}$ (*i.e.*, luminosity in particle flows) are naturally sensitive to the assumed values of the sound

velocity and the friction coefficient. We find that L_p can be of the same order as the radiation luminosity L_r (for Sikora's funnel) or somewhat lower for the range of parameters tried. This should be considered welcome in the context of the relativistic beams seen in active galactic nuclei. Unfortunately, the bulk γ of the particle beams does not seem to exceed 1.25 for any of the parameters we have considered. An important point to be kept in mind is that the original thick disc models were developed under the assumption of surface equilibrium and radiation outflow. Since we find that the mechanical luminosity can be considerable, one suspects that a more self-consistent theory is called for. This is particularly true for the optically thick funnels which are being considered nowadays (as opposed to our assumption that the accelerated matter remains stuck to the walls), where L_p is expected to dominate over L_r.

The arguments about how much luminosity the funnel can sustain still leave open the question of whether the luminosity can reach the funnel from where it is generated in the disc interior. Further, the radiation pressure gradients needed to do this should not violate the internal equilibrium of the disc. As Professor Rees remarked, the tendency in this field has been to worry about the surface and let the interior take care of itself. While this is perhaps justified by the complexity of the full problem, we have made some preliminary estimates which already seem to restrict the luminosity to $\lesssim L_E$ (Narayan & Nityananda 1983, unpublished). The first step in the argument is to realise that the bulk of the energy generated must come from rather near the black hole, say within $10\,r_s$ (r_s = Schwarzschild radius). This is of course reasonable since the basic source is gravity; however, it is also required on simple diffusion arguments if the bulk of the luminosity is to reach the funnels rather than the outer surface. Fig. 2 shows how the luminosity has to emerge nearly radially, turn, and reach the funnels. One can now construct an interior surface which all this energy has to cross, and investigate the vertical equilibrium condition there. This surface can easily be chosen to enclose most of the energy source. Noting that very little energy leaves directly through the funnel close to the black hole (*e.g.*, 86 per cent of the luminosity in Sikora's model *viz.* $7.3\,L_E$, emerges from a height greater than $35\,r_s$), we find that the bulk of the luminosity has to cross the interior surface. However, vertical bulk equilibrium requires that this interior luminosity be $< L_E$. This suggests that efficient thick discs, where the bulk of the energy generation takes place close to the central black hole, are restricted to $L \lesssim L_E$. We are at present trying to refine these arguments into a tight bound.

In conclusion, one must realise that even one Eddington luminosity emerging over two cones occupying $\sim 1/200$ of the full solid angle of the sphere represents a remarkable concentration of energy. Abramowicz & Calvani (1982) have recently invoked this to reconcile the high apparent luminosities and short variability timescales of some energetic extragalactic sources. The next stage in the theory will hopefully be to construct more globally consistent disc models incorporating both accretion and outflow.

References

Abramowicz, M. A., Calvani, M. 1982, *Nature*, **300,** 506.
Jaroszyński, M., Abramowicz, M. A., Paczyński, B. 1980, *Acta astr.*, **30,** 1.
Lynden-Bell, D. 1969, *Nature*, **223,** 690.
Lynden-Bell, D. 1978, *Phys. Scripta*, **17,** 185.
Nityananda, R., Narayan, R. 1982, *Mon. Not. R. astr. Soc.*, **201,** 697.

Paczynski, B., Wiita, P. J. 1980, *Astr. Astrophys.*, **88,** 23.
Shakura, N. I., Sunyaev, R. A. 1973, *Astr. Astrophys.*, **24,** 337.
Sikora, M. 1981, *Mon. Not. R. astr. Soc.*, **196,** 257.
Sikora, M., Wilson, D. B. 1981, *Mon. Not. R. astr. Soc.*, **197,** 529.

Discussion

Chitre: In your mechanical luminosity L_M, have you taken into account the mechanical dissipation due to shock waves which will arise when $V^* \gtrsim c_s$?
Nityananda: The calculations done so far have treated the sound velocity as a parameter. I agree that the sound velocity has to be determined self-consistently in a full treatment.
Rees: Have you considered the internal circulation which might be produced in matter which is not given enough energy to escape along the funnel?
Nityananda: In fact, our calculations were triggered off by some remarks by Blandford and our referee that the tangential forces would drive a circulation. But we have mainly pursued the escape case.

Kapahi, V. K. (Ed.)
Extragalactic Energetic Sources
Indian Academy of Sciences, Bangalore, 1985, pp. 133–134

Polarization Variability of Compact Extragalactic Radio Sources

M. M. Komesaroff *CSIRO Division of Radiophysics, P. O. Box 76, Epping NSW 2121, Australia*

Abstract. Results of a programme to measure the variability of both the linear and circular polarization of compact extragalactic sources are summarized.

Key words: compact extragalactic radio sources—linear and circular polarization—polarization variability

All four Stokes parameters of some 20 compact extragalactic radio sources were measured at roughly three-monthly intervals between late 1976 and early 1982 using the Parkes 64-m reflector at a frequency of 5 GHz. The observers were J. A. Roberts, D. K. Milne, P. T. Rayner, D. J. Cooke and myself. The observed sources were selected on the basis of small angular size ($\lesssim 1$ arcsec), known flux density variability, previously observed circular polarization and peaked or inverted spectra.

Most of the sources showed time variations in at least one polarization parameter. For one substantial group of sources the position angle of the linear polarization remained within about $\pm 10°$ of the same value throughout the observations, during which time there were large fluctuations in the linearly polarized flux density. For a second group there were sudden changes in position angle through about 90°. Both groups can be explained very simply in terms of a model comprising two components having approximately orthogonal position angles, whose relative contributions to the polarized flux changes with time. Provided one component remains predominant, the position angle varies only slightly, as in the first group of sources. On the other hand, if the initially weaker component becomes predominant, there will be a large and rapid swing in position angle, as observed in the second group. At the time this occurs we expect a drop in polarized flux density. Our results and those of other workers observed during this period indicate that in at least four cases this accompanying drop in polarized flux density did occur.

For the source 2134 + 004 the position angle of the linear polarization increased steadily with time at about 15° per year. This suggests that 2134 + 004 may be one of a class of sources described by Ledden & Aller (1979) and Aller, Hodge & Aller (1981). For three sources observed by them the same position angle was measured at three different frequencies. The most straight-forward explanation is a physical rotation of the emitting region.

Circular polarization was unambiguously detected in twelve sources at a level of a few tenths of one per cent. In at least four cases the circular polarization was variable on time scales as short as a few months. Our results, taken in conjunction with those in the

catalogue of Weiler & de Pater (1983) indicate that marked fluctuations in the *magnitude* of circular polarization often occur, but that reversals in the *sense* of circular polarization have been very rare over a wide range of frequencies and over a time interval of one decade. In the case of at least one source that we observed there was a marked change in the magnitude of the circular polarization in a time during which the total intensity and the linear polarization remained almost constant.

There are difficulties in explaining these results if the circular polarization is the polarization intrinsic to synchrotron radiation. This problem and others raised by our results could be further elucidated by simultaneous observations at two or more frequencies, particularly if a high resolution mapping technique could be used at one of these frequencies.

References

Aller, H. D., Hodge, P. E., Aller, M. F. 1981, *Astrophys. J.*, **248,** L5.
Ledden, J. E., Aller, H. D. 1979, *Astrophys. J.*, **229,** L1.
Weiler, K. W., de Pater, I. 1983, *Astrophys. J. Suppl. Ser.*, **52,** 293.

V. K. Kapahi (Ed.)
Extragalactic Energetic Sources
Indian Academy of Sciences, Bangalore, 1985, pp. 135–142

Backward Emission in Quasars

Jayant V. Narlikar *Tata Institute of Fundamental Research, Homi Bhabha Road, Bombay 400005*

Abstract. In the local Doppler theory of quasars the lack of observed blueshifts can be explained if quasars, ejected at high velocities from active galactic nuclei, radiate predominantly in a backward cone. An astrophysical single exhaust model has been proposed which not only explains why quasars emit radiation in the backward direction, but may also be able to account for some of their morphological features.

Key words: quasars—noncosmological redshifts—emission mechanisms

1. Introduction

In this Winter School we have seen excellent pictures of jets and beams in radio sources. I wish to describe a scenario where fast-moving quasars eject radiating material in the form of jets in the backward direction. The motivating idea is first described briefly.

From the early days of the discovery of quasars there have been several hypotheses concerning their redshifts. The most popular hypothesis known as the cosmological hypothesis (CH) interprets the redshift as due to the expansion of the universe. Other explanations come under the so-called noncosmological hypotheses (NCH) and include the Doppler redshift, the gravitational redshift and also other explanations involving variable masses, tired photons *etc.* (Terrell 1964; Hoyle & Burbidge 1966; Greenstein & Schmidt 1964; Bondi 1964; Hoyle & Fowler 1967; Das & Narlikar 1975; Das 1977; Narlikar & Das 1980; Narlikar & Edmunds 1981; Narlikar & Subramanian 1982; Pecker 1977). Burbidge has summarized the evidence suggesting the inadequacy of CH to account for the redshift phenomena in quasars. I will take it for granted that part of the redshift in a (high-redshift) quasar may well be of noncosmological origin. In particular I will explore the Doppler hypothesis further.

In the Doppler hypothesis it is assumed that quasars are ejected from explosions in active galactic nuclei (Hoyle & Burbidge 1966). In common with other NCH models it is presumed that most of the quasars now seen are comparatively nearby, at distances ranging from ~ 10 to ~ 100 Mpc. The Doppler redshift of a quasar ejected at speed V in a direction making an angle α with the line of sight away from the observer is given by

$$z = \frac{1 + (V/c)\cos\alpha}{(1 - V^2/c^2)^{1/2}} - 1. \tag{1}$$

Thus for example, for $\alpha = 0$ and $V = 0.8\,c$, we get $z = 2$. Here c = speed of light, and for a quasar of mass M, an ejection energy of γMc^2 [$\gamma = 1/(1 - V^2/c^2)^{1/2}$] is needed. Thus

the energy involved in the ejection of a quasar of $M \sim 10^6 M_\odot$ is $\sim 10^{60}$ erg. This is ~ 1 per cent of the energy commonly associated with active galactic nuclei.

The main problem with the Doppler theory is, however, with blueshifts. We should see quasars ejected towards us also, and these should exhibit large blueshifts. According to a calculation by Strittmatter (1967) if quasars are being ejected randomly in all directions and if a typical quasar radiates isotropically in its rest frame then in a flux-limited sample blueshifted quasars vastly predominate over the redshifted ones.

Strittmatter (1967) had sought a way out of this difficulty by arguing qualitatively that a typical quasar radiates, in its rest frame, in the backward direction. Hoyle (1980) has expressed the requirement more quantitatively as follows. In Fig. 1 we see a quasar Q moving with speed V in the direction of the arrow, relative to the intergalactic medium (IGM). The dotted cone in the backward direction has a semi-vertical angle θ_H given by

$$\cos\theta_H = \frac{c-(c^2-V^2)^{1/2}}{V}. \tag{2}$$

Then, provided the quasar emits all its radiation in this cone (in its rest frame), no observer at rest in the IGM will see it blueshifted.

Clearly an astrophysical explanation is needed to account for this emission property. Section 2 describes briefly the salient features of the model by Narlikar & Subramanian (1983).

2. The single-exhaust model

Our model is adapted from the original twin-exhaust model of Blandford & Rees (1974). In the Blandford-Rees (BR) model, a central engine ejects high-energy plasma which is collimated in two oppositely directed jets by a surrounding gas cloud which in turn is held together by the gravitational field of a massive matter distribution. To conserve momentum, two oppositely directed jets are necessary in the BR model.

The dynamical considerations are altered, however, when the object as a whole is moving rapidly through the IGM. The ram pressure exerted by the IGM can be considerable and may prevent a jet from emerging in the forward direction. The result is a single backward jet.

Fig. 2 illustrates our model qualitatively. C is the central source of fast-moving plasma. Although the plasma may initially come out isotropically, its flow pattern

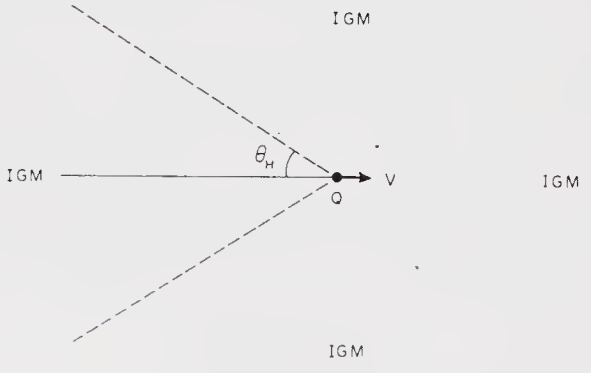

Figure 1. The permitted zone of backward emission is the dotted cone with semi-vertical angle θ_H. If quasars radiate (in their rest-frames) only within this cone, they are not seen blueshifted.

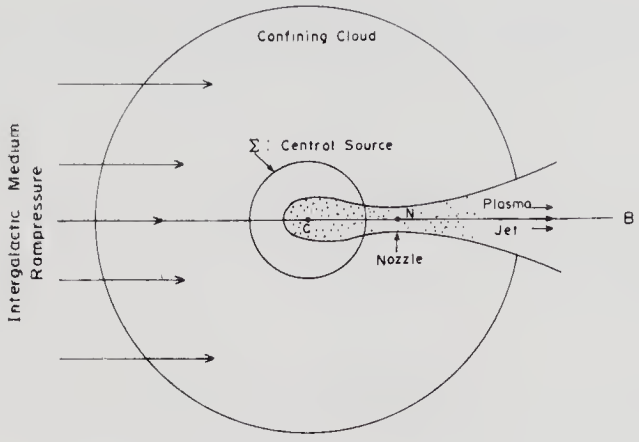

Figure 2. The components of the single-exhaust model where the gravitating mass is a compact object. The jet is in the backward direction. The dots denote emission-line clouds.

changes when it 'feels' the IGM ram pressure and selects the backward direction to come out since along there it encounters the least resistance. It carves out a channel in the backward direction CB, and forms a de Laval nozzle at N before emerging supersonically from the surrounding cloud. The cloud is held by a massive system, shown here as a compact object Σ, although as in the BR model it could also be in the form of a uniform distribution of stars. The optical and radio emission is supposed to come from the jet material. Forward emission is inhibited because (a) the jet as a source has a relativistic bulk motion in the backward direction and (b) a small fraction of dust in the surrounding cloud will absorb most of the forward (line and continuum) radiation.

These qualitative features need to be expressed in quantitative form. This can best be done through a discussion of various constraints on the model.

2.1 *Formation of Shocks*

The first question to be answered is whether any shocks are generated through collisions of the IGM with the enveloping cloud. Denoting by $n^{(c)}$ and $l^{(c)}$ the particle number density and linear size of the cloud and by σ the collision cross-section, the probability that an IGM particle collides with the cloud comes out to be

$$P \cong n^{(c)} \sigma l^{(c)}. \tag{3}$$

For the typical model parameters (given later in Table 1) we find $P \ll 1$, for $\sigma \sim 10^{-24}\,\mathrm{cm}^2$. Thus IGM just flows through the cloud without generating shocks. However, if magnetic fields are present in the vicinity of the gas cloud, collisionless shock can form. This may have relevance to an observed feature of radio-loud quasars to be discussed later.

2.2 *Survival of the Gas Cloud*

Will the gas cloud be swept away by the IGM? The answer is 'no' if the gravitational binding of the system is sufficiently high. The survival requirement gives us the

Table 1. Viable parameters for the single exhaust model.

	$n^{(I)}(\mathrm{cm}^{-3})$		
	10^{-5}	10^{-4}	10^{-3}
$l^*_{pc}(\gamma-1)^{1/2}$	2.26	0.72	0.23
$T\times 10^{-5}\,\mathrm{K}$	3	3	3
$M/10^5\,M_\odot$	60	20	6
K/K'	3.6×10^{-3}	1.4×10^{-2}	3×10^{-2}
$n_0^{(c)}$	1.9×10^2	1.9×10^3	1.9×10^4

Note: $n_0^{(c)}$ denotes the value of $n^{(c)}$ in the central part of the cloud.

inequality

$$\frac{GMm_p n^{(c)}}{R^{(c)2}} > n^{(c)} n^{(I)} \sigma m_p (\gamma^2-1)c^2. \tag{4}$$

Here m_p = proton mass (typical for cloud or IGM), $R^{(c)}$ = cloud radius, $n^{(I)}$ = particle number density in IGM. Parameters in Table 1 satisfy this inequality.

2.3 *Deformation of the Cloud*

The cloud will be significantly deformed by the IGM if the pressure scale height K is large compared to the distance K' over which the effect of IGM ram pressure is felt. We have

$$K = \frac{GMm_p}{2kT}, \quad K = \frac{2kT}{n^{(I)} m_p \sigma c^2 (\gamma^2-1)}, \tag{5}$$

where T = temperature of the isothermal cloud. For the parameter values in Table 1, $K \ll K'$ so that the cloud is *not* significantly deformed from its spherical shape.

2.4 *Physical Parameters of the Model*

The key quantity which determines the viable dimensions is the ram pressure exerted by the IGM on the object. This is given by

$$P^{(I)} = n^{(I)} m_p c^2 (\gamma^2-1). \tag{6}$$

The central pressure p_0 at the origin of the jet cannot exceed the above value, if the forward jet is to be effectively suppressed. We therefore set $p_0 \simeq P^{(I)}$. Then from the analysis given by BR, the nozzle radius l^* is given by

$$l^* = (3\sqrt{3}/8\pi)^{1/2} (L/p_0 c)^{1/2}, \tag{7}$$

where L is the quasar energy output from the jet. In NCH, L is typically in the range 10^{40}–10^{41} erg s^{-1}. We have assumed that the distance CN in Fig. 2 is $\sim 4l^*$. This is a compromise between the linear approximation CN $\gtrsim 10\,l^*$ of BR and the 'fat-jet' calculations of Norman *et al.* (1981) suggesting CN $\sim 2l^*$.

Since the cloud must be large enough to form the nozzle, the above considerations put a lower bound on M. Table 1 gives the ranges of viable parameters subject to such constraints. For details see the paper by Narlikar & Subramanian (1983).

3. Radiative features

We consider radiation in two forms: continuum and in lines, both taking place in the backward jet.

3.1 *Continuum Radiation*

Detailed calculations (Narlikar & Subramanian 1983) show that the most likely and energetically viable mechanism for continuum emission is the synchroton process. The characteristic magnetic field strength is $\sim 10^{-4}$ G, the electron density $n_e \sim 10^{-6}\,\mathrm{cm}^{-3}$ with relativistic γ-factor $\sim 10^6$. The characteristic lifetime for such energetic electrons is $\sim 10^2$–10^3 yr. This suggests that some *in situ* re-acceleration of electrons might be needed since the characteristic lifetime for these quasars ($\simeq$ time taken by the electrons to come out of the parent active galaxy) is expected to be $\sim 10^4$ yr.

Spectral analysis of the emitted radiation shows that a quasar is more powerful in optical and ultraviolet wavelengths than in radio. To be able to pick out a radio quasar one has to be preferentially located more or less along the direction of the backward jet. This may explain why radio-selected quasars are comparatively few.

A second mystery is the presence of only one radio jet in quasars. In twin-exhaust models it is difficult to explain why *all* radio quasars are seen with one jet only. In the present model this observation finds a natural explanation.

How is it then that ~ 40 per cent of all radio quasars show double lobes? The backward jet should form a radio lobe in the backward direction. To understand the possibility of forming the second lobe we recall the models with collisionless shocks. As shown in Fig. 3, a bow shock is formed in the forward direction. A weak forward jet develops which is stopped by the ram pressure of the IGM which has already been shocked this way. This weak jet may form the second lobe in the forward direction.

3.2 *Line Radiation*

Line radiation in the jet comes from emission-line clouds of characteristic mass $\sim 10^{-2} M_\odot$ and characteristic radius $\sim 5 \times 10^{-4}$ pc. These clouds can be driven forward (by ram pressure of the jet plasma) and backward (by gravity of the main object) so that their exact location in the jet may change. Some clouds may be driven away altogether.

Can the emission lines be seen in the forward direction? The cloud is optically thin unless it also contains dust. Calculations show that with dust forming only 10^{-3} of the cloud mass the radiation is absorbed over a distance of ~ 20 pc. Thus emission lines will not be seen unless we are viewing from the backward direction as explained in Fig. 4.

Thus the blueshift catastrophe mentioned earlier is resolved. First, quasars selected

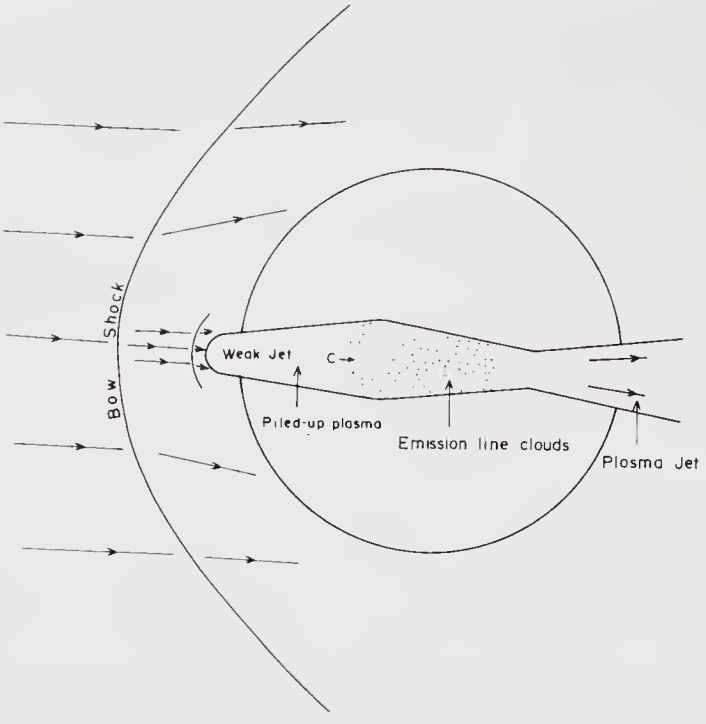

Figure 3. The formation of a collisionless bow shock allows the formation of a weak forward jet. The emission-line clouds are, however, prevented from entering the forward portion of the jet by the piled up plasma.

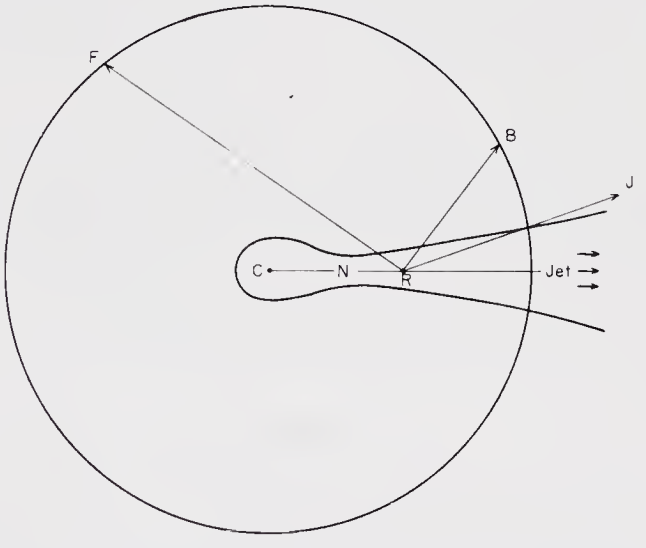

Figure 4. Because of ready absorption by dust in the cloud, emission lines are not seen in the forward direction like RF, but may be seen in the backward direction like RB through the cloud, or like RJ through the dust-free jet.

from their continuum radiation will have to be viewed from the backward direction. Second, even if some are bright enough to be seen from the forward direction they would appear as lineless objects. In an earlier paper (Narlikar & Edmunds 1981) the suggestion was made that BL Lacs may be such objects.

4. Observational tests

Besides the observation of single-jet quasars and the explanation of paucity of radio-loud quasars, the model makes further testable predictions:
(1) Proper motions of the order of 0.5–5 milliarcsec yr^{-1} should be seen. These could be detected by VLBI techniques if they can measure absolute movement across the sky.
(2) If proper motions are found they should be in a direction opposite to the observed jet.
(3) The cloud around the quasar could be detected as a fuzz. Since ram pressure is small for low-speed quasars, these should have a larger fuzz. Thus the size of the fuzz should be inversely correlated with the Doppler redshift.

References

Blandford, R. D., Rees, M. J. 1974, *Mon. Not. R. astr. Soc.*, **169**, 395 (BR).
Bondi, H. 1964, in *Proc. R. Soc. London Series A*, **282**, p. 303.
Das, P. K. 1977, *Mon. Not. R. astr. Soc.*, **177**, 391.
Das, P. K., Narlikar, J. V. 1975, *Mon. Not. R. astr. Soc.*, **171**, 87.
Greenstein, J. L., Schmidt, M. 1964, *Astrophys. J.*, **140**, 1.
Hoyle, F. 1980, *Astrophysics and Relativity, Preprint* 63, University College, Cardiff.
Hoyle, F., Burbidge, G. R. 1966, *Astrophys. J.*, **144**, 534.
Hoyle, F., Fowler, W. A. 1967, *Nature*, **213**, 373.
Narlikar, J. V., Das, P. K. 1980, *Astrophys. J.*, **240**, 401.
Narlikar, J. V., Edmunds, M. G. 1981, *J. Astrophys. Astr.*, **2**, 289.
Narlikar, J. V., Subramanian, K. 1982, *Astrophys. J.*, **260**, 469.
Narlikar, J. V., Subramanian, K. 1983, *Astrophys. J.*, **273**, 44.
Norman, M. L., Smarr, L., Wilson, J. R., Smith, M. D. 1981, *Astrophys. J.*, **247**, 52.
Pecker, J. C. 1977, in *IAU/CNRS Colloquia: Décalages vers le Rouge et expansion de L'universe; L'evolution de Galaxies et es Implications cosmologiques*, Eds C. Balkowski & B. E. Westerlund, CNRS, Paris, p. 451.
Strittmatter, P. 1967, in *Quasi Stellar Objects*, Eds G. R. Burbidge & E. M. Burbidge, Freeman, San Francisco, p. 164.
Terrell, J. 1964, *Science*, **145**, 918.

Discussion

Porcas: Quasars in your model must show appreciable proper motion. VLBI measurements of the proper motion between the quasar pair 1038 + 52 A,B, which have different redshifts, give stringent upper limits to such motion.
Narlikar: The proper motion expected to be observed in a quasar of distance d_{Mpc} from us is $\sim 60\, d_{\mathrm{Mpc}}^{-1}$ milliarcsec yr^{-1}. VLBI techniques should be able to detect such motions provided it is ensured that we are measuring motion relative to the IGM and not relative to separations between two moving objects. Naturally the model gets discredited if observations of a number of quasars show no proper motions.
Laing: Why, in your model, are radio sources in quasars double? One would expect extreme asymmetries if the jets pointing towards us are much stronger. Secondly, why are the radio structures of galaxies (presumed stationary) and quasars (moving relativistically) so similar?
Narlikar: The possibility of a weak forward jet may give rise to a lobe in the forward

direction also. I gather that less than 50 per cent of all quasars have double lobes. Regarding the second question, so far all radio quasars seem to have one jet while radio galaxies usually have two jets. This difference could be due to Doppler effect and ram pressure in the case of quasars.

van Speybroeck: How do absorption line systems occur in your model?

Narlikar: The absorption lines have to originate in the quasar, probably in the surrounding cloud. We have not investigated this as yet.

Kapahi, V. K. (Ed.)
Extragalactic Energetic Sources
Indian Academy of Sciences, Bangalore, 1985, pp. 143–148

Gravitational Lensing and Quasars

S. M. Chitre *Tata Institute of Fundamental Research, Homi Bhabha Road, Bombay 400005*

Abstract. A gravitational-lens model involving a spheroidal galaxy is shown to reproduce reasonably well the observed features of the triple quasar Q 1115 + 080 A,B,C. It is demonstrated that a double lens model made up of two intervening galaxies at different redshifts is required to account for the large separation of 7.3 arcsec between the components of the recently reported double quasar Q 2345 + 007 A,B. The abnormal brightness of the quasar 3C 273 and the VLBI observation of the structure within its component B showing an apparent superluminal motion upto $\sim 9c$ can both be explained in the framework of a gravitational lens model.

Key words: gravitational lens—quasars—superluminal motion

1. Introduction

The gravitational bending of light is one of the classical tests of Einstein's general theory of relativity. It is therefore remarkable that the properties of gravitational lenses which are a direct consequence of the gravitational deflection of light were not generally appreciated for some fifty years until quasars appeared on the cosmic scene. Barnothy (1965) pointed out that the brightening of quasars by gravitational lensing might explain the basic problem concerning the enormous energy output of all quasars. The first probable observation of lensing was reported by Walsh, Carswell & Weymann (1979) when they found two quasars (Q 0957 + 561 A,B) with nearly identical redshifts of 1.41 and a separation of 6.15 arcsec. It is now widely accepted that the twin quasar is a single object whose light has been split into two or more images by gravitational lensing. Young *et al.* (1981) have modelled the lensing action, by the combined gravitational effect of a massive elliptical galaxy and the surrounding cluster at a redshift of 0.39, to produce the observed separation and the intensity ratio between the components A, B.

The second gravitational lens Q 1115 + 080 A,B,C reported by Weymann *et al.* (1980) has a triangular configuration with a maximum separation of about 2.7 arcsec between components. The brightest image A was resolved with speckle interferometric observations by Hege *et al.* (1981) into components A_1, A_2 of almost equal intensity with a separation of ~ 0.5 arcsec. A third gravitational lens system Q 2345 + 007 A,B has been recently discovered by Weedman *et al.* (1982). The two components are separated by 7.3 arcsec and have nearly identical redshifts of 2.15 with an uncertainty of ± 0.005.

We shall describe in the next two sections, gravitational lens models which can

reasonably reproduce the observed features of the triple quasar Q 1115 + 080 A,B,C and the recently reported double quasar Q 2345 + 007 A,B. In the last section, we shall examine the possibility of explaining the extraordinary brightness and the superluminal motion observed, with VLBI, in quasar 3C 273.

2. The triple quasar Q 1115 + 080 A,B,C

We consider lens models similar to those constructed by Young *et al.* (1981) for the twin quasar Q 0957 + 511 A,B and adopt the mathematical formalism developed by Bourassa & Kantowski (1975). We follow the notation of Narasimha, Subramanian & Chitre (1982) to describe the source position and the image position projected onto the deflector plane which is taken perpendicular to the line of sight, by the complex numbers $z = x + iy$ and $z_0 = x_0 + iy_0$ respectively, and relate the source and image positions by the equation

$$z = z_0 - \mu g(z_0). \tag{1}$$

Here, all the length-scales are scaled in terms of the core-radius r_c of the lens galaxy having mass M, and, $\mu = 4\,\mathrm{GMD}/r_c^2 c^2$ where

$$D \equiv \frac{\text{(lens–observer distance) (lens–source distance)}}{\text{(observer–source distance)}} = \frac{D_d D_{ds}}{D_s}.$$

The function $g(z_0)$ is supposed to incorporate the properties like the mass distribution of the lens galaxy, which we assume to be an oblate spheroid given by

$$x^2 + y^2 + \frac{z^2}{1-e^2} = a^2. \tag{2}$$

We choose a geometry such that the centre of the galaxy is at the origin and the x-axis is along the major axis of the galaxy. The symmetry axis of the spheroid is chosen to be the z-axis which is tilted relative to the photon path by an angle γ. For computation, we adopt a galactic model with eccentricity e and mass distribution of the type given by the truncated King model

$$\begin{aligned} \rho(a) &\propto (1 + a^2/r_c^2)^{-3/2} \quad , \quad a/r_c \leqslant n, \\ &= 0 \qquad\qquad\qquad\quad , \quad a/r_c > n \end{aligned} \tag{3}$$

The parameter n refers to the cut-off radius in units of the core-radius, r_c.

This complex formalism is the basis for modelling the observed image configuration; the principal thrust of the calculation is to locate the roots of Equation (1) which give images consistent with the observed separation and intensity ratios, assuming a reasonable set of parameters for the lens galaxy. A typical solution displayed in Fig. 1 shows the contours $x = 0.15$ (solid lines) and $y = 0.24$ (dashed lines) giving the location of five images A_1, A_2, B, C and D. It turns out that the observed separation between images cannot be reproduced if the solutions are restricted to regions where three images form, which leads us to the five-image region to explain the observed features of this system. Notice that the solution displayed leads in a natural manner to the double nature of the brightest image A with a separation of ~ 0.5 arcsec between A_1 and A_2. In Table 1 we have shown the source position, image positions and separation between

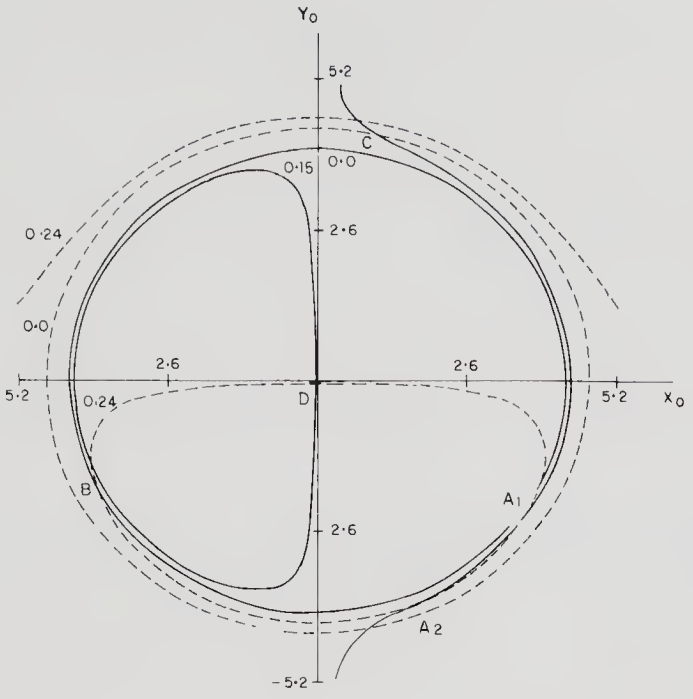

Figure 1. Contour diagram in the image plane for a source position (0.15, 0.24). The intersections of the solid lines $x = 0.15$ with the dashed lines $y = 0.24$ give the location of the five images A_1, A_2, B, C, D. The centre of the lens galaxy is chosen to be the origin and all lengths are expressed in units of the core-radius.

Table 1. The triple quasar Q1115+080 A,B,C: Predicted image positions, separations and intensity ratios for a choice of model parameters $e \sin\gamma = 0.6$, $n = 30$, $\mu = 40$.

	Image position*		Separation*		Intensity Ratio†	
	x_0	y_0				
A_1	3.95	−2.40	A_1A_2	1.47		
A_2	3.53	−3.80	AB	8.27	A_1/A_2	0.876
B	−4.30	−1.16	AC	8.29	B/A	0.121
C	−0.98	4.68	BC	7.87	C/A	0.138
D	−0.02	−0.02	DG	0.03	D/A	0.0005

* Position and separations are in the units of the core-radius r_c; the source position, in the same units, is $x = 0.15$, $y = 0.24$.
† $A = A_1 + A_2$.

various images in units of the core radius, r_c, along with the intensity ratios, for the following choice of the lens parameters: effective eccentricity $e \sin\gamma = 0.6$, cut-off radius $n = 30$ and $\mu = 40$. The fifth image D is very faint and appears very close to the centre of the galaxy. From Table 1 we have distances between images A, B and C in units of r_c which can be related to observed separations in arcsec. Thus, if S denotes the distance in units of r_c between images A and B, and θ is the observed separation A–B in arcsec, we can write $D_d\theta = r_cS$; in the Robertson-Walker universe with $q_0 = 0$, the

distance D_d from the observer to the lens galaxy is related to its redshift z_d by

$$D_d = \frac{c}{2H_0}\left[1 - \frac{1}{(1+z_d)^2}\right].$$

We take the Hubble constant to be $H_0 = 60$ km s^{-1} Mpc^{-1}. From the solution given in Table 1 we can determine the redshift $z_d = [1-(2r_c S H_0/c\theta)]^{-1/2} - 1$ for an assumed core-radius r_c. This enables us to fix the parameter $D = D_d D_{ds}/D_s$ knowing z_d and z_s, and hence the mass of the lens galaxy $M = r_c^2 c^2 \mu/4GD$, since the value of parameter μ is prescribed. The results are summarized in Table 2 where the apparent magnitude m_v is estimated assuming a mass-to-light ratio $M/L = 20$. The time-delay of $C/B = -39.1$ days, for example, implies that the intensity variation of image C lags behind that of B by 39.1 days.

It is clear from the solutions that for a reasonable choice of the lens parameters the observed characteristics of the triple quasar can be satisfactorily explained with the help of a spheroidal galaxy. The galaxy which we have postulated for modelling the triple quasar has not been detected as yet, but once its redshift is known, all the parameters of the lens galaxy, including its core-radius, could be determined.

Table 2. The triple quasar Q 1115+080 A,B,C: Deflector mass and time delay between the images for two values of r_c.

Redshift z_d	Core radius r_c (kpc)	Mass M (10^{11} $M_\odot$)	m	Time delay in days A_1/A_2	A_1/B	C/B	D/B
0.2	1	3.5	19.9	0.9	−3.4	−8.9	−28.1
0.6	2	12	20.8	3.8	−14.9	−39.1	−124.0

3. Double-lens model for Q 2345+007 A,B

The recently reported double quasar Q 2345+007 A,B at the redshift of 2.15, with a large separation ~ 7.3 arcsec between its components imposes stringent constraints on possible gravitational lens models. We can model the double quasar using a single lens with plausible values for the mass and velocity dispersion of the deflector galaxy, provided we place the lens close enough to us at a redshift $z_d \lesssim 0.1$. But then at such a redshift, a galaxy of mass 15×10^{11} $M_\odot$ should be easily observable unless its mass-to-light ratio M/L is large ($\gtrsim 900$). We therefore consider a double-lens model where we imagine a light ray from the quasar to get intercepted by two intervening galaxies $\mathscr{A}$ and $\mathscr{B}$ before reaching the observer O. A typical solution for the double lens is exhibited in Table 3 (based on Subramanian & Chitre 1984).

Amongst the gravitational lens models that we considered for Q 2345+007 A,B the one involving two intervening galaxies requires the most reasonable set of values for the lens parameters. However, a crucial question concerning the double lens models is their low probability. The probability of finding two quasars having redshifts of 2.15 with an uncertainty of ± 0.005, separated by 7.3 arcsec is 4×10^{-7}. On the other hand, the chance of finding two galaxies along the line of sight to a distant quasar may be

Table 3. A double-lens model for Q 2345+007 A,B.

Specification of the double lens*			Image position†			Intensity ratio‡	
z	μ	M ($10^{11}\ M_\odot$)		x_0	y_0		
0.45	49	11.8	A	9.48	9.48	A/B	5.428
0.18	44	7.8	B	−3.11	−3.11		
			C	−1.94	−1.94	C/B	0.085

* $n = 20$; $r_c = 1.4$ kpc.
† In units of r_c; source position, in the same units, is (5.0, 5.0).
‡ The time delay $t_B - t_A = 2.82$ yr.

evaluated by using the expression given by Bahcall & Spitzer (1969) for the number N of galaxies (within a cylinder of radius $R_g \simeq 10$ kpc) between the observer and quasar at redshift z_s:

$$N = 0.06\,(R_g/10\ \text{kpc})^2 (N_g/0.1\ \text{galaxy Mpc}^{-3})((1+z_s)^{3/2} - 1).$$

For a redshift $z_s = 2.15$ and a choice of $N_g = 0.01$ galaxy Mpc^{-3} for the number density of massive galaxies which we need for modelling the double quasar, we get $N \simeq 0.07$. A rough estimate of the probability for the double lens is then given by $N^2 F \simeq 3 \times 10^{-4}$, where the factor $F \simeq r^2/4R_g^2$ takes account of the fact that for the effectiveness of the double lens the amount of misalignment should not exceed r ($\simeq 5$ kpc) and one of the two deflectors should be within a certain angular distance from the line joining the source and the other deflector. Evidently, the probability of the double lens models is significantly larger than simply having two quasars with nearly identical redshifts within 7.3 arcsec of each other.

4. 3C 273, a gravitationally lensed quasar!

The quasar 3C 273 is known to be an abnormally bright optical object with an apparent magnitude of 12.8. Furthermore, of its two radio components A and B, the VLBI observations of structures within the component B show evidence for apparent superluminal motion up to $\sim 10c$. Both these features can be accommodated in the framework of a gravitational lens model, Chitre *et al.* (1984). The recent finding of a nebulosity around 3C 273 by Tyson, Baum & Kreidl (1982) is interpreted as a galaxy with the quasar embedded in its nuclear region. However, there remains the possibility of the nebulosity being a superposition of two galaxies one of which is at an intermediate redshift along the line of sight and which can act as a gravitational lens. We examine the consequence of such a hypothesis in the belief that an exceptionally brightened quasar is perhaps indicating the phenomenon of gravitational lensing.

To account for an apparent separation velocity of order $10c$ we need a linear amplification by at least a factor of 10 which would imply an intensity amplification of order 100. For the sake of illustration we consider a spherically symmetric lens galaxy with its centre at the origin of a coordinate system and the collinear image-system yielded by the spherically symmetric lens to be the x-axis. Equation (1) then reduces to

the one involving only one variable namely, x and takes the form $x = x_0 - \mu\, g(x_0)$. The linear scale amplification in the radial direction is $a_r = \mathrm{d}x_0/\mathrm{d}x$ and in the transverse direction it is given by $a_t = x_0/x$. Consequently, the intensity amplification $A = a_t a_r = (x_0/x)(\mathrm{d}x_0/\mathrm{d}x)$.

The image positions are yielded by the intersection of the two curves $y = x_0 - x$ and $y = \mu\, g(x_0)$. Note that the radial amplification turns out to be larger for those source positions where the straight line $y = x_0 - x$ is almost tangential to the curve $y = \mu\, g(x_0)$, while the transverse amplification is large when the source position is close to the origin. It is possible to produce an image configuration, for a small range of the parameter $\mu(\lesssim 5)$ which gives only one bright image and a significant superluminal motion of the components. A typical solution with the lens galaxy at a redshift 0.1 with a core-radius $r_c \simeq 1$ kpc and a mass $M = 1.7 \times 10^{11}\, M_\odot$ yields a linear amplification $a_t \simeq a_r \simeq 9$ and an intensity amplification $A \simeq 80$. Such a scenario can evidently yield an apparent superluminal motion of separating components up to $\sim 9c$ which is indeed observed in the case of 3C 273. Interestingly, an intensity amplification by a factor of 80 would imply that 3C 273 is really an 18-mag source like other typical quasars, and has been brightened by lensing to 12.8 mag.

References

Bahcall, J. N., Spitzer, L. 1969, *Astrophys. J.*, **156,** L63.
Barnothy, J. M. 1965, *Astr. J.*, **70,** 666.
Bourassa, R. R., Kantowski, R. 1975, *Astrophys. J.*, **195,** 13.
Chitre, S. M., Narasimha, D., Narlikar, J. V., Subramanian, K. 1984, *Astr. Astrophys.*, **139,** 289.
Hege, E. K., Hubbard, E. N., Strittmatter, P. A., Worden, S. P. 1981, *Astrophys. J.*, **248,** L1.
Narasimha, D., Subramanian, K., Chitre, S. M. 1982, *Mon. Not. R. astr. Soc.*, **200,** 941.
Subramanian, K., Chitre, S. M. 1984 *Astrophys. J.*, **276,** 440.
Tyson, J. A., Baum, W. A., Kreidl, T. 1982, *Astrophys. J.*, **257,** L1.
Walsh, D., Carswell, R. F., Weymann, R. J. 1979, *Nature*, **279,** 381.
Weedman, D. W., Weymann, R. J., Green, R. F., Heckman, T. M. 1982, *Astrophys. J.*, **255,** L5.
Weymann, R. J., Latham, D., Angel, J. R. P., Green, R. F., Liebert, J. W., Turnshek, D. A., Turnshek, D. E., Tyson, J. A. 1980, *Nature*, **285,** 641.
Young, P., Gunn, J. E., Kristian, J., Oke, J. B., Westphal, J. A. 1981, *Astrophys. J.*, **244,** 736.

Discussion

Swarup: For the double or triple quasar, do you expect any distortions in the shapes of the observed images over a scale of 1 kpc, which might predict differences in the shapes or widths of the emission lines.

Chitre: Although we do not expect much distortion in the shapes of the images for broad-line regions ($\lesssim 1$ pc) we might get a non-negligible distortion in the shapes over a scale of 100 pc–1 kpc. This could conceivably predict some observable difference in the widths of emission lines.

Rees: To explain the 'Mutel doubles', you probably need only a dwarf galaxy ($\sim 10^9\, M_\odot$).

Chitre: Yes, one could model the 'Mutel doubles' with a dwarf galaxy having a mass $\sim 10^9$–$10^{10}\, M_\odot$. The image separation scales as the square-root of the lens mass and consequently a deflector in the form of a dwarf galaxy could yield an image system with separation of the order of a fraction of a second.

Kapahi, V. K. (Ed.)
Extragalactic Energetic Sources
Indian Academy of Sciences, Bangalore, 1985, pp. 149–154

Gravitational Lenses—The Multiple Scattering Limit

Ramesh Narayan & Rajaram Nityananda *Raman Research Institute, Bangalore 560080*

Abstract. The unusually large angular separations in the three known cases of gravitational lensing coupled with the non-detection of any lensing galaxy in two of the cases suggest that multiple lenses may be involved. We consider the case when lenses are strongly clustered and develop a statistical theory to treat the distribution of images. In this multiple scattering limit, we automatically obtain large separations and asymmetric image configurations; the absence of a single, dominant lens is also natural. However, the observed degree of galaxy clustering does not seem to be as strong as this picture would require.

Key words: gravitational lens—clusters of galaxies—multipath propagation

The subject of gravitational lenses has gained importance in recent times with the discovery of three cases of lensing: (a) the double quasar Q 0957 + 561 A, B with an image separation of 6 arcsec and quasar redshift Z_q of 1.4, (b) the triple quasar Q 1115 + 080 A, B, C, separations AB = 1.9, BC = 2.4, CA = 2.0 arcsec, $Z_q = 1.7$ and (c) the double quasar Q 2345 + 007 A, B, separation = 7.3 arcsec, $Z_q = 2.15$. Young *et al.* (1981a, b) and Narasimha, Subramanian & Chitre (1982) have developed specific lens models involving galaxies and galaxy clusters to explain the observed component separations and ratios.

Let us for simplicity assume that the lenses involved in the above cases are spherically symmetric 'isothermal' galaxies and define a suitable cross-section for lensing events. The corresponding optical depth for lensing along the path to a quasar at $Z_q = y - 1$ has been given by J. P. Ostriker (1982, personal communication),

$$\tau = F[(y^4 + 4y^2 + 1)\ln y - 1.5\,(y^4 - 1)]/(y^2 - 1)^2 \tag{1}$$

and

$$F = 4\pi^3 n_0 (c/H_0)^3 (\sigma/c)^4, \tag{2}$$

where n_0 is the number density of galaxies at the present epoch with a line-of-sight velocity dispersion σ, and H_0 is the Hubble constant. Equation (1) has been derived assuming a Friedmann cosmology with $\Omega \ll 1$. Using the luminosity function of normal galaxies (Fall 1981),

$$\phi(L) = (\phi_*/L)\exp(-L/L_*)$$

$$\phi_* = 2.4 \times 10^{-3}\,\mathrm{Mpc}^{-3}, \quad L_* = 4 \times 10^{10}\,L_\odot, \quad H_0 = 50\,\mathrm{km\,s^{-1}\,Mpc^{-1}}, \tag{3}$$

and the Faber-Jackson relation (Fall 1981)

$$\sigma = 220(L/L_*)^{1/4}\,\mathrm{km\,s^{-1}}, \tag{4}$$

the mean value of F for all galaxies is estimated to be

$$F = 0.018, \tag{5}$$

leading to an optical depth at $Z_q = 2$ of

$$\tau_{\text{all galaxies}} = \sim 0.003. \tag{6}$$

This value is reasonably consistent with 3 cases of lensing seen in about 2000 known quasars.

However, there is a problem with the observed separations. The maximum gravitational deflection produced by an isothermal galaxy of velocity dispersion σ is

$$\theta_{\max} = 4\pi\sigma^2/c^2. \tag{7}$$

If we assume that the lens is generally approximately 'midway' between the quasar and the observer, then an observed component separation of θ implies that the rays on either side of the lens are also each deflected by θ. Combining Equation (7) with (4) and (3) we then find that for lensing with image separations greater than a given θ_0 (expressed in arcsec),

$$F(\theta \geqslant \theta_0) = 0.018\,\exp(-\theta_0^2/2). \tag{8}$$

This implies that the majority of lenses should produce small separations, say less than ~ 2 arcsec. The problem then is to understand why all the three known cases have separations larger than 2 arcsec, in fact very much larger in two of the cases.

If we decide to restrict ourselves to galaxy lenses, which is reasonable since a possible lensing galaxy has actually been identified in Q 0957, the way out is to assume that more than one lens is involved in all the known cases. There is support for this in the fact that a cluster of galaxies has been detected by Young *et al.* (1981b) in Q 0957; also, Narasimha, Subramanian & Chitre (1982) find that they need at least two lenses to reasonably model Q 2345 (see also Chitre 1984). If we invoke multiple lenses in all the three known cases, then the implication is that the conditional value of the optical depth τ, given the prior existence of one lens, is

$$\tau \lesssim 1. \tag{9}$$

To reconcile this with the intrinsically low probability of meeting the first lens, as given in (6), we need to invoke a remarkable degree of clustering in the lenses.

Although the known clustering properties of galaxies and other objects do not lead to the condition (9), it is still interesting to explore its consequences in view of the difficulty in understanding the known lensing events on the conventional picture. Thus we tentatively accept condition (9), and study the limiting case of lensing events caused collectively by a large number of lenses in a cluster. A theoretical framework to investigate this problem is discussed below.

For simplicity, let us model the gravitational deflection $\theta(r)$ due to a galaxy at an impact parameter r by

$$\begin{aligned} \theta(r) &= 8\sigma^2/c^2, \quad r \leqslant R, \\ &= 8\sigma^2 R/c^2 r, \quad r > R, \end{aligned} \tag{10}$$

where R is the outer radius of the galaxy. Consider a ray of light crossing a sheet of lenses. Let the surface number density of the lenses be η_s. The mean-square deflection of the ray in a direction parallel to an arbitrarily defined x-axis on the screen is

$$\langle \theta_x^2 \rangle = n_s \int_{r=0}^{r_c} \int_{\phi=0}^{2\pi} [\theta(r)\cos\phi]^2 \, r \, d\phi \, dr = A[1/2 + \ln(r_c/R)],$$
$$A = 64\pi n_s(\sigma/c)^4 R^2, \tag{11}$$

where r_c is some suitably chosen outer cut-off. This expression can be integrated over all sheets between the quasar and the observer to obtain the cumulative mean-square deflection. Considering a Friedmann cosmology with $\Omega = 0$ and taking $F = 0.018$, $Z_q = 2$, $R_{100} = R/100$ kpc, $H_0 = 50\,\mathrm{km\,s^{-1}\,Mpc^{-1}}$, and $r_c = c/H_0$, the rms deflection of a ray of light is $\sim 3.8\,R_{100}$ arcsec. Alternatively, if we assume strong clustering and take $F = 1.0$ and $r_c = 10$ Mpc, we obtain $\sim 94\,R_{100}$ arcsec. These numbers indicate that random multiple scattering by galaxies can indeed produce large deflections, particularly if there is clustering.

The above estimates are however not directly relevant for a theory of multiple images since the deflections of two neighbouring rays are always to a greater or lesser extent correlated. We therefore need the *differential* deflections $\langle [\Delta\theta_x(r)]^2 \rangle$ and $\langle [\Delta\theta_y(r)]^2 \rangle$ of two rays passing through a screen of lenses separated by a distance r parallel to the x-axis. We have computed these functions numerically for a random Poisson distribution of lenses on the screen and their dependence on (r/R) is shown in Fig. 1. Let us define

$$\langle [\Delta\theta_x(r)]^2 + [\Delta\theta_y(r)]^2 \rangle = A f(r/2R). \tag{12}$$

Consider two rays (Fig. 2) taking off from the distant quasar at a relative angle θ_0. Let the rays suffer random gravitational deflections due to lenses and be laterally displaced by amounts (X_1, Y_1) and (X_2, Y_2) at a screen placed at the location of the observer. For

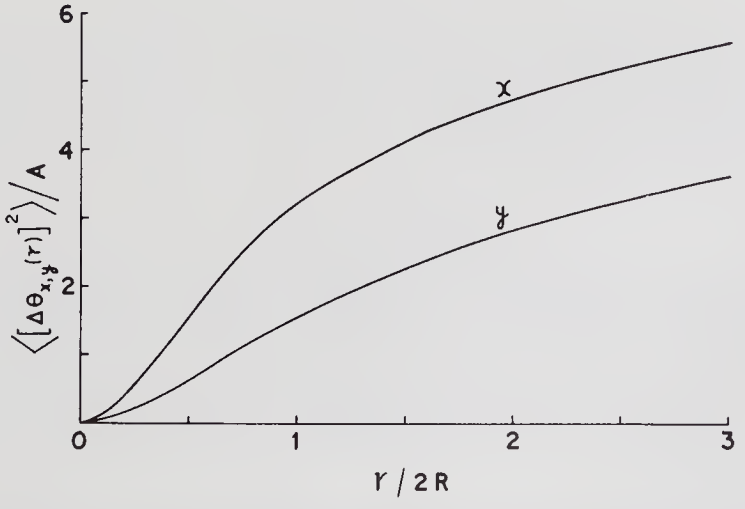

Figure 1. Mean square x and y differential deflections of two rays separated by a distance r along the x-axis on a screen of randomly distributed galaxy lenses. A is defined in Equation (11) and R is the radius of each galaxy.

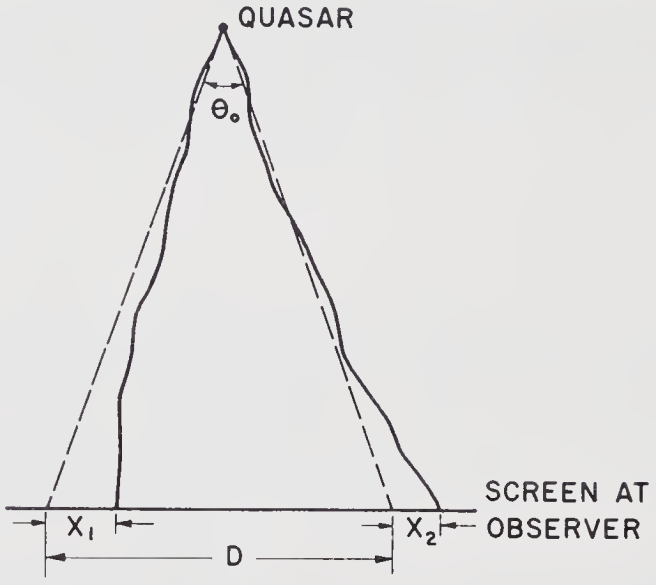

Figure 2. Two rays which take off at a relative angle θ_0 at the quasar would be separated by a distance D at the observer in the absence of deflections. In the presence of lenses, the rays are deflected by amounts (X_1,Y_1) and (X_2,Y_2). A suitably located observer sees two images if $X_1 - X_2 = D$ and $Y_1 = Y_2$.

$\Omega = 0$, it can be shown that

$$\langle (X_1 - X_2)^2 + (Y_1 - Y_2)^2 \rangle = (16F_0R^2/\pi^3) \int_0^{\chi_Q} f[(c/H_0)e^{-\chi}\theta_0 \sinh(\chi_Q - \chi)/2R] \times e^{2\chi} \sinh^2 \chi \, d\chi, \tag{13}$$

$$1 + Z_Q = \exp(\chi_Q).$$

If D is the expected separation between the two rays at the (observer) screen in the absence of lenses, we can define

$$g(\theta_0) = \langle (X_1 - X_2)^2 + (Y_1 - Y_2)^2 \rangle / D^2. \tag{14}$$

This function, which gives the dimensionless mean-square differential deflections of neighbouring rays, has the necessary information to treat the statistics of image formation by multipath propagation.

Longuet-Higgins (1956) has developed a detailed theory of various statistical properties of the sea surface in terms of the power spectrum of the waves. In particular, he has derived an expression for the density of maxima and minima, at which points the normal to the surface is vertical. In our problem, we are interested in the number of points in a randomly corrugated wavefront where the normal passes through the observer, producing an image. If we assume that the random gravitational deflections of rays can be described by Gaussian statistics, it turns out that Longuet-Higgins' formalism can be generalised to estimate the mean number of images $\langle N \rangle$ in our problem. The result is

$$\langle N \rangle = 1 + (\tau'/3.46) \exp(-4/3\tau'), \tag{15}$$

$$\tau' = d^2[g(\theta_0)]/d\theta^2. \tag{16}$$

We have made some preliminary estimates of τ' and N. For Z_q between 1.5 and 2.0 we find that

$$\tau' \sim 2.4\tau, \tag{17}$$

where τ is the single lens optical depth. This result has some very interesting implications. If we accept the hypothesis of strong clustering implicit in Equation (9), then Equation (17) shows that whenever there is lensing, there is a fairly good probability of getting multiple images from the collective 'many-lens' effects we have been considering. An immediate consequence is that one can no longer identify a single lens or a few lenses with the image splitting. This might explain why no massive lens galaxy has been seen in either Q 1115 or Q 2345 in spite of the large observed separations. Another consequence of our picture of multiple scattering is that the mean separation between images is not related to the angular scattering of a single lens (as in normal models) but rather depends on the radius R of an average lens (which is usually considered an irrelevant parameter). If we take R of the fiducial galaxy of luminosity L_* (Equation 3) to be 100 kpc, which implies $\Omega_{\text{galaxies}} = 0.077$, it appears that quite large image separations may be routinely expected. This is again a welcome feature. We also note that asymmetric image configurations should be the rule in the multiple scattering limit.

To summarize, if one is to attribute the three known cases of gravitational lensing to lensing by galaxies, then the large observed separations imply a very high degree of clustering. Our theory then shows that multiple scattering by a number of average lenses becomes important. The apparent absence of massive single lenses and the observed large separations appear to confirm this result. In this context, attempts to make models with one or a few lenses and to estimate H_0 from predicted time delays may be premature.

One must bear in mind that the calculations reported here are preliminary, and probably represent an extreme limiting case of multiple scattering because of the use of Gaussian statistics. It should also be mentioned that the degree of clustering seen in nearby galaxies does not appear to be strong enough to lead to Equation (9). It may then be necessary to abandon galaxies and look for other types of lenses. For instance, the universe may contain dark condensed massive ($10^{12-13}\,M_\odot$) lenses acting singly. These cannot however be black holes since the observed asymmetric image configurations imply that the lenses must be anisotropic. Alternatively, smaller dark lenses could be invoked. In this case, multiple scattering, presumably due to clustering, must become important, and the theory we have developed could again be relevant.

Acknowledgement

We gratefully thank J. P. Ostriker for several useful discussions on our work.

References

Chitre, S. M. 1984, in *Extragalactic Energetic Sources*, Ed. V. K. Kapahi, Indian Academy of Sciences, Bangalore, p. 143.

Fall, S. M. 1981, in *The Structure and Evolution of Normal Galaxies*, Eds S. N. Fall and D. Lynden-Bell, Cambridge University Press, p. 1.

Longuet-Higgins, M. S. 1956, *Phil. Trans. R. Soc. Lond.* **A, 249,** 321.
Narasimha, D., Subramanian, K., Chitre, S. M. 1982, *Mon. Not. R. astr. Soc.*, **200,** 941.
Young, P., Deverill, R. S., Gunn, J. E., Westphal, J. A., Kristian, J. 1981a, *Astrophys. J.*, **244,** 723.
Young, P., Gunn, J. E., Kristian, J., Oke, J. B., Westphal, J. A. 1981b, *Astrophys. J.*, **244,** 736.

Discussion

Porcas: My point is about the intrinsic improbability of a lens event which you give as $\sim 10^{-3}$. Since the lens effect also produces magnification of the images, lens systems will occur more frequently in flux-limited samples. In this context it may be significant that the second and third suspected cases of lensing occurred in optically selected samples. The first case, 0957 + 561 was radio selected and has significant extended emission at its selection frequency (966 MHz). However, statistics in this case are after the event, and in any case, here we see the galaxy and the cluster.

Narayan: Your point that image magnification changes the probability of detection is certainly true. We have not made any quantitative estimates but feel that the large separations that are observed will still be extremely unlikely even after allowing for this effect. The fact that a cluster has been seen in Q 0957 + 561 is actually support for our point of view. We say that there must be a cluster of some kind in all three cases. Note that in our approach a cluster is not treated as a single object but is handled statistically in terms of its constituent galaxies. There is a conceptual difference between this way of treating a cluster and the approach of Young *et al.* (1981a, b) which concentrates on the smooth overall potential.

Kapahi, V. K. (Ed.)
Extragalactic Energetic Sources
Indian Academy of Sciences, Bangalore, 1985, pp. 155–161

Mildly Active Nuclei of Galaxies

T. P. Prabhu *Indian Institute of Astrophysics, Bangalore 560034*

Abstract. Milder forms of activity in the nuclear regions of galaxies are reviewed. Three classes of activity are identified, namely starburst, high-excitation emission-line and low-ionization emission-line nuclei. Sérsic perinuclear systems are also briefly reviewed and it is pointed out that some interesting mildly active nuclei may lie hidden in these systems.

Key words: galaxies—active galactic nuclei—perinuclear systems

1. Introduction

The accumulating observations of galactic nuclei, in different bands of the electromagnetic spectrum, show that 'activity' is probably present in all nuclei, *albeit* in different degrees. On the other hand, it has proved frustrating to classify all the different observed properties into a sequence with a smoothly-varying degree of activity. Detailed investigations of different types of nuclei, whether highly active or quiescent, would improve our understanding of different processes that accompany 'activity' and also help in constructing the evolutionary sequence of an active galactic nucleus. Inclusion of all nuclei in an observational programme would enlarge the sample for any given flux limit, thus enabling one to arrive at a classification scheme; it also results in an increase in spatial resolution for a given limit on angular resolution.

The term 'nucleus' has been used in the past rather loosely, depending on the phenomenon addressed or the spatial resolution achieved. Following Ambartzumian (1971), I would define a 'nucleus' as a photometrically distinct structure unresolved or just resolved in ground-based optical photographs, and consequently also in the observations at short wavelengths using the Very Large Array (VLA). For a majority of nearby galaxies, the nucleus would thus have a size of a few hundred parsecs or less.

2. Nuclei of elliptical and lenticular galaxies

The classical active nuclei in elliptical (E) galaxies are associated with extended radio sources. A central, flat-spectrum, compact component is generally observed coincident with such nuclei. A new class of active nuclei identified in recent years is a compact flat-spectrum component in lenticulars (S0) and in some ellipticals. Some of these may be associated with either jets or haloes which do not extend beyond the optical size of the galaxy. Detailed observations may lead to a classification of such nuclei into two types: those which are actually milder versions of the strong sources and those in which the

beam is not able to penetrate outward through the interstellar gas in the galaxy. Clues to the latter class come from the following lines of evidence. Dressel (1981) finds that E and S0 galaxies are equally likely to be detected at a given radio power, though extended sources are predominantly found in ellipticals. It appears that ellipticals beam more efficiently than lenticulars. Even among ellipticals, Kapahi & Saikia (1982) find that the radio axis is aligned with the optical minor axis only for the group of galaxies for which a significant fraction of luminosity is contained in the core. Further, Prabhu & Kochhar (1984) find that the high core-strength radio galaxies may be flatter than the rest of the radio galaxies. Thus the fractional radio power retained in the nucleus could be related to the intrinsic shape of the galaxy and not to the intensity of activity. The milder nuclei in E/S0 galaxies should hence be identified only with those weak sources (see Jenkins 1982) which are compact and smooth, without any structure resembling beams or haloes.

3. Nuclei of spiral galaxies

The classical example of an active nucleus in a spiral galaxy is the Seyfert nucleus. Seyfert nuclei are characterized by broad optical emission lines of high excitation and ionization. They are classified into two types, type 1 being the ones with broad wings of Balmer lines that originate in the central 1 pc of the nucleus; the relatively narrower component of Balmer lines, as also the forbidden lines arise in an extended region (100–1000 pc). In Seyferts of type 2, only the latter region contributes to the emission lines. While both the types of Seyferts are characterized by strong non-thermal infrared (IR) and radio emission, type 2 Seyferts are brighter in the radio region and have strong thermal IR radiation attributed to hot dust. Type 1 Seyferts, on the other hand, emit intense X-ray radiation. The activity in Seyfert 1 is apparently more intense in the central parsec of the nucleus, and is characterized by broad wings of Balmer lines, intense X-rays and non-thermal continua.

3.1 *Optical Surveys of Bright Nuclei*

Morgan (1958, 1959), while classifying a large number of galaxies according to their central concentration, noted two types of morphological peculiarities in the central regions. The galaxies in which a bright nucleus was superposed on a considerably fainter background were termed as N galaxies and the ones with several bright spots in the nuclear region as hot-spot galaxies. Two central subsystems in galaxies could thus be recognized: the nucleus and the perinuclear system. The hot-spots were later shown to be giant H II regions. Sérsic & Pastoriza (1965) and Vorontsov-Vel'yaminov, Zaitseva & Lyutyi (1972) added a few more examples to this latter class while Sérsic (1973) gives a larger finding list of galaxies with a bright perinuclear system.

A large finding list of bright nuclei is now available through the Byurakan classification (class 4 and 5) and the RC2 classification (class 4 and 5; de Vaucouleurs, de Vaucouleurs & Corwin 1976). Keel & Weedman (1978) have surveyed photographically 448 such nuclei north of -20° declination and provide a brightness rank for these nuclei. Nuclear spectroscopic surveys are necessarily restricted to much smaller samples. A few distinct classes of mildly-active nuclei emerge through these surveys, which we describe in the following sections.

3.2 *Sérsic Perinuclear Systems*

The galaxies listed by Sérsic (1973) contain bright well-resolved structures of 1–2 kpc size in their central regions (Prabhu 1980b). While some galaxies have bright H II regions in these structures, others are of purely stellar constitution.

The relevance of Sérsic galaxies for a study of mildly active nuclei stems from two facts. First, a bright, red nucleus is hidden in probably all the bright perinuclear systems (Prabhu 1980a, b). Secondly, the observations imply that a few million solar masses of gas has been converted into stars in these perinuclear systems a few tens-of-million years ago (see *eg.* Alloin & Nieto 1982), implying a recurrent supply of gas. Active galactic nuclei face a similar problem of gas supply. Sørensen, Matsuda & Fujimoto (1976) have suggested that the bar may induce infall of gas from disc into the nuclear region. Observations tend to support this view (Prabhu 1980b; Kormendy 1982 and references therein). It also appears that the gas which funnels in through the bar does not fragment into stars until it reaches the nuclear region where it accumulates to the threshold density required (Tubbs 1982). A part of this gas may eventually fall into the nucleus and trigger the nuclear activity. At least in one case (NGC 1365, Véron *et al.* 1980), an active nucleus is detected hidden in a bright perinuclear system of hot spots. Clearly a detailed study of the nuclei of Sérsic galaxies would be of great importance.

3.3 *Low-ionization Nuclear Emission-line Regions (LINERs)*

Heckman (1980) has identified nuclei which fall in the low-ionization extension of Seyfert nuclei in the [O II]/[O III] *vs* [O I]/[O III] diagram. He also finds compact nuclear sources more often among these nuclei (termed 'liners') than among the remaining nuclei in his complete sample. Ionization in liners cannot be attributed to stellar ultraviolet (UV) flux. Shock heating and photoionization by power-law spectrum are two alternatives. Heckman (1980) lists 30 liners north of $+40°$ among the galaxies brighter than $B_T = 12$ and also 12 additional liners picked from literature. One would expect $\sim$ 50 liners south of $+40°$ in galaxies brighter than $B_T = 12$. Clearly, it is important to identify these and study the entire sample for a detailed comparison with Seyfert nuclei.

While liners can be found in all types of galaxies (E, S0 or S), we have discussed them here since a large number of spirals contain them.

3.4 *Starburst Nuclei*

Starburst nuclei are characterized by an intense burst of star formation in the nucleus ($\sim$ few hundred parsecs). These can be picked out easily since their spectra resemble the spectra of H II regions. Balzano (1983) lists 102 such nuclei largely drawn from Markarian's lists. The mass of young stars in these nuclei range from 10^7 to over 10^9 solar masses, comparable to the estimates for Sérsic perinuclear regions. Thus the burst of star formation is as intense as in 'hot spots', but takes place in a region ten times smaller in size.

3.5 *Brightness of Different Types of Nuclei*

We have thus identified three different types of nuclear and perinuclear activities. It would be of interest to see how they are distributed among the nuclear brightness ranks of Keel & Weedman (1978). The latter sample of 448 galaxies consists of 8 Seyferts, 40 Sérsic galaxies, 16 liners and 12 starburst nuclei. Dividing the sample into four unequal bins of 12, 55, 99 and 282 galaxies, it is seen (Table 1) that Seyferts are the brightest nuclei and liners are the next brightest, while Sérsic and starburst nuclei appear next. Eleven out of the twelve brightest nuclei in the sample exhibit one of the four kinds of activity, suggesting that the most common types of activity have all been identified. Two-thirds of active and mildly active nuclei from our sample are among the brightest one-third of Keel-Weedman sample. A spectroscopic investigation of the remaining nuclei from this sample, and an extension of the photographic survey to the southern hemisphere would certainly be rewarding.

3.6 *Observations in other Spectral Bands*

As already mentioned, liners are often associated with compact nuclear radio sources. Heckman's radio sample, however, did not include many starburst nuclei and Sérsic perinuclear systems. Van der Hulst, Crane & Keel (1981) have recently observed several nuclei at 6 cm using VLA. It appears from this survey that the ratio of radio to optical power is ~ 1 for liners and Sérsic perinuclear systems but exceeds ~ 10 for starburst nuclei. A significant fraction of radio emission from Sérsic galaxies is extended and coincides with the H II regions around the nucleus. Evidently, the radio emission from liners is of non-thermal origin while the free-free emission from H II regions dominates in the other two cases.

The thermal radiation from hot dust has been detected from 10 μm observations of several Sérsic and starburst nuclei (NN 2903, 5236, 1097; 2782, 3504, 4194, 4385, 4535, 4569, 7714). The dominant heating mechanism is certainly the UV radiation from young, hot stars. The near-IR *JHKL* bands are not significantly affected by dust reradiation. Hence, excess in these bands over composite starlight reflect contribution from the non-thermal continuum. Balzano & Weedman (1981) find that most nuclei with $J - K \geqslant 1.1$ in their sample of 107 galaxies are Seyferts. Almost all Seyferts (29/30) in their sample follow this criterion. There are several (21/77) non-Seyfert nuclei which also have such high IR colours. Ten of these are identified as starburst nuclei and one is

Table 1. Distribution of active and mildly-active nuclei in Keel-Weedman sample.

Rank	*N*	Seyfert	Liner	Sérsic	Starburst	Total
1–12	12	5	1	3	2	11
13–67	55	0	9	3	2	14
68–166	99	1	1	20	5	27
167–448	282	2	5	14	3	24
Total	448	8	16	40	12	76

of Sérsic type, while none of them is a liner. The total sample consists of 29 starburst nuclei, 5 Sérsic galaxies and two liners.

The ([O III] line width, $J-K$ colour) diagram of Balzano & Weedman (1981) shows a group of 16 galaxies occupying an intermediate location between most Seyferts and a majority of the remaining nuclei. This group has linewidths between 200 and 350 km s^{-1} and $J-K$ colours between 1.1 and 1.4. Of these 16, four are Seyferts (N4051, Mrk 352, 474 and 700), 10 are starburst nuclei and two (Mrk 359 and 518) do not fall into these two categories. Though data are meagre on Sérsic galaxies and liners, it may be stated with confidence that a significant fraction of mildly active nuclei may have non-thermal continuum and mild Seyfert-type activity.

It appears that X-ray observations provide a firm identification of Seyfert 1 type of activity. The existing X-ray data on normal spirals do not have sufficient angular resolution to enable a separation of the nuclear contribution from the total flux due to discrete sources in the disc. Observations with the high-resolution imager (HRI) aboard Einstein Observatory are available in a few individual cases, but even here the association can be narrowed down only to the central regions of the galaxy, and not to its nucleus. Yet, the X-ray flux far exceeding the flux expected from the disc ($\lesssim 10^{41}$ erg s^{-1} in 2–10 keV band) may certainly be attributed to an active nucleus. Several 'normal' galaxies have been detected at this level as reported in the literature (see *eg.* Wilson 1979). These are generally referred to as narrow-line (or sharp-line) X-ray galaxies, high excitation emission-line galaxies (HEXELG) or high-ionization nuclear emission-line regions (HINER). Specific example are NN 526 A, 1365, 2992, 5502, 7582, 2110 and MCG – 5-23-16. The last two are early-type galaxies. The underlying Seyfert 1 type nucleus has been detected in N 1365 (Véron *et al.* 1980) and it appears that the nuclei of HEXELG are milder versions of Seyfert 1 phenomenon. These nuclei are, however, extremely dusty unlike Seyfert 1 nuclei.

4. The galactic nucleus

At a distance of a mere 10 kpc, the nucleus of our Galaxy offers a very good opportunity to observe its internal structure (1 milli-arcsec = 10 a.u.) However, the very high ($\sim$ 25 mag) interstellar absorption in the optical region had rendered the galactic nucleus unobservable until observations became possible in various other bands of the electromagnetic spectrum. Comprehensive reviews of the present state of understanding are given by Oort (1977) and Townes *et al.* (1983).

The observations imply a dense star cluster consisting of $\sim 10^7$ stars in the central 3 pc, centred around an unusual IR source IRS 16 which houses a point-like radio source ($<$ 10 a.u.). There are several clouds of ionized gas interspersed in this cluster. The motions of these clouds are consistent with a point mass of $3 \times 10^6\, M_\odot$ at the centre. The observed X-rays ($\sim 10^{35}$ erg s^{-1}) probably originate near this supermassive object. There are clouds of neutral gas and dust at $\sim$ 100 pc from the centre. The gas motions are fairly circular here, but non-circular motions are present in the gas at radial distances of 1–4 kpc. The nucleus as defined for a sample of external galaxies would contain a few tens of arcmin of the central region of our Galaxy. The thermal radio emission extends to 250 pc while the non-thermal emission extends over 900 pc in diameter. Though there are a few H II regions close to the centre, the nucleus would give an overall appearance of a liner, though still milder in its activity.

5. Conclusions

As seen in the previous sections, the main forms of mild activity in the nuclei of spiral galaxies may be classified into three distinct types: (i) starburst nuclei; (ii) high-excitation emission-line nuclei and (iii) low-ionization emission-line nuclei. Each of these has some properties in common with Seyfert nuclei, though generally at a lower degree. Some such nuclei may be hidden among the perinuclear systems of Sérsic galaxies, and have been studied only in a few individual cases (*e.g.* N1365). While an abundance of gas appears to have given rise to a burst of star formation in starburst nuclei, liners generally have too low a gas content to lead to star formation.

The milder activity in the nuclei of ellipticals is generally seen as a weak compact nuclear radio source. Spectroscopically, these nuclei appear as liners. Indeed a majority of compact sources detected by Heckman (1980) in their sample of liners appear in E and S0 galaxies (5 out of 8) and a majority of E and S0 liners in their sample are known to be associated with a compact radio source (7 out of 9). It would be worthwhile to study the properties of these three classes of objects in comparison with Seyfert and radio galaxies. It would also be of interest to study the nuclei of Sérsic galaxies and to identify whether they would belong to one of the above three categories, or would exhibit a different type of activity.

References

Alloin, D., Nieto, J.-L. 1982, *Astr. Astrophys. Suppl. Ser.*, **50,** 491.
Ambartzumian, V. A. 1971, in *Nuclei of Galaxies.*, Ed. D. J. K. O'Connell, North-Holland, Amsterdam, p. 9.
Balzano, V. A. 1983, *Astrophys. J.*, **268,** 602.
Balzano, V. A., Weedman, D. W. 1981, *Astrophys. J.*, **243,** 756.
de Vaucouleurs, G., de Vaucouleurs, A., Corwin, H. G. 1976, *Second Reference Catalogue of Bright Galaxies*, Univ. of Texas Press, Austin.
Dressel, L. L. 1981, *Astrophys. J.*, **245,** 25.
Heckman, T. M. 1980, *Astr. Astrophys.*, **87,** 152.
Jenkins, C. R. 1982, *Mon. Not. R. astr. Soc.*, **200,** 705.
Kapahi, V. K., Saikia, D. J. 1982, *J. Astrophys. Astr.*, **3,** 161.
Keel, W. C., Weedman, D. W. 1978, *Astr. J.*, **83,** 1.
Kormendy, J. 1982, *Astrophys. J.*, **257,** 75.
Morgan, W. W. 1958, *Publ. astr. Soc. Pacific*, **70,** 364.
Morgan, W. W. 1959, *Publ. astr. Soc. Pacific*, **71,** 394.
Oort, J. H. 1977, *A. Rev. Astr. Astrophys.*, **15,** 295.
Prabhu, T. P. 1980a, *Astrophys. Space Sci.*, **68,** 519.
Prabhu, T. P. 1980b, *J. Astrophys. Astr.*, **1,** 129.
Prabhu, T. P., Kochhar, R. K. 1984, *Astrophys. Space Sci.*, **102,** 29.
Sérsic, J. L. 1973, *Publ. astr. Soc. Pacific*, **85,** 103.
Sérsic, J. L., Pastoriza, M. 1965, *Publ. astr. Soc. Pacific*, **77,** 287.
Sørenson, S.-A., Matsuda, T., Fujimoto, M. 1976, *Astrophys. Space Sci.*, **43,** 491.
Townes, C. H., Lacy, J. H., Geballe, T. R., Hollenbach, D. J. 1983, *Nature* (*London*), **301,** 661.
Tubbs, A. D. 1982, *Astrophys. J.*, **255,** 458.
van der Hulst, J. M., Crane, P. C., Keel, W. C. 1981, *Astr. J.*, **86,** 1175.
Véron, P., Lindblad, P. O., Zuiderwijk, E. J., Véron, M. P., Adam, G. 1980, *Astr. Astrophys.*, **87,** 245.
Vorontsov-Vel'yaminov, B. A., Zaitseva, G. V., Lyutyi, V. M. 1972, *Soviet Astr.*, **16,** 71.
Wilson, A. S. 1979, *Proc. R. Soc. London*, **A366,** 461.

Discussion

Venugopal: How is gas forced into the nucleus by the bar?
Prabhu: Bars in spiral galaxies are prolate ellipsoidal bodies rotating end-over-end. These are known to be rotating fairly rapidly (Kormendy 1982), with a constant angular velocity. The gaseous disc, on the other hand, rotates differentially, the angular velocity decreasing outwards. Thus, the velocity of the tip of the bar very much exceeds the velocity of the gas in the disc at the corresponding position. Hence the gas near the ends of the bar is shocked and loses a part of its angular momentum. Consequently, it streams radially inward and settles into a disc around the nucleus, the scale-length depending on the residual angular momentum.

Note added in proof

An extensive nuclear spectroscopic survey of disc galaxies was recently undertaken by John Stauffer. The data on 139 field disc galaxies (Stauffer, J. R. 1982a, *Astrophys. J. Suppl. Ser.*, **50,** 517) and 67 Virgo cluster galaxies (Stauffer, J. R. 1983, *Astrophys. J.*, **264,** 14) have already been published while data on many more cluster galaxies are yet to appear in print. Based on these data, Stauffer (1983) finds no significant difference in emission-line strengths in Virgo cluster and field galaxies suggesting that there is no stripping of nuclear gas due to cluster environment. On the other hand, galaxies with detectable emission lines occur preferentially in pairs and groups suggesting that the gas infall into the nucleus is triggered by tidal encounters (Stauffer, J. R. 1982b, *Astrophys. J.*, **262,** 66). Stauffer also separates the nuclei with emission lines not excited by stellar photoionization (and hence related to Liners) and classifies them further into shock-ionized and power-law-ionized nuclei following the spectral-line diagnostics already suggested (Baldwin, J., Phillips, M., Terlevich, R. 1981, *Publ. astr. Soc. Pacific*, **93,** 5).

Kapahi, V. K. (Ed.)
Extragalactic Energetic Sources
Indian Academy of Sciences, Bangalore, 1985, pp. 163–170

M 82—A Nearby Laboratory for Rapid Star Formation and the Phenomena of Active Galactic Nuclei

P. P. Kronberg *Scarborough College, Toronto, Ontario M1C 1A4, Canada & David Dunlap Observatory, University of Toronto, Richmond Hill, Ontario L4C 4Y6, Canada*

Abstract. A brief summary of the properties of, and objects within, M 82 is given. Recent radio and optical observations show that the intense activity within the inner 1 kpc of the M 82 nucleus is accompanied by the presence of several energetic objects which are exotic by the standards of our Galaxy and other 'normal' spirals. Recent observations reveal several very luminous objects which are presumably stellar in origin. These are being seen in some detail for the first time, thanks to improved observational techniques and the proximity of M 82. These luminous objects are, however, probably very common, and important constituents of most 'starburst' galaxies. The nucleus of M 82 therefore provides us with a useful laboratory for furthering our understanding of star-formation cycles in the universe.

The newest Very Large Array (VLA) data are described in some detail: large numbers (~ 30) of supernova-remnant candidates have been revealed in the inner 600 pc of M 82 with sub-arcsec resolution. The flux-density decrease of the bright source 41.9 + 58 in the nuclear region of M 82 occurs with an approximately constant spectral index of -0.9 at $\nu > 3$ GHz, and the low-frequency turnover has moved from ~ 700 MHz in 1974–1975 to ~ 400 MHz in 1979–81. A model of 41.9 + 58 is proposed in which it is, at least initially, confined by its own hot, pre-supernova ejecta.

Key words: galaxies, individual—active galactic nuclei—'starburst' galaxies—extragalactic supernova remnants

1. Introduction

The nearby irregular galaxy M 82 is perhaps the most puzzling and intriguing of all nearby galaxies. Its unusual morphology (Fig. 1) shows why it has been called an 'exploding galaxy', and also that it is difficult to relate, *prima facie*, to other morphologically standard galaxies. In terms of the attention M 82 has received in the literature, and because of the wide variety of astrophysical phenomena it exhibits, it can be called the 'Crab Nebula' of the nearby universe.

A summary of what we have learned about M 82 from observations over the past two decades has been given by O'Connell & Mangano (1978) and a more recent discussion of M 82's radio properties can be found in Kronberg, Biermann & Schwab (1981). I shall give only a brief and incomplete survey here. What I shall concentrate on are some

recent radio observations which put a few more pieces into the M 82 puzzle. Recent VLA* observations show that the inner 600 pc of M 82 contains many radio sources—presumably stellar in origin—which are 10–200 times more luminous than Cassiopeia A, the radio-brightest supernova remnant in the Milky Way. Observations of the brightest radio hotspot in the M 82 nucleus reveal a new kind of—presumably stellar—radio source, which is brighter than any current galactic supernova remnant and is probably associated with the pre-supernova remnant phase of a massive star. I shall discuss its physical properties as far as they can be deduced from the latest VLA and VLBI observations.

The inner zone of intense star formation activity in M 82 is probably displaying a scenario similar to that in the nuclei of all or most active galaxies, including those which conform better to the Hubble classification scheme. Our interest in M 82 lies not so much in its morphological uniqueness, but rather in the likelihood that the physical processes occurring near its nucleus are typical of most, or all galaxies undergoing bursts of star formation. The relative proximity of M 82 (3.2 Mpc) makes it one of the first 'laboratories' for understanding the physical processes in regions of active star formation, especially those undergoing tidal interaction with consequent infall of matter.

H I observations of the M 81–M 82 system confirm that M 82 is a tidally interacting galaxy (Gottesman & Weliachew 1977; Cottrell 1977). The inner 1 kpc is heavily obscured by gas and complex dust features. However, two very large H II complexes are at sufficiently low optical depth that they can be individually distinguished. These are denoted as regions A and C by O'Connell & Mangano (1978) and I and II respectively by Recillas-Cruz & Peimbert (1970) who first called attention to their interesting properties. O'Connell & Mangano (1978) find that the H II region A, the largest single complex in the M 82 nucleus, is at least partially dynamically detached from the other material visible near the nucleus. From its velocity gradient they determine a dynamical mass for region A of $\sim 10^8\ M_\odot$. This can be combined with the estimated intrinsic luminosity of region A ($L_v \sim 10^9\ L_\odot$) to estimate the M/L ratio which is ~ 0.1. This in turn implies that a substantial fraction of the light from region A comes from massive pre-main sequence stars. Combining these facts with the assumption of a conventional initial mass function with limits 50 $M_\odot$ and 1 $M_\odot$ it can be concluded that star formation in A has been going on for less than $\sim 5 \times 10^7$ yr (O'Connell & Mangano 1978). I shall call this 'timescale 1'

$$\tau_1 \sim 5 \times 10^7 \text{ yr}.$$

The supposition that region A is only the 'tip of the iceberg' is suggested by the very large dust obscuration in the M 82 nuclear region. The total infrared (IR) luminosity of $\sim 8 \times 10^{43}$ erg s^{-1} (Kleinmann, Wright & Fazio 1976), if powered by clusters similar to region A, implies that up to 10 additional regions similar to A and C must lie at larger optical depths to us within the inner ~ 1 kpc.

The optical observations provide us with a second relevant timescale (τ_2) of nuclear activity, namely the collapse time of the interstellar clouds. Both the Hα intensities and the [S II] ($\lambda\lambda$6717, 6731) line ratios indicate interstellar densities of a few hundred to

* The Very Large Array is operated by the U.S. National Radio Astronomy Observatory under contract with the National Science Foundation.

Figure 1. Photograph of the Irr II galaxy M 82, taken on Kodak 103a-E emulsion with an Hα interference filter using the Hale Observatories 5-m telescope (by A. Sandage, and reproduced with his kind permission). P. P. KRONBERG

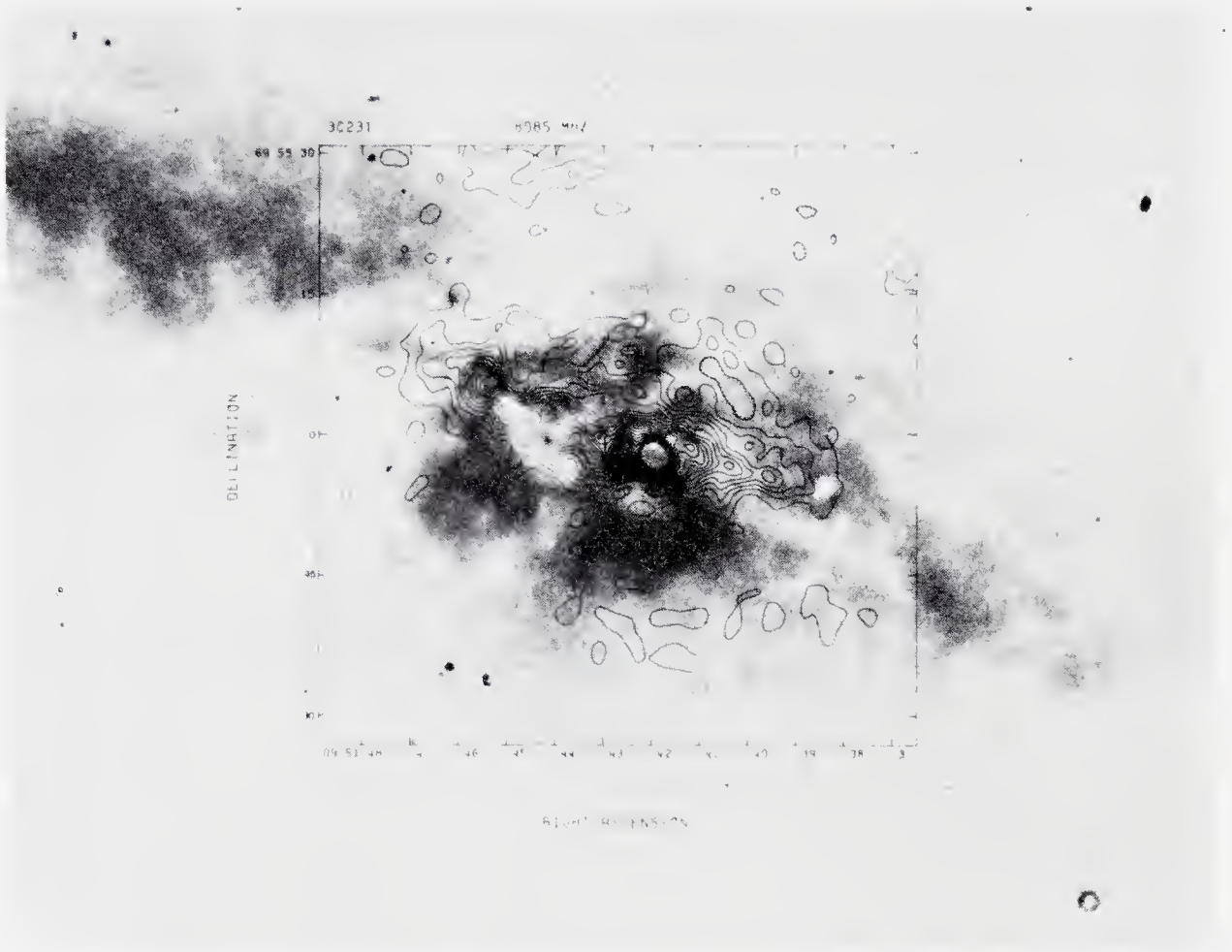

Figure 2. The 8085-MHz supersynthesis radio map superposed on an IR – red composite photograph in which sources prominent in the *near IR* are bright and the *red* sources are dark. The red plate (103a-E emulsion and RG2 filter) was taken by R. Racine and the IR (Kodak I-N emulsion and Wr 89B filter) by S. van den Bergh, both with the Hale Observatories 5-m telescope. The exposure was adjusted to show the two large H II regions in isolation from other emission. Some of the IR knots are also visible—see also Fig. 3. (Kronberg & Wilkinson 1975). P. P. KRONBERG

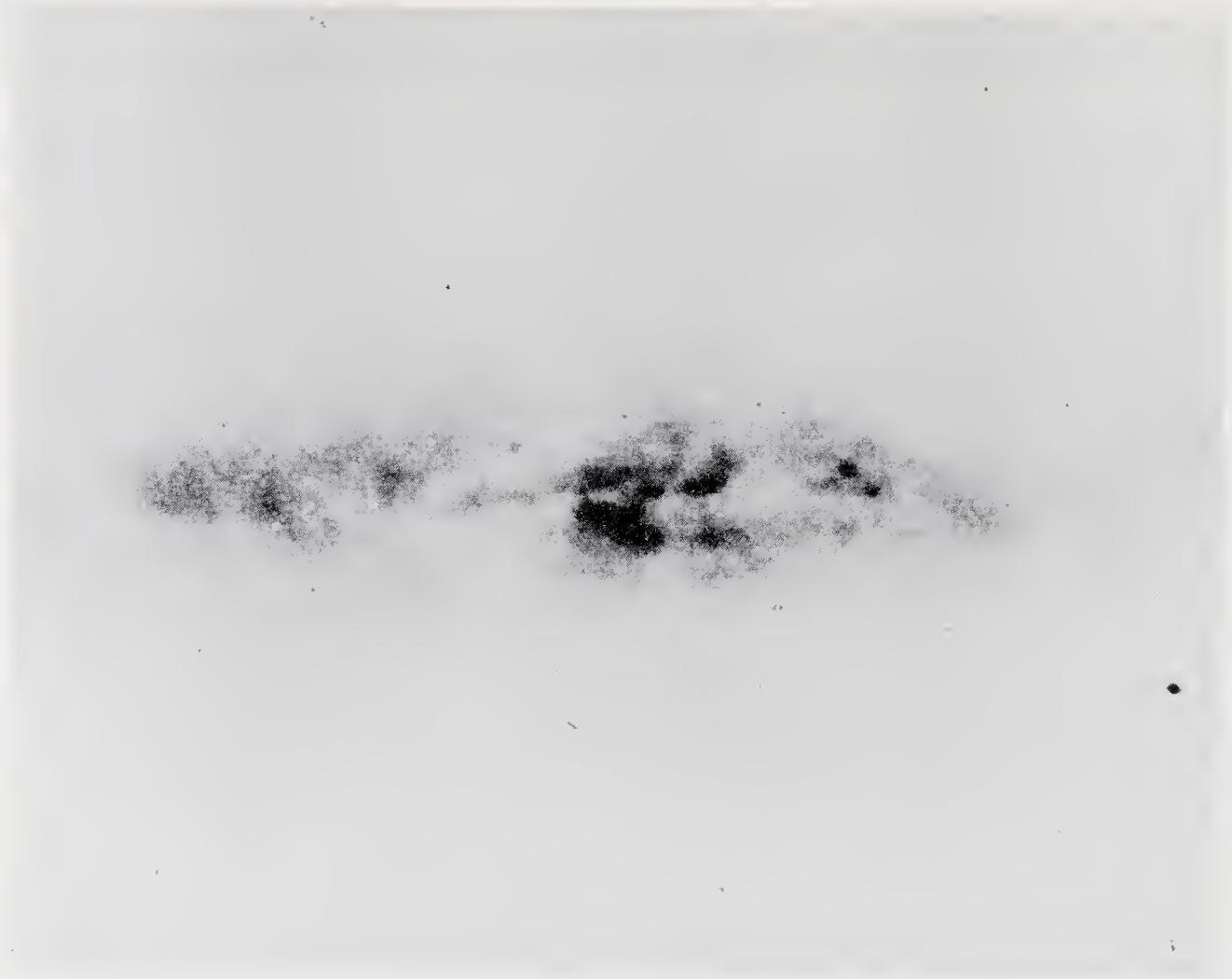

Figure 3. Near-IR (I-N + RG5) photograph of M 82 which shows the bright compact stellar knots which are prominent near 1 μm. (Taken by F. Bertola on the 182-cm Asiago telescope and reproduced here with Dr. Bertola's kind permission.) P. P. KRONBERG

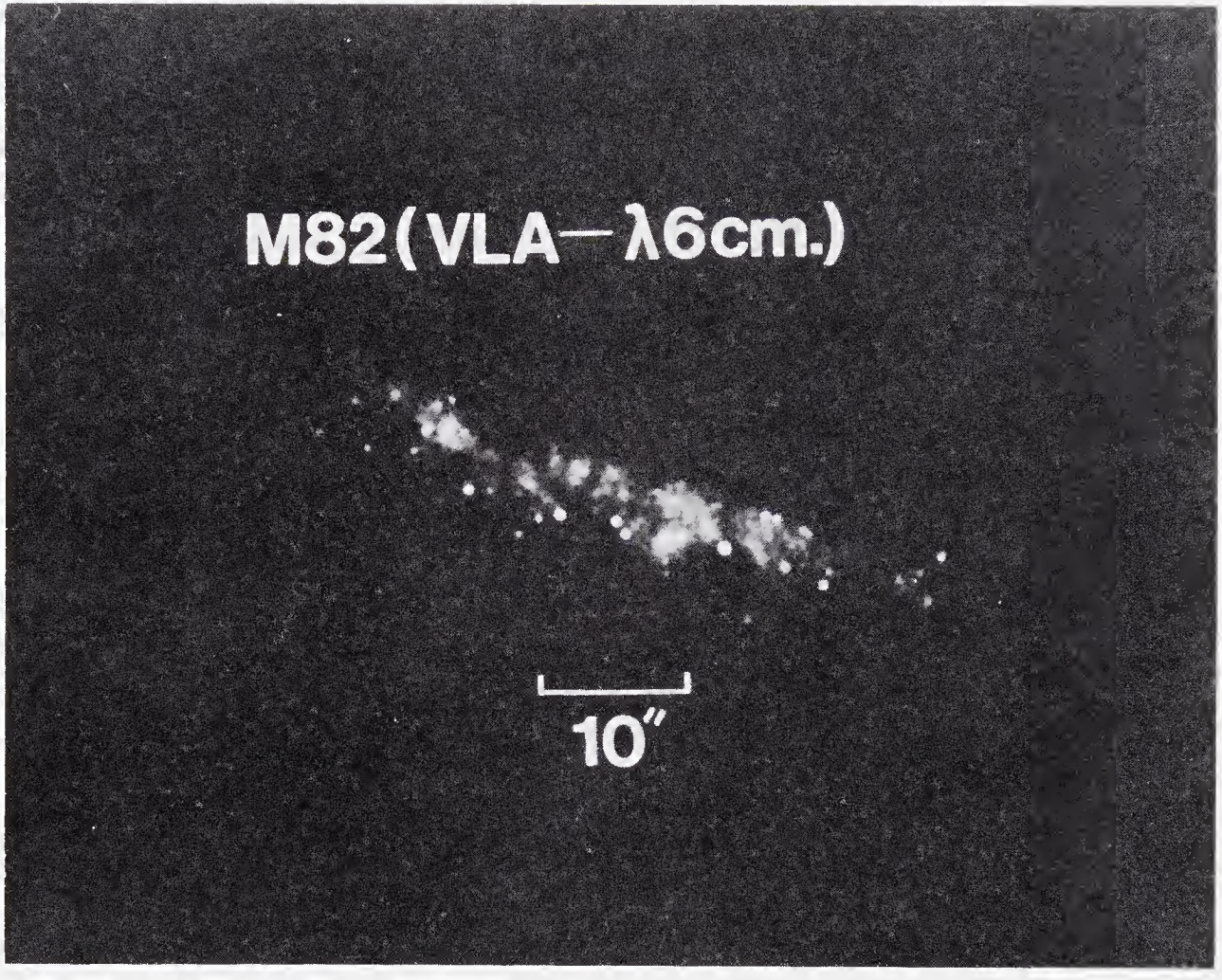

Figure 4. The radio emission from the inner 600 pc of the M 82 nucleus, mapped at 0.4 arcsec resolution with the NRAO Very Large Array in 1981. The brightest point source is 41.9 + 58. The faintest point sources visible in this picture have radio luminosities comparable with that of Cassiopeia A. (Kronberg & Biermann 1983). P. P. KRONBERG

$\sim 2000\,\mathrm{cm}^{-3}$. I shall call τ_2 the free-fall time,

$$\tau_2 \simeq 10^7 n^{-1/2} = 6 \times 10^5\,\mathrm{yr} \quad \text{for} \quad n = 300\,\mathrm{cm}^{-3}$$

and although τ_2 is only a crude time estimate given for the large range of densities, it is clearly compatible with τ_1 above.

Both τ_1 and τ_2 should be less than time τ_3 ago when the violent activity in M 82 was initially triggered off. Further optical evidence for τ_3 comes from the fact that the outer disc of M 82 beyond ~ 1 kpc from the nucleus has no detectable H II regions, Balmer emission lines, or individual supergiant stars which should be visible if $M_v \lesssim -6$. The light from the outer disc is characteristic of spectral types *F*0–*F*5 (O'Connell & Mangano 1978) which, combined with the absence of young stars, means that star formation in the outer disc of M 82 has stopped a few hundred million years ago; *i.e.*,

$$\tau_3 \sim 2 \times 10^8\,\mathrm{yr}.$$

Thus the timescales τ_1, τ_2 and τ_3 are all consistent with the hypothesis that the disc of M 82 was disrupted, probably by gravitational interaction with M 81, some 10^9 yr ago, and that infalling debris in consequence of this began the evident activity which is now observed. We shall see below that new VLA observations of M 82 by Kronberg, Biermann & Schwab (1983) can give us another independently determined *radio-activity* timescale, τ_4.

Fig. 2 shows an 8.1-GHz NRAO Interferometer synthesis map of the radio emission in M 82 (Kronberg & Wilkinson 1975), superimposed on a red-IR photograph which shows the approximate locations of H II regions A and C, and the fact that the bulk of the radio emission is generated within the inner 600 pc of the M 82 nucleus. The bulk of the X-ray emission (Griffiths 1980) and the 5–20 μm IR emission (Rieke *et al.* 1980) are also generated in this region.

Another interesting constituent of the inner regions of M 82 are the dense optical knots first discovered by van den Bergh (1971) and which are best seen at $\lambda \sim 1$ μm (Fig. 3). These highly reddened knots are thought to be very dense star clusters ~ 100 times brighter than our Galaxy's most luminous known clusters. Although we, as yet, know relatively little about their physical properties, they most likely occur commonly in other active galaxies. Some of the 1 μm knots of M 82 occur outside the 600 pc nucleus, and so far none has been unambiguously associated with detectable radio emission. Some of these knots, if we correct for reddening on the assumption of their intrinsic $(B-V) = 0$, have as much as $10^8\ L_\odot$, comparable with the superassociations seen in some luminous spirals (Ambartsumian 1964). Whereas the superassociations have sizes of ~ 500 pc, the M 82 stellar knots are $\lesssim 15$ pc (the seeing limit at M 82), *i.e.*, $\lesssim 3 \times 10^{-5}$ of the volume of the former. Our most recent VLA maps show that any radio emission is < 0.5 mJy from at least 2 of the brightest of these knots—K and L of Kronberg, Pritchet & van den Bergh (1972). This is less than Cas A at the distance of M 82.

2. New radio observations of M 82

The M 82 nucleus has been observed with the full resolution of the VLA (0.4 arcsec) at λ 6 cm (5 GHz). At this resolution, as Fig. 4 shows, a large number of compact ($\lesssim 0.2$ arcsec) sources are visible from 100 mJy down to 0.5 mJy—the current limit of

dynamic range at λ 6 cm. Within this flux-density range, at least 30 discrete sources can be identified, 16 of which are stronger than 2 mJy. If the majority of these are supernova remnants, they are all more radio luminous than Cassiopeia A, which, at the assumed 3.2 Mpc distance of M 82, would have a 5-GHz flux density of 0.8 mJy and an angular size of ~ 0.2 arcsec.

A preliminary spectral index comparison at cm wavelengths for the stronger sources in Fig. 4 shows that the vast majority have steep spectra, which is consistent with their being powerful supernova remnants. Their luminosities range from 1 to 200 times that of Cas A. In an earlier astrometric comparison between the radio hotspots and optical knots, Kronberg, Pritchet & van den Bergh (1972) and O'Connell & Mangano (1978) determined that there was little, if any, correspondence between radio knots at 2 arcsec resolution and compact features in the optical and near-IR. A preliminary comparison at the present, higher radio resolution indicates that this is still the case, which is not too surprising in view of the high optical obscuration within most of the inner 600 pc. A more detailed analysis of these new radio maps is in progress, and comparison of the radio features with those in the optical and X-ray bands (Kronberg, Biermann & Schwab 1983) will be published elsewhere.

The new VLA map at 0.4-arcsec resolution resolves out a significant portion of the radio emission. This gives us, for the first time, a direct measurement of the radio surface brightness in the M 82 nucleus, and hence an estimate of the energy density of the relativistic electron gas on the assumption of equipartition between particles and magnetic field energy and that protons and electrons have equal energies. The result is that the electron cosmic-ray clouds (which generate the synchrotron radiation seen in Figs 2 and 4) have $\varepsilon \sim 10^{-9}\,\mathrm{erg\,cm^{-3}}$. This gas, being bounded by interstellar clouds having $10 \lesssim n \lesssim 2000\,\mathrm{cm^{-3}}$, will advance with a ram-pressure determined velocity of $\sim 100\,\mathrm{km\,s^{-1}}$ (we ignore adiabatic losses). We can thus calculate that the present configuration of radio-emitting clouds will have dispersed in $\sim 10^6$ yr. This is the *radio cloud dispersal timescale*, τ_4 which independently agrees with τ_1 and τ_2, and like τ_1 and τ_2 is compatible with, *i.e.* much less than τ_3, the time since the initial primary triggering event. Thus the observations support a scenario in which chaotic and expanding cosmic-ray clouds envelop and statically or quasi-statically compress dense interstellar gas clouds which are induced to collapse into massive stars. The end phases of stellar evolution generate the next generation of cosmic-ray clouds directly through supernovae, pulsars, *etc.*, and/or indirectly through interstellar turbulence. A self-perpetuating (for a time) scenario of this sort is the most likely explanation of the active condition of the M 82 nuclear region. The large implied numbers of massive stars make the M 82 nucleus an interesting laboratory for supernovae and their remnants—which we apparently see in large numbers and with very high luminosities, by galactic standards. The next section discusses the properties of the most luminous—presumably stellar—object, namely the variable source labelled 41.9 + 58 by Kronberg & Wilkinson (1975).

3. The compact, variable source, 41.9 + 58

This source is the most luminous radio object within the 600 pc long M 82 nuclear region. Its spectrum was first defined by Kronberg & Wilkinson (1975) between 408 MHz, where it was optically thick, and 8085 MHz where its spectral slope was steep and close to -0.9 ($S \propto \nu^{\alpha}$). Successive NRAO interferometer observations made

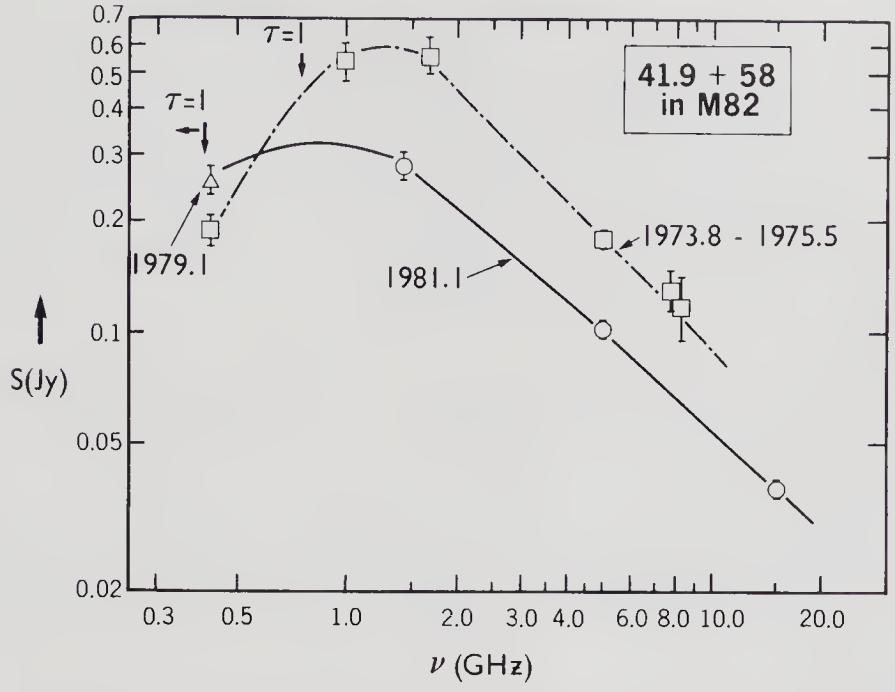

Figure 5. The radio spectrum of 41.9 + 58 for two epochs. The eariler epoch was chosen to include flux-density measurements which are relatively close in time to that of the VLBI measurement of the angular size (1974.6) by Geldzahler *et al.* (1977) (Kronberg & Biermann 1983).

between 1971 and 1975 showed further that the 8085-MHz flux was decreasing with time (Kronberg & Clarke 1978), which fact was later confirmed by VLA measurements in 1978 and 1981. VLBI measurements in 1974 by Geldzahler *et al.* (1977) revealed the remarkable result that most of the 8-GHz flux from 41.9 + 58 came from a region only 1.5 milli-arcsec in diameter ($\sim$ 1 light month). Fig. 5 shows the spectrum of 41.9 + 58 at two epochs. I have chosen the first to be closest to the VLBI measurement of Geldzahler *et al.* and then 1981, when simultaneous 20, 6 and 2 cm measurements were made with the VLA. A repeat by Conway in 1979.1 of Kronberg & Wilkinson's 408 MHz flux measurement indicates that the optically thick flux is increasing, whereas at higher frequencies it is decreasing *with a nearly constant slope* and *e*-folding time of $\sim$ 15 yr. Furthermore, the low-frequency turnover ($\tau = 1$) frequency, $\sim$ 700 MHz in $\sim$ 1975, has decreased to $\lesssim$ 400 MHz in 1981. The spectral index in 1981 is -0.9, so that the index of the relativistic electron energy spectrum is 2.8. The earliest measurement of the flux from 41.9 + 58 in 1966 at 11 cm (Bash 1968) is consistent with a backward extrapolation of the spectrum in Fig. 5. It sets a conservative lower limit of 9 yr to the age in 1975, and also an *upper limit* of 1270 km s^{-1} to the average velocity of expansion. Unfortunately no definitive VLBI map has been made since, although more recent low-frequency (18-cm) observations by Jones, Sramek & Terzian (1981) indicate elongated structure up to 15 mill-arcsec in p.a. 56° (epoch 1979.4). It is unfortunate that since 1974 no detailed VLBI map has been obtained at $\nu > 3$ GHz (where interstellar scattering is not likely to obscure the true radio size).

If we assume incoherent synchrotron radiation and use the spectrum measured $\sim$ 1975 (Fig. 5) and the size at 7.8 GHz, some interesting requirements will have to be imposed on the physical parameters of this source (*cf.* Kronberg & Clarke 1978; Brown

& Neff 1980): The very well-defined low-frequency spectral turnover (Fig. 5) establishes a firm upper limit on the synchrotron self-absorption (ssa) frequency (ν_{ssa}), as well as the *combination* of thermal absorption (ν_{th}) both *within* and *in front of* the radiating volume. *If* $\tau = 1$ at 700 MHz is due to ssa, then the 1.5 milli-arcsec size and observed luminosity of 6×10^{37} erg s^{-1} (integrating between 10^7 and 2×10^{10} Hz) require that the magnetic field strength, $B \sin\theta \approx 2 \times 10^{-4}$ G. This, being far below the equipartition field [0.13 G for equal proton and electron energies ($k = 1$) or 0.4 G if ($k = 100$)], requires a high energy density of relativistic particles, $E_p = 3.2 \times 10^{47}$ erg ($k = 1$), or 1.6×10^{-3} erg cm^{-3}.

The fact that any non-relativistic electrons within the source must also cause $\tau_{th} = 1$ at $\lesssim 700$ MHz requires that *at most* $2.5\, T_8^{3/4}\, M_\odot$ of nonrelativistic gas exists *within* the radiating volume, *i.e.*, $n_{th} \lesssim 1.16 \times 10^7\, T_8^{3/4}$ cm^{-3}. This puts an upper limit of 6.3×10^{49} erg at $T = 10^8$ K to its thermal gas component of total energy. Comparing n_{th} with the likely density of relativistic electrons, we conclude that the thermal and relativistic particles are present in roughly comparable numbers. This, in turn, means that the acceleration mechanism for the relativistic electrons is a very efficient one.

It must be noted here that both the total particle energy and the ratio of n_r/n_{th} are highly sensitive to the dimensions of the radiating volume, and may have changed significantly from 1975 to 1981. The fact that the frequency at which $\tau = 1$ moved significantly downward between 1975 and 1981 (Fig. 5) suggests that the sharp turnover in the 1975 spectrum was indeed due to synchrotron self-absorption, and that 41.9 + 58 has expanded and decreased in surface brightness. We can then conclude that the $\tau = 1$ frequency due to thermal absorption *in front of the source* (and probably within the source) lies *below* 400 MHz (the $\tau = 1$ frequency in 1981), on the grounds that the optical depth of the foreground material is unlikely to change so quickly with time, being less sensitive to the radius of the source than the 'ssa' turnover frequency.

Assuming that the foreground ionized gas is part of a shell of hot thermal gas having thickness ΔR, the requirement that $\tau_{th} = 1$ at $\nu \lesssim 400$ MHz now requires that the *density* in the shell has an upper limit given by

$$n_{shell} \lesssim \frac{6.7 \times 10^6\, T_8^{3/4}}{\Delta R^{1/2}_{(3.10^{16}\,\mathrm{cm})}}\ \mathrm{cm}^{-3}.$$

The shell must be sufficiently hot and dense to restrain the expansion of the cloud of energetic relativistic electrons and at the same time have an optical depth less than unity at 400 MHz. We find that, for $T = 10^8$ K and $n_{shell} \simeq 10^7$, these conditions are just satisfied for the source parameters of epoch 1975. This also limits the mass of the shell at $M_{shell} \lesssim 20 T_8^{3/4}\, M_\odot$. A mass in the range of 1 to $10 M_\odot$ is probably more realistic, in which case $\Delta R \simeq R$ in 1975.

The foregoing arguments and discussion suggest a 'first-order' physical model for 41.9 + 58, illustrated in Fig. 6, as recently proposed by Kronberg & Biermann (1983). According to this model, most of the synchrotron radio emission in 1975 was within a diameter of $\sim 7 \times 10^{16}$ cm (~ 25 light days) and confined by a hot shell of density 10^7 cm^{-3} and temperature $\sim 10^8$ K (Fig. 6a). The radio source is expanding slowly (at $v \sim 1000$ km s^{-1} as required by its size, and minimum age in 1975) and contains a magnetized rotator, probably a pulsar, whose rapidly rotating magnetosphere efficiently accelerates the radiating relativistic electrons. The mass of the surrounding thermal shell is too great to be swept-up interstellar matter. We postulate that it is the *ejecta from the massive star* which is undergoing a supernova-like explosion.

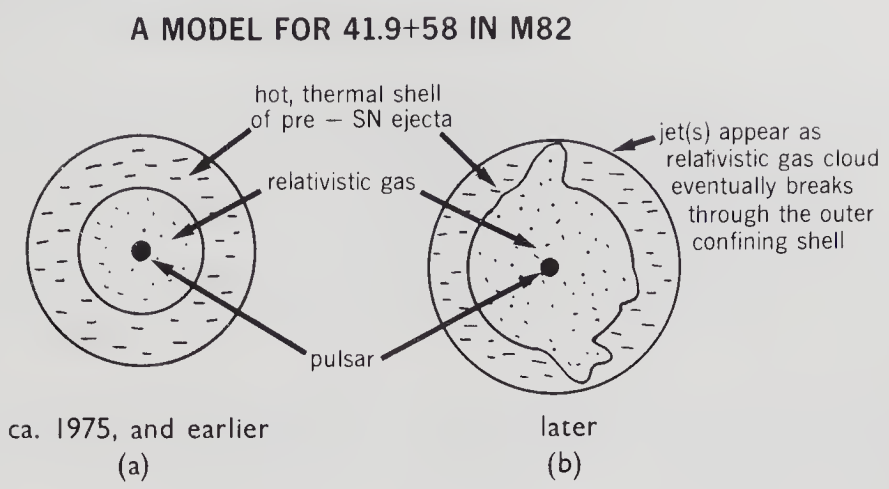

Figure 6. A suggested physical model for 41.9 + 58, (a), which is consistent with the physical parameters as measured around 1975. Instabilities will develop quickly in the surrounding hot ejecta (b) which will be punctured by the relativistic gas, and an asymmetric growth of overall radio dimensions will develop within a short period of time (right side). (Kronberg & Biermann 1983).

The configuration in Fig. 6(a) is not stable, and the hot, light relativistic gas will expand into instabilities in the surrounding shell as Fig. 6(b) illustrates schematically. An asymmetrical source and/or jets will develop quickly, and such a phenomenon might explain the asymmetrical source shape observed using 18-cm VLBI by Jones, Sramek & Terzian (1981). If so, then by the late 1970s a jet-like protrusion had already formed.

The confining shell will be a source of bremsstrahlung X-rays. We note that the extrapolation of the synchrotron spectrum in Fig. 5 to X-rays would give only 1/20 of the value of $\sim 10^{39}$ erg s^{-1} reported by Griffiths (1980), and likely associated with 41.9 + 58. A shell near $2M_{\odot}$ having a temperature between 10^7 and 10^8 K in our model would provide about the same amount of X-ray emission; however it is also possible that inverse compton emission, at least at epoch 1975, also contributed to the X-ray flux. Our calculations serve to show that the X-ray flux from 41.9 + 58 will be an important guide in a more detailed model than that described in this lecture. A more refined model will require definitive VLBI maps, which are now needed to provide the crucial observational clues to the interesting nature of 41.9 + 58. A further monitoring of its radio spectrum and X-ray flux is also being undertaken.

It is premature to classify 41.9 + 58 with other galactic supernovae, since its luminosity exceeds that of Cas A by a factor of $\sim$ 200. Considering the large number of luminous (relative to Cas A) objects in Fig. 1 it appears that a much more luminous supernova-like object may commonly exist, at least in regions of very active star formation. It is likewise premature to compare 41.9 + 58 with comparably luminous supernova-like radio source recently discovered in M 100 (Weiler *et al.* 1981). Whatever the type of star associated with 41.9 + 58, it provides us with one of the first opportunities to study the early phase of an explosive stellar event—one which we have not seen in our Galaxy, but which may be very common in active or 'starburst' galaxies.

References

Ambartsumian, V. A. 1964, in *IAU-URSI Symp.* 20: *The Galaxy and the Magellanic Clouds*, Eds F. J. Kerr & A. W. Rodgers, Australian Academy of Sciences, Canberra, p. 122.
Bash, F. N. 1968, *Astrophys. J. Suppl. Ser.*, **16,** 373.
Brown, R. L., Neff, S. G. 1980, *Astrophys. J.*, **241,** 561.
Cottrell, G. A. 1977, *Mon. Not. R. astr. Soc.*, **178,** 577.
Geldzahler, B. J., Kellermann, K. I., Shaffer, D. B., Clark, B. G. 1977, *Astrophys. J.*, **215,** L5.
Gottesman, S. T., Weliachew, L. 1977, *Astrophys. J.*, **211,** 47.
Griffiths, R. E. 1980, in *Highlights of Astronomy*, **5,** Ed. P. A. Wayman, D. Reidel, Dordrecht, p. 641.
Jones, D. L., Sramek, R. A., Terzian, Y. 1981, *Astrophys. J.*, **246,** 28.
Kleinmann, D. E., Wright, E. L., Fazio, G. G. 1976, preprint.
Kronberg, P. P., Biermann, P. 1983, in *IAU Symp.* 101: *on Supernova Remnants and their X-ray Emission*, P. Gorenstein & I. J. Danziger, D. Reidel, Dordrecht.
Kronberg, P. P., Biermann, P., Schwab, F. R. 1981, *Astrophys. J.*, **246,** 751.
Kronberg, P. P., Biermann, P., Schwab, F. 1983, (in preparation).
Kronberg, P. P., Clarke, J. N. 1978, *Astrophys. J.*, **224,** L51.
Kronberg, P. P., Pritchet, C. J., van den Bergh, S. 1972, *Astrophys. J.*, **173,** L47.
Kronberg, P. P., Wilkinson, P. N. 1975, *Astrophys. J.*, **200,** 430.
O'Connell, R. W., Mangano, J. J. 1978, *Astrophys. J.*, **221,** 62.
Recillas-Cruz, E., Peimbert, M. 1970, *Bol. Obs. Tonantzintla Tacubaya*, No. 35.
Rieke, G. H., Lebofsky, M. J., Thompson, R. I., Low, F. J., Tokunaga, A. T. 1980, *Astrophys. J.*, **238,** 24.
van den Bergh, S. 1971, *Astr. Astrophys.*, **12,** 474.
Weiler, K. W., van der Hulst, J. M., Sramek, R. A., Panagia, N. 1981, *Astrophys. J.*, **243,** L151.

Kapahi, V. K. (Ed.)
Extragalactic Energetic Sources
Indian Academy of Sciences, Bangalore, 1985, pp. 171–176

Nuclear Activity and Supernova Occurrence

R. K. Kochhar *Indian Institute of Astrophysics, Bangalore 560034*

Abstract. It is argued that the occurrence of nuclear activity and supernovae in E and S0 galaxies are correlated and a result of accretion of gas by the galaxy.

Key words: nuclear activity—extragalactic radio sources—supernovae

1. Introduction

We shall argue that there is a correlation between the occurrence of nuclear activity and supernovae (SN); both occur only in those E and S0 galaxies which accrete matter from outside and form stars. In the next section we review the arguments in favour of the hypothesis that SN I come from short-lived stars (Oemler & Tinsley 1979) and show that contrary to the general belief the colour observations of ellipticals do not rule out this hypothesis. It is our contention that a typical isolated E/S0 galaxy, which is gas-free and does not form stars will not produce SN. Indeed, we introduce the concept of a *supernovic* elliptical. An elliptical which can produce SN is called here supernovic (just as a nation which produced heroes is called a heroic nation). Of course some supernovic E/S0s may be more supernova-prone than the others, but a non-supernovic E/S0 galaxy will not produce a SN at all.

A supernovic elliptical may accrete gas from its own halo (*e.g.* M 86) or from the intergalactic or intracluster medium (N 1275 = Perseus A, M 87) or from a neighbouring galaxy (N 3226). Alternatively or simultaneously an elliptical may swallow gas clouds or gas-rich dwarf galaxies (N 1316 = Fornax A).

Nuclear activity of E/S0 galaxies is interpreted in terms of a central engine (*e.g.* a black hole) which uses gas as fuel and converts energy from a passive into an active form (*e.g.* Rees 1977). Now since a typical galaxy is gas free, a central engine in such a galaxy—if it existed—would lie idle for want of fuel. However if an E/S0 accretes gas from outside, in course of time this gas would find its way to the nuclear regions and give rise to nuclear activity (Shklovskiĭ 1963). Thus the presence of gas and dust, star formation, occurrence of SN, and nuclear activity in E/S0 galaxies are all interrelated and a consequence of accretion of gas by the galaxy.

2. Progenitors of SN I

The occurrence of SN I in E/S0 galaxies has been interpreted to mean that SN I progenitors are low-mass stars. In recent times this picture has come under severe

strain. Oemler & Tinsley (1979) have argued, on the basis of SN I rates in I0 and spiral galaxies and other evidence, that SN I come from stars in the mass range 4–7$M_\odot$. Recent theoretical work supports this view; the most plausible models for SN I are the carbon deflagration models, in which a star of mass $(6 \pm 2) < M/M_\odot < (8 \pm 2)$ loses its hydrogen envelope, by being in a binary or otherwise, and explodes as SN I (Nomoto 1981). This picture is consistent with the absence of a hot neutron star in the remnants of historical SN I, Tycho and Kepler, and with the recent estimates of pulsar and stellar birthrates (Kochhar 1981).

The fact that E/S0 galaxies have produced only SN I means that stars more massive than $7M_\odot$ do not form in them. It seems that as one moves along the Hubble sequence and towards a decreasing bulge-to-disc ratio, the IMF becomes shallower. This has an interesting consequence. If very many massive stars form, the associated energetics will heat and disperse the interstellar gas with the result that the next phase of star formation would be delayed (Seiden & Gerola 1982). By the time the next phase of star formation takes place, the earlier stars would have completed their evolution, returning most of the gas back to the interstellar medium. Thus a shallow IMF will ensure a perennial availability of gas. On the other hand, if IMF is steep, all the available gas will be used up in the formation of long-lived stars.

If SN I come from short-lived stars, the E/S0 galaxies that produce SN should be bluer than the ones which do not. Sandage & Visvanathan (1978a, b) give corrected photoelectric colours for a sample of 354 unambiguous E/S0s out of which 12 have produced SN. For these 12 galaxies one obtains $\langle (u-V)^{\rm KEM}_{0.5} \rangle = 2.32 \pm 0.08$ which is not significantly different from the value 2.33 ± 0.09 for the whole sample. Before one jumps from this to the conclusion that the supernovic E/S0s are not bluer than the nonsupernovic ones, one must examine the various corrections that have gone into obtaining these numbers from the raw data.

Since an error of 10 per cent in the distance translates into an error of 0.5 mag in $(u-V)^{\rm KEM}$ colours through the colour–magnitude (C–M) relation, it is advisable to confine one's attention to a single cluster while comparing the supernovic and the nonsupernovic E/S0s. The well-studied Virgo I cluster of galaxies—usually referred to as the Virgo cluster—is a small, irregular, dynamically unevolved, spiral-rich cluster containing 205 Shapley–Ames galaxies of which 19 per cent are elliptical. It contains eight supernovic E/S0s making it an obvious choice for a study of the difference between the supernovic and nonsupernovic E/S0s. Six of the eight supernovic E/S0s are 0.06 ± 0.01 mag bluer than the general sample taken from Visvanathan & Sandage (1977). (See Fig. 1.) Kochhar & Prabhu (1984) point out that the colours of the E/S0s should be seen in the light of their metallicities. Fig. 2 shows a plot of Mg index versus absolute magnitude (Mg–M) for 54 E/S0s for which data are available in the literature. Significantly, all the supernovic E/S0 have higher line-strength than expected from the mean Mg–M relationship. (The only exception is the interacting dwarf elliptical N 3226.) In particular the supernovic Virgo galaxies N 4374, 4486 and 4621, which are on an average 0.027 mag bluer in $(u-V)$, have 0.019 mag excess line-strength. If their colours were to reflect this excess metallicity, these galaxies should have been 0.1 mag redder than expected from the mean C–M relation. In other words, these supernovic E/S0 are 0.13 mag bluer than they would have been if star formation had not occurred in them. Their excess metallicity may itself have resulted from such recurrent bursts of star formation.

Thus the spread in the C–M relation is not all intrinsic and is in part due to star

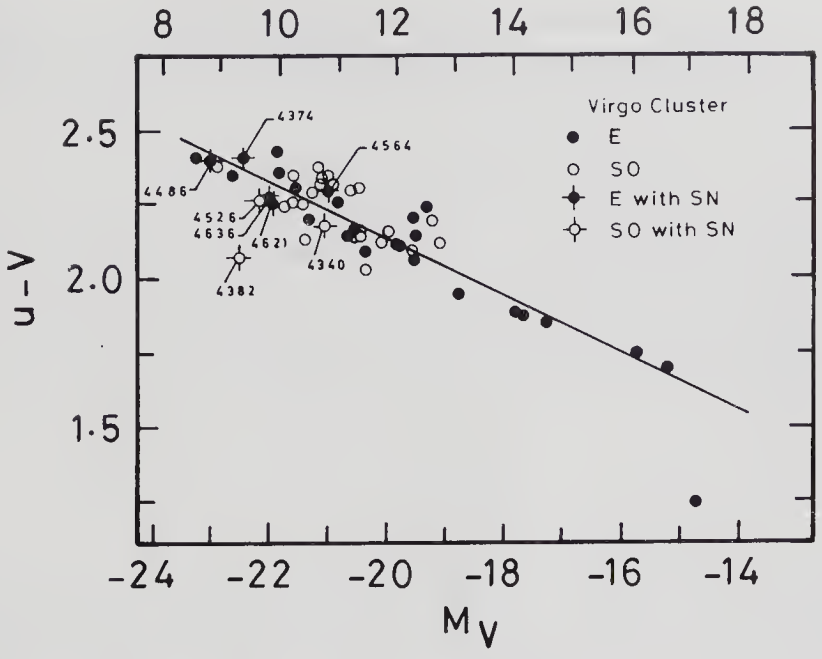

Figure 1. The colour–magnitude diagram of Virgo E/S0 galaxies. Supernovic ones are marked.

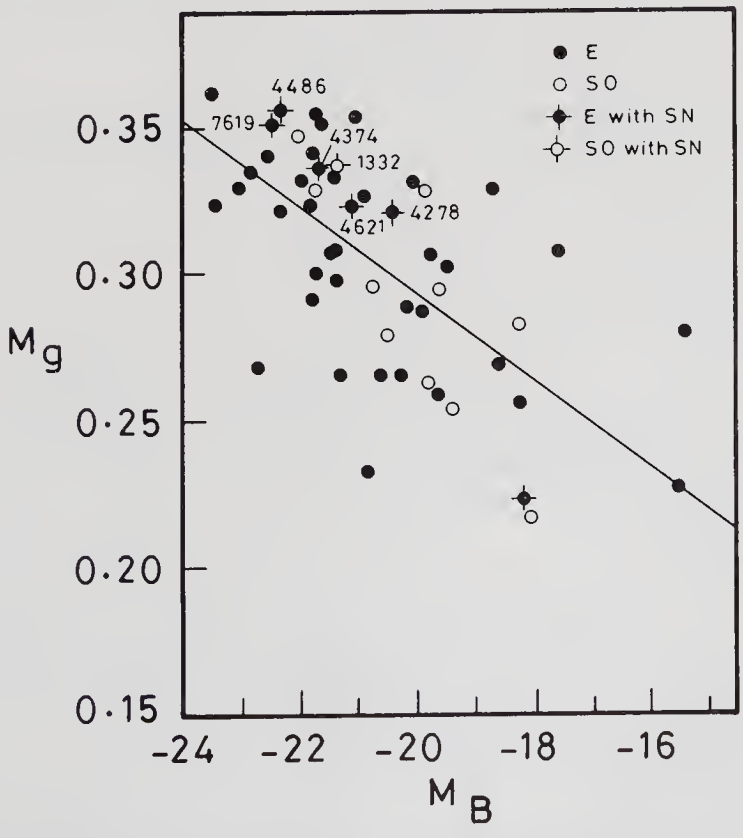

Figure 2. The Mg-index–absolute magnitude diagram for E/S0 galaxies. Supernovic ones are marked.

formation in some of the galaxies. However, the star formation is not so extensive as to make a galaxy bluer than the scatter. But these galaxies are metal-richer than normal.

3. Galactic ecology

If an elliptical accretes matter, it may show up as neutral hydrogen and/or dust. Hummel (1980) has convincingly shown that elliptical galaxies with detected H I are much more likely to contain nuclear emission-line regions and nuclear continuum radio emission than ellipticals without detected H I, suggesting that the accreted gas fuels the central source. Shostak *et al.* (1983) find that the H I detection rate in radio galaxies is consistent with the presence of thin H I discs of galactic dimensions in all radio galaxies. In the case of 8 radio ellipticals with dust lanes, radio axis is perpendicular to the dust lane (Kotanyi & Ekers 1979) again highlighting the connection between accretion and radio activity. Out of these 8 galaxies, N 1316 has had two SN and N 4374 one.

The suggestion that it is gas accreted by an E/S0 galaxy from outside which fuels the nuclear activity finds support from observations of radio spirals. Nuclear sources in barred spirals are on an average brighter than those in non-barred spirals, and nuclear sources in double galaxies are brighter than in isolated galaxies (Hummel 1980). Whereas in the case of paired galaxies the supply of gas to the central regions is ensured by tidal interaction, the centres of barred spirals receive their fuel supplies as a result of the interaction of the bar with the gas in the disc.

The environments of an E/S0 galaxy play the same role as the disc of a barred spiral, that is, they ensure the central regions of fuel supply. Thus an elliptical galaxy is more likely to be a radio source if it is in a Zwicky cluster, and is still more likely to be a radio source if it is in a group within a cluster (Dressel 1981).

The Virgo cluster shows a two-component X-ray spectrum; the cluster is permeated by a hot ($\sim 10^8$ K) intracluster gas in which are embedded galaxies with individual cool ($\sim 10^7$ K) atmospheres (Forman *et al.* 1981). The non-thermal activity in the central regions of N 4486 (M 87) is explained in terms of accretion from its massive halo (Mathews 1978). We hold this accretion responsible for the SN also (A similar case is that of the powerful X-ray and radio source N 1275 = Per A [Fabian & Nulsen 1977], which has also produced a SN). X-ray haloes have been detected around M 84 and M 86 (Forman *et al.* 1981). It is reasonable to suppose that other ellipticals in the Virgo cluster too would have similar haloes, confined by the hot intracluster gas (Fabian, Schwartz & Forman 1980). The presence of individual gas reservoirs around ellipticals from which they can accrete gas explains why Virgo ellipticals are predominantly supernovic and radio active.

The hot gas (10^8 K) in the compact, dynamically evolved, spiral-poor Coma cluster is associated with the cluster as a whole and not with any individual galaxy. It approximates an isothermal gas sphere and shows no sign of radiatively regulated accretion (Forman *et al.* 1981). There are indications that SN rate in Coma is about a factor of 3 lower than in Virgo (Barbon 1978).

Coma cluster is fairly uniform in galaxy type and shows a central maximum density with a symmetrical decrease towards the boundaries. If all galaxies were equally likely to produce SN, we should expect the supernovic ellipticals to have the same distribution as the galaxies in general. This, however, is not the case. All supernovic E/S0 in Coma are confined to a plane (Barbon 1978). Presumably, some gas in Coma has settled down

in a disc and is accreted by the galaxies there, giving rise to supernovic activity. Of the seven SN in the central regions of Coma, two have occurred in I0 galaxies, four in E/S0 galaxies and only one in an Sb galaxy (Thomson 1981). At the centre of the cluster and the disc lies the giant elliptical radio galaxy N 4874 which has produced two SN.

Further support for the accretion hypothesis comes from Caldwell & Oemler (1981), who find that the spiral-rich outer regions of rich clusters of galaxies have higher SN rate in the E/S0 galaxies as compared to the spiral-poor and gas-poor central regions of such clusters. They also find that the E/S0 galaxies in the outer regions of rich clusters are bluer than the ones in the inner regions suggesting that recent star formation is more active in the E/S0 galaxies embedded in gas-rich outer regions of the rich clusters.

4. Conclusions

We have argued in favour of the assertion that all SN I come from short-lived stars. We have, however, suggested that a typical, isolated E/S0 galaxy will not produce SN. Only if an E/S0 galaxy accretes matter from outside and forms stars will it produce SN. Thus not all E/S0 galaxies are *supernovic*.

We have discussed some aspects of what may be termed *galactic ecology*, that is, the role of environment in determining the properties of an E/S0 galaxy. We have argued that occurrence of supernovae and nuclear activity in elliptical and lenticular galaxies are interrelated and a consequence of accretion of gas and resultant star formation.

Acknowledgement

The work reported here has been done in collaboration with Dr T. P. Prabhu.

References

Barbon, R. 1978, *Astr. J.*, **83,** 13.
Caldwell, C. N., Oemler, A. 1981, *Astr. J.*, **86,** 1424.
Dressel, L. L. 1981, *Astrophys. J.*, **245,** 25.
Fabian, A. C., Nulsen, P. E. J. 1977, *Mon. Not. R. astr. Soc.*, **180,** 479.
Fabian, A. C., Schwarz, J., Forman, W. 1980, *Mon. Not. R. astr. Soc.*, **192,** 135.
Forman, W., Bechtold, J., Blair, W., Jones, C. 1981, in *X-ray Astronomy with the Einstein Satellite*, Ed. R. Giacconi, D. Reidel, Dordrecht, p. 187.
Hummel, E. 1980, *Ph D Thesis, University of Groningen.*
Kochhar, R. K. 1981, *J. Astrophys. Astr.*, **2,** 87.
Kochhar, R. K., Prabhu, T. P. 1984, *Astrophys. Space Sci.*, **100,** 369.
Kotanyi, C. G., Ekers, R. D. 1979, *Astr. Astrophys.*, **73,** L1.
Mathews, W. G. 1978, *Astrophys. J.*, **219,** 413.
Nomoto, K. 1981, in *IAU Symp. 93: Fundamental Problems in the Theory of Stellar Evolution*, Eds D. Sugimoto, D. Q. Lamb & D. N. Schramm, D. Reidel, Dordrecht, p. 295.
Oemler, A., Tinsley, B. M. 1979, *Astr. J.*, **84,** 985.
Rees, M. 1977, *Q. J. R. astr. Soc.*, **18,** 429.
Sandage, A., Visvanathan, N. 1978a, *Astrophys. J.*, **223,** 707.
Sandage, A., Visvanathan, N. 1978b, *Astrophys. J.*, **225,** 742.
Seiden, P. E., Gerola, H. 1982, *Fund. Cosmic Phys.*, **7,** 241.

Shklovskiĭ, I. S. 1963, *Sov. Astr.*, **6**, 465.
Shostak, G. S., van Gorkom, J., Ekers, R. D., Sanders, R. H., Goss, W. M., Cornwell, T. 1983, *Astr. Astrophys.*, **119**, L3.
Thompson, L. A. 1981, *Publ. astr. Soc. Pacific*, **93**, 176.
Visvanathan, N., Sandage, A. 1977, *Astrophys. J.*, **216**, 214.

Other Seminar Talks not Included in the Proceedings

R. Cowsik: The Knots of M 87
(see R. Cowsik *et al.* 1983, in *Proc. 18th International Cosmic Ray Conference*, Bangalore, **2,** p. 234).

Gopal-Krishna: Reflection Symmetry in Double Radio Sources
(see Gopal-Krishna & S. M. Chitre 1983, *Nature*, **303,** 217).

Participants

Ambastha, A. K. *Physical Research Laboratory, Ahmedabad.*
Ananthakrishnan, S. *Radio Astronomy Centre (TIFR), Ootacamund.*
Anantharamaiah, K. R. *Raman Research Institute, Bangalore.*
Arora, S. *Raman Research Institute, Bangalore.*
Bagri, D. S. *Radio Astronomy Centre (TIFR), Ootacamund.*
Banhatti, D. G. *Radio Astronomy Centre (TIFR), Ootacamund.*
Bhandari, R. *Raman Research Institute, Bangalore.*
Burbidge, G. R. *Kitt Peak National Observatory, Tucson, USA.*
Chitre, S. M. *Tata Institute of Fundamental Research, Bombay.*
Cohen, M. H. *California Institute of Technology, Pasadena, USA.*
Cowsik, R. *Tata Institute of Fundamental Research, Bombay.*
Dadhich, N. *University of Poona, Pune.*
Das, P. K. *Indian Institute of Astrophysics, Bangalore.*
Das Gupta, P. *Tata Institute of Fundamental Research, Bombay.*
Datta, Bhaskar *Indian Institute of Astrophysics, Bangalore.*
Deo, P. P. *Tata Institute of Fundamental Research, Bombay.*
Deshpande, A. A. *Raman Research Institute, Bangalore.*
Deshpande, M. R. *Physical Research Laboratory, Ahmedabad.*
Dwarakanath, K. S. *Raman Research Institute, Bangalore.*
Ghosh, P. *Tata Institute of Fundamental Research, Bombay.*
Gopal-Krishna *TIFR Centre, Indian Institute of Science Campus, Bangalore.*
Gopal Swamy, N. *Indian Institute of Astrophysics, Bangalore.*
Gupta, S. S. *Indian Institute of Astrophysics, Bangalore.*
Iyer, B. R. *Raman Research Institute, Bangalore.*
Jacob, B. V. *Indian Institute of Astrophysics, Bangalore.*
Joseph, Samuel *Raman Research Institute, Bangalore.*
Jyotsna, Vijapurkar *Indian Institute of Astrophysics, Bangalore.*
Kapahi, V. K. *TIFR Centre, Indian Institute of Science Campus, Bangalore.*
Kapoor, R. C. *Indian Institute of Astrophysics, Bangalore.*
Kembhavi, A. K. *Tata Institute of Fundamental Research, Bombay.*
Kochhar, R. K. *Indian Institute of Astrophysics, Bangalore.*
Komesaroff, M. *Radio Physics, CSIRO, Epping, Australia.*
Krishna Mohan, S. *TIFR Centre, Indian Institute of Science Campus, Bangalore.*
Kronberg, P. P. *Universi.y of Toronto, Ontario, Canada.*
Kulshrestha, A. K. *Physical Research Laboratory, Ahmedabad.*
Kundu, M. R. *University of Maryland, College Park, USA.*
Laing, R. A. *NRAO, Charlottesville, USA.*
Lokanandham, B. *Osmania University, Hyderabad.*
Marar, T. M. K. *ISRO Satellite Centre, Bangalore.*
Mohanty, D. K. *TIFR Centre, Indian Institute of Science Campus, Bangalore.*
Murray, S. S. *Centre for Astrophysics, Cambridge, USA.*
Namboodiri, B. M. S. *Indian Institute of Astrophysics, Bangalore.*

Narayan, R. *Raman Research Institute, Bangalore.*
Narlikar, J. V. *Tata Institute of Fundamental Research, Bombay.*
Nataraja, B. V. *Raman Research Institute, Bangalore.*
Nityananda, R. *Raman Research Institute, Bangalore.*
Padmanabhan, T. *Tata Institute of Fundamental Research, Bombay.*
Padmavathy, A. S. *Indian Institute of Astrophysics, Bangalore.*
Patnaik, A. R. *TIFR Centre, Indian Institute of Science Campus, Bangalore.*
Porcas, R. W. *Max Planck Institute for Radio Astronomy, Bonn, FRG.*
Prabhu, T. P. *Indian Institute of Astrophysics, Bangalore.*
Radhakrishnan, V. *Raman Research Institute, Bangalore.*
Ramadurai, S. *Tata Institute of Fundamental Research, Bombay.*
Ramanujan, M. N. *Raman Research Institute, Bangalore.*
Rana, N. C. *Tata Institute of Fundamental Research, Bombay.*
Ravindra, D. K. *Raman Research Institute, Bangalore.*
Ray, A. *Tata Institute of Fundamental Research, Bombay.*
Rees, M. J. *Institute of Astronomy, Cambridge, UK.*
Saikia, D. J. *TIFR Centre, Indian Institute of Science Campus, Bangalore.*
Sarma, N. V. G. *Raman Research Institute, Bangalore.*
Seetha, S. *ISRO Satellite Centre, Bangalore.*
Sharma, D. P. *ISRO Satellite Centre, Bangalore.*
Shastri, Prajval *TIFR Centre, Indian Institute of Science Campus, Bangalore.*
Singal, A. K. *Radio Astronomy Centre (TIFR), Ootacamund.*
Singh, K. P. *Tata Institute of Fundamental Research, Bombay.*
Sivaram, C. *Indian Institute of Astrophysics, Bangalore:*
Smiles, M. *Raman Research Institute, Bangalore.*
Sreekantan, B. V. *Tata Institute of Fundamental Research, Bombay.*
Srinivasan, G. *Raman Research Institute, Bangalore.*
Steppe, H. *Max Planck Institute for Radio Astronomy, Bonn, FRG.*
Strittmatter, P. A. *Steward Observatory, Tucson, Arizona, USA.*
Subrahmanya, C. R. *TIFR Centre, Indian Institute of Science Campus, Bangalore.*
Subramaniam, K. R. *Raman Research Institute, Bangalore.*
Subramanian, K. *Tata Institute of Fundamental Research, Bombay.*
Sukumar, S. *Radio Astronomy Centre (TIFR), Ootacamund.*
Surendiranath, R. *Indian Institute of Astrophysics, Bangalore.*
Swarup, G. *Radio Astronomy Centre (TIFR), Ootacamund.*
Thejappa, T. *Indian Institute of Astrophysics, Bangalore.*
Thakur, R. K. *Ravishankar University, Raipur.*
Udaya Shankar, N. *Raman Research Institute, Bangalore.*
Usha, S. *Radio Astronomy Centre (TIFR), Ootacamund.*
van Speybroeck, L. *Centre for Astrophysics; Cambridge, USA.*
Varghese, B. V. *Indian Institute of Astrophysics, Bangalore.*
Vasanthi, M. M. *Tata Institute of Fundamental Research, Bombay.*
Vasundhara, R. *Indian Institute of Astrophysics, Bangalore.*
Venugopal, V. R. *Radio Astronomy Centre (TIFR), Ootacamund.*
Vinod Krishan *Indian Institute of Astrophysics, Bangalore.*
Visveshwara, C. V. *Raman Research Institute, Bangalore.*
Vivekanand, M. *Raman Research Institute, Bangalore.*

Cover printed at Eastern Press, Bangalore